UNIVERSITÀ DEGLI STUDI DI MILANO

FACOLTÀ DI SCIENZE E TECNOLOGIE
SCUOLA DI DOTTORATO IN INFORMATICA
DIPARTIMENTO DI INFORMATICA
DOTTORATO DI RICERCA IN INFORMATICA, XXVI CICLO

CONTACTLESS AND LESS-CONSTRAINED PALMPRINT RECOGNITION

INF/01 INFORMATICA

TESI DI DOTTORATO DI RICERCA DI:
Angelo Genovese

RELATORE:
Prof. Vincenzo Piuri

CORRELATORE:
Dott. Ing. Fabio Scotti

DIRETTORE DELLA SCUOLA DI DOTTORATO:
Prof. Ernesto Damiani

Anno Accademico 2012/13

"Anybody who has been seriously engaged in scientific work of any kind realizes that over the entrance to the gates of the temple of science are written the words: Ye must have faith."

— Max Planck

"Research is to see what everybody else has seen, and to think what nobody else has thought."

— Albert Szent-Gyorgyi

ACKNOWLEDGMENTS

I would like to thank Vincenzo Piuri and Fabio Scotti for their collaboration, their support, and their advice during the research activities that led to the writing of this thesis. Without their presence, this work would not have been possible. I want to thank also Ruggero Donida Labati for his help and support during the research work, and for his company in the laboratory.

I thank all the people I worked with, my friends, and all the people that volunteered for the numerous biometric acquisitions I needed in order to evaluate my work. Among them I want to mention, with no particular order, Ravi Jhawar, Massimo Rivolta, M. Aktaruzzaman, Jonatan Maggesi, Michele Zanchetta, Alice Moscovali, Giulio Vinci, Stefano Ferrari, Elisa Venturelli, Roberta Arrigoni, Manuel Vailati, Fulvio Frati, Daniela Mutti, Guido Lena Cota, Marco Casazza, Mirko Bodini, Valerio Bellandi, Claudio Ardagna, Olga Scotti, Danio Asinari, Andrea Mangiavini, Claudia Piana, Claudio Moretti, Cristina Salice, Davide Rebeccani, Giovanni Livraga, Sara Foresti, and Annamaria Pavesi. I thank them for their willigness and patience.

I also want to thank the referees Prof. Pau-Choo Chung, Prof. Konstantinos N. Plataniotis, and Dr. Qinghan Xiao for their time spent in reading my thesis and for giving me valuable suggestions for improving my work.

Lastly, I want to thank everyone that will read this thesis and use it as a way of developing new ideas, improving existing methods, or implementing innovative technologies and solutions.

ABSTRACT

Biometric systems consist in the combination of devices, algorithms, and procedures used to recognize the individuals based on the characteristics, physical or behavioral, of their persons. These characteristics are called biometric traits.

Nowadays, biometric technologies are becoming more and more widespread, and many people use biometric systems daily. However, in some cases the procedures used for the collection of the biometric traits need the cooperation of the user, controlled environments, illuminations perceived as unpleasant, too strong, or harmful, or the contact of the body with a sensor. For these reasons, techniques for the contactless and less-constrained biometric recognition are being researched, in order to increase the usability and social acceptance of biometric systems, and increase the fields of application of biometric technologies.

In this context, the palmprint is a biometric trait whose acquisition is generally well accepted by the users. Moreover, palmprints can be captured using low-cost devices, and even in the case of elder people or manual workers. However, biometric systems based on the palmprint traditionally use contact-based acquisitions, with pegs used to constrain the position of the hand in a specific way.

For these reasons, this thesis has the objective of researching innovative methods for the contactless and less-constrained recognition of the palmprint. In particular, the researched methods allow to recognize the individuals without the contact of the hand with any surface, and a metric three-dimensional representation is used to eliminate the need for the user to place his hand in a specific position. The originality of the researched techniques allow to perform an accurate biometric recognition, with a focus on the usability, computational speed, and social acceptance of the system. Moreover, the cost of the final device is also taken into consideration. The novelty of the described method, with respect to similar methods in the literature based on contactless three-dimensional acquisitions, resides in the use of an innovative setup, which has a lower cost and captures the images faster.

In particular, innovative multiple view acquisition systems, based on CCD cameras and a led illumination, are designed in order to capture the palmprint samples, and original image processing algorithms are implemented to process the samples. Three-dimensional reconstruction techniques are used in order to achieve a metric representation of the hand, invariant to the pose and orientation. Then, pattern recognition methods are implemented in order to extract and match the distinctive features of the palmprints.

The novel methods researched in this thesis obtained a good recognition accuracy, in many cases superior to the most recent approaches in the literature. Moreover, good results were obtained regarding the computational speed, usability and social acceptance of the considered methods.

CONTENTS

1 INTRODUCTION

The focus of this thesis is on the research of innovative methods for the biometric recognition of the individuals based on the characteristics of their palm. In particular, the researched methods focus on the study and implementation of original methods able to perform the recognition in a contactless and less-constrained manner.

In order to better understand the described research, an introduction to biometrics and biometric recognition is presented, then the contactless and less-constrained biometric systems are introduced, followed by an introductory state of the art on palmprint recognition. The objective of the thesis, the performed research, and the obtained results are described. To conclude, the structure of the thesis is detailed.

1.1 BIOMETRICS

Biometrics refers to the discipline that studies the measurement of bodily features typical of human beings. In particular, the term biometrics is defined by the International Organization for Standardization (ISO) as "*the automated recognition of individuals based on their behavioral and biological characteristics*" [1].

The main applications of biometrics are in the medical and security fields. In the medical field, biometrics can be used as a support for performing diagnoses, together with other techniques for medical analysis. In the security field, biometric measurements are used for regulating the access to restricted areas (e.g., military zones, airports, stadiums, banks), for government applications (e.g., border control, ID cards, identification of wanted people), for controlling the access to logical resources (e.g., home banking, ATMs, e-commerce, personal devices), or for forensic analyses (e.g., identification of suspects, analysis of kinships).

Biometric systems consist in the combination of devices, algorithms, and procedures used to recognize the individuals based on the characteristics of their persons, rather than using something known (e.g., a password) or something possessed (e.g., a smart-

card). The advantages of biometric features lay in the fact that they are distinctive of each individual, and do not risk to be forgotten (like a password), nor stolen (like a smartcard).

A biometric trait is defined as the particular characteristic of the person that is being considered in order to perform the recognition [2]. In particular, biometric traits can be physiological (biological) or behavioral: in the first case, the recognition is based on physical traits related to the body of the person, such as the fingerprint, the iris, the face, or the shape of the hand. Behavioral traits, on the other hand, are related to the actions performed by a person and include, for example, the gait, the voice, or the signature.

Moreover, biometric systems can work in two modalities: authentication and identification. In the case of a biometric system working in the authentication mode, the individual states his identity and gives his biometric trait to the biometric system, which compares the biometric trait presented to the system with the one previously stored, in order to determine if the traits match and the person is recognized. Examples of biometric systems working in the authentication mode are the systems that regulate the access to restricted areas. In a biometric system working in the identification mode, the individual does not state his identity, and the systems compares the biometric trait of the individual with all the traits stored in the database, in order to ascertain his identity. An example of a biometric system working in the identification mode is the analysis of a latent fingerprint found at a crime scene, which is compared with all the fingerprints present in the law-enforcement databases, in order to determine the identity of the person.

1.2 CONTACTLESS AND LESS-CONSTRAINED BIOMETRICS

Traditionally, most biometric systems require the user to be cooperative and willing to give his trait to the sensor. In many cases, biometric acquisitions require controlled procedures, or the contact of the trait with the sensor. For example, the user must assume a certain pose, place his biometric trait in a particular place, and remain still for the duration of the biometric acquisition.

Examples of biometric traits that traditionally require constrained acquisition procedures are the face, the iris, the fingerprint, or the palmprint. In the case of a face acquisition, the user must stand still in a specified position, and with a neutral expression. The illumination conditions are controlled. Iris acquisitions are performed by placing the eye, properly open, in a specific position. An infrared illumination, often perceived as unpleasant or harmful, is used. Fingerprints are captured by touching a small sensor with the proper pressure. However, in many cases the hands can be dirty or sweaty, and the sensor can easily be dirty, which can pose a problem to the user acceptability. In fact, some people might have problems in touching a sensor that has been touched by the hands of many people. Palmprint characteristics are measured by placing the hand on a surface, where pegs are used to constrain the hand in a specific pose. Like fingerprint sensors, palmprint acquisition surfaces can be dirty. Moreover,

the presence of pegs can be a problem in the case of elder people, or people with muscular or joint problems (e.g., arthritis).

Techniques for a less-constrained biometric recognition are being researched in order to reduce or eliminate these constraints. A less-constrained recognition could result in shorter acquisition times, a greater usability, and a greater social acceptance, which in turn could lead to the use of accurate biometric traits in more applicative scenarios. For example, a less-constrained iris recognition would make possible a high recognition accuracy in surveillance applications, mobile phones, gates, etc. Similar applications can be foreseeable also in the case of contactless systems based on the fingerprint, or on the palmprint.

1.3 PALMPRINT RECOGNITION: INTRODUCTION AND OVERVIEW OF THE STATE OF THE ART

Palmprint recognition has been increasingly investigated over the past fifteen years, since it has many points in common with biometric systems based on the fingerprint trait, and the research in the field of palmprint recognition spread rapidly due to the experience maturated for the recognition of fingerprints. As fingerprints, palmprints present many distinctive features and can be used for a highly accurate biometric recognition. However, on the contrary to fingerprints, palmprint recognition can use low-cost acquisition devices, feature a greater user acceptability, and has the possibility to extract biometric samples even from elder people or manual workers. Moreover, numerous kinds of features, at different levels of details, can be extracted according to the type of acquisition used.

It is possible to divide the methods for the palmprint recognition into contact-based and contactless methods, according to the type of contact with the sensor needed to perform the acquisition. Moreover, each category can be further divided into methods based on two-dimensional samples, and methods based on three-dimensional samples.

Currently, the majority of the approaches in the literature perform the palmprint recognition by using contact-based two-dimensional acquisitions, performed by using flatbed scanners or CCD-based acquisition devices. In particular, flatbed scanners allow to implement low-cost palmprint recognition systems, while CCD-based acquisitions offer good quality samples and short acquisition times. Moreover, in order to increase the recognition accuracy, contact-based three-dimensional acquisition devices based on CCD cameras and projectors were proposed. However, they require a complex and more expensive setup.

Contact-based methods have the problem of distortion, dirt, and user acceptability. In fact, distortions are caused by the non-uniform pressure of the hand on the sensor, and at the same time dirt is accumulated after continued acquisitions. Then, user acceptability can be a problem if the people do not want to touch surfaces touched by other people, also possibly dirty with sweat.

For these reasons, contactless acquisition devices were studied. However, contactless methods might feature disadvantages such as a lower contrast, a more complex background, and non-uniform acquisition distances. Moreover, they are sensible to differ-

ences in the lighting conditions. For these reasons, three-dimensional contactless methods were described. These methods are more robust to different acquisition distances, lighting conditions, different backgrounds, noise, and spoofing attacks. However, they require more complex and more expensive setups, with respect to two-dimensional contactless methods.

1.4 NOVELTY AND OBJECTIVE OF THE THESIS

Methods for the biometric recognition based on the palmprint are being increasingly studied in the literature, since palmprints present many distinctive features and can be used for a highly accurate biometric recognition. Moreover, similarly to many hand-based biometric systems, palmprint recognition systems feature a good user acceptability, low-cost acquisition devices, and the possibility to extract biometric samples even from elder people or manual workers.

The objective of this thesis is the research of innovative methods for the contactless, less-constrained biometric recognition based on the characteristics of the palmprint. Original methods are studied in order to perform the recognition without the contact of the palm with a surface, and without the need for the user to place his hand in a specific position. In particular, three-dimensional reconstruction techniques are used in order to compute a metric representation of the palm, which is invariant to the position, distance, and orientation of the hand. By using these techniques, it is be possible to perform an accurate biometric recognition, and increase the usability, computational speed, and social acceptance of the biometric recognition systems based on the palm. Moreover, the cost of the final device is also taken into consideration.

The novelty of the described approach, with respect to the methods in the literature that perform contact-based acquisitions, reside in the fact that the researched methods do not have the problems caused by the contact of the palm with the sensor, such as distortion, dirt, sweat, or latent impressions, nor they require the back of the hand to be placed against a fixed surface. In this manner, the problem of uncomfortable positions for the acquisition of biometric data are reduced. Moreover, the absence of contact increases the usability and acceptability of the system, especially since no pegs are used. With respect to other methods in the literature that only use two-dimensional samples, the original methods researched in this thesis use the three-dimensional information in order to achieve a metric and more accurate representation of the palm, invariant to the position, orientation, and distance of the acquisition. Then, a less-constrained acquisition can be performed, with a relaxed and non-fixed position of the hand. With respect to the other methods in the literature based on a contactless three-dimensional acquisition of the palmprint, the novelty of the described approach consists in the fact that an innovative hardware acquisition setup is used, which has a lower cost and captures the images considerably faster.

1.5 PERFORMED RESEARCH AND RESULTS

The performed research started with the preliminary study of a contactless and less-constrained biometric system based on the fingerprint. The fingerprint trait was chosen because fingerprint-based biometric systems are a mature and widely used technology, and standard methods for the acquisition, preprocessing, enhancement, and matching of fingerprint samples are already available. For these reasons, it was possible to develop methods for the contactless and less-constrained recognition of the fingerprints that produce images compatible with traditional contact-based samples, in order to evaluate the performance of the methods in comparison with contact-based systems, using common biometric matching algorithms.

In particular, the researched methods for the fingerprint recognition are based on two-view acquisitions using CCD cameras, and do not require the contact of the fingerprint with a sensor or the need for the finger be placed in a specific position. The implemented methods are based on optical acquisition systems, image processing techniques, and pattern recognition algorithms. Moreover, three-dimensional reconstruction techniques were studied and applied to fingerprint acquisitions, in order to increase the accuracy of the recognition system. Then, the reconstructed models are processed using ad-hoc algorithms able to work on three-dimensional models, also to ensure the compatibility with current contact-based biometric systems.

Since similar techniques can be used to capture and process contactless fingerprint and palmprint samples, the obtained results in the field of fingerprint recognition allowed to extend the studied methods for the palmprint recognition. First, a feasibility study for a contactless palmprint recognition was performed, by researching a method based on two-view acquisitions performed at a fixed distance. The method achieved a good recognition accuracy, comparable with the accuracy of the most recent methods in the literature, without the distortions present in contact-based acquisitions, and without the need to touch any surface. However, the back of the hand needs to be placed against a fixed surface.

The obtained recognition accuracy allowed to design and implement an innovative fully contactless and less-constrained palmprint acquisition method, which does not require the contact of the palm with any surface, nor a fixed position of the hand. The method uses three-dimensional reconstruction techniques in order to achieve a metric representation of the hand, invariant to the pose and orientation. This original researched method obtained a good recognition accuracy, in many cases superior to the most recent approaches in the literature, and a good robustness to changes in the hand orientation and to differences in the environmental illumination situations.

Moreover, other biometric aspects were considered and evaluated, in order to estimate the feasibility of the innovative researched method for large-scale biometric recognition scenarios. In particular, good results were obtained in the evaluation of the aspects related to the usability and social acceptance of the researched method. Moreover, other aspects related to the computational speed, cost, interoperability, security, and privacy were considered and discussed.

1.6 STRUCTURE OF THE THESIS

The thesis is structured as follows:

- *Chapter 2*: contains an introduction to the biometric recognition, the biometric modalities, and the general structure of the biometric systems. A survey of the main biometric traits is presented, and the methodologies used for the evaluation of biometric systems are described. The research trends in biometric recognition are also presented.

- *Chapter 3*: presents an introduction to less-constrained biometric systems, then a survey of the research in the field of contactless and less-constrained recognition is proposed. First, the methods that perform the contactless recognition of biometric traits traditionally captured using contact-based sensors are presented. Then, less-constrained techniques for the biometric recognition using traits traditionally captured using contactless acquisitions are described.

- *Chapter 4*: provides an overview of the state of the art in the field of palmprint recognition. First, an introduction to palmprint recognition, including the main characteristics and its applications, is presented. Then, the contact-based and contactless palmprint recognition systems are reviewed. The methods are divided into methods based on two-dimensional samples and methods based on three-dimensional samples. A review of the methods for the quality estimation and the classification of palmprints is also presented.

- *Chapter 5*: contains the descriptions of the original researched methods. First, a feasibility study for a contactless palmprint recognition based on acquisitions at a fixed distance, which require the back of the hand to be placed against a fixed surface, is described. Then, the design and implementation of the innovative fully contactless and less-constrained methods, based on acquisitions with uncontrolled distance, are described.

- *Chapter 6*: presents the experimental results related to the described methods. The collections of the datasets and the used parameters are described, then the accuracy, robustness, computational speed, cost, interoperability, usability, social acceptance, security, and privacy are evaluated, in order to assess the feasibility of the considered innovative methods.

- *Chapter 7*: summarizes the work and the obtained results, the originality of the contribution, then presents a series of possible future works.

- *Appendix A*: contains the list of publications in which some of the ideas and significant results present in this thesis were published.

2

BIOMETRIC SYSTEMS

This chapter presents an overview of biometric systems, in order to better contextualize the technology described in the presented work. The principles of biometric recognition, their general structure and their basic functioning methods are introduced, and the most used biometric traits are described. Then, the methods used for evaluating the biometric systems are detailed. To conclude the chapter, the current research trends in the field of biometric recognition are discussed.

2.1 INTRODUCTION TO BIOMETRIC RECOGNITION

Biometrics refers to the discipline that studies the measurement of bodily features typical of human beings. As defined by the International Organization for Standardization, biometrics is "*the automated recognition of individuals based on their behavioral and biological characteristics*" [1].

Nowadays, biometric systems are becoming more and more widespread, and the costs for their deployment are decreasing. For these reasons, the market of biometric technologies is showing a positive increase in size [3]. In particular, the biometric market reached in 2011 an amount of 5 billion dollars, and forecasts indicate it will reach 12 billion dollars in 2015 [4].

The main applications of biometrics are in the medical and security fields. In the medical field, biometrics can be a support for performing diagnoses, together with other techniques for medical analysis. In the security field, biometric measurement is used for regulating the access to restricted areas (e.g., military zones, airports, stadiums, banks), for government applications (e.g., border control, ID cards, identification of wanted people), for controlling the access to logical resources (e.g., home banking, ATMs, e-commerce, personal devices), or for forensic analyses (e.g., identification of suspects, analysis of kinships) [2].

Then, biometric systems for security applications consist in the combination of devices, procedures, and algorithms used to recognize the individuals based on their bodily features, rather than using something known (e.g., a password) or something possessed (e.g., a smartcard). For example, the details of the fingerprint, the face, or the shape of the hand can be used to determine the identity of a person and regulate the access to restricted services, instead of requiring to type a password (e.g., for accessing a video terminal) or to scan a magnetic card (e.g., for withdrawing money from an ATM). The advantages of biometric features lay in the fact that they do not risk to be forgotten nor stolen, and they are typical of each individual. In this way, it is increased the confidence that the person to be recognized is actually who he claims to be.

A biometric trait consists in the particular characteristic that is measured. Biometric traits can be physiological or behavioral: in the first case, the recognition is based on physical traits related to the body of the person, such as the fingerprint, the iris, the face, or the shape of the hand. Behavioral traits are related to the actions performed by a person, which include the gait, the voice, or the signature.

Nowadays, a multitude of biometric systems is used, with different traits and technologies chosen according to factors such as accuracy, speed, cost, usability, and privacy risks. The choice of the biometric system to be used in a specific operational scenario must consider these different factors. For example, in an environment where high-security is needed (e.g., a military structure), the recognition performance of the system must be as high as possible, and speed and privacy can be sacrificed if needed. On the other hand, a biometric system installed in a low-security environment (e.g., an amusement park) must put the focus on a high speed, a low invasiveness, and low privacy risks.

2.2 STRUCTURE OF BIOMETRIC SYSTEMS

Biometric recognition consists in the procedures used for comparing the biometric traits of the individuals, in order to compute their similarity and determine if they belong to the same person or not. In particular, the recognition process performed by the biometric systems can be divided in five modules:

1. *Acquisition*: based on the used biometric trait, a specific sensor is used to capture the trait belonging to the user. The captured trait can be an image, an audio sample, or a frame sequence. The trait captured by the sensor is called the "sample".

2. *Segmentation*: the region of the sample containing the biometric information is isolated. For example, in the case of an image of an iris acquisition, the background and occlusions are eliminated, and only the iris region is considered.

3. *Feature extraction*: an abstract representation of the biometric trait (the "template") is computed. The template is more suited to be stored in a database and processed by an automatic information processing system. Templates can be strings of bit, coordinates of particular points in the image, images, signals, or algebraic functions.

4. *Identity matching*: the template is compared with one or more templates present in the database. The database can be centralized or also, for authentication modalities, stored on a device possessed by the user. The result of the identity matching step is a "match score", which measure the similarity of the templates.

5. *Decision*: the match score is used to produce the final decision of the biometric system. In most cases, a threshold on the matchscore value is used in order to transform the match score into a boolean decision, which determines if the compared templates belong to the same individual.

In particular, biometric systems can work in two modalities: authentication and identification. In the case of a biometric system working in the authentication mode, the individual states his identity (for example, by showing an ID card) and gives his biometric trait to the biometric system that regulates the access (for example, by placing his fingerprint on the sensor), which captures the corresponding sample. Then, a template is computed using the captured sample, and a biometric matching algorithm is used to compare the template with the template previously stored in the database, corresponding to the presented identity. The system realizes a $1 : 1$ matching between the identities, and grants the access based on a thresholding operation on the resulting match score. A biometric system working in authentication mode can be included in any system that regulates the access to a sensitive resource, such as an ATM, a personal device, or the entrance to a restricted area.

In a biometric system working in the identification mode, the individual does not state his identity, and the systems performs a $1 : N$ matching, by comparing the template computed from the biometric trait presented (or extracted from) the individual with all the templates stored in the database. Then, the identity of the individual associated to the most similar template, based on the resulting match scores, is extracted. The identification modality is typical of biometric systems present in law-enforcement installments, such as the Automated Fingerprint Identification Systems (AFIS). In the case of the AFIS, for example, a particular fingerprint extracted from a crime scene must be compared with every fingerprint present in the database, in order to obtain the identity of the associated individual.

In most cases, in order to refer to the process of biometric matching, and where there is not the need to make a distinction between the authentication and identification modes, the general term "recognition" is used.

Both biometric systems functioning in the authentication and identification modality require an enrollment step, in which a template is computed using the biometric trait of the user, and then stored in the database of the system, together with the associated identity. A graphical representation of the enrollment step is shown in Fig. 2.1. A biometric system working in authentication mode is shown in Fig. 2.2, while the identification mode is shown in Fig. 2.3.

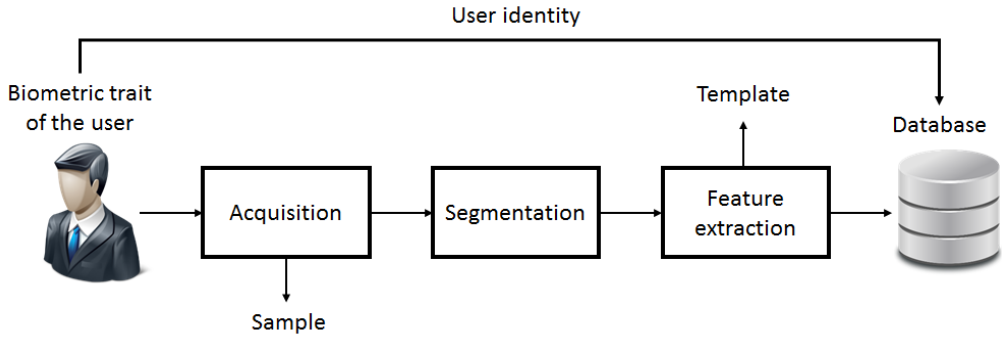

Figure 2.1: Schema of the enrollment step in a biometric system.

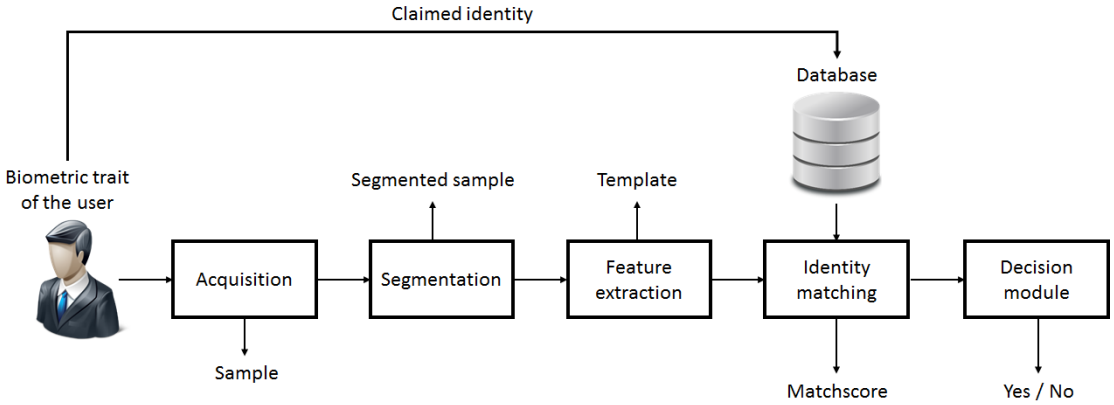

Figure 2.2: Schema of a biometric system working in the authentication mode.

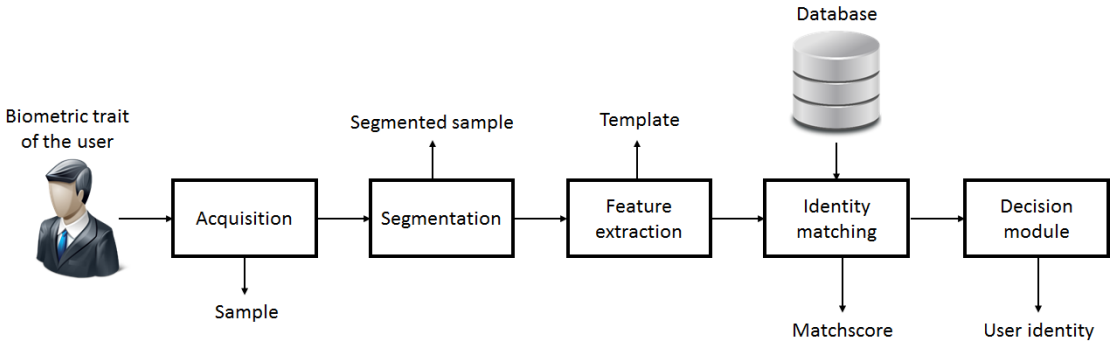

Figure 2.3: Schema of a biometric system working in the identification mode.

2.3 BIOMETRIC TRAITS

Biometric traits can be divided in physiological and behavioral traits. Physiological traits refer to features physically possessed by the body of the person to be recognized. Examples of physiological traits include the fingerprint [14, 15], the palmprint [16], the iris [17, 18], the face [19], the hand geometry [20], the vein pattern of the hand (or palm vein) [21], the shape of the ear [22], the DNA [23], and the ECG [24] (Fig. 2.4). Behavioral traits are related to the actions undertaken by the person in order to be rec-

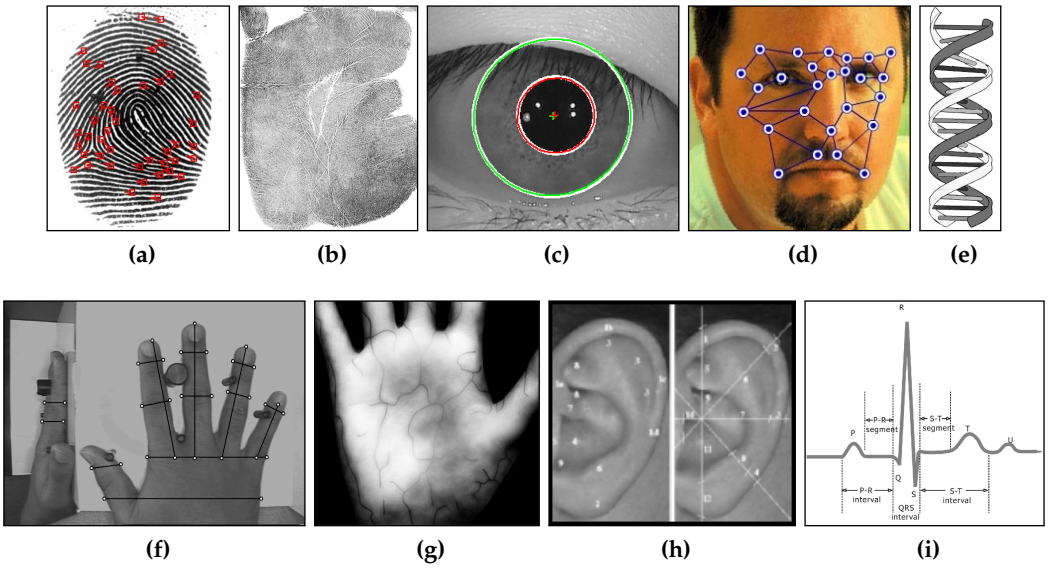

Figure 2.4: Examples of physiological biometric traits: (a) fingerprint [5]; (b) palmprint [6]; (c) iris [7]; (d) face [8]; (e) DNA [9]; (f) hand geometry [10]; (g) vein pattern of the hand [11]; (h) shape of the ear [12]; (i) ECG [13].

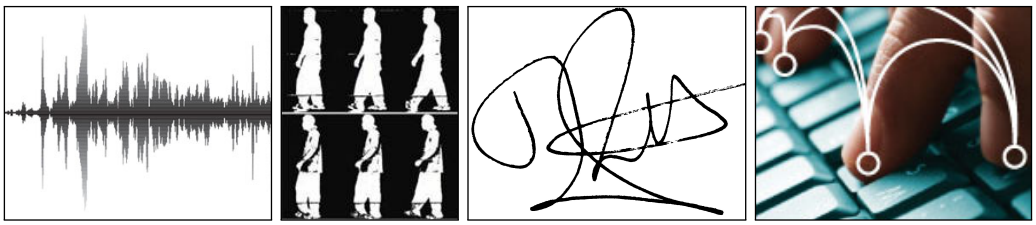

Figure 2.5: Examples of behavioral biometric traits: (a) voice [29]; (b) gait [30]; (c) signature [31]; (d) keystroke [32].

ognized, and include the voice [25], the gait [26], the signature [27], and the keystroke [28] (Fig. 2.5).

The use of innovative biometric traits for recognition purposes is constantly being investigated, in order to improve the performance, speed, cost, or reduce the privacy risks. However, in order to be used for recognition purposes, a biometric trait must possess certain characteristics [33]:

- *Universality*: the biometric trait should be possessed by everyone;
- *Distinctiveness*: the biometric trait should be able to distinguish the individuals;
- *Permanence*: the biometric trait should not change over a period of time;
- *Collectability*: it should be possible to measure quantitatively the biometric trait.

Moreover, other important characteristics are to be considered in order to use the biometric trait in a biometric system for practical purposes:

(a) (b)

Figure 2.6: Examples of fingerprint acquisition sensors: (a) state-of-the-art sensor [42]; (b) portable sensor mounted on a laptop [43].

- *Performance*: it refers to the accuracy and speed that can be obtained by using the biometric trait;
- *Acceptability*: it refers to how much people are willing to give their biometric traits in order to be recognized;
- *Circumvention*: it refers to the difficulty to hack the biometric system in order to gain unauthorized access.

Biometric traits can also be divided in hard and soft biometric traits. The first category includes the aforementioned traits, which have the features of distinctiveness and permanence. Soft biometric traits, on the other hand, have a low distinctiveness or a low permanence of the trait. This kind of traits cannot be used to recognize individuals with a sufficient confidence over a period of time, but can be used for low security environments or for situations where an individual must only be recognized for a short period of time. Moreover, these traits usually present a low invasiveness and can be combined in order to increase the performance of the biometric system [34].

Soft biometric traits can be either continuous or discrete [35]. Continuous soft biometric traits include the height [36], weight [37, 38], and measurement of the size of body parts in general [39]. Discrete biometric traits are the gender [40], race [40], eye color [41], and also the color of the clothes [39].

Today, biometric systems based on the fingerprint (Fig. 2.6) are the most widespread. In fact, they present limited costs (fingerprint sensors can even be placed on laptops or on USB pen drives, as shown in Fig. 2.6b), and good performances. Moreover, they are not considered too invasive by the majority of people. Due to their good accuracy and speed, biometric systems based on the fingerprint trait can be used both for authentication and for identification purposes. Typical biometric systems based on the fingerprints are used for access control (Fig. 2.7a) and for forensic applications (Fig. 2.7b). Centralized fingerprint databases are present in many countries for large scale identification of fingerprints [44]. The analysis of the fingerprint features can be performed in three levels, according to the resolution of the imaging device. In particular, the Level 1 analysis extracts the features related to the ridge flow, orientation, frequency, and

(a) (b)

Figure 2.7: Examples of fingerprint applications: (a) access control [45]; (b) forensic analyses [46].

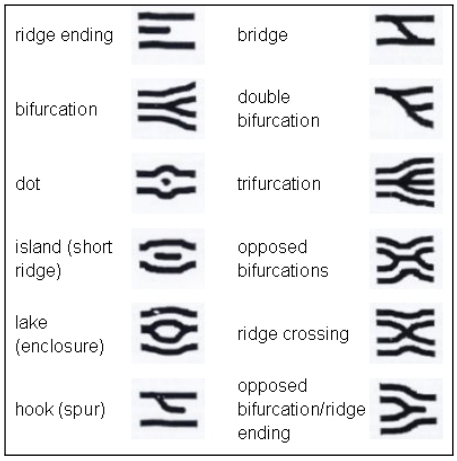

Figure 2.8: Examples of minutiae used for fingerprint recognition [47].

the position of the singular points. The Level 2 analysis is the most used, and is based on the extraction and matching of the positions of particular points called minutiae (Fig. 2.8). The Level 3 analysis considers the position of the pores of the skin, and the incipient ridges.

Biometric systems based on the iris (Fig. 2.9) are being increasingly used, especially in the situations where a high recognition accuracy and a high speed are required, such as border control stations and airports. Iris-based systems, in fact, present the highest accuracy among other biometric traits (except DNA), and the identification procedure is very fast, allowing to perform a real-time identification over a large-scale database. However, biometric systems based on the iris have high costs, and can be perceived as invasive. The acquisition procedure, in fact, requires the user to place his open eye near an IR illumination. One of the most used iris recognition algorithms is based on the IrisCode [17], a bit string representation of the random pattern typical of the iris (Fig. 2.10).

Face recognition systems (Fig. 2.11) are a widely studied type of biometric system. These kind of systems, in fact, offer a low invasiveness since people recognize them-

(a) (b)

Figure 2.9: Examples of iris acquisition sensors: (a) fixed sensor [48]; (b) portable sensor [49].

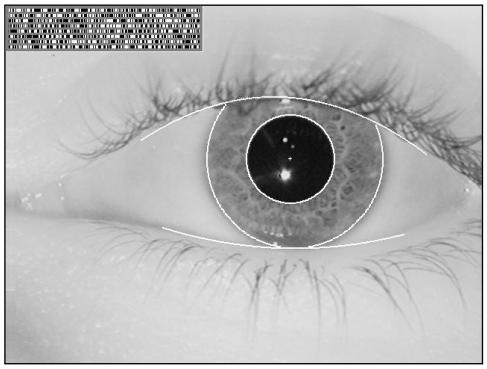

Figure 2.10: Example of a segmented iris image and the corresponding IrisCode [17].

selves naturally by looking at each other's face. Moreover, the acquisition of the face samples is performed contactless by using cameras. For this reason, face recognition systems can be used in surveillance applications, to recognized people at a distance, and in unconstrained scenarios. However, biometric systems based on face recognition do not possess the same accuracy as the systems based on the fingerprint or the iris, since they are greatly influenced by differences in pose, illumination, facial expressions, occlusions (e.g., hat, glasses, etc.) and by the change of physical attributes over time (e.g., beard, hair). The algorithms used for face recognition can use techniques based on transformation or based on the definition of attributes [19].

Systems based on hand geometry (Fig. 2.12), while characterized by a low accuracy, have a very low invasiveness and are very much accepted by the users. Moreover, a biometric system based on hand geometry can be realized with low hardware costs [20]. Then, biometric systems that use the hand geometry can be used positively in situations where a high recognition accuracy is not needed. Some methods described in the literature focus especially on the recognition based on the finger shape [52, 53, 54, 55] or the finger knuckle [56, 57].

Other biometric recognition systems based on the features of the hand, such as the palmprint [16] (Fig. 2.13) or the vein pattern of the hand [21] (Fig. 2.14) also possess a low invasiveness and are positively accepted by the users. These systems usu-

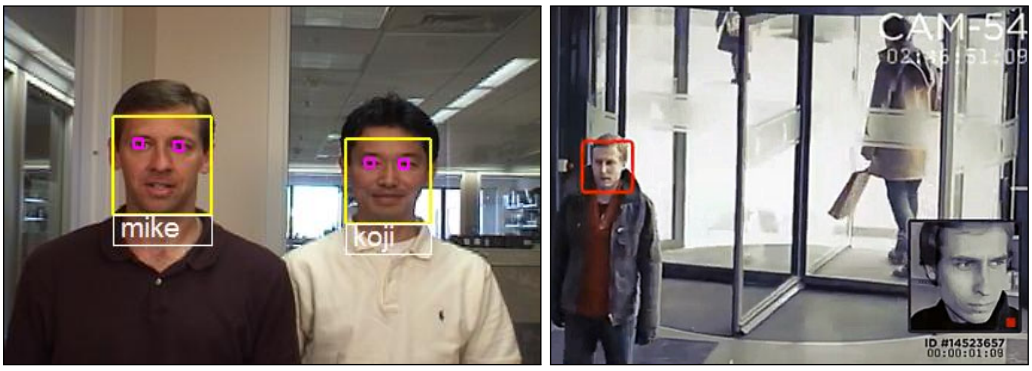

(a) (b)

Figure 2.11: Examples of face recognition systems: (a) face recognition of collaborative subject [50]; (b) face recognition in surveillance applications [51].

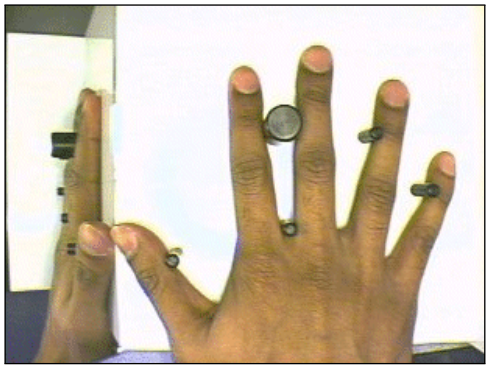

Figure 2.12: Example of a biometric system based on hand geometry [10].

ally present a higher accuracy with respect to the systems based only on geometric measures of the hand. Biometric systems based on palmprint can use optical sensors (Fig. 2.13a), low-cost flatbed scanners (Fig. 2.13b) or CCD-based devices (Fig. 2.13c). However, some systems based on the vein pattern use an infrared camera, which can raise the costs of the biometric system.

Biometric systems based on the DNA [23] are the most accurate mean of performing the recognition of an individual. However, the procedure is extremely expensive and time consuming. Moreover, by using DNA it is not possible to discern identical twins.

In the literature, some works describe also the use of the ear shape to perform a biometric recognition [22] (Fig. 2.15). In particular, the shape of the ear can be acquired in a contactless manner, and even at long distances.

Systems based on retinal scans are also present in the literature [63], and perform the biometric recognition by acquiring the pattern of veins present in the back region of the eye.

Facial thermography is a technology based on the acquisition of the vein pattern on the face of the individual. In most cases, an infrared camera is used. The recognition algorithms are similar in most aspects to the ones used in face recognition systems [64].

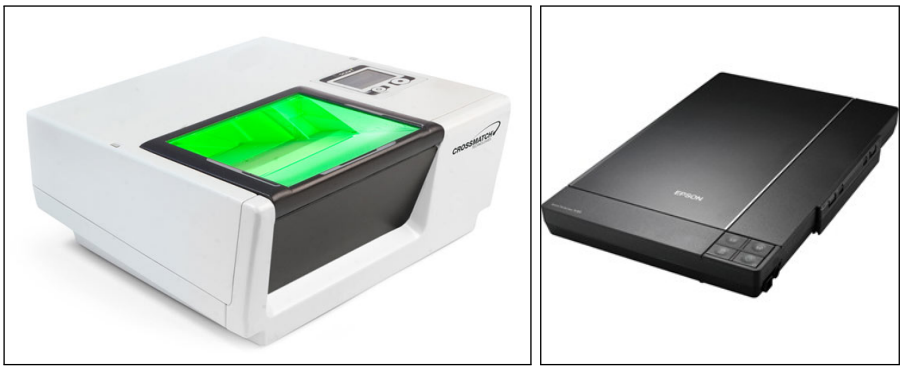

(a) (b)

(c)

Figure 2.13: Example of palmprint acquisition devices: (a) optical device [58]; (b) flatbed scanner [59]; (c) CCD-based device [60].

Figure 2.14: Example of a palm vein scanner, able to capture the vein pattern of the hand [61].

Behavioral traits, like the voice [25], the gait [26], the signature [27], and the keystroke [28] are usually well-accepted by the users, also because they can be partially altered to prevent recognition (e.g., a person can change the way he walks or talks) , or even hidden (e.g., a person can refuse to speak or to sign). However, they present a lower recognition accuracy.

Similarly, soft biometric traits do not allow to perform the univocal recognition of an individual [35], but they can be used in the case of a very limited number of users, or to perform a preliminary screening of a large database, in order to save time by

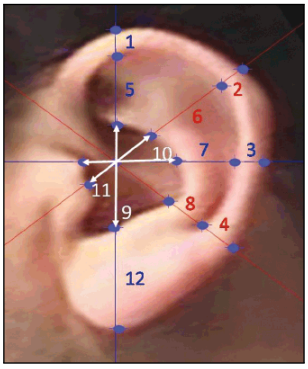

Figure 2.15: Examples of features used for the recognition of the shape of the ear [62].

Table 2.1: Characteristics of the main biometric traits.

Trait	Univ.	Uniq.	Perm.	Coll.	Perf.	Acc.	Circ.
Face	H	L	M	H	L	H	L
Fingerprint	M	H	H	M	H	M	H
Hand geometry	M	M	M	H	M	M	M
Keystrokes	L	L	L	M	L	M	M
Hand vein	M	M	M	M	M	M	H
Iris	H	H	H	M	H	L	H
Retinal scan	H	H	M	L	H	L	H
Signature	L	L	L	H	L	H	L
Voice	M	L	L	M	L	H	L
Face thermograms	H	H	L	H	M	H	H
Odor	H	H	H	L	L	M	L
DNA	H	H	H	L	H	L	L
Gait	M	L	L	H	L	H	M
Ear	M	M	H	M	M	H	M

Notes: Univ. = Universality; Uniq. = Uniqueness; Perm. = Permanence; Coll.= Collectability; Perf. = Performance; Acc. = Acceptability; Circ. = Circumvention; H = High; M = Medium; L = Low.

performing a lesser number of hard biometric comparisons. Moreover, soft biometric traits can be used for an unobtrusive, continuous authentication [65] (e.g., it is possible to monitor the user in front of a terminal by simply checking his clothes).

In order to increase the biometric recognition accuracy, multimodal or multibiometric systems can be obtained by combining the information of multiple biometric traits, multiple samples, or different recognition algorithms [34, 66, 67, 68]. Multibiometric systems can combine multiple hard biometric traits (e.g., iris and face) in situations where a very high security is critical, or can combine multiple low-accuracy traits (e.g., height and weight) in order to obtain a low-invasiveness system with an increased accuracy.

An overview of the characteristics of the main biometric traits is presented in Table 2.1.

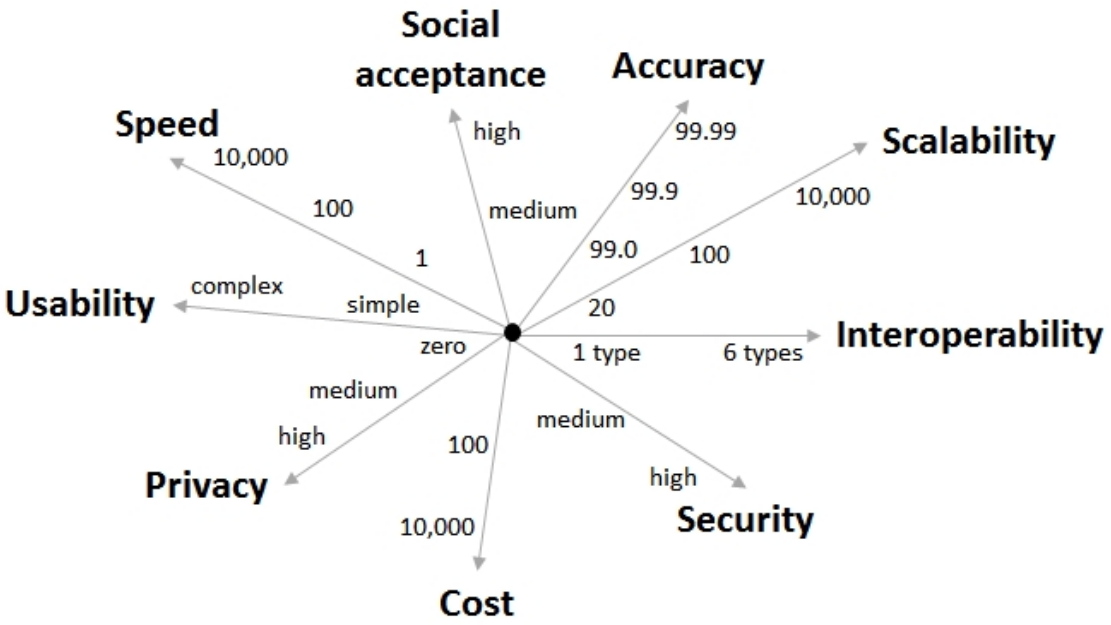

Figure 2.16: The different aspects of biometric systems.

2.4 EVALUATION OF BIOMETRIC SYSTEMS

Biometric systems can be evaluated by considering a multitude of different aspects, such as accuracy, speed, usability, cost, privacy, social acceptance, scalability, interoperability, and security (Fig. 2.16). The methods used for evaluating the different aspects belong to numerous different fields, ranging from engineering and computer science, to social sciences and economics.

In this section, the different aspects used for the evaluation of biometric systems are described, along with the different used strategies. A particular focus is placed on the methods for accuracy and privacy evaluation.

2.4.1 EVALUATION ASPECTS

Usually, accuracy metrics are the most important mean of evaluating biometric systems, and they are always used as a measure of every biometric method. However, an efficient trade-off of all the aspects is necessary in order to create a successful biometric technology. Nine different aspects can be considered:

- *Accuracy*: measures the ability of the biometric system to discriminate the individuals based on biometric trait used. Accuracy measures are described in more detail in Section 2.4.3.
- *Speed*: measures the amount of time needed to perform the enrollment, the authentication, or the identification processes. Speed is particularly important in the case of identification processes. Moreover, it is necessary to consider separately the time needed by the different steps of the biometric system. For example, a long acquisition time could result in a less usable system.

- *Usability*: measures how easy the system is to use, and how much easily people learn to use it. The usability is influenced by the acquisition time, and by the number of incorrectly captured samples. However, social and personal factors could influence the usability of the system, and surveys are often used for a better evaluation [69].

- *Cost*: measures the cost of the design, the development of the hardware system, and the implementation of the recognition algorithms. Expensive biometric systems usually have better performances with respect to cheaper ones, but a limited cost can favor a widespread diffusion of the systems.

- *Privacy*: measures the possibility that the biometric trait is stolen or misused by the biometric system. Since biometric traits cannot be changed, a biometric system must enact efficient ways to protect personal data. Privacy considerations related to biometric systems are described in more detail in Section 2.4.4.

- *Social acceptance*: refers to how the system is perceived by the users. The measure can be related to the public knowledge about the performance of the system, to the perceived privacy risks, to its invasiveness, and to its usability. Personal factors can also play an important role in determining the social acceptance of a biometric system (e.g., some people do not like to touch biometric sensors) [70].

- *Scalability*: measures the ability of the system to function efficiently as the number of enrolled users, or the number of queries to the central biometric database, increases. This aspect can be related to the chosen hardware architecture (e.g., CPU frequency, hard drive speed, network bandwidth), to the software implementation of the biometric recognition algorithms, or to the ability of the recognition algorithms to function with more templates (e.g., amount of time needed for one comparison).

- *Interoperability*: it refers to the compatibility of different biometric systems based on the same biometric trait. It can be influenced by the different types and qualities of the biometric sample (e.g., a low-cost device will produce a sample different from a high-end device), by the data format used for storing the templates, by the measure of similarity used as the output of the matching process, etc. In order to overcome this problem, biometric standards are used [71].

- *Security*: measures how much the system is robust to attacks. In particular, the robustness to fake biometric traits must be investigated in order to design an efficient biometric system. Moreover, the robustness of the computer architecture and the network infrastructure to attacks, and the robustness of processing software to malicious software must be taken into consideration.

2.4.2 EVALUATION STRATEGIES

Different evaluation strategies can be used to assess the performances and usability of the biometric systems at different stages of their design and implementation. In

particular, it is possible to divide the evaluation strategies in technology evaluations, scenario evaluations, and operational evaluations. These strategies are characterized by an increasing number of uncontrolled variables:

- *Technology evaluations*: this kind of procedure has the purpose of evaluating the performance of the biometric system, in order to measure how accurate the system is. Usually, technology evaluations are performed on standard databases of biometric samples, which are made public in order to provide a common ground for the comparison of the performances of different recognition algorithms. An example of technology evaluation is the ICB Competition on Iris Recognition [72].
- *Scenario evaluations*: consider the application of the biometric technology in a particular applicative context. In a scenario evaluation, different biometric technologies are tested in a particular applicative context. For example, biometric systems based on the iris, or on the fingerprint can be tested for the realization of a fast, accurate, access control system to critical areas. Scenario evaluations are performed using the different biometric traits from the same individuals, and usually a large number of samples is collected in order to have statistically significant results. An example of a scenario evaluation is the UK Biometric Product Testing [73]. However, scenario evaluations can be difficult to repeat completely.
- *Operational evaluations*: these evaluations are performed using the chosen biometric system operating in the real applicative scenario, and considering the real users (every user, or a subset) that will be using the biometric system. Operational evaluations are not used to measure the performance of the biometric system, but to analyze the impact on the workflow caused by the introduction of the biometric system, and the possible advantages and disadvantages. Operational evaluations are often difficult or impossible to repeat.

The three different evaluation strategies should be performed in sequence in order to successfully pass from the design phase to the actual installation of the biometric system. First, the technology evaluation should be performed in order to ensure that the biometric system has sufficient performances. Then, the scenario evaluation must be used to determine the best biometric technology for a particular situation. In the end, the operational evaluation permits to analyze the economic impacts and generate the business reports necessary for potential installations.

2.4.3 ACCURACY EVALUATION

In the literature, common figures of merit in the form of standard indexes [33] are used in order to measure the accuracy of a biometric system. These indexes can be used to describe the performance of a biometric system in a synthetic way, and to compare the results obtained by different methods. Standard databases of biometric samples are often used in order to produce results, described by indexes, that can be easily compared with other results obtained on the same database [74].

In this section, B_{ij} is used to describe the $j-th$ biometric sample pertaining to the $i-th$ individual, T_{ij} indicates the corresponding biometric template, n_i describes the

number of templates available for individual i, N indicates the number of enrolled identities, and $M(\cdot)$ represents the biometric matching function.

Matching functions can be symmetrical or asymmetrical. In particular, in symmetrical matching functions the following equation is respected:

$$M(T_{ij}, T_{kl}) = M(T_{kl}, T_{ij}) \qquad (ij) \neq (kl) \ , \tag{2.1}$$

where $M(\cdot)$ represents the matching function. In the case of asymmetrical matching functions:

$$M(T_{ij}, T_{kl}) \neq M(T_{kl}, T_{ij}) \qquad (ij) \neq (kl) \ . \tag{2.2}$$

In the literature, some accuracy measures are valid only for symmetrical matching functions [75]. However, the procedures for the accuracy evaluation described here are usable on both symmetrical and asymmetrical matching functions [76, 77].

Accuracy evaluation procedures are usually used to describe the performance of biometric systems by considering the results of the enrollment step, the identity matching step, and the decision module.

2.4.3.1 ENROLLMENT STEP

In this step, the index REJ_{ENROLL} describes the number of errors that prevent the creation and storage of a biometric template T_{ij}, using the sample B_{ij}. Possible errors can be caused by failures in the acquisition process, timeouts (the algorithms exceeds the maximum allowed time), or crashes.

In particular, the Failure to Accept Rate (FTAR) is used to describe the expected proportion of enrollment tries for which it is not possible to generate a sample with sufficient quality. Moreover, the Failure to Enroll Rate (FER) describes the expected percentage of the population for which it is not possible to generate a repeatable template [14].

2.4.3.2 IDENTITY MATCHING STEP

The procedure used to evaluate the biometric system in the identity matching step, using symmetrical matching functions, is based on matching each template T_{ij}, with the samples B_{ik}, with $j < k \leqslant n_i$. The resulting match scores are stored in the genuine match score matrix gms_{ijk}, where the term "genuine" is used to refer to matching scores obtained by matching identities pertaining to the same individual i. Then, a genuine match score matrix is computed for each individual i (Fig. 2.17a). The matrix is square, and since it is symmetrical, only the upper triangular matrix is computed.

In the case of asymmetrical matching functions, the match scores are computed by matching each template T_{ij}, with the samples B_{ik}, with $k \neq j$. For each individual, the matrix gms_{ijk} is computed. The resulting matrices are square but not symmetrical (Fig. 2.17b).

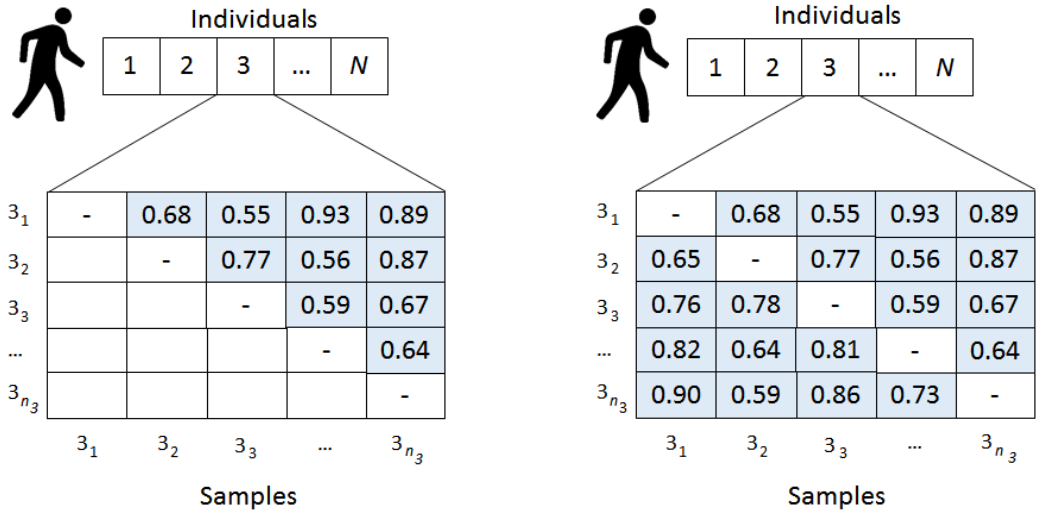

Figure 2.17: Matrices of genuine matching scores gms_{ijk} in the case of symmetrical and asymmetrical matching functions: (a) gms_{ijk} for symmetrical matching functions; (b) gms_{ijk} for asymmetrical matching functions.

It is possible to define the number of genuine recognition attempts (NGRA), in the case of symmetrical matching functions, as:

$$NGRA_{symmetric} = \frac{1}{2}\sum_{i=1}^{N} n_i(n_i - 1) \ , \tag{2.3}$$

assuming $REJ_{ENROLL} = 0$.

In the case of asymmetrical matching functions, and $REJ_{ENROLL} = 0$, the NGRA is defined as:

$$NGRA_{asymmetric} = \sum_{i=1}^{N} n_i(n_i - 1) \ . \tag{2.4}$$

Then, it is necessary to consider the match scores relative to impostor comparisons, which are the comparison of templates pertaining to different individuals. In the case of symmetrical matching functions, each template T_{i1}, relative to individual i, is matched against the first sample of the other different individuals B_{k1}, with $i < k \leqslant N$. The resulting match scores are stored in the impostor match score matrix ims_{ik}, which is square and upper triangular (Fig. 2.18a).

In the case of asymmetrical matching functions, each template T_{i1} is matched against the first sample of the other different individuals B_{k1}, with $i \neq k$. The resulting match scores are stored in the impostor match score matrix ims_{ik}, which is square but not triangular (Fig. 2.18b).

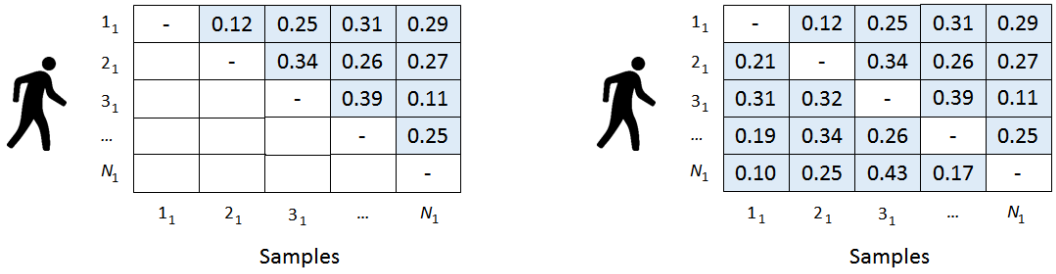

(a) **(b)**

Figure 2.18: Matrices of impostor matching scores ims_{ik} in the case of symmetrical and asymmetrical matching functions: (a) ims_{ik} for symmetrical matching functions; (b) ims_{ik} for asymmetrical matching functions.

The number of impostor recognition attempts (NIRA) in the case of symmetrical matching functions, assuming $REJ_{ENROLL} = 0$, is defined as:

$$NIRA_{symmetric} = \frac{1}{2}N(N-1) \ . \tag{2.5}$$

In the case of asymmetrical matching functions, and assuming $REJ_{ENROLL} = 0$, the NIRA is defined as:

$$NIRA_{asymmetric} = N(N-1) \ . \tag{2.6}$$

During the identity matching step there is the possibility of errors due to fails (the biometric sample cannot be processed), timeouts (the algorithms exceeds the maximum allowed time), or crashes (the algorithm crashes). These events result in missing values in the matrices gms_{ijk} and ims_{ik}, and they are respectively accumulated in the variables REJ_{NGRA} and REJ_{NIRA}.

2.4.3.3 DECISION MODULE

The computed values, relative to both genuine and impostor identity comparisons, can be used to determine the aggregate indexes that describe the accuracy of the biometric system. The accuracy indexes are computed by considering biometric systems that have multiple templates or permit multiple recognition attempts, and considering each match score as comparison of a single submitted sample against a single enrolled template.

In particular, the most important indexes are the False Match Rate (FMR(t)) and the False Non-Match Rate (FNMR(t), and they are functions of the threshold value t used in the decision module. The threshold is used to classify each match score as the result of a comparison of identities pertaining to the same individual, or to different individuals.

In particular, the FMR describes the expected probability that a sample will be incorrectly declared to match a template pertaining to a different individual (false positive),

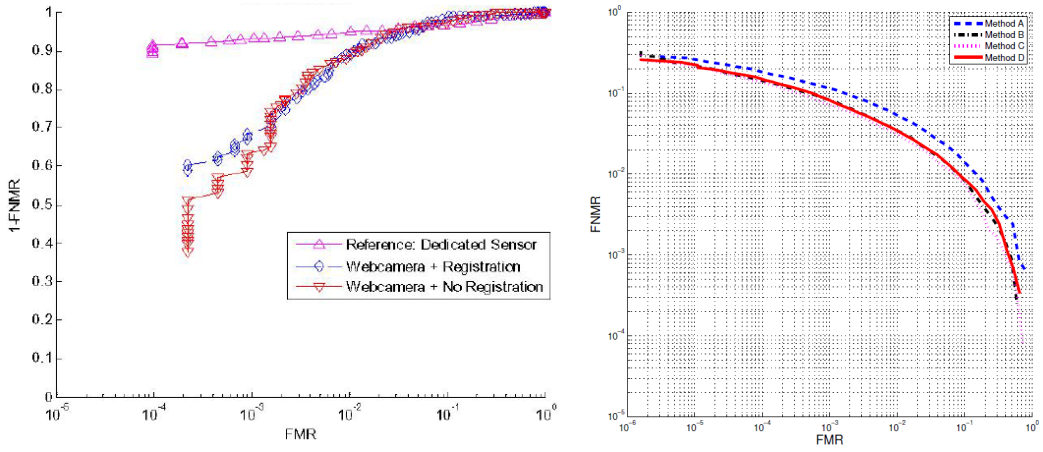

(a) **(b)**

Figure 2.19: Example of ROC and DET curves: (a) example of ROC curves [78]; example of DET curves [79].

while the FNMR describes the expected probability that a sample will be incorrectly declared not to match a template pertaining to the same individual (false negative).

The FMR and FNMR are computed by classifying each match score in ims_{ik} and gms_{ijk} with the values of the threshold ranging from 0 to 1, where 0 corresponds to the minimum possible similarity between the template and the sample, and 1 corresponds to the maximum possible similarity between the template and the sample.

The FMR and FNMR are defined as [14]:

$$\begin{aligned} FMR(t) &= \frac{card\{ims_{ik} | ims_{ik} \geqslant t\}}{NIRA} \\ FNMR(t) &= \frac{card\{gms_{ijk} | gms_{ijk} < t\}}{NGRA} + REJ_{NGRA} \ , \end{aligned} \tag{2.7}$$

where $card(\cdot)$ represent the cardinality of the set. To summarize the FMR and FNMR values, in the literature it is often used the EER value, corresponding to the threshold value t for which FMR(t) = FNMR(t).

The resulting FMR and FNMR values are usually visualized in a synthetic way by using two error plots, the Receiver Operating Curve (ROC) and the Detection Error Tradeoff (DET). Linear or logarithmic axes can used for visualization purposes.

The ROC curve shows the percentage of false negatives as a function of the percentage of false positives, according to the value of the threshold t. The ROC curve is used in the case of binary classification systems, of which biometric systems are a particular case, and is computed by plotting the FMR values on the x axis, and the (1 - FNMR) values on the y axis (Fig. 2.19a).

The DET plot is computed by plotting the FMR values on the x axis, and the FNMR values on the y axis (Fig. 2.19b).

The advantage of the ROC curves is that they allow to easily compare the accuracies of different biometric systems, since the most accurate system corresponds to the curve that remains above all the other curves for all the values of the threshold t. In the case

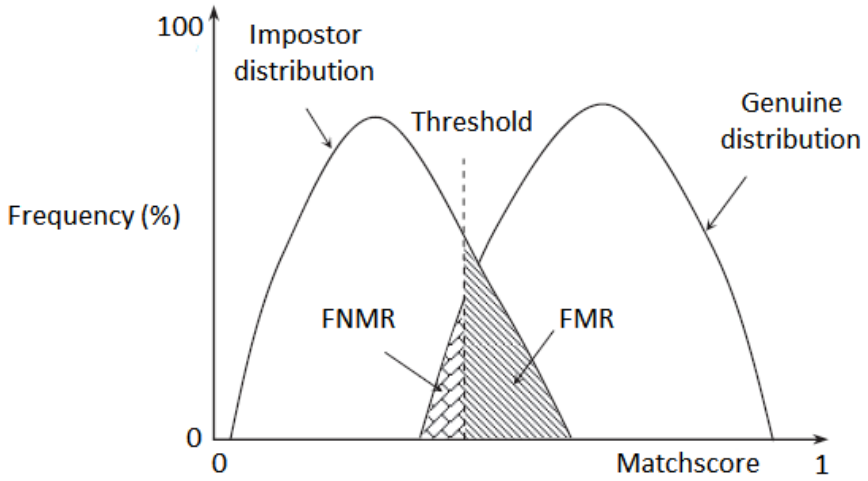

Figure 2.20: Example of score distributions for genuine and impostor matching scores.

of the DET plot, the curve corresponding to the most accurate systems remains below all the other curves for all the values of the threshold. However, in most of the cases a system has a better accuracy only in a certain region of the ROC curve, corresponding to a particular range of values of the threshold.

In order to evaluate the distribution of genuine and impostor matching scores, in most cases it is useful to plot a graph describing separately the frequency of the genuine and impostor comparisons, contained in the matrices gms_{ijk} and ims_{ik}, for each possible matching score value. In particular, if the two distributions are completely separated, a threshold value t exists that can classify the matching scores with $FMR = FNMR = 0$. An example of two genuine and impostor distributions is shown in Fig. 2.20.

Other indexes used in the literature include the False Accept Rate (FAR) and the False Reject Rate (FRR). The FAR indicates the number of times a non-authorized person is accepted as authorized, while the FRR describes the number of times an authorized person is rejected as non-authorized. These indexes are different from the FMR and FNMR because they consider also the errors in the acquisition step.

2.4.3.4 CONFIDENCE ESTIMATION

Since it is not possible to evaluate the accuracy of biometric systems on the entire human population, but limited databases must be used, it is necessary to use techniques to estimate the confidence of the performed measurements.

For this reason, two rules have been proposed in the literature [80] in order to estimate the necessary size of the testing database: the Rule of 3 [81, 82] and the Rule of 30 [83].

The Rule of 3 is used to compute the lowest error rate that can be statistically determined using N biometric comparisons. This error rate p is the error value for which

the probability of 0 errors in N trials is equally to a fixed value (usually this value is 5%). It is also possible to express the rule as:

$$p \approx \frac{3}{N} \quad \text{with 95\% confidence.} \tag{2.8}$$

For example, if a test on 300 samples yields no errors, it is possible to compute that the biometric system has an error rate $\leqslant 1\%$, with a 95% confidence.

The Rule of 30 states that, to have a 90% confidence that the true error rate of the biometric system differs no more than $\pm 30\%$ from the computed error rate, at least 30 errors must be present. For example, if there are 30 false non-match errors in 3000 genuine comparisons, there is a 90% confidence that the true error is between 0.7% and 1.3%.

Moreover, if the number of samples is sufficiently large, it is possible to evaluate the confidence of the measured accuracy by using the central limit theorem [84], which states that the error rate should follow a normal distribution. In this case, $100(1-\alpha)\,\%$ confidence bounds can be estimated by using the equation:

$$\hat{p} \pm z\left(1-\frac{\alpha}{2}\right)\sqrt{\hat{V}(\hat{p})}\ , \tag{2.9}$$

where $\hat{p}$ is the observed error rate, $\hat{V}(\hat{p})$ is the estimated variance of the observed error rate [80], and $z(\cdot)$ is the inverse of the standard normal cumulative distribution. For example, for 95 % confidence limits, the value $z(0.975)$ is equal to 1.96.

Non-parametric methods based on the bootstrap technique have also been proposed in the literature [85, 86]. These techniques do not have the need of making assumptions about the distribution of the error rate, and do not need to assume dependencies among the different attempts. In fact, the distributions and dependencies are computed by observing the used samples, in particular by using a subset of samples, obtained by sampling with replacement the original samples. Then, the extracted samples are used for the bootstrap technique, in order to estimate the distribution of the accuracy indexes, and the confidence interval values. The robustness of the bootstrap techniques is studied in several works in the literature [87, 88].

Using the bootstrap methods, it is possible to directly compute the $100(1-\alpha)\,\%$ confidence limits, which include a lower limit L and an upper limit U, in order to have only $\alpha/2$ bootstrap values lower than L, and only $\alpha/2$ bootstrap values higher than U. In the method used in [84], at least 1000 are recommended in order to have 95 % limits, and at least 5000 for 99 % limits.

A bootstrap technique that considers also a statistical correlation between the templates computed from the same biometric trait is described in [89]. In particular, the approach uses a sampling with replacement technique that extracts only certain subsets of the original data, in order to have templates pertaining to a single biometric trait or individual.

Some works are present in the literature with the purpose of estimating the confidence of the accuracy of biometric systems based on different techniques. In particular, the method described in [90] proposes a semi-parametric technique based on the mul-

tivariate copula model, in order to account for correlated biometric acquisitions. Moreover, the method describes a technique for the computation of the minimum number of samples necessary to have the confidence intervals for the ROC curve of the desired width. Another method in the literature [91] deals specifically with the confidence estimation in multibiometric systems.

2.4.4 PRIVACY AND SECURITY EVALUATION

As stated in Section 2.1, biometric systems allow to recognize individuals with a greater accuracy with respect to traditional methods. Moreover, the accuracy of biometric systems is commonly known by people, who in many cases consider the accuracy of the biometric system equal to 100 %. On one hand, this leads to a greater confidence of the users towards the system, because a recognition error is considered impossible. On the other hand, some people might believe that the acquired biometric trait could be used to track their activities and be a risk to his privacy.

In fact, while it is true that the biometric traits are more accurate and secure than traditional recognition methods, they are strictly associated to each person, and cannot be rejected or altered if a person does not wish to be recognized anymore. Moreover, if biometric data is stolen, the thief can impersonate the victim for a long time. On the other hand, passwords and smartcards can be easily changed or discarded in the case of thefts or misuses of personal data.

For this reasons, it is necessary to accurately design the biometric system considering the privacy and security risks involved in the handling of personal data, especially in the case of systems that use hard biometric traits (e.g., fingerprint, iris, or face).

The protection of the privacy must consider different aspects, such as the real and perceived risks for the users, the specificity of the application, the use of correct policies, and the used methods for the protection of sensible data [92, 93, 94, 95]. Both real and perceived risks must be considered, since a system might enforce techniques for the privacy protection, but the users could still perceive that their privacy is violated. Moreover, to ensure security it is necessary to include techniques for data verification, integrity, confidentiality, and non-repudiation.

In order to design a privacy-compliant biometric system, it is possible to distinguish three different perspectives, which consist in the risks perceived by the user, in the application context, and in the used biometric trait:

- *Risks perceived by the user*: this aspect describes the way the biometric system is perceived, in particular regarding its privacy risks. The analysis of the risks perceived by the users directly influences the acceptability of the system. The evaluation of this aspect can be difficult, since biometric systems can be perceived in a different way by different persons. Moreover, the evaluation can also fall outside the technical aspects of the biometric system. For example, most people think that biometric systems have a 100 % accuracy, or that the biometric traits can be always captured from a high distance and be used to identify them in every situation, track their activities, operate proscription lists, or be used for malicious purposes.

Table 2.2: Application contexts and privacy risks.

Lower risk	Question	Higher risk
Overt	Is the system deployed overtly or covertly?	Covert
Optional	Is the system optional or mandatory?	Mandatory
Verification	Is the system used for Identification or Verification?	Identification
Fixed Period	Is the system deployed for a fixed period of time?	Indefinite
Private Sector	Is the system deployed in the private or public sector?	Public Sector
Individual/Customer	In what role is the user interacting with the system?	Employee/Citizen
Enrollee	Who owns the biometric information?	Institution
Personal storage	Where is the biometric data stored?	Database Storage
Behavioral	What type of biometric trait is being used?	Physiological
Templates	Does the system use templates, samples or both?	Sample/Images

In some cases, biometric systems can be perceived as a dangerous to the health. For example, the infrared illuminators used in iris scanners can be erroneously regarded as a danger to the eyes.

In order to ensure a widespread distribution of the biometric system, the procedures for a correct use of the system and the real dangers must be explicitly reported, together with the methods used for protecting the privacy of personal data.

- *Application context*: the context in which the biometric system operates directly influences the privacy risks, real and perceived. A series of application contexts, and the corresponding possible privacy risks, is reported by the International Biometrics Group [96] and is shown in the Table 2.2. It is possible to observe that the privacy risk can be lower or higher according to how the system is used (e.g., identification or verification, optional or mandatory, etc.), to how the data are stored and who owns the information, and to which traits are used. Behavioral traits, in fact, can be more easily altered or not given to the biometric system.

- *The used biometric trait*: according to the biometric trait used, different privacy risks can arise. In particular, it is necessary to consider if the biometric trait can be used for identification, in covert systems, if the trait is physiological, and if the template databases are compatible. In fact, incompatible template databases can greatly limit the risk of spreading the biometric data and violating the user's privacy. On the other hand, using compatible databases allow the possibility that the biometric data collected in particular situation is used in different situations, and so the privacy risks are higher.

Biometric traits that can be used in identification systems can present more privacy risks, since the users can be recognized also against their will (e.g., by extracting a latent fingerprint). For similar reasons, covert biometric systems can pose threats to the privacy, since the users can be recognized without their knowledge (e.g., from surveillance videos).

Physiological traits are more privacy-invasive than behavioral traits, because they cannot be altered and they are more permanent.

Lastly, the more the biometric databases are compatible, the more privacy risk can arise, because the biometric templates can be used in applications different from the one where the user enrolled his trait.

By considering these aspects, it is possible to perform an assessment of the privacy and security risks involved in the biometric system. In particular, the face and fingerprint are the traits that present the most risks, while medium risks can be assigned to the systems based on the iris and the retina. The systems based on the hand geometry, the signature, the keystroke, and the voice are the ones that present the lower risks.

2.5 RESEARCH TRENDS IN BIOMETRIC RECOGNITION

Many research groups are working towards the design and implementation of enhanced biometric systems. In particular, some aspects are mostly researched:

- *Improvement of accuracy*: numerous works in the literature deal with the improvement of the recognition accuracy of the biometric systems, by using better sensors [97, 98, 99, 55, 100, 101, 102, 103] and better recognition algorithms [104, 105, 106, 107].

- *Use of multimodal and multibiometric systems*: the combined use of multiple biometric traits or multiple recognition algorithms allows to improve the accuracy and robustness of the biometric system. However, better techniques for an efficient fusion of the information are being researched [34, 66, 67].

- *Reduction of costs*: reducing the costs of the acquisition sensors is important in helping a more widespread distribution of biometric systems. For example, the sensor used to capture the iris uses infrared illuminators, and it can be very expensive [17]. For this reasons, many methods for the recognition of the iris in visible light illumination are being researched [108, 109, 110, 111].

- *Use of less-cooperative acquisition techniques*: many biometric techniques require that the subject is cooperative and willingly to give his biometric trait (e.g., the fingerprint and the iris). Methods for a less-cooperative biometric acquisition are being studied, in order to increase the speed and the usability of the biometric systems, or use the biometric traits in surveillance applications [112].

- *Increase of the distance between the trait and the sensor*: by increasing the distance needed for a correct acquisition of the biometric trait, it is possible to reduce

the perceived invasiveness of the acquisition, increase the acquisition speed, and allow the use of the biometric systems for new applications. Many works deal with the design of iris recognition systems able to work with a greater distance [113].

- *Improvement of usability and acceptance*: the design of biometric system with an increased usability, and more accepted by the general population, can result in a wider distribution and in a greater confidence towards the biometric recognition [114, 115]. The use of less-cooperative acquisition techniques, along with the increase of the distance between the trait and the sensor, can help in the improvement of the usability and acceptance.
- *Use of three-dimensional samples*: three-dimensional samples do not present the distortions caused by the perspective transformation of the biometric trait on a two-dimensional plane. Moreover, three-dimensional models can describe a wider area of the trait, which would not be possible to capture using a single image, and can also use the depth information to increase the accuracy. For example, three-dimensional models can be used in biometric applications [116] for the recognition of face [117, 101], ear [22], fingerprint [98, 103], and palmprint [97, 100].
- *Improvement of security and privacy*: as stated in Section 2.4.4, better techniques for the protection of the users' privacy and security could permit a greater distribution of biometric systems, by preventing misuses of biometric data and thus increasing the confidence of the users. However, the speed performances of security-hardened systems can decrease, and for this reasons more secure and more efficient methods for the improvement of security [118] and the protection of privacy [119] are being researched.
- *Use of new biometric traits*: new biometric traits for recognition purposes could allow to use biometric systems in different applicative contexts. For example, the electrocardiogram (ECG) [24, 120, 121] and the photoplethysmogram (PPG) [122] are recently being researched for biometric recognition.

In this thesis, the work is focused on the study of less-constrained methods for palmprint recognition. In order to achieve a less-constrained recognition, it is necessary to use less-cooperative acquisition techniques, increase the distance between the trait and the sensor, and improve the usability of the system.

2.6 SUMMARY

Biometric systems have the advantages of allowing to recognize individuals based on the characteristics of their persons, rather than using something possessed or something known. In fact, biometric traits cannot be lost or forgotten, and the risks of impersonating a different individual is highly reduced. For this reasons, biometric systems are increasingly used in several applications, especially when it is necessary to grant access to sensitive areas or resources.

Biometric systems can work in authentication mode, when it is necessary to confirm the identity stated by an individual, or in identification mode, when it is necessary to establish an unknown identity from a biometric trait. The general structure of the biometric systems is based on the five steps of acquisition, segmentation, feature extraction, identity matching, and decision.

Biometric traits can be divided into physiological, behavioral, and soft biometric traits. Physiological traits are related to the characteristics of the body of the person (e.g., fingerprint, iris, face), behavioral are related to the actions and gestures (e.g., voice, signature, keystroke), and soft biometric traits include the features that have a low distinctiveness and permanence (e.g., height, weight, age, gender).

The fingerprint is currently the most used biometric trait, since it offers a good compromise between accuracy, speed, and costs. Biometric systems based on the iris possess the greatest accuracy and speed, but have high costs and can be perceived as invasive. Face recognition systems are considered less invasive, but have a low accuracy and suffer from the differences in the acquisitions. The systems based on hand geometry are very well accepted and have low costs, but also a limited accuracy. The systems based on the palmprint or the vein pattern have a greater accuracy. Other used biometric traits include the ear shape, the retinal pattern, the facial thermography, and behavioral traits such as the gait, the voice, the signature, and the keystroke. Soft biometric traits are also used to perform continuous authentications, or combined to improve the accuracy using a multibiometric system.

In order to choose the best trait to be used in a particular situation, different aspects need to be evaluated. In particular, it is necessary to analyze the accuracy, speed, usability, cost, privacy, social acceptance, scalability, interoperability, and security of the system. The techniques for the evaluation of the accuracy, and its confidence values, are the most important and used metrics. However, the methods used to evaluate the privacy risks are important in ensuring a widespread diffusion of the biometric systems.

Currently, the research is focused on improving several aspects of the biometric systems, in order to improve their accuracy, speed, the fusion of information in multibiometric systems, the usability and acceptance, and the security and privacy techniques. Many methods investigate the possibility to use three-dimensional models in order to increase the accuracy. Moreover, several methods are being researched in order to reduce the level of cooperation needed and the costs, and to increase the distance needed between the trait and the sensor. The use of new biometric traits is also being investigated.

3

LESS-CONSTRAINED BIOMETRIC SYSTEMS

The research for less-constrained biometric systems has the purpose of designing and implementing biometric systems able to overcome the limitations in the usability of traditional systems. In particular, the goals of less-constrained systems is to perform a biometric recognition with contactless acquisitions, using less cooperation from the users, and at higher distances, in order to increase the speed, usability and acceptance of the biometric systems.

In this chapter, an overview of the less-constrained biometric systems is presented. First, the less-constrained biometric recognition is introduced. Then, the techniques for performing a contactless, less-constrained recognition are reviewed, by first describing the methods based on the traits that are traditionally acquired using the contact with the sensor (e.g., fingerprint, palmprint). Then, the innovative methods for a less-constrained recognition of the traits usually captured using a contactless acquisition (e.g., face, iris) are presented.

3.1 INTRODUCTION TO LESS-CONSTRAINED BIOMETRIC RECOGNITION

Traditionally, most biometric traits require that the user is cooperative and willing to give his trait to the sensor. Moreover, in some cases biometric acquisitions require controlled procedures, or the contact of the trait with the sensor. For example, the user must assume a certain pose, place his trait on a particular place, and remain still for the duration of the biometric acquisition.

Techniques for a less-constrained biometric recognition are being researched in order to reduce or eliminate these constraints. A less-constrained recognition could result in shorter acquisition time, a greater usability, and a greater acceptance. Moreover, more applicative scenarios would be made possible by using accurate biometric traits in a greater number of situations. For example, a less-constrained iris recognition would

permit a high recognition accuracy in surveillance applications, mobile phones, gates [123], etc.

Three main goals are the focus of the research on less-constrained biometric recognition:

- *Increasing the distance between the trait and the sensor*: increasing the distance needed for a correct biometric acquisition could increase the usability, acceptance, and speed of the system. In the case of biometric traits traditionally captured using contact-based systems (e.g., fingerprint), increasing the distance would result in the use of contactless acquisition techniques (e.g., CCD cameras instead of capacitive sensors). In the case of traits traditionally captured contactless (e.g., face, iris), increasing the distance could result in the ability to perform the biometric acquisition without the need for the user to come close to the sensor.

- *Reduction of user cooperation*: less-cooperative systems require the user less time to learn how to produce a correct acquisition, and a minor effort. This would result in a higher acceptability and acquisition speed. For example, a less-cooperative acquisition system could eliminate the need for the user to stand still during the acquisition, and capture his traits as he walks.

- *Use of uncontrolled light conditions*: the use of uncontrolled, natural light illumination can make possible a biometric recognition in a greater number of situations, and also can reduce the level of cooperation needed. If the system can work in uncontrolled light conditions, the user does not need to stand in a particular place.

However, innovative methods for capturing and processing the biometric data must be studied:

- *Adaptive acquisition systems*: if the acquisition procedure can adapt to the different situations, generating a biometric sample with a sufficient quality, the level of user cooperation is reduced, and the system can work in a greater number of situations without the intervention of an operator.

- *Adaptive preprocessing methods*: if adaptive acquisition procedures are used, it is necessary to design methods able to process the biometric samples in a high variety of situations. In fact, differences in the acquisition distance and light conditions can create high variations between the samples.

- *Innovative feature extraction and matching methods*: in most cases, less-constrained systems produce samples that are different from traditional samples. It is necessary to adopt new methods for the feature extraction and matching.

- *Compatibility of less-constrained systems with traditional systems*: it is not possible to replace the existing databases with templates computed using less-constrained systems. For this reason, it is necessary to ensure the compatibility of new templates with the existing ones.

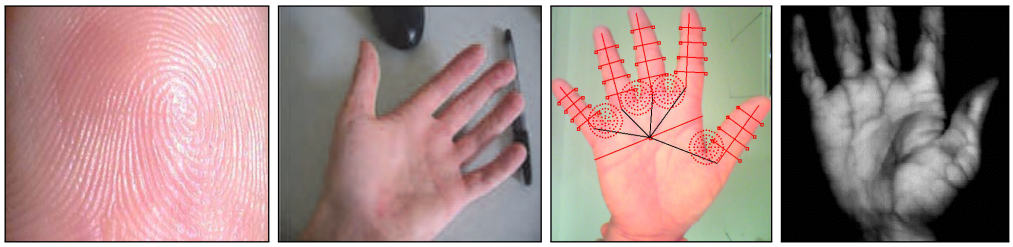

(a) (b) (c) (d)

Figure 3.1: Examples of contact-based traits, captured using less-constrained contactless acquisitions: (a) fingerprint [124]; palmprint [125]; (c) hand geometry [126]; (d) palm vein [127].

Less-constrained biometric systems are usually based on CCD cameras for the acquisition of the biometric trait. In fact, cameras are the most common mean of performing a contactless acquisition with a natural light illumination [123]. In some cases, multiple cameras can be combined to create a multi-view acquisition system, in order to increase the captured area or create three-dimensional models of the biometric trait. A greater captured area or a three-dimensional modeling of the biometric trait can increase the robustness of the recognition.

However, the design of less-constrained system is a difficult task, and the elimination of constraints inevitably leads to a reduction of the recognition accuracy. According to the biometric trait, different challenges must be considered for reducing the constraints in the case of biometric traits traditionally captured using a contact-based acquisition, and in the case of biometric traits traditionally captured in contactless way.

In the case of contact-based traits, the main goal is the design of acquisition procedures capable of capturing the trait in a contactless manner using a CCD camera, and the implementation of preprocessing methods able to extract the distinctive features from the obtained image, especially taking into account the light conditions. Currently, in less-constrained biometric systems that use traits traditionally captured using contact-based sensors, user cooperation is still required and light conditions must still be partially controlled. For example, in the case of fingerprints, the distinctive pattern is much less visible in images captured using a CCD camera, and special algorithms for its extraction must be used. Moreover, a contactless fingerprint recognition is not possible if the user is not cooperative, or if the light conditions are completely uncontrolled.

In the case of contactless traits, the research is oriented towards the design and implementation of biometric systems able to work at greater distances, with a moving or non-cooperative subject, and with uncontrolled light conditions. However, the problems caused by non-frontal poses, adverse illumination, or excessive distances are still being studied. For example, in the case of the iris, off-axis poses and reflections can seriously reduce the recognition accuracy. Moreover, if the user is too distant from the camera, the iris pattern could be unusable.

Currently, there is no complete unconstrained biometric system with an accuracy comparable to the corresponding traditional system [128]. However, promising results

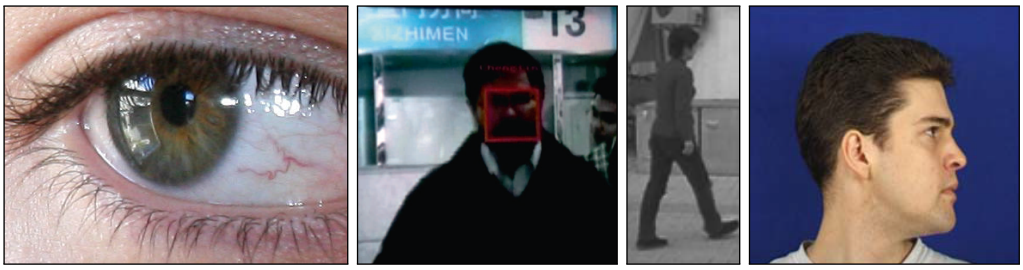

(a) (b) (c) (d)

Figure 3.2: Examples of contactless traits, captured using less-constrained acquisitions: (a) iris; face [134]; (c) gait [135]; (d) ear shape [136].

have been obtained in the fields of fingerprint [129, 103], palmprint [130], palm vein [131, 127], hand geometry [132], iris [133], face [134], gait [135], ear shape [136]. Unconstrained recognition using soft biometric traits has also been researched [39]. Some examples of less-constrained contact-based traits captured using contactless acquisitions are shown in Fig. 3.1. Some examples of contactless traits captured using less-constrained acquisitions are shown in Fig. 3.2.

3.2 CONTACTLESS RECOGNITION OF CONTACT-BASED BIOMETRIC TRAITS

This section presents the methods in the literature for the contactless recognition of the biometric traits that are traditionally captured using contact-based acquisitions. In particular, the most used contact-based biometric systems are based on the features of the hand, which include the fingerprint, the palmprint, the palm vein, and the hand geometry. Palmprint recognition systems are described in more detail in Chapter 4.

3.2.1 CONTACTLESS FINGERPRINT RECOGNITION

In the literature, several methods describe techniques for a contactless fingerprint recognition. Traditional contact-based methods, in fact, have the problems of distortions and elastic deformations caused by the contact of the finger with the sensor and by the different pressures exerted on the sensor. Moreover, different conditions of the skin can cause problems (e.g. dry/wet skin, worn-out ridges, sweat, etc.). Then, dirt and latent fingerprints are left by the contact of the finger after each acquisition, causing reductions in the accuracy or even security problems [129, 137].

Biometric systems based on fingerprints captured using contactless sensors are designed to overcome these problems, and to increase the user acceptability. Some people, in fact, are not willing to touch dirty sensors due to personal culture and fears about the transmission of diseases. Moreover, a contactless sensor could reduce the level of cooperation needed and the speed of the acquisition. Typically, contactless fingerprint systems are based on CCD cameras. However, the images captured by a CCD camera present a lower contrast, a more complex background, and the problems related to perspective effects (Fig. 3.3).

(a) (b)

Figure 3.3: Comparison of contact-based and contactless fingerprints: (a) contact-based; (b) contactless.

Contactless fingerprint systems can be divided into systems based on two-dimensional samples, and systems based on three-dimensional models. In the first case, the recognition is performed by using a single sample captured by a CCD camera. These systems have the aforementioned advantages of contactless acquisition methods, but suffer from perspective effects and have a smaller area usable for the biometric recognition [78, 138, 139, 140, 141, 142, 143, 144, 79, 145, 146, 147]. Systems based on mosaicking [148] or ring mirrors [149] have been proposed to solve these problems.

On the other hand, systems based on three-dimensional models allow to use a greater area for the recognition, and can use a metric representation of the captured data. In particular, multiple-view setups [103, 102, 129, 150, 151], photometric techniques [152], or structured light techniques [153, 98, 154] are used to reconstruct the three-dimensional model. However, specific procedures must be used in order to map the three-dimensional model on a two-dimensional image, in order to ensure the compatibility with the existing databases [155, 153, 156, 157, 158]. In the majority of the cases, a guided fingerprint placement and controlled light conditions are needed for a correct recognition. Some examples of systems used for the three-dimensional reconstruction of fingerprints are shown in Fig. 3.4.

Generally, fingerprint images captured using a contactless acquisition are not compatible with the current recognition algorithms, which use grayscale high-contrast image [159] (Fig. 3.3a). For this reason, many methods in the literature deal with the problem of enhancing the images, in order to compute a contact-equivalent acquisition [78, 160, 161, 162, 163].

3.2.2 CONTACTLESS PALM VEIN RECOGNITION

Currently, palm vein biometric recognition systems use a CCD camera, or a NIR camera for the acquisition of the vascular pattern of the hand. However, the majority of these systems require that the user places his hand on a glass support. Pegs can also be used to guide the user's hand into the correct position [131].

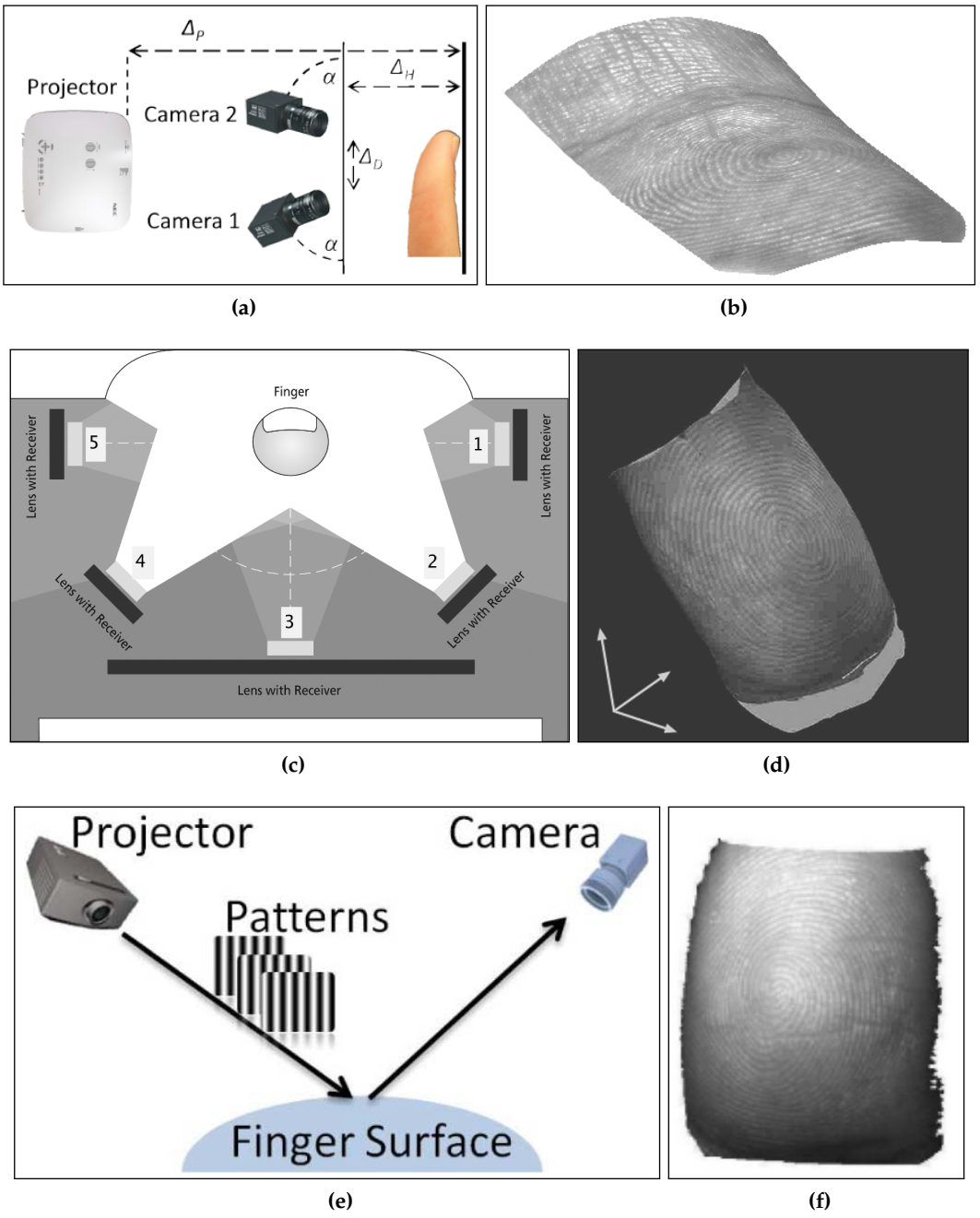

Figure 3.4: Example of three-dimensional reconstruction setup and the corresponding models: (a) two-view setup [103, 102]; (c) multiple-view setup [150]; (e) structured light illumination setup [153]; (b,d,f) corresponding models.

Similarly to the aforementioned problems for contact-based fingerprint acquisitions reported in Section 3.2.1, the contact of the hand with a support can cause problems due to different pressures, dirt, skin conditions, or latent impressions.

For this reason, contactless palm vein acquisition systems have been proposed in the literature [131, 127, 164, 165, 166, 167]. The main challenge of the contactless acquisition devices is represented by the need of performing a fast capture, in order to avoid

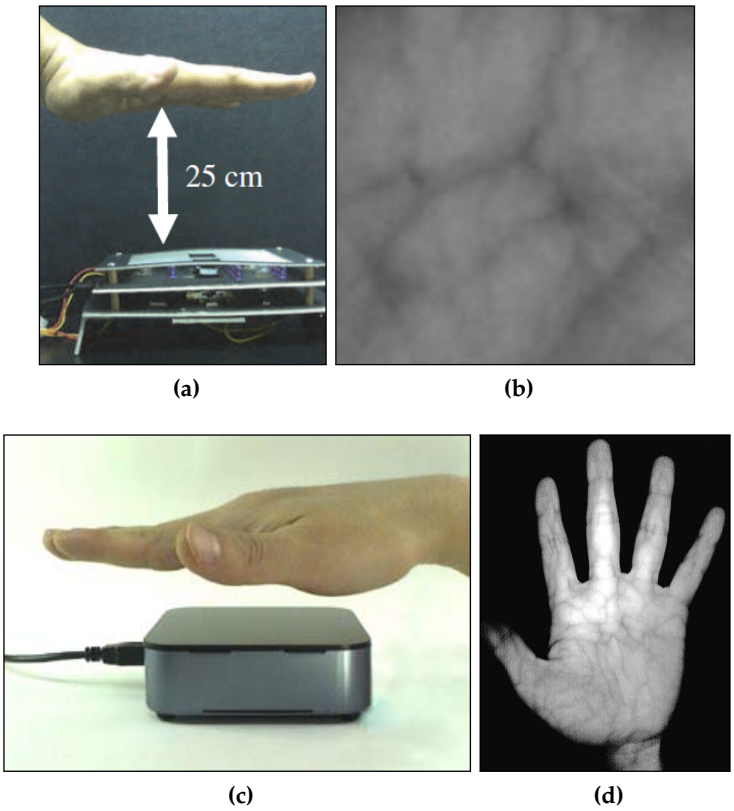

Figure 3.5: Example of contactless palm vein acquisition setups: (a) setup described in [131], (c) setup realized in [127]; (b,d) corresponding samples.

motion blur effects. Moreover, it is necessary to design the acquisition setup in order to have a sufficient depth of focus and a controlled, uniform illumination [131]. However, the position of the hand must still be partially controlled, since it must be open and oriented frontally towards the sensor. Examples of contactless palm vein setups are shown in Fig. 3.5.

3.2.3 CONTACTLESS HAND GEOMETRY RECOGNITION

Biometric systems that use a contact-based analysis of the geometry hand can be divided into two categories [20, 168]: contact-based systems that use pegs to correctly place the hand on the sensor [169, 170] and contact-based systems that do not use pegs [171]. In particular, the majority of the commercial systems fall into the first category.

However, while the systems based on the hand geometry are among the systems with a greater user acceptability, several problems limit the use of traditional contact-based system with pegs. In particular, elder people or people with impaired movements can have difficulties in placing the hand according to the placement of the pegs. Moreover, there are the problems typical of contact-based sensors, caused by dirt, sweat, or different pressures applied on the sensor.

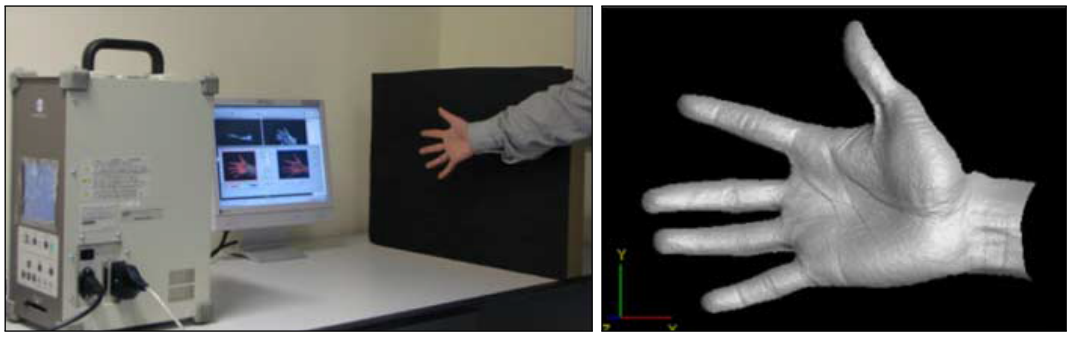

(a) (b)

Figure 3.6: Example of a laser scanner for the contactless acquisition of the three-dimensional hand geometry: (a) the laser scanner used in [168, 100, 99]; (b) the corresponding model.

For these reason, several methods have been proposed in the literature with the purpose of performing a contactless recognition based on the geometry of hand. In particular, it is possible to divide the methods in techniques that use two-dimensional samples and techniques that use three-dimensional models. The techniques based on two-dimensional samples are based on CCD cameras [172, 99, 173, 174, 126, 175], mobile phone cameras [132], or NIR cameras [176, 177].

The techniques that use three-dimensional models are based on 3D laser scanners [168, 100, 99] or structured light illumination [55, 178]. An example of a laser scanner for the contactless acquisition of the three-dimensional hand geometry is shown in Fig. 3.6.

3.3 LESS-CONSTRAINED RECOGNITION OF CONTACTLESS BIOMETRIC TRAITS

This section describes the methods in the literature that have the purpose of performing a less-constrained recognition using the biometric traits that are traditionally captured with a contactless acquisition. In particular, the techniques for a less-constrained face and iris recognition are described. Moreover, methods based on gait, ear shape, and soft biometric traits are presented.

3.3.1 LESS-CONSTRAINED FACE RECOGNITION

Face recognition systems have the characteristic of being very accepted by the users, since the face is naturally used by everyone to recognize each other. Traditionally, face recognition systems use controlled acquisitions with a high level of cooperation, and usually require the user to stand still, with a neutral expression, at a certain distance, and without covering parts of his face. In some cases, a uniform background is used. For these reason, face recognition system are usually used for access control to borders, airports, or buildings, where a trained user performs the recognition.

In fact, uncontrolled situations pose very difficult problems for biometric systems based on face recognition, since they are extremely sensitive to illumination, pose, aging, and distance [19, 134, 179]. Moreover, uncooperative subjects pose great difficulties in the recognition process. For this reasons, many methods in the literature have been proposed in order to design less-constrained face recognition systems. In particular, different methods have been especially described in order to solve (or mitigate) the problems of illumination, pose, and aging:

- *Illumination*: the variations in the illumination conditions are one of the greatest challenges in the design of less-constrained face recognition systems. Different techniques have been proposed in the literature to achieve illumination invariance, and it is possible to divide them in subspace methods, reflectance model methods, and methods based on three-dimensional models. In particular, subspace methods have the purpose of capturing the generic face space, and recognize samples that were not previously analyzed. Modified subspace methods have been proposed in order to achieve more robustness to illumination variations [180]. The methods based on a reflectance model use a Lambertian description of the reflections, by considering a varying albedo field [181]. The methods based on three-dimensional models can use the depth information to be more robust to local illumination variations, but more complex setups and algorithms are needed [182, 183].

- *Pose*: differences in the pose can cause problems to face recognition algorithms. For this reason, methods for the compensation of pose variations are described in the literature. Usually, this class of methods needs to compute the correspondences of the same points in multiple acquisitions, and estimate the positions of the common points in the three-dimensional space. For this reason, the methods based on three-dimensional models are more suited to compensate for pose variations [179, 117, 184].

- *Aging*: the aging of the subjects can be a problem both in short time intervals (e.g., bear, hair) or in long time intervals (e.g., matching the face of a kid with the face of an adult). In particular, long time intervals can be present in the case of investigative or forensic applications. For this reason, some methods have been proposed to compensate the aging by simulation of older facial features [185], or by extracting features invariant to age differences [186].

The achievement of less-constrained face recognition system could greatly increase the range of applications in which a biometric systems based on the face traits can be used. For example, applications of less-constrained face recognition could be in the fields of surveillance, for the authentication in mobile devices, or for designing advanced human-computer interfaces:

- *Surveillance applications*: the ability to perform a face recognition in unconstrained (or less-constrained) situations could be used for the recognition of individuals from surveillance footages, in an automatic way and without the subjects' knowledge. Currently, the analysis of surveillance footages is performed off-line, and

only after in the case of a particular event (e.g., the search of a wanted person). However, face recognition from surveillance videos require the design of algorithms able to work with subjects captured at a great distance, with great variations in the pose, with uncontrolled light conditions (e.g., dark images, reflections). Moreover, the subjects can be partially covering their face (e.g., hats, scarves). Some works in the literature are showing improvements in the fields of face recognition systems for surveillance applications [112, 187], also at distance greater than 15 m [188]. Automatic face indexing systems have also been proposed [189].

- *Authentication in mobile devices*: face recognition systems can be integrated in mobile phones for their authentication. However, the systems need to function with low-quality, noisy acquisitions, and strongly uncontrolled light situations. Moreover, the algorithms need to be fast in order to function correctly with low computational resources. Some works in the literature describe face recognition systems implemented in mobile devices [190].

- *Advanced human-computer interfaces*: less-constrained face recognition systems could be used for the design of advanced human-computer interfaces, such as adaptive home environments, handless control of electronic devices (e.g. personal computer, consoles, home entertainment centers), or indoor monitoring of human activities [191, 192].

Some examples of the applications of less-constrained face recognition techniques are shown in Fig. 3.7.

3.3.2 LESS-CONSTRAINED IRIS RECOGNITION

Traditionally, iris recognition techniques use very controlled acquisition procedures, require a cooperative subject, and are based on complex, expensive equipment. Moreover, the procedure is often considered invasive, and the infrared illumination is in some cases perceived (erroneously) as dangerous for the health. For these reason, biometric systems based on iris recognition have a limited diffusion, and are used only when high accuracies and speed are crucial (e.g., airports, borders, military installations).

Currently, less-constrained iris recognition techniques are being studied in order to increase the distance between the eye and the sensor, to decrease the level of cooperation needed, and to decrease the need for controlled illumination techniques. In fact, many techniques have been studied for performing the recognition of the iris at a distance, on the move, or with natural illumination.

However, the research for a less-constrained iris recognition presents several challenges. The iris region of the eye, in fact, is a relatively small area, wet, constantly moving, often presents reflections, and is occluded by eyelids and eyelashes. Even with traditional iris sensors, some trials could be necessary in order to acquire a correct sample from a non-expert user.

(a) (b)

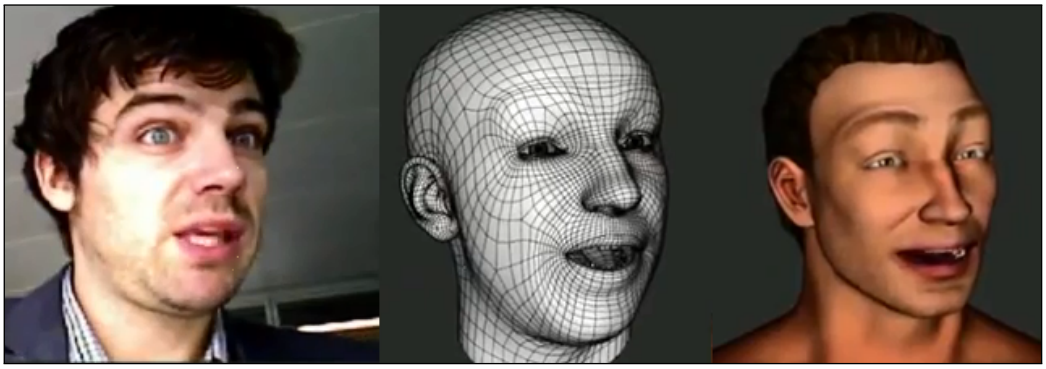

(c)

Figure 3.7: Example of applications of less-constrained face recognition: (a) surveillance [51]; (b) mobile devices [193]; (c) videogames [194].

Currently, the research is working in the improvement of the different steps that compose the iris recognition systems. In particular, innovative methods for the segmentation, the gaze assessment, and the recognition algorithms are being studied:

- *Segmentation*: the segmentation step has the purpose of locating the iris region of the eye in the captured images. This task is particularly critical in less-constrained systems, since the iris region can be small, partially occluded, or with off-axis problems [18] (Fig. 3.8). A correct segmentation is crucial and directly affects the accuracy of the iris recognition system. For these reasons, several methods in the literature deal with the problem of segmenting the iris in less-constrained acquisitions, using computational intelligence [195], active contours [196], or incremental approaches [108]. Moreover, methods based on statistical approaches [18], or more complex techniques [197, 198], are used for the segmentation of reflections and occlusions.

- *Gaze assessment*: in less-constrained iris recognition systems, there is the problem of iris acquisitions captured using a non-frontal point of view. This kind of acquisitions could reduce the accuracy of the biometric recognition, and it is necessary to design methods for the estimation of the gaze [199], or use multiple cameras in order to compensate the effect [200].

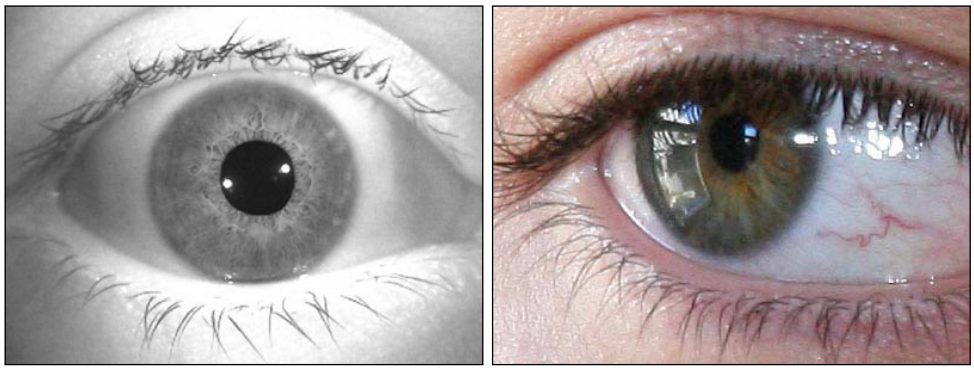

(a) (b)

Figure 3.8: Comparison of irises captured using a traditional acquisition and a less-constrained acquisition [18]: (a) traditional acquisition with infrared light; (b) less-constrained acquisition captured with natural illumination. The image (b) presents problems related to off-axis, reflections, and occlusions.

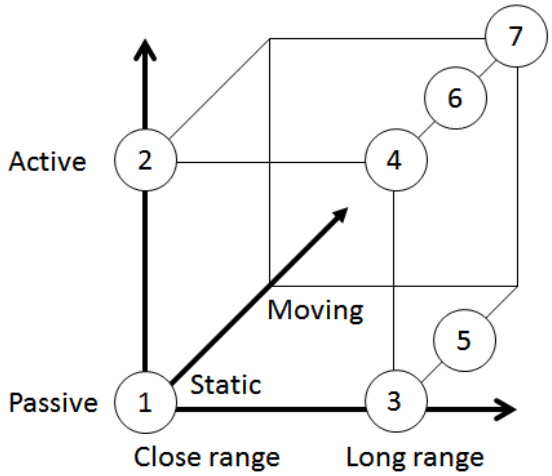

Figure 3.9: Classification of the different less-constrained iris recognition systems [202].

- *Recognition*: the images acquired in less-constrained conditions present a less visible iris pattern, with respect to images captured using a traditional constrained setup with infrared illumination. For this reason, it is necessary to design dedicated methods for the enhancement, feature extraction, and matching of iris images captured in less-constrained situations. A method for the enhancement of iris images captured using a biometric portal is described in [201]. A comparison of the matching performances of different methods, operating in different less-constrained situations, is described in [111].

It is possible to divide the iris recognition systems based on the techniques used to locate the iris in the captured image, on the distance between the user and the sensor, and on the level of cooperation required [202]. Based on the combination of these features, seven types of iris recognition systems can be defined (Fig. 3.9):

1. *Close range iris recognition*: it is the most diffused type of iris recognition, in which the eye needs to be placed at a small distance from the sensor, and the user must stand still during the acquisition.

2. *Active iris recognition*: in this type of systems, the iris is captured at a small distance, but the user does not need to stay still during the acquisition, since active cameras automatically locate the iris and adjust their position accordingly. Usually, a wide-angle camera is used for the estimation of the position of the iris, then the camera used for acquiring the iris is moved to the correct position [203].

3. *Iris recognition at a distance*: these systems are based on passive cameras capable of long-range acquisitions. However, the user must be cooperative and stay still for the time of the acquisition. Dedicated algorithms must be used to locate and process the iris from high distances [204].

4. *Active iris recognition at a distance*: with respect to the methods that perform the iris recognition at a distance, this typology of systems use also active cameras, which allow to autonomously locate the iris and reduce the level of cooperation needed. However, the user needs to be standing still during the acquisition [205].

5. *Passive iris recognition on the move*: in this type of systems, the iris is captured as the user moves. However, the walking paths must be controlled and the cooperation of the user is needed. Examples of these systems are the iris recognition systems installed on gates. A system composed of multiple passive cameras for the iris recognition on the move is described in [113].

6. *Active iris recognition on the move*: in these systems, active cameras are used to automatically locate the iris of people moving in front of the camera. With respect to passive systems that perform the iris recognition on the move, these systems can reduce the level of cooperation needed. However, no example of this kind of system is present in the literature.

7. *Active iris recognition for surveillance*: in surveillance applications, iris recognitions would be performed in a complete unconstrained way, using a network of active cameras, capable of locating and extracting the iris of individuals walking in non-predetermined paths. This kind of system is not yet designed, and its design would open iris recognition systems to a wider range of applications.

Some examples of the described categories are shown in Fig. 3.10.

3.3.3 LESS-CONSTRAINED GAIT RECOGNITION

Biometric systems based on gait use frame sequences captured with CCD cameras in order to perform the recognition [26]. Currently, gait recognition methods require little cooperation by the users, are non-intrusive, and can work at distances up to tens of meters. However, some works in the literature have been proposed with the purpose of designing gait recognition systems that can be even less-constrained, for example by

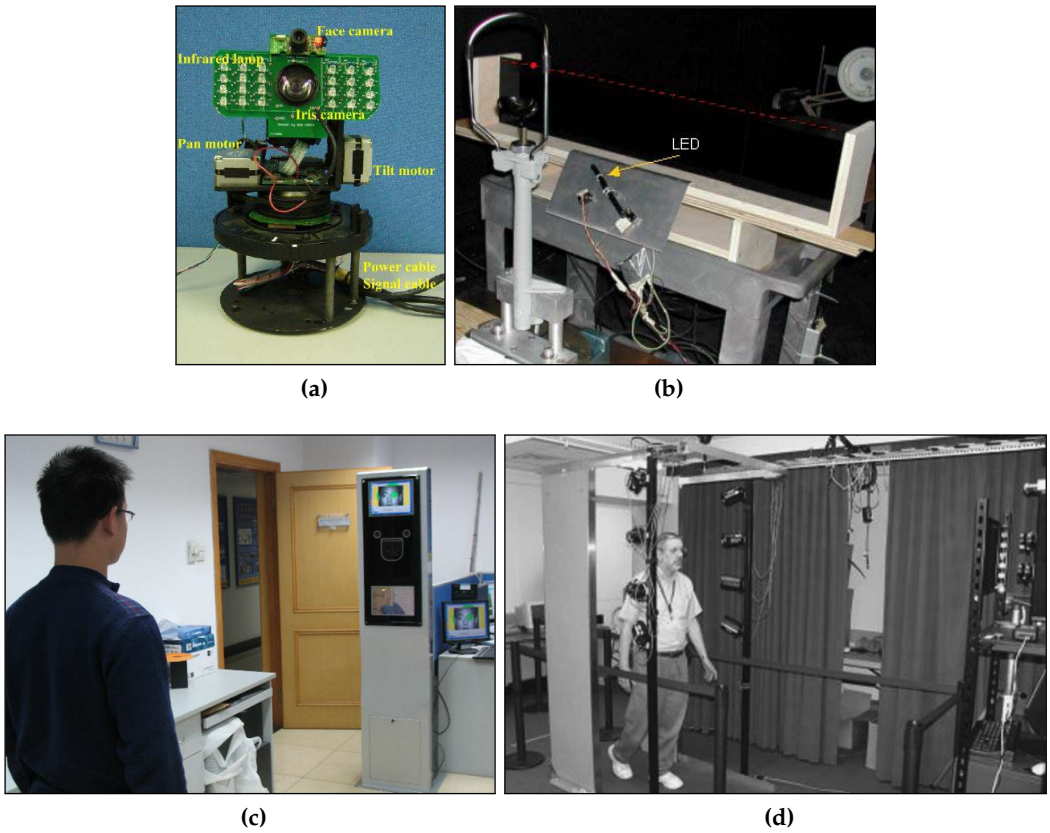

Figure 3.10: Example of less-constrained iris recognition systems: (a) active iris recognition [203]; (b) iris recognition at a distance [204]; (c) active iris recognition at a distance [205]; (d) passive iris recognition on the move [113].

achieving the pose invariance [135], or by performing the recognition at great distances [206].

3.3.4 LESS-CONSTRAINED EAR SHAPE RECOGNITION

Biometric systems based on the ear shape currently represent a non-intrusive means of recognition, able of working at great distances and with low quality images [22]. However, some studies have been recently proposed in order to achieve a complete unconstrained ear shape recognition [136], even in the case of moving subjects [207].

3.3.5 LESS-CONSTRAINED SOFT BIOMETRIC RECOGNITION

Soft biometric traits are particularly suited to be used for a less-constrained recognition. While they cannot be used to perform a strong biometric recognition, since their lack of distinctiveness, it is possible to capture them from uncooperative subjects, using unobtrusive methods, and at great distances [35, 39, 34]. In particular, soft biometric traits can be used where it is not possible to use stronger biometric recognition methods (e.g., surveillance applications), the number of user to be recognized is sufficiently

small, or a high accuracy is not necessary (e.g., applications that use a continuous authentication).

The method described in [40] is used in surveillance applications, and uses the information of gender and race in order to act as a preliminary screening for different biometric recognition methods. The deployment of a multi-camera network is proposed in [36] in order to recognize individuals using their color and height information. The method described in [39] uses the color information, and the height information divided into three parts (head, torso, legs). Gait, height, size, and gender are used in combination in the work described in [208]. A method designed for the unconstrained estimation of the weight of walking individuals is described in [38]. In particular, the techniques for weight estimation can be particularly useful in aid to forensic applications, since in many cases the weight of a person can be inferred from the analysis of a scene. A biometric system for a continuous authentication is proposed in [65], and uses the information related to the face and to the clothes.

3.4 SUMMARY

Less-constrained biometric systems have the purpose of overcoming the limitations of traditional biometric systems, which in most cases require high levels of cooperation, controlled situations, and constraints on the user placement. Less-constrained biometric systems have the purpose of performing the recognition of the individuals with the less possible degree of cooperation, control, and number of constraints. In order to achieve these goals, it is necessary to develop advanced techniques for the adaptive acquisitions and preprocessing of biometric samples. Moreover, innovative biometric features must be defined. However, the compatibility with existing systems must be ensured.

Currently, less-constrained systems have a lower accuracy with respect to traditional biometric systems. Moreover, the research for less-constrained systems has different challenges in the case of traditional contact-based traits, and in the case of contactless traits. In the first case, it is necessary to develop techniques for a biometric acquisition and processing using images captured using a CCD camera. Less-constrained systems for a contactless fingerprint, palmprint, hand geometry, and palm vein have been proposed in the literature. In the second case, it is necessary to design techniques in order to correctly acquire the biometric traits at higher distances, with less user cooperation, or with uncontrolled light conditions. In this context, less-constrained systems for face, iris, gait, ear shape, and soft biometric traits have been reviewed.

4

PALMPRINT BIOMETRICS

Palmprint recognition is a relatively recent technology, which has been increasingly investigated over the past fifteen years. Palmprint recognition has many points in common with biometric systems based on the fingerprint trait, and the research in the field of palmprint recognition spread rapidly due to the experience maturated for the recognition of fingerprints. As fingerprints, palmprints present many distinctive features and can be used for a highly accurate biometric recognition. However, on the contrary to fingerprints, palmprints feature a greater user acceptability, low-cost acquisition devices, and the possibility to extract biometric samples even from elder people or manual workers. Moreover, numerous kinds of features, at different levels of details, can be extracted according to the type of acquisition used.

Traditionally, contact-based acquisition systems are used for capturing palmprint samples. In some cases, physical constraints are used in order to guide the placement of the hand. However, physical constraints can pose difficulties in the case of elder people, and contact-based systems have the problems of dirt, sweat, latent impressions, or cultural factors. For these reasons, the research is currently oriented towards the use of contactless and less-constrained acquisition systems.

In this chapter, the state of the art of palmprint recognition systems is described. After an introduction on palmprint recognition and an overview of its main advantages, a survey of the possible applications of palmprint recognition is presented. Then, the biometric systems based on the palmprint are introduced: first, the contact-based methods are reviewed, then the contactless methods for the palmprint recognition are described. In both cases, the methods that use two-dimensional samples and the methods that use three-dimensional models are considered. The techniques used for the quality estimation of palmprint samples and their classification are reviewed, and the methods used for generating synthetic palmprint samples are introduced.

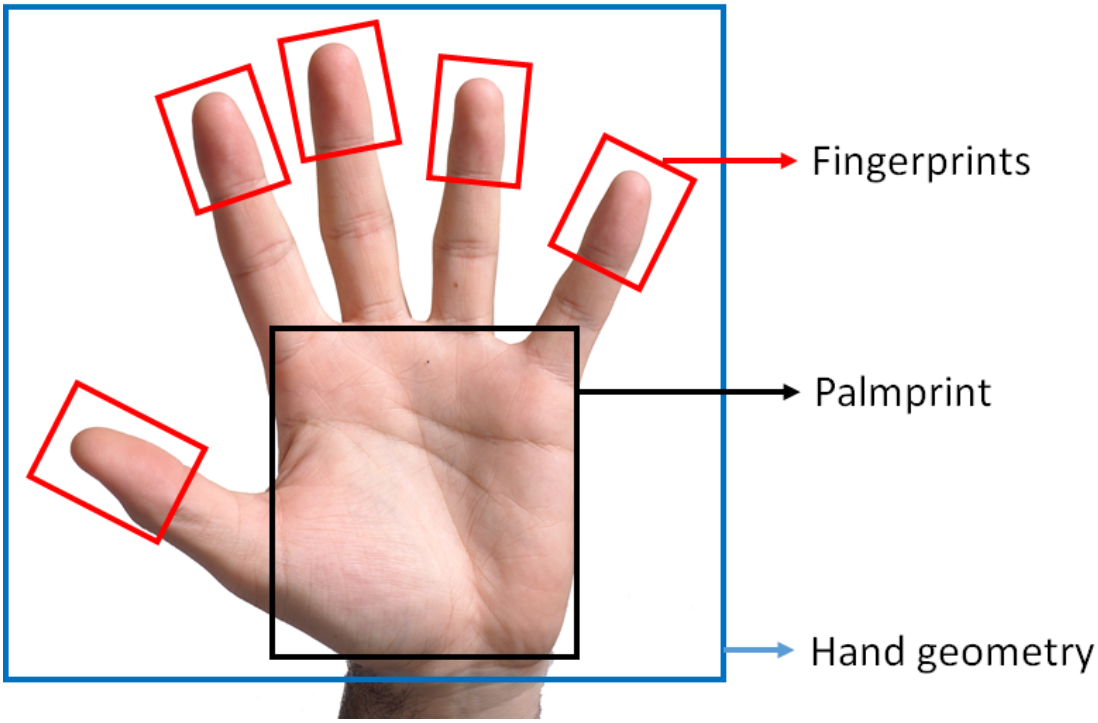

Figure 4.1: Schematic overview of the biometric traits of the hand according to the size of the analyzed area.

4.1 INTRODUCTION TO PALMPRINT RECOGNITION

Palmprint recognition systems are a particular category of hand-based biometric systems, which focus on the area of the hand from the wrist to the base of the fingers. A schematic overview of the biometrics traits of the hand, according to the size of the analyzed area, is shown in Fig. 4.1. In particular, palmprint-based systems analyze the skin that covers the inner surface of the hand, which is of the same type of the skin that covers the fingerprints.

The palmprint area is covered by three principal lines (or flexion creases), several wrinkles (or secondary creases), and a series of ridges (similar to the ones that compose the fingerprints) covering the entire palm area. Moreover, the ridges create several features similar to the ones found in fingerprints, such as singular points and minutiae.

It has been studied that the principal lines and the major wrinkles are formed between the third and fifth month of pregnancy [209], while the other lines appear only after the birth. Moreover, the three principal lines are dependent on genetic information, while the other lines are not [210]. Different relationship have been established between palmprint features and genetic diseases [211]. Like in the case of fingerprints, also identical twins possess different palmprint features [210].

Palmprints can be analyzed at different levels of details, starting from a high-detail analysis of the minutiae and ridges, to the analysis of texture information captured using low-resolution images, making it possible to perform an accurate recognition

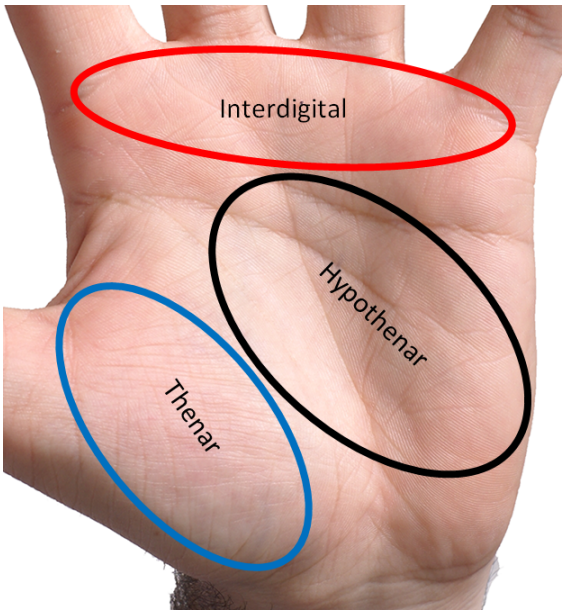

Figure 4.2: The different regions of the palm.

even using low-cost hardware and at distances higher than the ones possible for the recognition of fingerprints.

Moreover, it is possible to divide the palm area in three zones: the thenar, hypothenar, and interdigital zones [212] (Fig. 4.2). In particular, some works in the literature are proposed especially for the biometric recognition of the individuals using the thenar area of the palmprint [213, 214, 215].

In this section, the main palmprint features are described, then the structure of the biometric systems based on the palmprint is presented. Then, the approaches used for classifying the various methods in the literature are detailed.

4.1.1 PALMPRINT FEATURES

It is possible to divide the features used for the palmprint recognition in five categories, according to the level of detail used in analyzing the palmprint images [217]:

- *Geometry features*: they comprehend the features related to the geometrical shape of the palm, for example its width, length, and area (Fig. 4.3a). In some cases, this kind of features is considered as part of the features related to the hand geometry, and not typical of the palmprint itself.

- *Principal line features*: there are three principal lines (or flexion creases) on the palm of every hand, important for palmprint recognition since they feature a high distinctivity and permanence (Fig. 4.3a). In particular, four different principal palm lines can be defined, namely the heart line, the head line, the life line, and the fate line (Fig. 4.4).

- *Wrinkle features*: they can be considered also as secondary lines (or secondary creases), and they are distinctive since they are highly irregular (Fig. 4.3a).

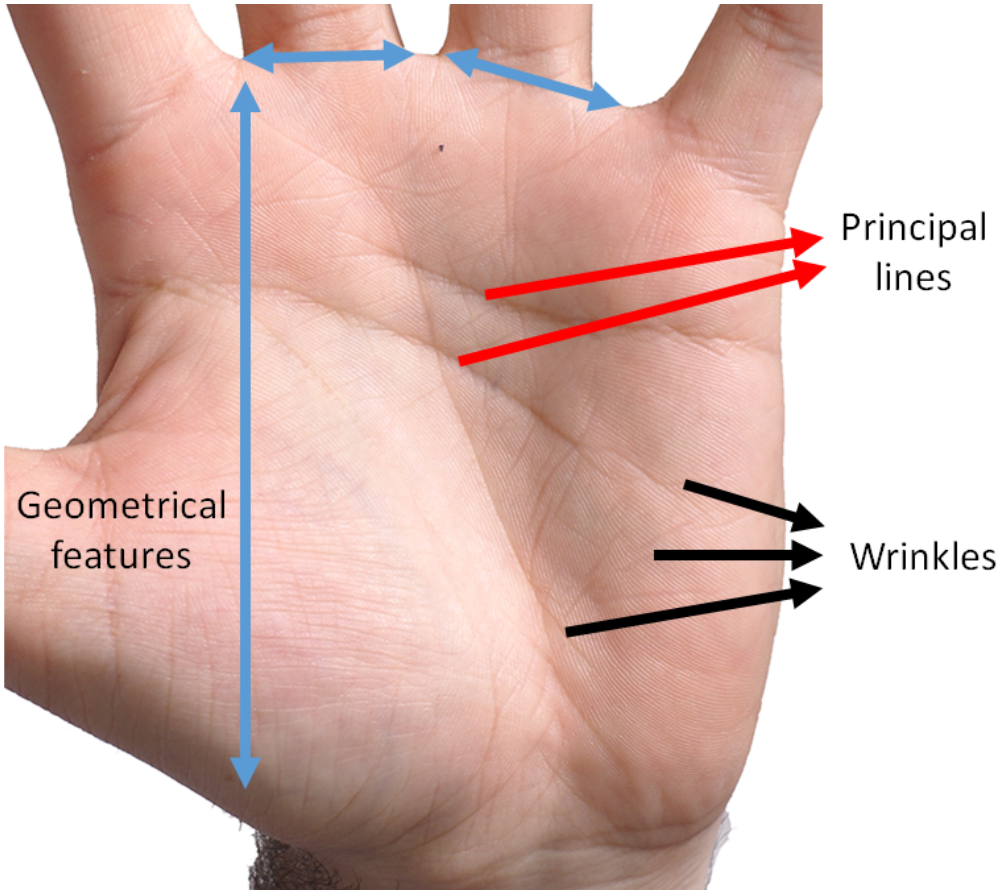

(a)

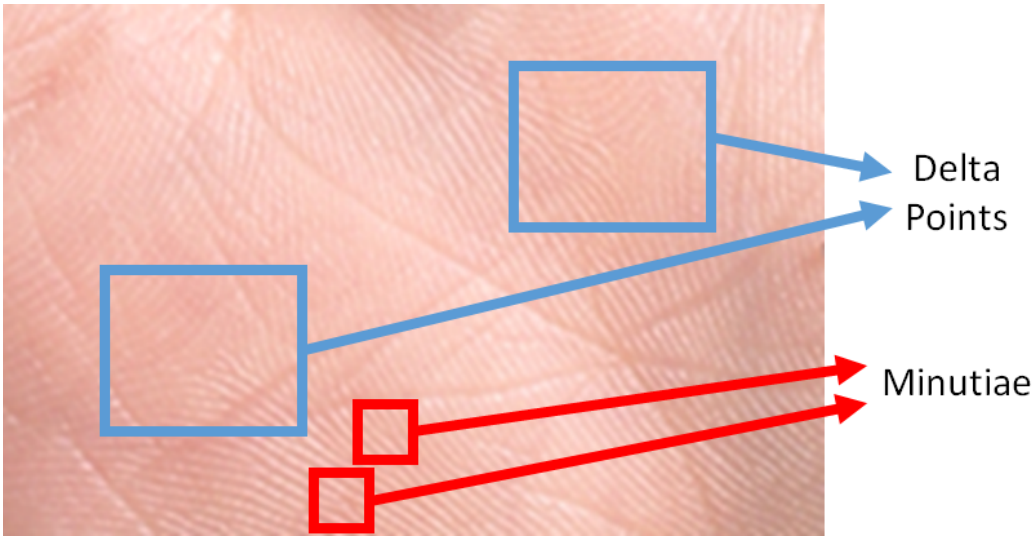

(b)

Figure 4.3: Different features of the palmprint, according to the level of detail: (a) Geometry features, principal line features, and wrinkle features; (b) Delta point features and minutiae features.

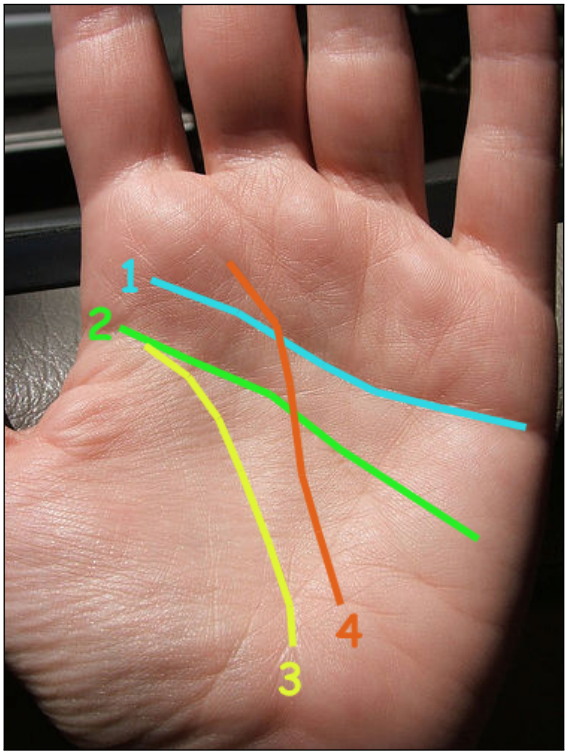

Figure 4.4: The four principal palm lines [216]: (1) the heart line; (2) the head line; (3) the life line; (4) the fate line (not always present).

- *Delta point features*: they are similar to the delta points extracted from fingerprints, and they correspond to the points where the local ridge orientation is similar to the Greek letter Δ (Delta) (Fig. 4.3b).
- *Minutiae features*: correspond to the points where the ridges of the palmprint merge, bifurcate, end, or start (Fig. 4.3b).

According to the level of detail, it is possible to use images captured with a resolution ranging from 150 dpi or less, up to 400 dpi or more [16]. Some palmprint recognition systems use high resolution images in order to capture the details of the ridges and the minutiae [218, 219]. High resolution images are often used for forensic applications [220, 58]. However, the majority of the research is currently oriented towards the use of low-resolution images for civil and commercial applications.

Recently, several methods that use the three-dimensional structure of the palmprint, in order to perform the recognition, have been proposed. In particular, the information related to three-dimensional depth of the palmprint features is difficult to fake, and is more robust to spoofing attacks [221]. An example of a three-dimensional model of a palmprint is shown in Fig. 4.5.

Table 4.1 summarizes the features used for palmprint recognition, the resolution of the imaging device needed to collect them, their collectability, permanence, distinctiveness, the possibility of circumvention, and their ability to be extracted from latent impressions [221].

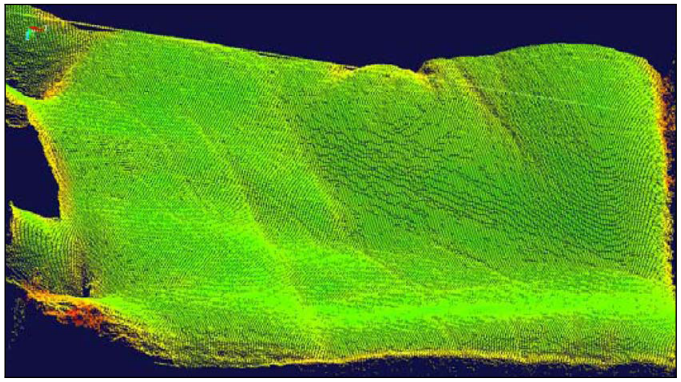

Figure 4.5: Example of a three-dimensional model of a palmprint [222].

Table 4.1: Characteristics of the features used for palmprint recognition [221].

Feature	Res.	Coll.	Perm.	Dist.	Circ.	Latent impr.
Geometry features	L	H	H	L	H	N
Principal line features	L	H	H	L	H	N
Wrinkle features	M	H	M	H	H	N
Delta point features	H	M	H	M	M	Y
Minutiae features	H	M	H	H	M	Y
3D structure features	M	L	M	M	M	N

Notes: Res. = Resolution; Coll. = Collectability; Perm. = Permanence; Dist. = Distinctiveness; Circ. = Possibility of circumvention; Latent impr. = Possibility to be extracted from latent impressions; H = High; M = Medium; L = Low; Y = Yes; N = No.

4.1.2 STRUCTURE OF PALMPRINT RECOGNITION SYSTEM

According to the definition of the modalities of biometric systems defined in Section 2.2, palmprint recognition systems can be used both in the authentication and in identification modalities [217]. In particular, methods for optimizing the performances of systems working in the identification modality have been presented [223, 224].

Moreover, palmprint recognition systems follow the general structure of biometric systems described in Section 2.2, and can be divided into the following steps [217]:

1. *Acquisition*: the techniques used for the acquisition of palmprint samples can be divided into offline or online techniques. Offline acquisition techniques include rolled inked acquisitions and forensic methods for the extraction of latent palmprints. Online acquisition techniques can be based on optical devices, digital scanners, CCD (or CMOS) cameras, or video cameras. CCD-based and video-based techniques can require the contact of the palmprint with a surface, or use contactless acquisition methods. Structured light illumination systems, based on a DLP projector and a CCD camera, are also used in order to capture the three-dimensional model of the palmprint.

2. *Segmentation and registration*: the methods for the segmentation and registration of palmprint samples usually binarize the input image in order to extract the

contour of the hand, then detect some keypoints which are used to align the images. Usually, the spaces between the fingers are used as reference points. Then, a reference coordinate system is adjusted using the extracted keypoints, and the central part of the hand (the actual palmprint) is extracted.

3. *Image enhancement*: different image enhancement procedures have been proposed, according to which features are used to perform the recognition. The image enhancement algorithms used for palmprint recognition include edge detectors (e.g., Canny, Sobel, derivative, or ad-hoc edge detectors), Hough transform, wavelet transforms, Fourier transform, and Gabor filters.

4. *Feature extraction*: the features used for palmprint recognition can include the edges corresponding to the principal and secondary lines, their magnitude and orientation, the coefficients of the used transform function (e.g., Hough, wavelet, Fourier), the magnitude and orientation of the filter response (e.g., magnitude of Gabor-filtered image), texture descriptors (e.g., Local Binary Pattern), statistical measures, or the position of certain points of interest (e.g., Delta points, minutiae). Some methods use feature extraction methods based on Principal Component Analysis (PCA), Linear Discriminant Analysis (LDA), or Independent Component Analysis (ICA).

5. *Matching*: matching functions include the Euclidean distance between the feature vectors, Artificial Neural Networks, Support Vector Machines (SVM), the Root Mean Square distance, or the Hamming distance.

4.1.3 CLASSIFICATION OF PALMPRINT RECOGNITION APPROACHES

It is possible to classify the palmprint recognition methods according to the techniques used to extract and match the features, or according to the type of acquisition device used.

In the literature, the most used classification is the one performed according to the techniques used to extract and match the features [16]. In particular, it is possible to distinguish ridge-based, line-based, subspace-based, statistical, or coding-based approaches:

1. *Ridge-based approaches*: these approaches use the pattern of the ridges, the position of the Delta points, and the location of the minutiae in order to perform the recognition. These methods are derived from the methods used for contact-based fingerprint recognition, and they are traditionally adopted in the case of offline palmprint acquisitions, or palmprints captured using an optical device.

2. *Line-based approaches*: these methods focus on the extraction of the lines of the palmprint, principal or secondary, in order to perform the recognition. They are traditionally based on the use of edge detectors to extract the lines. The extracted lines are matched according to their position, direction, or by using edge descriptors.

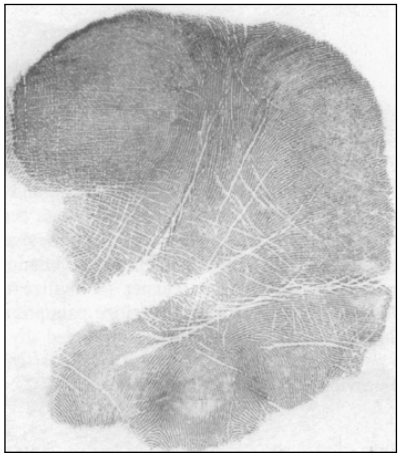

Figure 4.6: Example of an inked palmprint acquisition [225].

3. *Subspace-based approaches*: these approaches use feature extraction methods such as the PCA, LDA, or ICA. The feature extraction is performed directly on the input sample, or on the image obtained after performing a transformation using wavelets, Fourier transform, kernels, or Gabor filtering. The subspace coefficients are considered as features, and different distance measures can be used to classify the extracted features.

4. *Statistical approaches*: statistical methods can be divided into methods based on local statistics or methods based on global statistics. In the first case, the image is divided into several subregions, and local statistics (e.g., mean and variance) are computed on each region, and considered as features. In the second case, global statistics are computed directly on the entire image. Image transformations (e.g., wavelets, Gabor filters, Fourier transform) can be applied. Several distance measures can be used for the classification.

5. *Coding-based approaches*: these methods perform a preliminary filtering of the image, then encode the result by quantizing the magnitude or the phase of the response. The most diffused coding-based methods are based on the PalmCode and its derivatives, and use a Gabor filtering procedure on the input image, then encode the phase information as a bit string. The Hamming distance is used to compute the similarity of the templates.

It is possible to divide the palmprint recognition approaches also based on the type of the acquisition device used to capture the samples. In particular, four categories can be defined, according to the type of contact needed (contact-based or contactless), and on the type of sample used (two-dimensional or three-dimensional):

1. *Contact-based two-dimensional methods*: these methods can be divided into offline and online methods. In particular, offline methods include the scanning of inked palmprints (Fig. 4.6), and the lifting of latent impressions (Fig. 4.7).

   Online methods use an acquisition device that requires the user to place the hand on a fixed support, in order to capture a two-dimensional sample of the

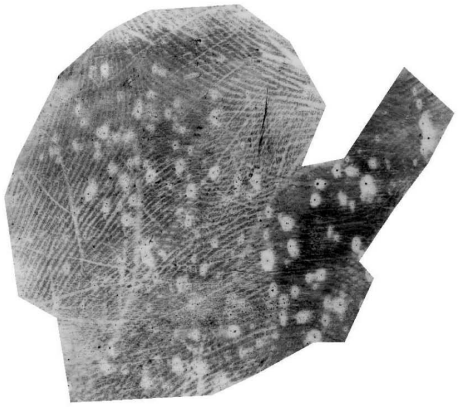

Figure 4.7: Example of a latent palmprint [212].

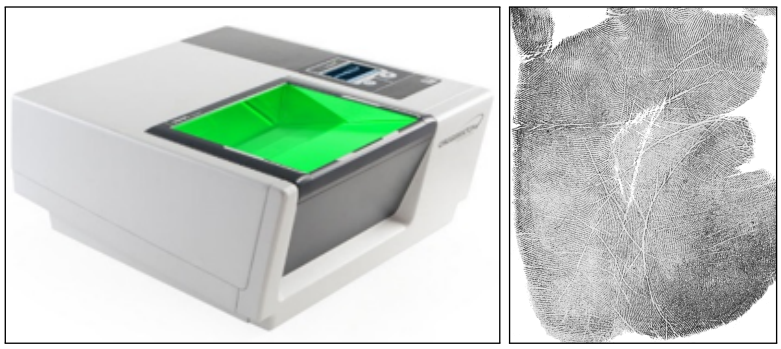

(a) **(b)**

Figure 4.8: Example of an optical device for contact-based, two-dimensional palmprint acquisitions [58]: (a) the device; (b) the corresponding sample.

palmprint. This category includes the methods based on optical devices (Fig. 4.8), digital scanners (Fig. 4.9), and CCD-based devices (Fig. 4.10).

2. *Contact-based three-dimensional methods*: these methods use an acquisition device that requires the user to place the hand on a fixed support. Then, structured light illumination techniques are used to reconstruct the three-dimensional model of the palmprint (Fig. 4.11). In most cases, a two-dimensional sample is captured as well.

3. *Contactless two-dimensional methods*: the methods that use a contactless two-dimensional acquisition are based on CCD cameras (Fig. 4.12), smartphone cameras, or video cameras. These methods can be used to design a low-cost, less-constrained palmprint recognition.

4. *Contactless three-dimensional methods*: currently, the methods based on the reconstruction of a three-dimensional model of the palmprint using a contactless acquisition are based on 3D laser scanners (Fig. 4.13). These methods permit an accurate, less-constrained palmprint recognition. However, the cost of the acquisition devices is high.

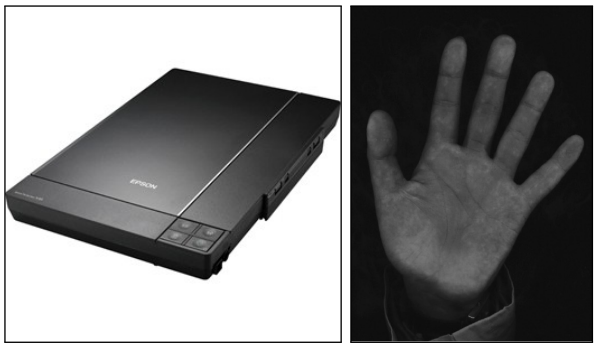

(a) (b)

Figure 4.9: Example of a digital scanner for contact-based, two-dimensional palmprint acquisitions: (a) a digital flatbed scanner [59]; (b) a sample captured with a flatbed scanner [226].

(a) (b)

Figure 4.10: Example of a CCD-based device for contact-based, two-dimensional palmprint acquisitions [217]: (a) the device; (b) the corresponding sample.

A taxonomy of the methods based on the type of the acquisition device used is shown in Fig. 4.14.

Offline palmprint recognition methods, based on two-dimensional samples, are usually used for investigative and forensic applications, and are not suited for real-time applications.

Online palmprint recognition methods based on contact-based, two-dimensional CCD acquisition devices offer good quality samples, and short acquisition times. For this reason, they can be used for real-time applications. Moreover, with respect to optical devices, they can offer a greater number of details, and at minor resolutions. Contact-based CCD acquisition devices usually use pegs in order to constraint the user's hand in a particular position [225]. However, the presence of pegs can be a problem in the case of elder people, or people with muscular or joint problems (e.g., arthritis).

For these reasons, some methods use pegless CCD-based acquisition devices [229], or are based on digital scanners [230]. In particular, palmprint recognition systems based on digital scanners can be realized with a low cost equipment (e.g., off-the-

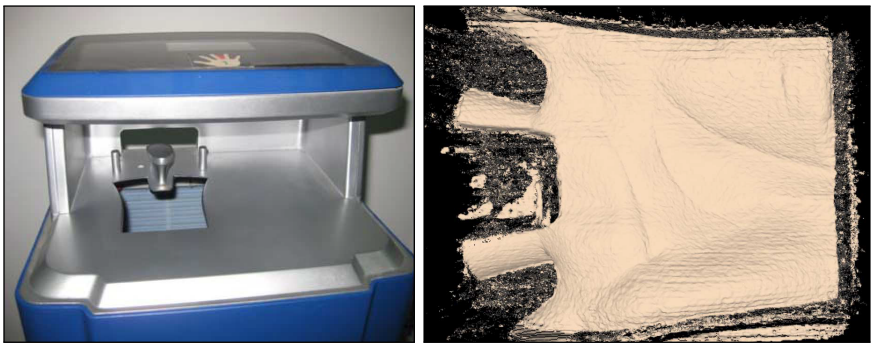

(a) (b)

Figure 4.11: Example of a structured light illumination device for contact-based, three-dimensional palmprint acquisitions [227]: (a) the device; (b) the corresponding sample.

(a) (b)

Figure 4.12: Example of a CCD camera for contactless, two-dimensional palmprint acquisitions [228]: (a) the device; (b) the corresponding sample.

shelf scanners), but they require a long scanning time and are not suited for real-time applications.

Recently, three-dimensional contact-based methods were developed in order to increase the recognition accuracy and the robustness to lighting, occlusions, noise, and spoofing attacks [97], with respect to two-dimensional CCD acquisition devices.

However, all contact-based methods have the problem of distortion, dirt, sweat, and possible problems of user acceptability. In fact, some people might have problems in touching a sensor that has been touched by the hands of other people. In many cases, in fact, hands can be dirty or sweaty.

For these reasons, contactless acquisition devices have been studied [231]. However, contactless methods might have the problems of a lower contrast, a more complex background, non-uniform acquisition distances, and they are sensible to lighting conditions.

In order to overcome these problems and achieve a greater accuracy, three-dimensional contactless methods [100] have been proposed. In particular, three-dimensional contactless systems are more robust to different acquisition distances, lighting condi-

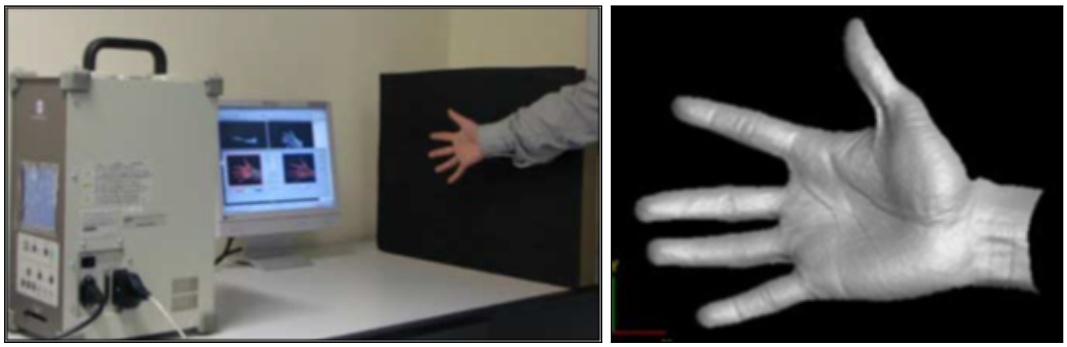

(a) (b)

Figure 4.13: Example of a 3D laser scanner for contactless, three-dimensional palmprint acquisitions [100]: (a) the device; (b) the corresponding sample.

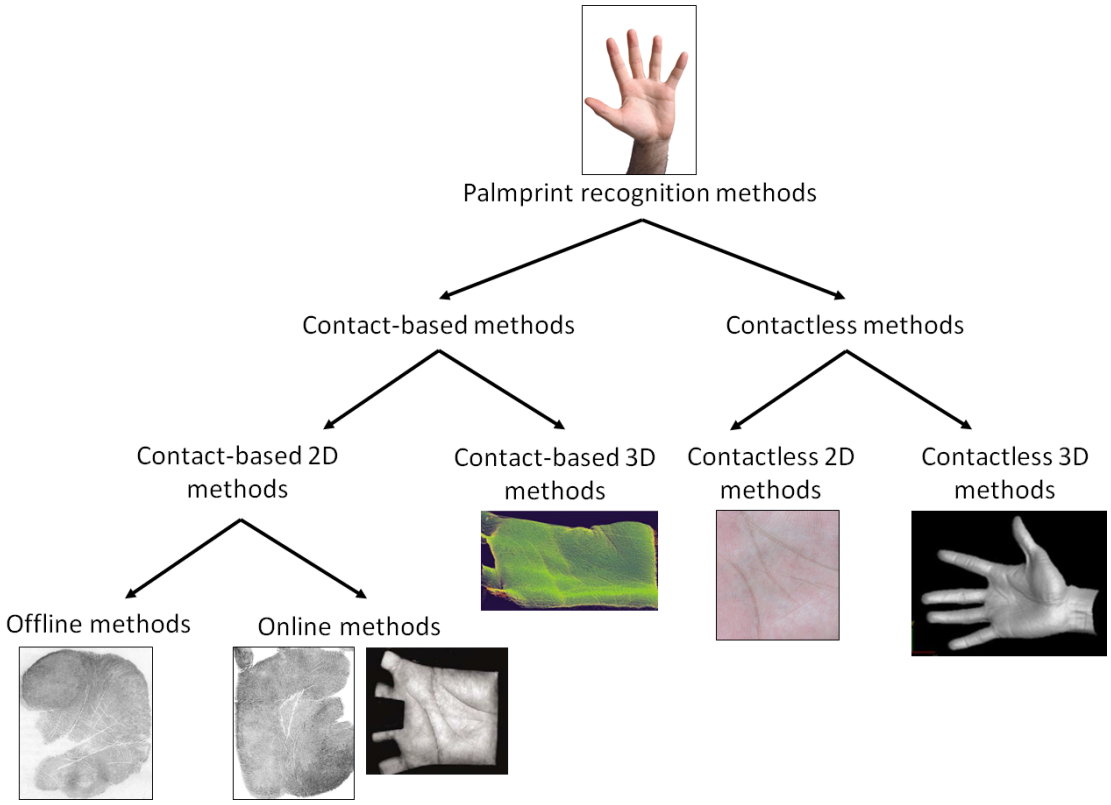

Figure 4.14: Classification of palmprint recognition approaches according to the type of the acquisition device.

tions, different backgrounds, noise, and spoofing attacks. However, they require more complex and more expensive setups.

In this chapter, the palmprint recognition methods are classified according to the type of the used acquisition device. For each category, the different methods used in each step of the recognition process are be described, including the acquisition, the segmentation, the image enhancement, the feature extraction and matching.

In the remainder of the chapter, some applications of the palmprint recognition systems are discussed (Section 4.3), then the contact-based methods for palmprint recognition are described (Section 4.4), with a distinction of the methods based on two-dimensional images and the methods based on three-dimensional samples. Then, the contactless methods are described (Section 4.5), including the methods that use two-dimensional images and the methods based on three-dimensional samples. Then, the methods used for estimating the quality of palmprint biometric samples (Section 4.6) and perform their classification (Section 4.7) are reviewed. The methods for the generation of synthetic palmprint samples (4.8) are introduced.

4.2 ADVANTAGES OF PALMPRINT RECOGNITION

As mentioned before, palmprints have many points in common with fingerprints, since details similar to the ones used for recognizing fingerprints are present in the palms. Similarly to fingerprints, palmprints present many distinctive features and can be used for a highly accurate biometric recognition.

However, on the contrary to fingerprints, palmprints feature a greater user acceptability, since the inner surface of the hand is commonly used by the people to interact with the environment. Moreover, palmprint recognition systems are generally more usable, since they require to position the entire open hand over the acquisition surface, and not just the fingertip. In fact, in the case of fingers different from the index finger, the procedure necessary for the fingerprint recognition can be difficult to perform (e.g., the ring finger is difficult to be captured singularly). Moreover, with respect to fingerprints, palmprint-based systems can use a greater area for the biometric recognition, and it is possible to extract biometric samples even from elder people or manual workers, since palmprints are less likely to be damaged [225].

Another advantage of palmprint recognition systems reside in the fact it is possible to use low-cost acquisition devices, such as off-the-shelf flatbed scanners or webcams [16], and numerous kinds of features, at different levels of details, can be extracted according to the type of acquisition device used. The use of low-resolution images makes the recognition robust to the noise in the acquisition process and to the dirt on the surface of the hand, and allows to quickly process the samples [225]. Moreover, palmprint recognition methods can be easily integrated in hand-based multibiometric systems [100].

4.3 APPLICATIONS OF PALMPRINT RECOGNITION SYSTEMS

Palmprint recognition systems can be used in different applicative contexts. One of the first applications of palmprint recognition was the analysis of latent palmprints in forensic applications [234, 212, 235], since latent palmprints can be often found at crime scenes [236], and can provide a greater recognition area with respect to fingerprints. For these reasons, high resolution devices for palmprint scanning [58] were designed, and Automated Palmprint Identification Systems (APIS) were also deployed [220].

Figure 4.15: Examples of palmprint applications: (a) forensic analyses [232]; (b) access control [60]; (c) personal authentication using a webcam [233]; (d) mobile identification [228].

However, the majority of palmprint recognition devices is designed for civil access control applications [217] and uses contact-based acquisition systems. Different acquisition techniques can be used to capture the palmprint sample, such as digital scanners, CCD cameras, or video cameras [16]. Multispectral imaging systems are also used [237].

Recently, several approaches have been described for personal authentication systems using palmprint information, based on webcams [231, 238, 239], or mobile phones [228, 240, 241, 242, 243, 244]. Studies for palmprint recognition in less-constrained environments are also present [231, 239, 245].

Examples of palmprint applications are shown in Fig. 4.15.

4.4 CONTACT-BASED PALMPRINT RECOGNITION

This section contains the description of the methods used for performing the palmprint recognition using a contact-based acquisition of the hand. Methods based both on two-dimensional images and three-dimensional samples are reviewed.

4.4.1 TWO-DIMENSIONAL CONTACT-BASED PALMPRINT RECOGNITION

Two-dimensional contact-based palmprint recognition methods require the user to place the palm of his hand on a surface, then they capture a two-dimensional image to be used as a biometric sample. Different acquisition devices can be used, for example optical devices, digital scanners (with live or inked acquisitions), and CCD-based acquisition devices. In this section, the methods that use contact-based two-dimensional acquisition methods are reviewed. In particular, four different steps are analyzed: acquisition, segmentation and registration, image enhancement, feature extraction and matching.

4.4.1.1 ACQUISITION

It is possible to divide the two-dimensional contact-based palmprint acquisition techniques in offline and online techniques. Offline techniques include the scanning of ink-based acquisitions and the lifting of latent prints. Online acquisition devices include optical devices, digital scanners, and CCD-based devices operating in visible light, or with different wavelengths:

- *Offline techniques*:
  1. Ink-based acquisition using a digital scanner;
  2. Latent acquisition.
- *Online techniques*:
  1. Acquisition using an optical device;
  2. Live acquisition using a digital scanner;
  3. CCD-based acquisition in visible light;
  4. CCD-based multispectral acquisition.

INK-BASED ACQUISITION USING A DIGITAL SCANNER The use of ink-based offline acquisitions with a low resolution (100 dpi) has been investigated in preliminary works for palmprint recognition, in order to study the feasibility of palmprints as a biometric recognition system [246, 247]. Currently, some methods are still being researched for forensic applications [248, 249, 250, 251], using high resolution (500 dpi) images.

In particular, the ink-based acquisition method is based on inking the palm of the user and pressing it onto a white paper. Then, the paper is digitized using a flatbed scanner in order to capture the palmprint (Fig. 4.16). A particular method, based on placing the hand on a rubber surface that prints the palmprint on a sheet of paper, is described in [252]. Then, the sheet is scanned using a digital scanner.

This kind of methods can be used only for offline recognition, and it is not suited for real-time acquisitions. Moreover, the acquisition procedure is highly dependent on the expertise of the operator, since the right amount of ink must be used. Both too much and too little ink can cause acquisitions of a minor quality. A document containing

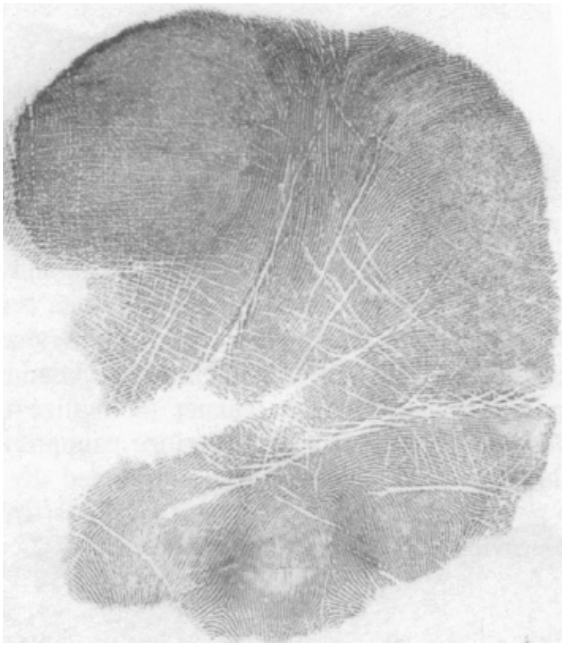

Figure 4.16: Example of an inked palmprint acquisition [225].

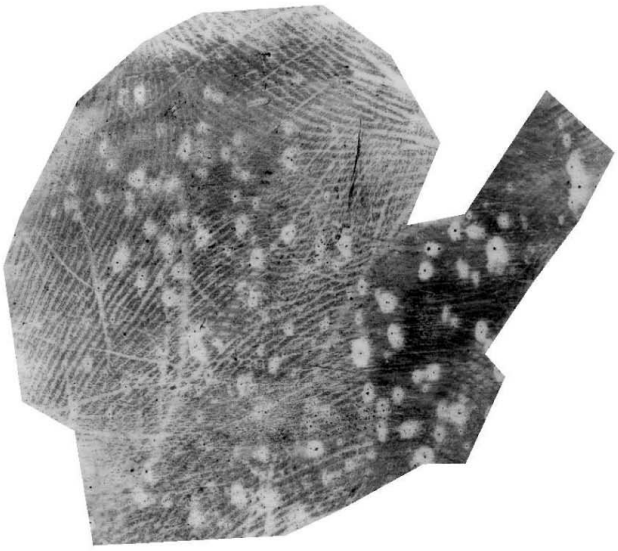

Figure 4.17: Example of a latent palmprint [212].

practical guides for a correct inked palmprint acquisition is released by the FBI [253]. Currently, the revision of the standard ANSI NIST ITL-2000 Type 15 for the exchange of palmprint data is underway [254].

LATENT ACQUISITION Several works deal with the offline analysis of latent palmprints [212, 235, 255, 256, 257, 258, 259, 260, 261]. In particular, a resolution of 500 dpi is the standard in forensic applications [212]. However, specific techniques must be used by an expert operator in order to lift latent palmprints [262] (Fig. 4.17). A particular

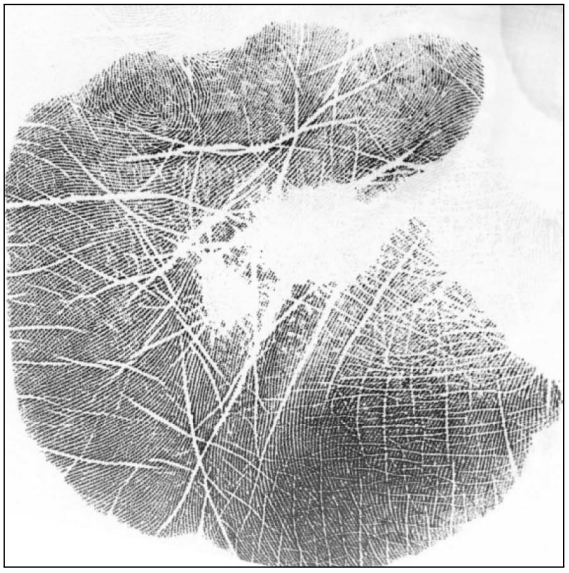

Figure 4.18: Example of a palmprint captured using an optical device [264].

work was proposed in order to identify the left palm given the right palm, and vice versa, using latent palmprints [263].

ACQUISITION USING AN OPTICAL DEVICE Some methods for palmprint recognition use samples captured using an optical device [58] (Fig. 4.18), similar to the ones used for contact-based fingerprint recognition. These category of methods use high resolution images (500 dpi) in order to extract features related to ridges, singular points, or minutiae, in addition to the features related to the principal and secondary palm lines [264, 265, 105, 266]. Some databases of palmprints captured using optical devices are publicly available [264].

LIVE ACQUISITION USING A DIGITAL SCANNER Digital scanners are used in several cases for palmprint acquisition since they allow to design low-cost palmprint recognition system. Moreover, it is relatively easy to place the hand in a correct position, because the majority of the users has some familiarity with the device. However, the acquisition times can be long, according to the resolution used and the quality of the hardware used in the scanner. Moreover, distortions due to the pressure of the hand on the surface of the scanner are often present in the thenar and hypothenar regions of the palm (Fig. 4.19).

In the literature, several methods use images captured using digital scanners in order to design a low-cost palmprint recognition system [267, 226, 230, 268, 269, 270, 271, 272, 273, 274, 275, 276, 277, 278, 279, 280, 281, 282, 283, 284, 285, 286, 287]. Moreover, a great variety of different resolution is used, ranging from 72 dpi to 300 dpi.

Multibiometric methods based on palmprints captured using digital scanners are also present in the literature, and combine palmprint samples with face features [288], hand geometry [289, 290, 291], or fingerprints [292].

Figure 4.19: Example of a palmprint captured using a digital scanner [226]. Distortions are visible in the thenar and hypothenar regions of the palm.

CCD-BASED ACQUISITION IN VISIBLE LIGHT The majority of the devices for the contact-based acquisition of palmprint images, that a CCD camera operating with visible light illumination, follow a general structure that include a camera and a transparent support. In order to perform the acquisition, the user needs to place his hand on the transparent surface. In particular, the advantages of a CCD-based device are in the fact that the acquisition can be performed in a short period of time (almost instantly), and the use of a surface placed at a fixed distance helps in reducing the motion blur and controlling the focus and the acquisition distance. Moreover, the surface help in enhancing the user experience, since people naturally tend to place their hand on a surface. However, this kind of acquisition methods can feature the problems typical of contact-based acquisitions, such as dirt, sweat, or latent impressions.

The majority of the palmprint recognition methods described in the literature [293, 294, 295, 296, 223, 297, 298, 299, 300, 301, 302, 303, 304, 305, 306, 224, 307, 308, 309, 310, 311, 312, 313, 314, 315] use palmprint samples captured using the CCD-based acquisition device described in [293]. This device requires the user to place his hand on a glass surface, and includes a series of pegs used for constraining the position of the hand in a fixed position, in order to simplify the subsequent segmentation and

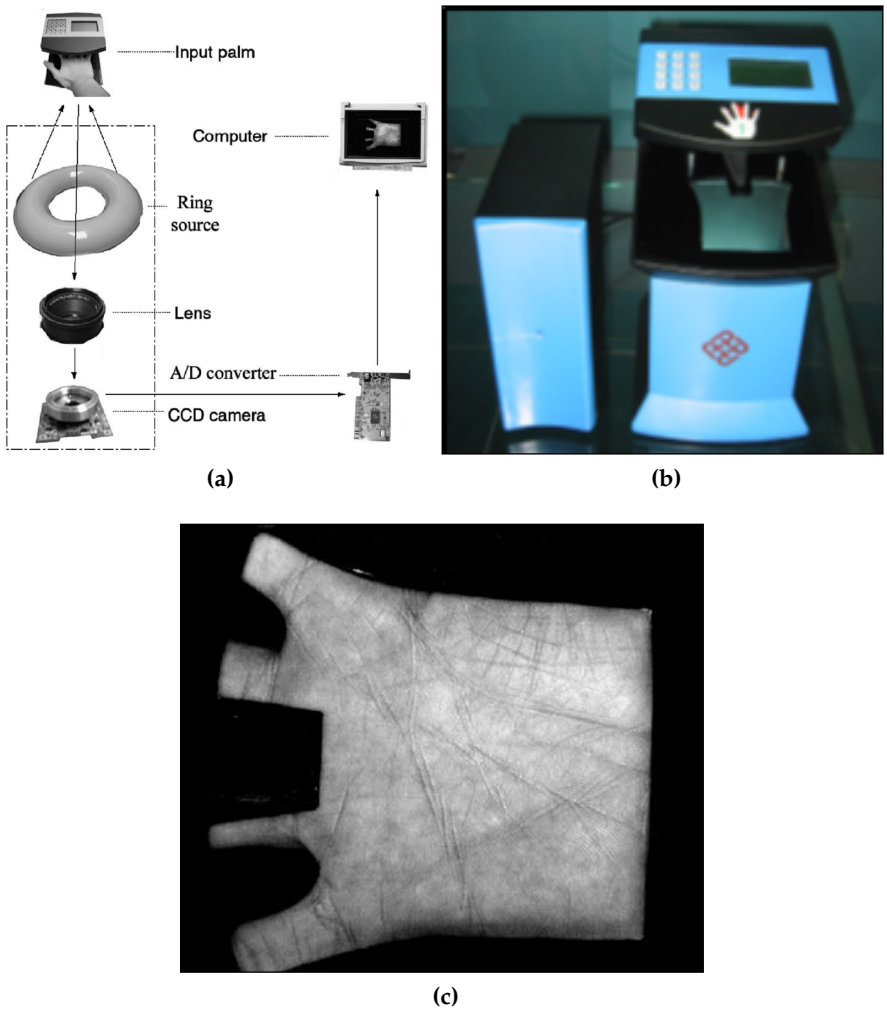

Figure 4.20: The contact-based two-dimensional CCD acquisition device described in [293]: (a) schema of the device; (b) the device; (c) example of an acquisition.

alignment processes [293] (Fig. 4.20a). The device captures images at 75 dpi (Fig. 4.20b). A database of palmprints captured using this device is publicly available [316].

In the literature, several multibiometric systems based on the samples captured using the device described in [293] have been proposed. In particular, the fusion of palmprint biometric data with face features [317, 318, 319, 320, 321, 322, 323, 324], and features obtained from the finger knuckle [325], have been described.

Other contact-based two-dimensional acquisition devices based on digital cameras have been described in the literature [326, 327, 229, 328]. A device based on a low-cost CMOS camera, a ring illuminator, and a casing which provides a transparent support to place the palm of the hand is described in [326] (Fig. 4.21a). The device is designed to be small in order to be used as a personal identification device for online applications. The devices captures images with a resolution of 65 dpi (Fig. 4.21b). A similar device for a low-cost recognition is described in [229] (Fig. 4.22)

A real-time recognition device is described in [327], and is composed by a CCD camera, a ring illuminator, and a casing in order to provide the support for the user's

(a) (b)

Figure 4.21: The contact-based two-dimensional CCD acquisition device described in [326]: (a) the device; (b) example of acquisition.

(a) (b)

Figure 4.22: The contact-based two-dimensional CCD acquisition device described in [229]: (a) the device; (b) example of acquisition.

(a) (b)

Figure 4.23: The contact-based two-dimensional CCD acquisition device described in [327]: (a) the device; (b) example of acquisition.

(a) (b)

Figure 4.24: The contact-based two-dimensional CCD acquisition device described in [328]: (a) the device; (b) example of acquisition.

hand (Fig. 4.23a). The device captures high-resolution samples, in order to use the pattern of the ridges for recognition (Fig. 4.23b).

A low-cost device that offers a higher degree of freedom is described in [328]. In particular, the user is free to move the hand across the acquisition surface, and the background is uncontrolled (Fig. 4.24).

CCD-BASED MULTISPECTRAL ACQUISITION In the literature, several methods propose acquisition devices able to capture palmprint samples under different wavelengths. In fact, different wavelengths penetrate the human skin at different depths, and enhance different details [329].

The majority of multispectral palmprint recognition methods [237, 330, 331, 332, 333, 334, 335, 336, 337, 338, 339, 340] use the samples captured using the device described in [237, 340] (Fig. 4.25), which uses four different illuminators emitting light at the red, green, blue, and NIR wavelengths, in order to enhance the different details of the palmprint. Then, a standard low-cost CCD camera is used to capture the images, which are taken at short time intervals (Fig. 4.25b–e). A database of multispectral palmprint samples captured using the device described in [237] is publicly available [341]. Moreover, a study on the best wavelengths for the enhancement of palmprint details is proposed in [342]. In particular, it is shown that the combination of the 580 nm (yellow spectrum), 760 nm (red spectrum) and 990 nm (NIR spectrum) wavelengths provides the best results. The database used for the experiments is publicly available [343]

Multibiometric systems based on multispectral acquisition devices are often described in the literature for the joint recognition of palmprint and palm vein features [344, 345, 346, 347, 348]. In particular, the device described in [344, 345] uses two light sources to illuminate the palm, which is placed on a glass surface (Fig. 4.26a). A blue LED is used as the illumination source for capturing the palmprint in visible light, while a NIR illuminator is used to enhance the details of the vein pattern of the hand. A standard low-cost CCD camera is used to capture the two images (Fig. 4.26b–c), with a short time interval between the two acquisitions.

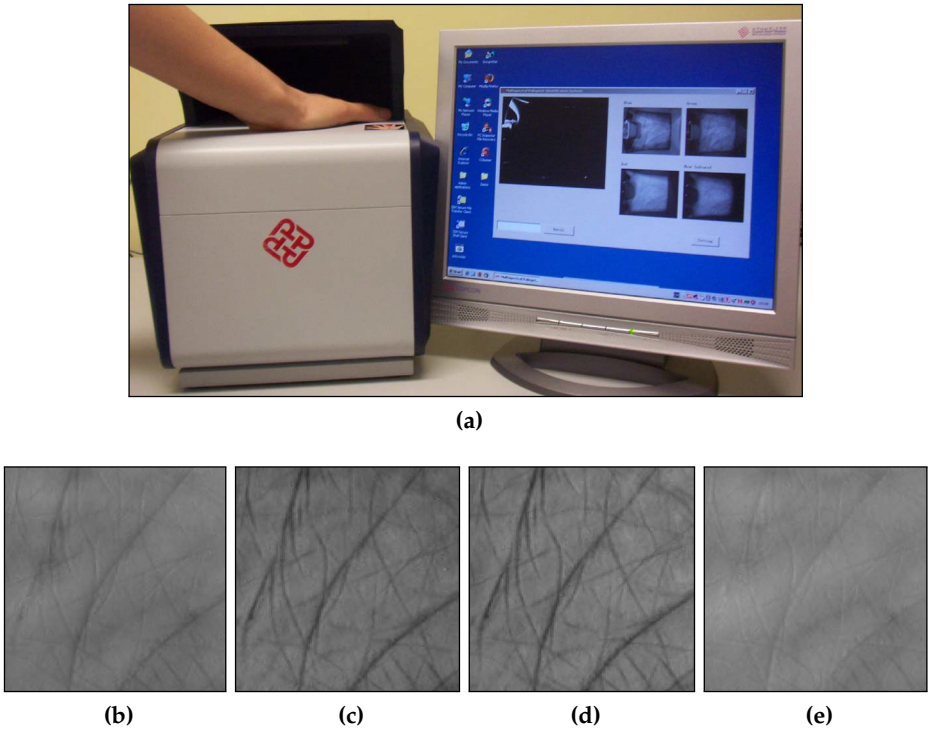

(a) (b) (c) (d) (e)

Figure 4.25: The contact-based two-dimensional CCD multispectral acquisition device described in [237]: (a) the device; (b) acquisition with the red illuminator; (c) acquisition with the green illuminator; (d) acquisition with the blue illuminator; (e) acquisition with the NIR illuminator.

Similar devices are proposed in [346, 347, 348]. In particular, the methods described in [346, 348] use an image-level fusion scheme, in order to generate a combined image from the two acquisitions, one captured with visible light and one captured using a NIR illumination.

4.4.1.2 SEGMENTATION AND REGISTRATION

The segmentation and registration step (or preprocessing) has the purpose of extracting and aligning correctly the region of interest (ROI) of the palmprint image. In the majority of the approaches in the literature, the segmentation and registration step can be divided into four phases:

1. Binarization of the palm image and extraction of the contour of the hand;
2. Detection of the keypoints and establishment of a coordinate system;
3. Extraction of the central part of the palm;
4. Registration.

In this section, the most significant methods for the each phase of the segmentation process of palmprint acquisitions are reviewed.

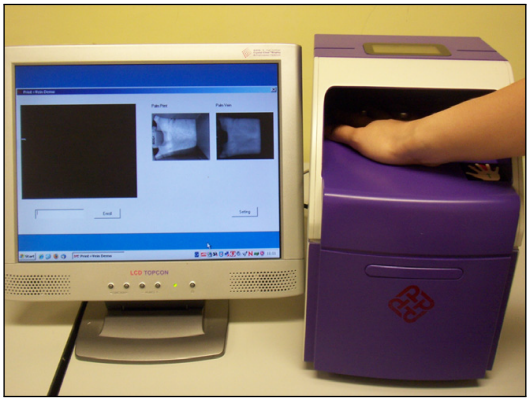

(a)

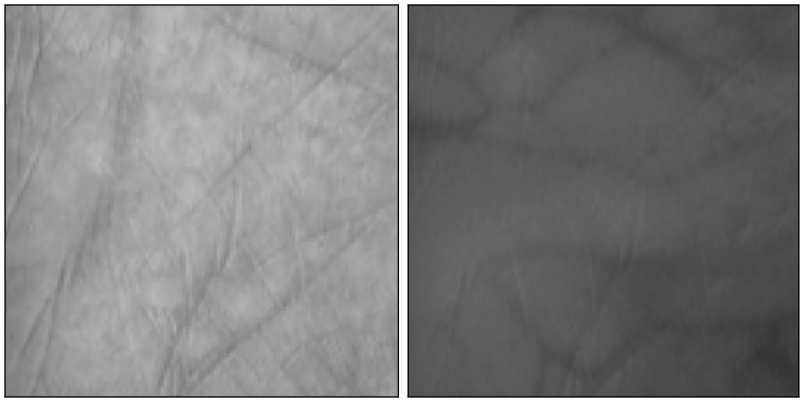

(b) (c)

Figure 4.26: The multispectral multibiometric acquisition device described in [344]: (a) the device; (b) palmprint acquisition with the blue LED illuminator; (c) palm vein acquisition with the NIR illuminator.

BINARIZATION OF THE PALM IMAGE AND EXTRACTION OF THE CONTOUR OF THE HAND The methods for the binarization of the palm image and the extraction of the contour of the hand are different in the case of offline and online acquisitions.

Usually, variance-based approaches are used to binarize offline and optical-based palmprint acquisitions, and to extract the contour of the hand. However, particular approaches are described in [250, 258, 261, 105]. In the case of offline palmprint acquisitions, the binarization step and the extraction of the contour are usually the only steps needed for the segmentation of the region of interest.

The approach described in [250] divides the image in several blocks and computes the variance and proportion of white pixels for each block, in order to discriminate palmprint regions from blank regions. A connected component analysis is used to eliminate the isolated knuckle regions, and a convex component analysis is used to eliminate the connected knuckle regions.

A method for the segmentation of latent palmprint images is described in [258]. The method is based on the use of gradient functions in the spatial domain, and on the use of energy functions in the frequency domain, in order to describe the orientation and

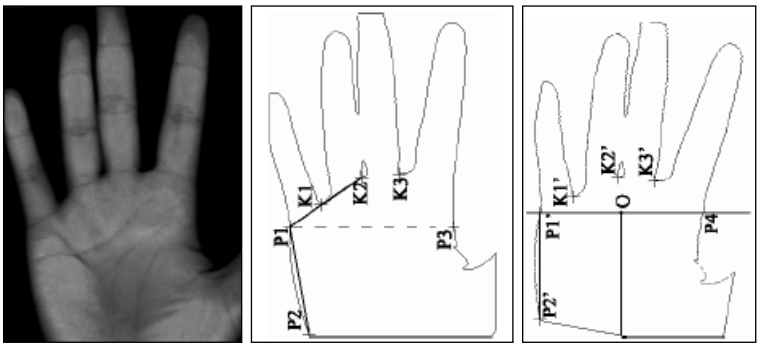

Figure 4.27: The keypoint extraction method described in [287]: (a) the original image; (b) the extracted gaps K1, K2 and the points P1, P2; (c) the aligned image and the center O of the reference system as the middle point of the segment P1′P4.

periodicity of the palmprint texture. A dissimilarity threshold is used to segment the palmprint regions from the non-palmprint regions.

An Active Contour Model (ACM) is used in [261] for the segmentation of latent palmprint images. The method uses a Gabor filtering step in order to enhance the details of the palmprint, divides the image in several blocks, then computes the Average Absolute Deviation (AAD) for each block of the image. A spline function is used to enclose the region corresponding to high AAD values.

A binarization method based on the thresholding of the gradient intensity map is used in [105] for the segmentation of palmprints captured using an optical device.

Online palmprint acquisition methods often use global thresholding methods in order to binarize the palm image and extract the contour of the hand, especially when the acquisition is controlled and the background is uniform. In this case, in fact, there is a high difference between the foreground and background. However, particular methods have been described in the literature [286, 269, 292], also in order to consider uncontrolled backgrounds [328].

A method for the extraction of the central region of the palm using acquisitions made using a digital scanner is described in [286]. The method is based on a threshold operation, then the region corresponding to the pixels with the most homogeneity of intensity, color, texture, and shape is extracted.

A method based on hysteresis thresholding is used in [269].

The method described in [292] uses a Gabor filtering step to enhance the fingerprint and palmprint image, then uses Otsu's thresholding to automatically compute the best threshold for binarizing the image.

DETECTION OF THE KEYPOINTS AND ESTABLISHMENT OF A REFERENCE COORDINATE SYSTEM The detection of the keypoints allows to define a reference coordinate system, in order to robustly align the palmprint images and extract the central part of the palmprint, which contains the majority of the information. In particular, most of the palmprint recognition methods described in the literature use the spaces between the fingers as the keypoints.

(a) (b)

Figure 4.28: The method for determining the orientation of the hand described in [276]: (a) the left region is extracted; (b) the number of connected components is $\geqslant 3$ so the hand is oriented towards the left.

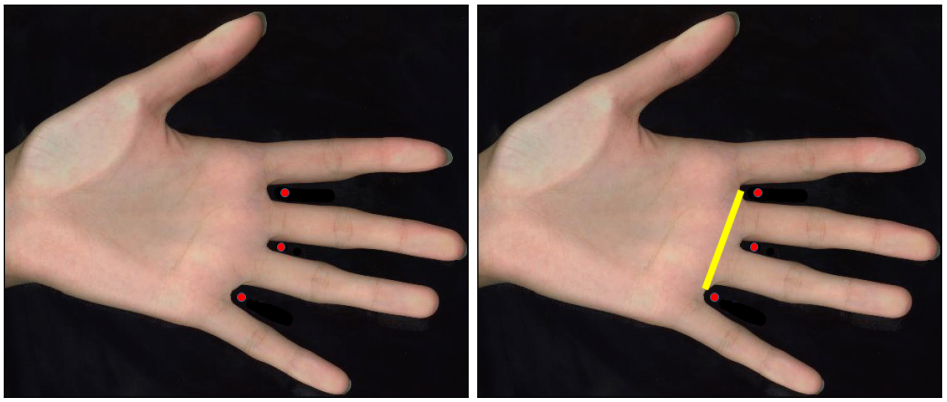

(a) (b)

Figure 4.29: The method for extraction of the keypoints described in [276]: (a) the gaps between the fingers, and the corresponding centers of gravity; (b) the baseline of the reference system.

The method described in [287] uses the position of two gaps between fingers in order to compute a reference system (Fig. 4.27). The gaps $K1, K2$ are connected in order to find a reference point $P1$ on the boundary of the palm (Fig. 4.27b), which is connected to the lower end $P2$ of the palmprint. The segment $P1P2$ is used to align the palmprint image. The middle point of the perpendicular segment $P1'P4$ in the aligned image is used as the center O of the reference system (Fig. 4.27c).

The approach described in [276] computes the number of connected components in the right and left region of the hand in order to determine the orientation of the hand (Fig. 4.28). Then, the images are oriented in a common direction. Subsequently, the positions of the three gaps between the fingers are extracted and the centers of gravity for each gap are computed (Fig. 4.29a). The outermost centers of gravity are connected in order to form the baseline of the reference system (Fig. 4.29b).

A similar method is used in [267], and is based on the extraction of the center of the gaps $v1, v2, v3$ between the fingers. The segments $v1v2$ and $v2v3$ are extended to intersect the boundary of the hand, and the middle points $m1, m2$ between the valleys $v1$ and $v3$ and the corresponding intersection points are extracted. These points are

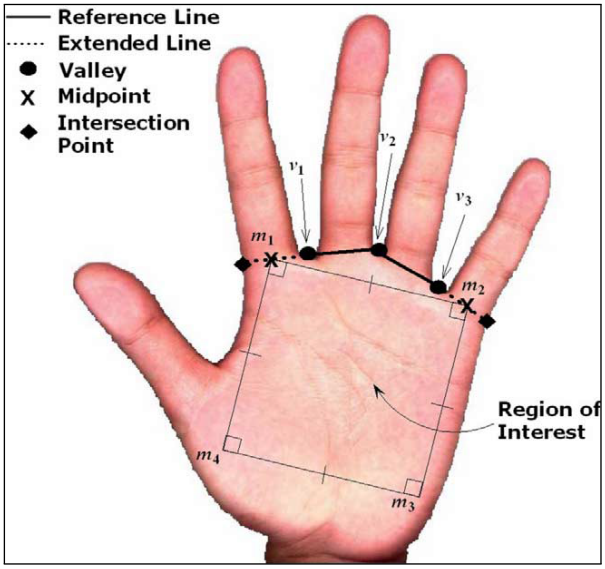

Figure 4.30: The method for extraction of the keypoints described in [267].

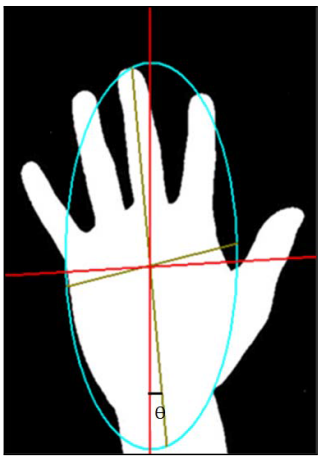

Figure 4.31: The method for extraction of the keypoints described in [269].

used as the baseline of the reference system (Fig. 4.30). A similar method is used in [314], and a fixed angle is used to compute the segment connecting the valleys with the boundary of the palm.

A method based on fitting an ellipse through the binarized shape of the hand is proposed in [269]. Then, the centers of the two axes of the ellipse are used as the base of the reference system (Fig. 4.31).

The method described in [293] uses a boundary tracking algorithm in order to compute two gaps between the fingers. In particular, the first gap is between the forefinger and the middle finger, while the second gap is between the ring finger and the little finger (Fig. 4.32b). These two points are used as the coordinates of the reference system (Fig. 4.32c).

A method based on two points, the root of the middle finger and the center of the wrist, is described in [304]. A linear boundary search algorithm is used to find

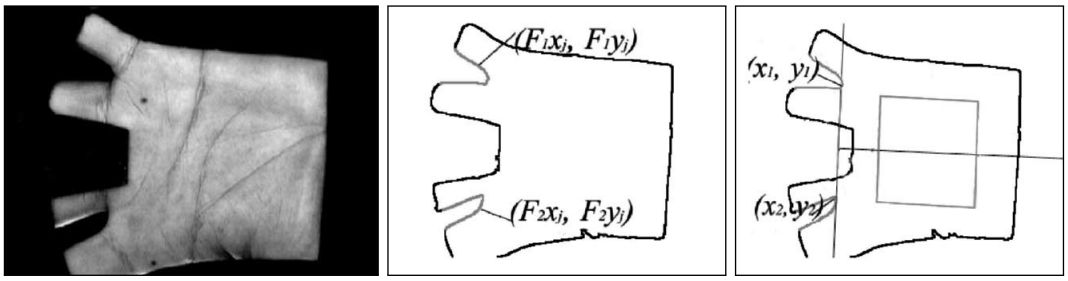

(a) (b) (c)

Figure 4.32: The keypoint extraction method described in [293]: (a) the original image; (b) the extracted gaps; (c) the extracted reference system.

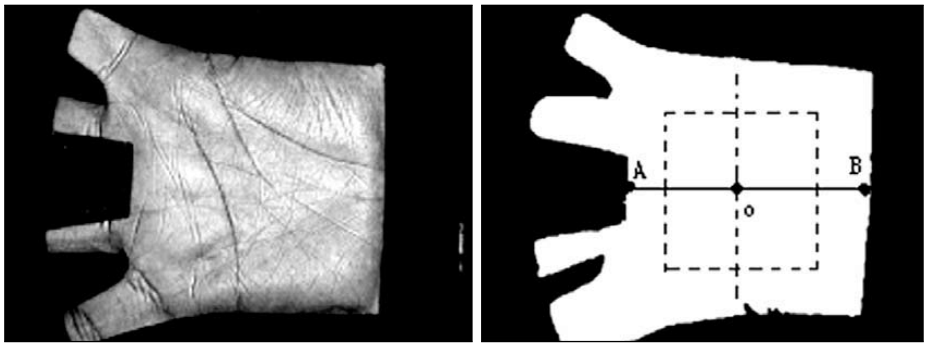

(a) (b)

Figure 4.33: The keypoint extraction method described in [304]: (a) the original image; (b) the extracted keypoints and the reference system.

the points, and the center of the segment connecting them is used as the base of the reference system (Fig. 4.33).

A method based on Active Appearance Models (AAM) is used in [328] for the segmentation of palmprint images captured with a CCD-based device, with uncontrolled background conditions. In particular, AAMs are a statistical method that has the purpose of matching a previously computed model of the shape and texture to unseen samples.

EXTRACTION OF THE CENTRAL PART OF THE PALM The majority of the methods for the segmentation of the palmprint uses the computed reference coordinate system for the extraction of a square region containing the central part of the palmprint [287, 276, 267, 314, 293].

REGISTRATION In the majority of the palmprint recognition methods, if the region of interest is extracted according to a computed reference system based on keypoints, the registration of the images is trivial. Moreover, if the acquisition is based on a constrained hand position, a registration step might be not necessary. However, some approaches in the literature have been proposed in order to perform a finer registration

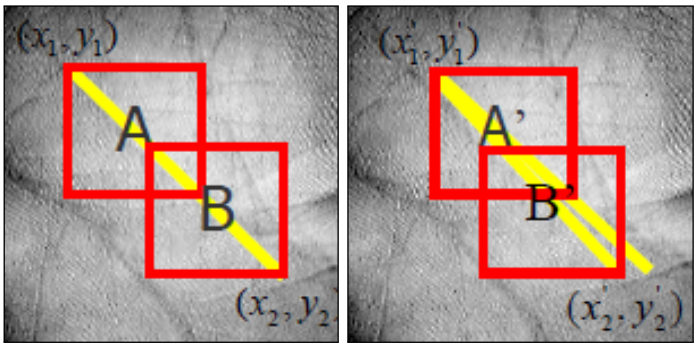

(a) (b)

Figure 4.34: The registration method described in [326]: (a) two blocks A and B are extracted from the first image; (b) two matching blocks A′ and B′ are extracted from the second image: the line connecting them is used to align the image.

[311], or for the cases when the region of interest is not extracted using a reference system [265, 326].

A method based on the alignment of the orientation field is used in [265] for the registration of high-resolution palmprint images captured using an optical device.

The method proposed in [311] first extracts the region of interest using the method described in [293], then computes the position of the principal lines of the palm. Then, an Iterative Closest Point (ICP) algorithm is applied on the binarized images of the principal lines, in order to align the palmprint acquisitions with a better precision.

The method described in [326] extract two blocks from the first image (Fig. 4.34a), with a 45° degree line connecting them, and searches the best matching blocks in the second image. The angle of the line connecting the blocks in the second image is used to align the image (Fig. 4.34b). A similar procedure is used to find the translation between the two images.

4.4.1.3 IMAGE ENHANCEMENT

Image enhancement techniques for palmprint recognition are strongly correlated with the typology of features used for the recognition. Moreover, different enhancement methods are used according to the device used for the acquisition of the samples. In this section, the most significant methods used for the enhancement of palmprint acquisition are reviewed.

An enhancement method used for offline palmprint acquisitions is described in [248]. The method is based on computing the orientation field of the palmprint, then a series of O'Gorman and Nickerson oriented filters are used to reduce the noise and enhance the pattern of the ridges. Otsu's threshold method is used to binarize the image (Fig. 4.35).

The method described in [212] is used for the enhancement of latent palmprints, and computes the orientation field and the frequency map of the palmprint image. Then, a series of oriented Gabor filters is used to enhance the details of the ridge pattern and

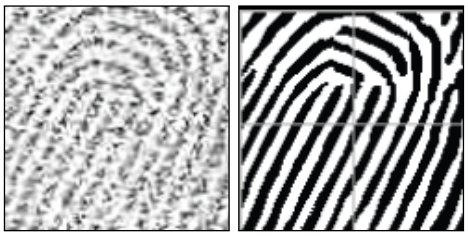

(a) (b)

Figure 4.35: The enhancement method described in [248]: (a) a particular of the original image; (b) the enhanced image.

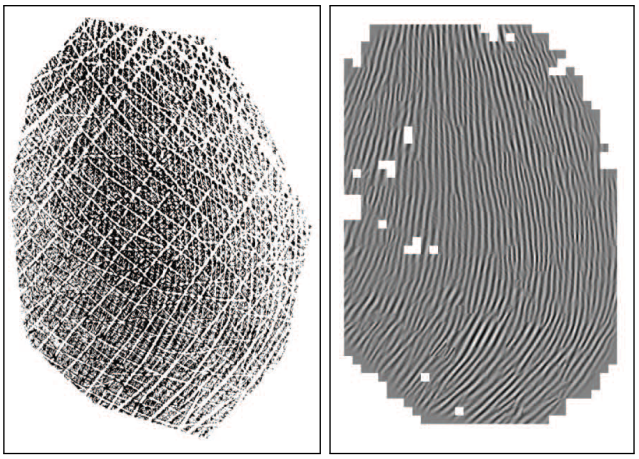

(a) (b)

Figure 4.36: The enhancement method described in [212]: (a) the original image; (b) the enhanced image.

the minutiae. A region growing algorithm is applied in order to connect broken ridges and avoid the introduction of false minutiae (Fig. 4.36).

A contrast-limited adaptive histogram equalization technique is used in [261] for the enhancement of latent palmprints. The method is based on an improved version of the adaptive histogram equalization technique, which divides the image in several regions and performs the histogram equalization separately on each region.

Methods based on the computation of the orientation field and frequency map, and the subsequent enhancement using Gabor filters, are typically used for online palmprint acquisitions captured using optical devices [264, 105].

Palmprint recognition methods that use a feature extraction step based on the extraction of the principal lines typically adopt edge detectors to enhance the images. Examples of edge detectors used in the literature are the Canny edge detector [286, 282, 290], the Sobel operator [296], or derivative-based operators [291]. Steerable filters are used in [285]. Ad-hoc edge detectors are also used [288], including a Fuzzy Unsharp Masking Method [284].

Several methods use an enhancement step based on Gabor filtering [230, 226, 281, 275, 276, 291, 293, 298, 302, 303, 305, 306, 310, 322], Wavelet Transforms [267, 280, 279,

274, 291, 289, 309, 312], Fourier Transform [294, 256], Contourlet Transform [269, 270, 315], Radon Transform [299, 300, 301], Discrete Cosine Transform (DCT) [317], Directional Filter Bank Transform [307], Riesz transform [325], or Karhunen-Loève transform [349]. In most cases, the values of the resulting image after the transformation are directly used as features.

4.4.1.4 FEATURE EXTRACTION AND MATCHING

As mentioned in Section 4.1.3, the methods used for the extraction and matching of the features can be divided into the sequent categories:

1. Ridge-based approaches;
2. Line-based approaches;
3. Subspace-based approaches;
4. Statistical approaches;
5. Coding-based approaches;
6. Other approaches.

In this section, the most relevant methods for the feature extraction, according to the described categories, are reviewed.

RIDGE-BASED APPROACHES The method proposed in [248] is designed for offline palmprint acquisitions, and combines the positions of the minutiae and the local structure of the ridge orientation around each minutia point in order to perform the recognition. For each minutiae, a descriptor is computed using the extracted information and the information of the neighboring minutiae. The Euclidean distance between the descriptors is used as the match score.

A minutiae-based method for latent palmprint matching is proposed in [235]. First, a clustering algorithm is used to group the minutiae points in several clusters, according to local features such as local orientation and frequency. For each cluster, a reduced number of correspondences between minutiae is computed. A local structure for each minutia, based on the position and type of the surrounding minutiae [212], is used to compute the similarity. Each minutia correspondence is used as the start of a propagation algorithm, in order to search for other matching minutiae. The match score is computed as the longest computed propagation.

A local minutiae descriptor, which combines minutiae features with SIFT features, is used in [255] for partial palmprint matching. A Euclidean distance-based matching is used to compare the descriptors and compute the match score.

A minutia matching scheme based on triangulation is adopted in [257]. The method compares the radial triangulations computed using restricted sets of minutiae in order to perform the matching of partial latent palmprints. The result of the comparison between triangulations is used to align the image, in order to perform a global minutiae comparison.

A 2D wavelet transform is used in [263] to extract the features of the palmprint in order to recognize a right hand given his left hand, and vice versa. A clustering algorithm is used to classify the features in order to find the most similar ones.

A method that combines minutiae and SIFT keypoints is used in [261] for matching latent palmprint acquisitions. A weighted sum is used for combining the two match scores.

LINE-BASED APPROACHES A method based on the extraction of feature points lying on the principal lines of the palmprint is described in [252]. The feature points are chosen as the points lying on the lines that have the maximum intensity in their local block. Then, for each point, the local ridge orientation is computed. The images are aligned and the feature sets of the extracted points are matched in the Euclidean space. The number of matching pairs and the average distance are used as match scores. A discriminant analysis is used to reduce the two-dimensional classification problem into a one-dimensional problem.

The position of the datum points, corresponding to the endpoints and midpoints of the principal lines, is used in [247], along with the direction of the palm lines, subdivided into several straight-line segments. The positions of the endpoints of each segment, expressed in the coordinate system based on the positions of the datum points, are used as features. The number of segments for which their Euclidean distance is less than a threshold is used as the match score.

The method described in [313] is based on the extraction of feature points corresponding to the intersection of palm lines and creases. Then, the SIFT descriptors are computed for each point and used for matching different palmprint acquisitions. Moreover, a SVD of the proximity matrix, constructed using the positions of the points, is used for matching the points based on their position.

A Sobel operator is used in [296] to extract the palm images, then a series of features related to the magnitude and direction of the lines is computed. A method based on HMMs is used for the classification.

SUBSPACE-BASED APPROACHES The method proposed in [226] first enhances the image using Gabor filters, then uses a 2D PCA analysis followed by a Locality Preserving Projection (LPP) to extract the features. The Euclidean distance is used as a measure of the similarity of the palmprint acquisitions.

The combination of palm lines and LPP is used in [299]. First, the palm lines are extracted from the images, then a matching is performed by considering the percentage of lines in common [300]. Then, the LPP is applied on the images, and the Euclidean distance is used to compute the similarity of the LPP feature set. A method based on the product rule is used to combine the two measures.

A Gabor filtering step, followed by a 2D PCA analysis, is used in [281] for the extraction of the features from the R, G, B channels of the image separately. The Euclidean distance is used for measuring the similarity between the feature sets.

A method which compares PCA, Fisher Discriminant Analysis (FDA), and Independent Component Analysis (ICA) is described in [267]. The use of a preliminary

enhancement using a wavelet transform is also proposed. A Probabilistic Neural Network (PNN) is used to classify the features.

A method proposing the use of FDA to extract the features is described in [279]. As a preliminary step, a Dual-Tree Complex Wavelet Transform is used to enhance the images. However, instead of directly using the wavelet coefficients as features, the wavelet response is modeled using Gaussian shape descriptors.

The method described in [273] uses a techniques based on Non-negative matrix factorization (NMF) in order to extract the local features of the palmprint image. Then, a PCA analysis is used to extract the image features at a global level. Different fusion rules are tested for combining the local and global features, then a Nearest Neighbor classifier is used.

A method that uses 2D PCA and LDA is used in [277] in order to extract the distinctive features. A Nearest Neighbor classifier is used for classification. A similar method, using Kernel Fisher Discriminant Analysis (KFDA), is proposed in [278].

The method described in [307] uses an enhancement procedure based on Shiftable Complex Directional Filter Banks (CDFB), which achieves a representation of the image invariant to gray scale values. Then, the Histograms of Local Binary Patterns are computed for each subregion of the image, and a Fisher Linear Discriminant classifier is used to compare the palmprint samples.

A sparse representation of the palmprint images is computed in [308] by solving a minimization problem, in order to increase the efficiency of the matching process. Then, a comparison of PCA and LDA for the feature extraction step is described.

STATISTICAL APPROACHES The method described in [280] uses the texture features of palmprint images by expressing the palm lines as direction fields in the Riemannian geometry. Then, a Dual-Tree Complex Wavelet Transform is used to enhance the images, and the histograms of the Local Binary Patterns (LBP) are extracted and used as the distinctive features.

The combined use of geometrical features and texture features is proposed in [268]. In particular, Zernike Moments are used as descriptors of the characteristics of the palmprint texture. A combined computational intelligence approach, based on Self Organizing Maps (SOM) and Backpropagation Neural Networks (BPNN) is used to classify the features.

Different feature vectors extracted from several color spaces are used in [271] for palmprint recognition. In particular, for each colorspace used, the mean and entropy of each subregion of the image are extracted. The feature vectors corresponding to the same color spaces are compared using the Euclidean distance, and the match scores obtained by comparing the feature vectors of the different color spaces are combined using different fusion rules.

CODING-BASED APPROACHES The method described in [293] uses a Gabor filtering scheme in order to extract the phase information relative to the direction of the palm lines. Then, the Gabor response is quantized in order to compute a bit string representing the information of the palmprint (PalmCode). The Hamming distance is used

for comparison. A similar method that uses multiple Gabor filters is described in [350] (FusionCode). In particular, the filter that produces the maximum intensity response is considered. In the work described in [295], their bitwise angular distance is used for comparison (Competitive Code). In the work described in [306] a Binary Orientation Co-occurrence Vector (BOCV), obtained by concatenating the normalized responses obtained using multiple Gabor filters, is used to describe the palmprint.

A method based on a fuzzy C-means clustering algorithm is used in [305] to determine the best orientations of the Gabor filters to be applied on the image.

A similar coding scheme, called Robust Line Orientation Code (RLOC), is used in [301] to encode the orientation information of the image, after an enhancement step based on the Radon transform.

OTHER APPROACHES A correlation approach, based on the phase information obtained by applying a modified Fourier transform on the image, is used in [256] for the matching of degraded palmprint images.

A representation of the palm lines based on a Quad-tree decomposition is described in [282]. The decomposition has the purpose of splitting the image into smaller and smaller blocks, until the pixels within a block have an intensity value smaller than a threshold. Using this technique, it is possible to efficiently analyze the image, using the required resolution only in the block that contains the information.

The use of the Contourlet Transform is proposed in [269] in order to obtain the feature descriptors used for the recognition. The Euclidean distance is used for classification.

The combined use of the Contourlet Transform and fractal dimensions is described in [270]. In particular, the fractal dimension feature of an image is used as an indicator of the roughness of its texture. The Manhattan distance and the nearest neighbor classifier is used for classification. Multifractal characteristics are also used by the method described in [304].

In the method described in [294], the Fourier response in the frequency domain is subdivided into several zones, and the intensity values of the different zones are used as features. Two feature set are constructed by dividing the frequency image using concentric rings, or by using triangular sectors. Then, a hierarchical matching is used for comparing the similarity of the samples.

Features at different levels are extracted in [223]. In particular, geometrical features, global texture energy, palm lines, and local texture energy are used for recognition. A hierarchical matching method is used to speed up the identification in large databases. Euclidean distance and angular distance between feature vectors are used as similarity measures.

The method described in [303] uses Gabor-based Region Covariance Matrices, which contain the information related to both the magnitude and the phase of the Gabor response.

A method which combines the features extracted from a Discrete Wavelet Transform with the estimation of the illumination quality is proposed in [309].

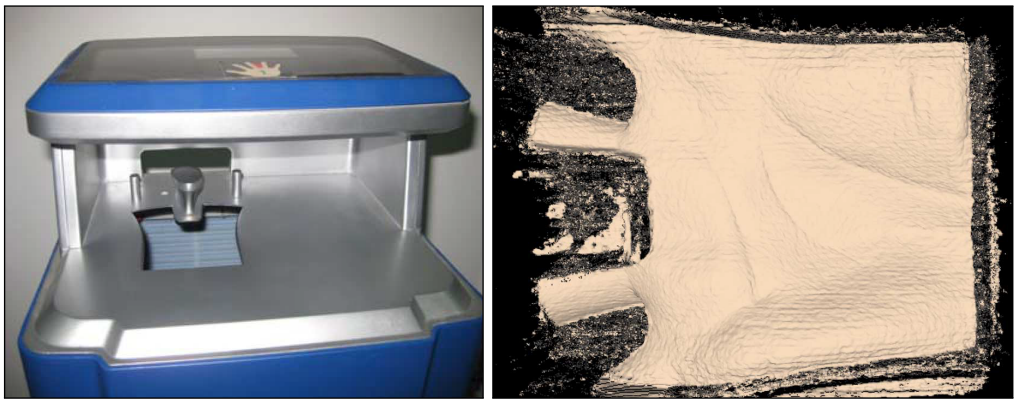

(a) (b)

Figure 4.37: The contact-based three-dimensional acquisition device described in [227]: (a) the device; (b) example of a three-dimensional acquisition.

The method proposed in [310] enhances the images using 2D Gabor Wavelets, then uses a Pulse Coupled Neural Network (PCNN) to decompose the Gabor-filtered images into a series of binary images. The entropies of the binary images are used as features, and a SVM classifier is used for comparison. An efficient implementation, designed for on-line fast palmprint identification, is proposed in [312].

The use of SIFT features for palmprint matching is proposed in [314]. The Euclidean distance between SIFT descriptors is used a measure of comparison between samples.

4.4.2 THREE-DIMENSIONAL CONTACT-BASED PALMPRINT RECOGNITION

Three-dimensional contact-based palmprint recognition systems require the user to place the palm of the hand on a surface, then they compute a three-dimensional model of the hand. This category of acquisition systems use CCD-based acquisition devices, and capture a two-dimensional image of the palm of the hand as well. Usually, structured light illumination setups, based on a CCD camera and a DLP projector, are used to perform the acquisition and the three-dimensional reconstruction of the palm.

In this section, the methods that use contact-based three-dimensional acquisition methods are reviewed. In particular, the four different steps are analyzed: acquisition, segmentation and registration, image enhancement, feature extraction and matching.

4.4.2.1 ACQUISITION

The majority of the approaches in the literature that use a contact-based three-dimensional reconstruction of the palmprint [227, 97, 351, 106, 352, 353] use the acquisition system proposed in [227, 97]. This system is based on a structured light illumination setup, and is composed by a CCD camera and a DLP projector (Fig. 4.37). The projector emits a series of shifted stripes onto the surface of the palm, then a CCD camera is used to capture the different images. A phase unwrapping technique is used to compute the depth information relative to each point in the image. The acquisition device has a

resolution of 150 dpi, with an error of 1 mm in the estimation of the three-dimensional depth of the points. Moreover, the device captures a two-dimensional image as well, similar to the one used in the method described in [293].

An enhanced version of the acquisition device is described in [351], and introduces the use of infrared sensors to detect when a hand is placed on the sensor, in order to start automatically the acquisition. Moreover, when the stripes are projected on the palm, different brightness levels are used in each stripe, in order to simplify their distinction and the phase unwrapping process.

A database collected using this device is publicly available [354].

4.4.2.2 SEGMENTATION AND REGISTRATION

As mentioned before, in the method described in [227, 97] a two-dimensional acquisition is collected along with the corresponding three-dimensional model. Since there is a point-to-point correspondence between the two acquisitions, the same methods used for the segmentation and registration of two-dimensional images are used in the case of the three-dimensional palmprint models. In particular, the segmentation method described in [293] for two-dimensional, contact-based acquisitions is the mostly used technique for the samples captured using the device described in [227, 97].

An improvement of the technique described in [293] is proposed in [355]. In particular, the region of interest of both the two-dimensional and three-dimensional acquisitions is extracted using the method described in [293]. Then, the palm lines are extracted from the two-dimensional image, and an ICP algorithm is used to register both the two-dimensional image of the palm lines, and three-dimensional acquisition.

The method described in [356] segments the samples by using the technique proposed in [293], then uses a cross-correlation approach to refine the registration of the images.

4.4.2.3 IMAGE ENHANCEMENT

In some cases, image enhancement algorithms are applied on the two-dimensional acquisitions. However, they are similar to the ones mentioned in Section 4.4.1.3. Gabor filters are used in [227, 106, 351] as a preliminary step before the computation of the Competitive Code [295].

The method described in [357] computes a Mean Curvature Image (MCI) and a Gaussian Curvature Image (GCI) from the three-dimensional model of the palmprint, in order to describe the three-dimensional shape of the palm using two-dimensional images. Then, a Gabor filtering step is applied in order to compute the Competitive Code.

The method described in [355] computes the MCI and GCI images, then uses a Radon transform for the extraction of the palm lines from the two-dimensional acquisition, and from the MCI and GCI images. A Gabor filtering step is applied for the computation of the Competitive Code.

4.4.2.4 FEATURE EXTRACTION AND MATCHING

The techniques for the feature extraction and matching can be divided into methods used for two-dimensional images, and method used for three-dimensional models. In many cases, the methods used for two-dimensional images are similar to the ones described in Section 4.4.1.4. In particular, the Competitive Code method is used in [227, 351] for the feature extraction and matching of the two-dimensional images.

Moreover, the Competitive Code method is used in [355, 357] also for matching the MCI and GCI images, which use a two-dimensional representation for the three-dimensional shape of the palmprint.

In the method described in [227], the MCI and GCI images are computed from the three-dimensional sample, along with the ST features, that describe the local structure of the shape. The GCI and MCI images are matched using the AND operator, while the ST images are matched by considering their absolute difference. Then, different schemes for match score fusion are tested.

A method based on a PCA analysis, followed by a Two-phase Test Sample Representation (TPTSR), is used in [352] for extracting the features from both the two-dimensional and three-dimensional samples. In particular, the TPTSR method uses a series of samples in the training phase, and is based on representing the features of each samples as a linear combination of the features of all the training samples. Then, the matching sample is searched among the nearest samples in the feature space.

The method described in [106] computes a binary image describing the palm lines from the MCI image, then uses the Competitive Code method to extract the orientation feature from the MCI. The AND operator is used to match the images describing the palm lines, while the angular distance between orientations is used in the Competitive Code method. Several match score fusion methods are tested.

A cross-correlation approach is used in [351] for matching the MCI images.

A local contrast measure is used in [358] for extracting the features from the two-dimensional and three-dimensional samples of the palmprint, and a PCA analysis is used to reduce the dimensionality of the feature space. Then, a method based on Hidden Markov Models is used to model the feature vector, and the Log-likelihood measure is used as the match score.

A method based on Linear Discriminant Analysis (LDA) is used in [359] to extract the features from the MCI image.

A method based on the analysis of the different depth levels of a three-dimensional model of the palmprint is described in [97]. In particular, a fixed number of isodepth curves is used to represent the sample, and the absolute difference between the values of the curves in each point of the shape is used as a match score.

4.5 CONTACTLESS PALMPRINT RECOGNITION

In this section, the methods that perform the palmprint recognition using contactless acquisition devices are reviewed. In particular, the acquisition procedure is considered without contact if the palm of the hand does not touch any surface. Some contactless systems, in fact, require the user to place the back of his hand on a surface. In this sec-

(a) (b)

Figure 4.38: The two-dimensional contactless acquisition device described in [360]: (a) the device; (b) example of a palmprint sample.

tion, both the contactless methods based on two-dimensional images, and the methods based on three-dimensional models are described.

4.5.1 TWO-DIMENSIONAL CONTACTLESS PALMPRINT RECOGNITION

The methods that perform the recognition of palmprint samples using a two-dimensional contactless acquisition device use CCD-based devices, such as cameras or video cameras. This category of systems do not require the contact of the palm with a sensor, and can use partially constrained setups (e.g., the back of the hand must be placed on a fixed support) or unconstrained setups (e.g., the hand does not touch any surface). Moreover, different constraints can be posed to the position and orientation of the hand with respect to the camera. In this section, the four different steps for palmprint recognition are analyzed: acquisition, segmentation and registration, image enhancement, feature extraction and matching.

4.5.1.1 ACQUISITION

Based on the type of illumination used, it is possible to divide the two-dimensional contactless acquisition techniques in two-categories:

1. CCD-based acquisition in visible light;
2. CCD-based multispectral acquisition;

CCD-BASED ACQUISITION IN VISIBLE LIGHT A semi-constrained contactless acquisition system is described in [360], and is based on a digital camera which captures the images of the hand at a resolution of 1280×960. In particular, the back of hand must be placed on a flat table with the fingers open. An image of the proposed system, and an example of the corresponding contactless acquisition, are shown in Fig. 4.38.

A similar acquisition method is used in [361, 362, 363]. The user needs to place the back of his hand on a flat surface, with the fingers separated. A digital camera with a resolution of 1024×768 is used to capture the images (Fig. 4.39).

The acquisition device used in [364] requires the user to place the back of the hand on a flat surface with a uniform background, and a digital camera placed in a fixed

Figure 4.39: Example of a two-dimensional contactless acquisition captured using the system described in [361].

(a) **(b)**

Figure 4.40: The two-dimensional contactless acquisition device described in [364]: (a) the device; (b) example of a palmprint sample.

position is used to capture the sample. The device and an example of the corresponding acquisition are shown in Fig. 4.40.

A device based on a tripod is described in [365, 366]. The acquisition is performed when the back of the hand of the user is placed on the surface beneath the camera (Fig. 4.41).

The method described in [367] uses a dark-colored enclosure with a digital camera mounted on top (Fig. 4.42a). The user must place the back of his hand on a flat surface, and a ring illuminator is used to enhance the visibility of the details of the palm. The images are captured at a distance of 350 mm with a 75 dpi resolution. An example of an acquisition is shown in Fig. 4.42b.

A contactless palmprint acquisition system is proposed in [368]. The system is composed by a webcam, a light source, and an enclosure used to partially control the position of the users' hand. However, the hand does not touch any surface. A warm (yellow) light source is used to enhance the pattern of the palmprint. The system is designed to capture 640×480 images at a 25 fps. An image of the system and the corresponding captured sample are shown in Fig. 4.43.

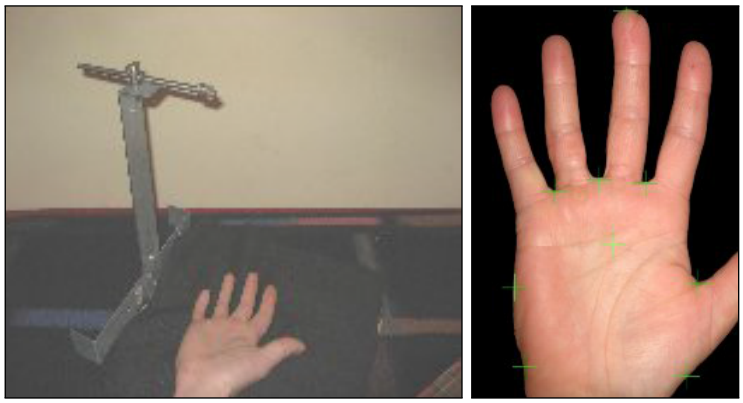

(a) (b)

Figure 4.41: The two-dimensional contactless acquisition device described in [365]: (a) the device; (b) example of a palmprint sample.

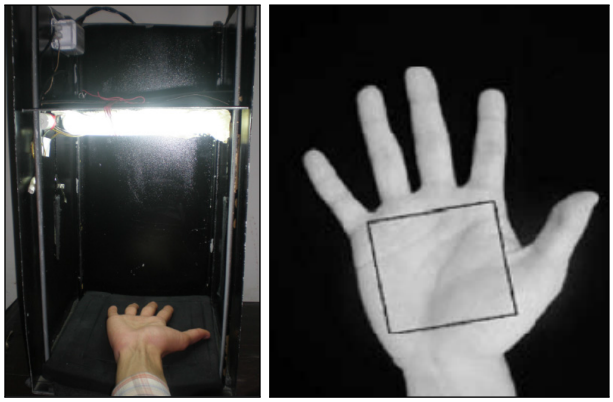

(a) (b)

Figure 4.42: The two-dimensional contactless acquisition device described in [367]: (a) the device; (b) example of a palmprint sample.

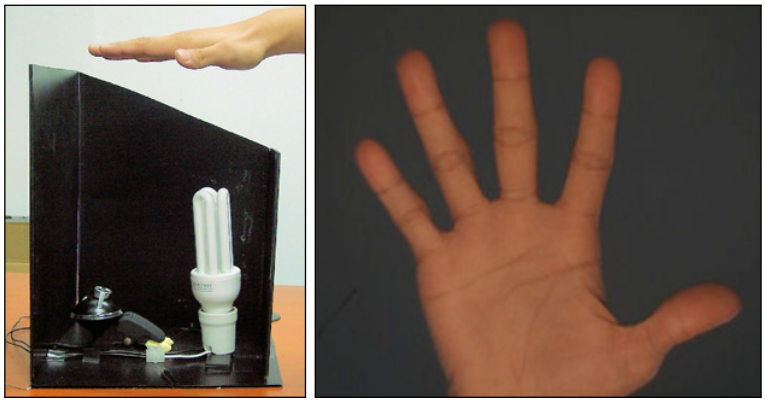

(a) (b)

Figure 4.43: The two-dimensional contactless acquisition device described in [368]: (a) the device; (b) example of a palmprint sample.

Figure 4.44: Example of a two-dimensional contactless acquisition captured using the system described in [369].

(a) **(b)**

Figure 4.45: Examples of unconstrained palmprint acquisitions captured using the devices used in [373]: (a) acquisition from a high distance; (b) acquisition from a shorter distance.

A webcam with a 640×480 resolution is used also in the method described in [369, 370, 371]. An example of a captured sample is shown in Fig. 4.44.

A method based on a webcam, which is used to collect frame sequences of a palm positioned in front of the camera, is described in [372].

An unconstrained acquisition setup based on a webcam is described in [373]. The method uses a webcam, which captures images with a 640×480 resolution, to collect the palms of the users. The position, orientation, and pose of the hand are unconstrained, and distances from 80 to 300 mm are possible. Moreover, the background and illumination are not controlled. Examples of acquisitions are shown in Fig. 4.45.

A method for the unsupervised acquisition of palmprints is proposed in [374]. The method can work using distances from 300 to 500 mm, with uncontrolled pose, background and illumination conditions. The imaging device has a resolution of 1024×768.

The unconstrained acquisition setup described in [375] uses a webcam with a 1600×1200 resolution, and performs the acquisition of the palmprint without requiring the

Figure 4.46: Example of a two-dimensional contactless acquisition captured using the system described in [375].

Figure 4.47: Example of a two-dimensional contactless acquisition captured using the system described in [376].

Figure 4.48: Example of a two-dimensional contactless acquisition captured using the system described in [377].

user to place his hand at a particular distance. However, the hand must be placed horizontally with the fingers spread apart (Fig. 4.46).

A digital camera-based acquisition device, which uses a resolution of 1792×1200, is used in [376]. An example of a captured sample is shown in Fig. 4.47.

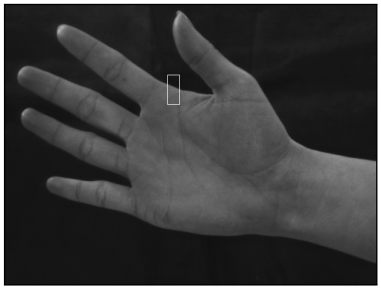

Figure 4.49: Example of a two-dimensional contactless acquisition captured using the system described in [380].

(a) **(b)**

Figure 4.50: The two-dimensional contactless acquisition device used in [381]: (a) the device; (b) example of a palmprint sample.

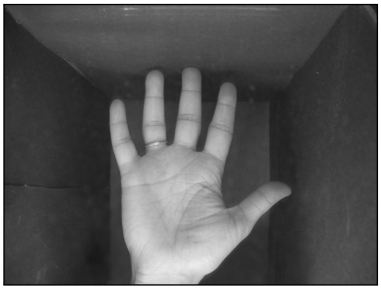

Figure 4.51: Example of a two-dimensional contactless acquisition used in [395].

The method described in [377, 378, 379] uses image captured with a digital camera at a resolution of 2048×1536 (Fig. 4.48).

A method based on a digital camera and a ring-shaped led illuminator is proposed in [380]. A uniform dark background is used to facilitate the segmentation process. An example of an acquisition is shown in Fig. 4.49

A database of contactless palmprint acquisitions, captured using an ad-hoc designed device at 96 dpi with a 640×480 resolution, is available at [381]. The device and a corresponding sample are shown in Fig. 4.50. Several methods in the literature [382, 383, 384, 385, 386, 387, 388, 389, 390, 391, 392, 393, 394] use this database.

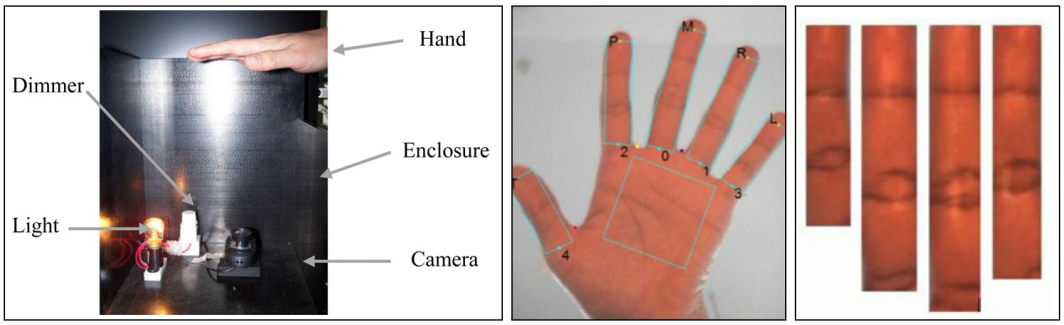

(a) (b) (c)

Figure 4.52: The two-dimensional contactless acquisition device used in [402] for capturing the palmprint and the knuckle print: (a) the device; (b) example of a palmprint sample; (c) example of a knuckle print sample.

A database of palmprints captured in a contactless way is available at [395]. In particular, the hands of the users are captured with differences in the pose of the hand during the acquisition. The used background and illumination are controlled. In particular, a circular fluorescent light is used to illuminate the palms, and a resolution of 800×600 is used to capture the images. An example of an acquisition is shown in Fig. 4.51. Several methods in the literature [130, 396, 397, 398, 399, 400, 401] use this database.

Mobile palmprint acquisition methods have been described in the literature. The use of a 100 dpi camera mounted on a PDA is proposed in [243]. A guided alignment procedure is used to capture the images with the correct position of the hand. Experiments on palmprint recognition performance using images captured with different mobile phones are proposed in [242, 241, 244, 228]. The method proposed in [240] combines palmprint and knuckle print features for the recognition using mobile devices.

Two-dimensional contactless palmprint acquisition systems have also been proposed in the context of multibiometric recognition systems.

The method proposed in [402, 403] captures both the palmprint and the finger knuckle using a low-cost webcam positioned with an upward orientation. The cameras captures a video stream at 30 fps, with a 640×480 resolution. A real-time algorithm is used to extract the ROI from the image. The device and an example of an acquisition are shown in Fig. 4.52.

In the literature, several methods propose acquisition setups that capture both the palmprint and the hand shape. In most cases, in fact, the hand shape can be captured without increasing the complexity of the acquisition system. In particular, several methods use an acquisition setup composed by a camera facing downwards, which require the user to place the back of his hand on a flat surface [360, 404, 405].

A less-constrained setup is described in [406] for the acquisition of the palmprint and the hand shape, and requires the user to position his hand vertically in front of the camera. Two common light bulbs are used for the illumination (Fig. 4.53).

(a) (b)

Figure 4.53: The two-dimensional contactless acquisition device used in [406] for capturing the palmprint and the hand shape: (a) the device; (b) example of an acquisition.

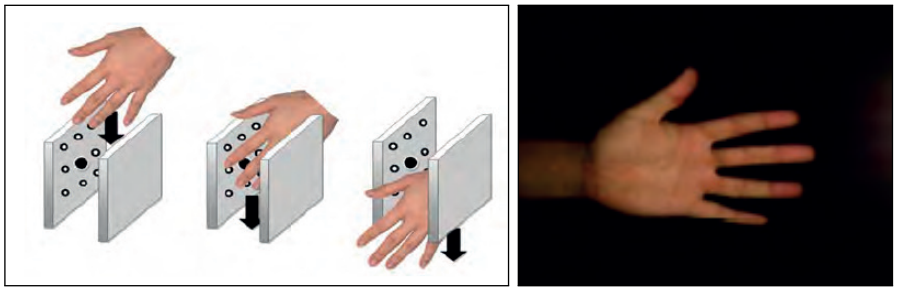

(a) (b)

Figure 4.54: The two-dimensional contactless acquisition device used in [407] for capturing the palmprint and the hand shape: (a) the device; (b) example of an acquisition.

The acquisition system described in [407] requires the user to pass his hand vertically from up to down with the palm facing rightwards, while multiple images are captured (Fig. 4.54).

In the literature, some multibiometric systems are proposed for combining palmprint features with features extracted from face acquisitions [408, 375], fingerprint [405, 409], and finger geometry [410].

CCD-BASED MULTISPECTRAL ACQUISITION An unconstrained contactless acquisition setup for the capture of multispectral palmprint images is proposed in [411]. The acquisition system is composed by two digital cameras, a CMOS camera working with natural illumination, and a NIR camera. Both environmental lighting and a NIR illuminator are used. The palm must be placed at a distance between 350 and 500 mm, and facing the camera with a direct angle. The device and an example of an acquisition are shown in Fig. 4.55.

Six groups of LED illuminators, ranging from violet wavelength to the near infrared, are used in [412]. The LEDs are positioned in a circular fashion for uniform illumination. In particular, the different wavelengths are absorbed by the skin at different levels, and enhance different details of the palmprint pattern. A public database containing

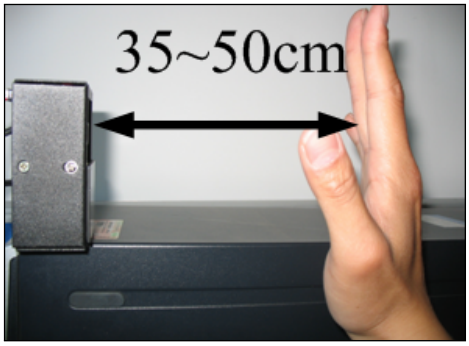

(a)

(b)

(c)

Figure 4.55: The two-dimensional contactless multispectral acquisition device used in [411] for capturing multispectral palmprint images: (a) the device; (b) example of a palmprint sample captured with the CMOS camera with environmental lighting; (c) example of a palmprint sample captured with the NIR camera.

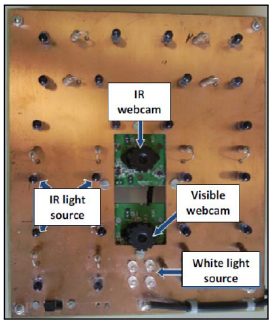

(a)

(b)

(c)

Figure 4.56: The two-dimensional contactless multispectral acquisition device used in [416] for capturing multispectral palmprint images: (a) the device; (b) example of a palmprint sample captured with visible light illumination; (c) example of a palmprint sample captured with the IR camera.

the multispectral acquisitions is available at [413]. Some methods in the literature use this database [414, 415].

Two webcams are used in [416] for a bispectral palmprint acquisition, respectively operating with visible light and with IR light. In particular, the IR webcam is a normal webcam, which was modified by removing the IR filter and using a visible light filter.

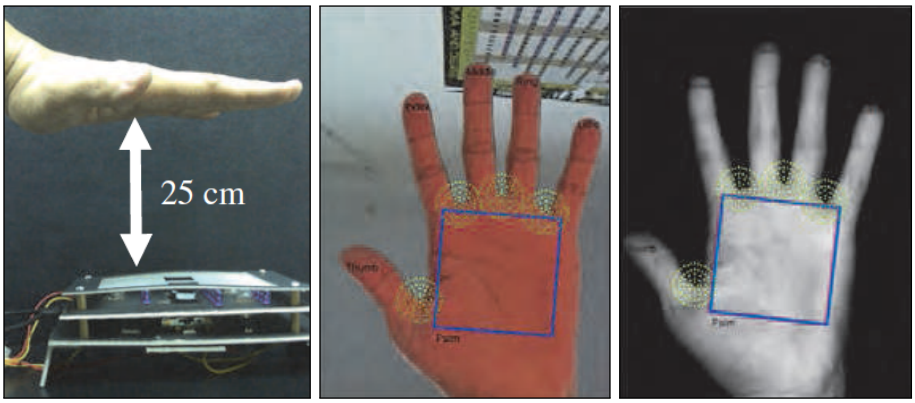

Figure 4.57: The two-dimensional contactless multispectral acquisition device used in [131] for capturing multispectral palmprint images: (a) the device; (b) example of a palmprint sample captured with visible light illumination; (c) example of a palmprint sample captured with the IR camera.

A white LED and a IR illumination are respectively used during the acquisition. The device and an example of an acquisition are shown in Fig. 4.56. A database of bispectral acquisitions is publicly available at [417].

Multibiometric systems based on multispectral palm acquisitions are also present in the literature. In particular, methods that combine palmprint and palm vein images are described. The method proposed in [131] is based on a contactless multispectral acquisition device which uses two cameras, one used for capturing images with visible light illumination, and one for capturing images with IR illumination. The second camera is a normal low-cost camera modified with a visible light filter. Both visible light and IR illuminators are used, and diffuser paper is used for a uniform illumination. The device and an example of an acquisition are shown in Fig. 4.57.

4.5.1.2 SEGMENTATION AND REGISTRATION

It is possible to divide the methods for the segmentation and registration of contactless palmprint acquisitions in methods used in the case of a uniform background, and methods used in the case of uncontrolled background. Moreover, methods for the registration and fusion of multispectral acquisitions have been proposed in the literature.

UNIFORM BACKGROUND In the case of acquisitions with uniform background and the fingers spread apart, the segmentation and registration methods are in most of the cases similar to the ones described in the Section 4.4.1.2 for contact-based acquisitions. In fact, the majority of the segmentation methods is based on a global thresholding in order to obtain the binary image, and on contour tracking algorithms used to find the intersection between the fingers. These intersections are used as reference points in order to extract the central square region of the palmprint.

The method described in [360] first binarizes the image using the Otsu's threshold, then uses an ellipse fitting method to compute the major axis and the orientation of the

hand. Then, a morphological erosion is performed, and the center of the eroded area is used as a reference point, in order to extract a square region containing the palm.

The method described in [368] uses a model of the skin color in order to segment the hand image from the background. In particular, the color of the skin is described by a Gaussian distribution of the color values, and the likelihood of each pixel to be a part of the background or the foreground is computed. A contour tracking algorithm is then used to detect the intersections of the fingers, which are used as reference points to extract the square region containing the palm.

A method based on Otsu's thresholding is described in [361]. After binarizing the image, the point corresponding to the middle of the wrist, and the points corresponding to the intersection of the fingers are used to align the image and to extract the central square region of interest.

The method described in [364] computes the line that intersects the four main fingers in eight points, and then extracts the position of the valley points corresponding to the intersections of the fingers.

The method described in [396] binarizes the image using a threshold computed based on the histogram of the image, then detects the valleys between the fingers and computes the line connecting the first and the last valley. The line is used as reference to extract the central square region of the palm.

A Hysteresis thresholding is used in [367], then the longest line passing through the palm is computed and used as reference to align the image, by comparing it with the direction of the major axis of the fitted ellipse. Then, a fixed-size area is cropped around the center of the hand.

The maximum inscribed circumference is used in [407] to determine the central region of the hand, then the inner square region is extracted.

The minimum circumscribed rectangle is used in [404] to segment the hand region in the image.

The method described in [406] binarizes the image using a threshold computed from the histogram, then a Sobel filter is used to detect and track the edge of the hand. The valleys between the fingers are used as the reference points in order to extract the central region of the palm.

A segmentation performed in the R channel is used in the method described in [375], since the images are captured on a green background. A contour tracking algorithm is used to detect the local minima and maxima of the border, corresponding to the fingertips and the valleys. The central region is extracted accordingly.

After the extraction of the valley points, a variable-size central region extraction is performed in [165], in order to account for differences in the size of the hand.

The method proposed in [415] binarizes the images, then uses a morphological closing operator to regularize the borders. A column-wise search for discontinuities is used to extract the position of the valleys, then the central region of the palm is extracted accordingly.

UNCONTROLLED BACKGROUND In the case of less-constrained or unconstrained acquisitions, different methods have been studied.

A method based on the extraction of reference points is used in [245] for aligning the hand images captured using an unconstrained setup. The method uses the intersection between the fingers as the initial reference points, which are increased by sampling the points extracted using an edge detector. A RANSAC algorithm is used to compute the alignment between the set of points.

A method based on a Multi-Layer Perceptron (MLP) is used in [374] for the segmentation of the hand images captured in unconstrained conditions, with an uncontrolled background.

A method based on a neural network is used in [369] for binarizing the input image, then a contour tracking algorithm is used to detect the fingertips and the intersections between the fingers. These points are used to extract the center of the palm image.

A neural network approach based on the YCbCr color space is proposed in [418] for the segmentation of the hand in situations when a complex background is present.

The method described in [373] is proposed for the real-time segmentation of palmprint images in the case of unsupervised acquisitions. First, an object detection algorithm is used to determine whether a hand is present in the image. Then, the histogram models of skin and non-skin regions are computed, and the Bayesian maximum likelihood is used to compute the probability of a pixel to belong to the foreground. A method based on an edge detector is used to compute the contour of the hand even in the case of non-spread fingers. Then, a contour tracking algorithm is used to find the positions of the valleys between open fingers, and possible candidates of the valleys between closed fingers. An analysis of the neighboring points is performed in order to determine the correct points. Then, a shape context descriptor is used to discard the false keypoints, and a central square region is then extracted, based on the position of the computed keypoints.

The method proposed in [240] uses a set of rules for the R, G, B values in order to segment the skin from an uncontrolled background, in the case of hand images captured using a mobile camera. A contour tracking algorithms is used to detect the fingertips and the valleys. Then, the image is aligned and the central square region is extracted.

A method for the segmentation of palm images captured using mobile devices is proposed in [228]. The method first binarizes the image using the Otsu's threshold, then the center of the wrist is computed, and the valleys between the fingers are detected. The position of the valleys is used to align the images to a horizontal orientation. Then, a rectangle corresponding to the lower side of the hand is extracted and enhanced using the Radon Transform. The position of the maximum value of the enhanced region is used to normalize the images to the same scale. Then, the center region of the palm image is extracted.

The method described in [241] analyzes the central region of the images, which is supposed to be occupied by the hand, in the nRGB color space. The median and variance of the intensity of the pixels in the central region is computed, and compared with the remaining pixels, in order to determine whether they belong to the foreground or the background. Then, a preliminary detection of the valleys is performed, and the lines from each valley to the finger border are computed. The most frequent orientation

is used as the reference orientation of the hand, and used to align the image. The position of the valleys is refined by searching a horizontal row with eight transitions. Then, the central region of the hand is extracted according to the position of the valleys.

The center of gravity of the palmprint images is extracted in the method described in [419], then a two-dimensional Hanning window is used to extract the central region. The DFT of the region is computed, and a correlation-based approach is used to align the images and to normalize the scale.

A cascade classifier is used in [411] to segment hand regions in unconstrained acquisitions. In particular, hand acquisitions with excessive in-plane rotations must be rejected. The AdaBoost algorithm is used to select the most distinctive Haar features from the learning dataset. The orientation of the image is computed by calculating its moments. Then, a morphological erosion is used to remove the finger regions, and the central rectangular region is extracted.

MULTISPECTRAL ACQUISITIONS The method proposed in [414] merges the images captured using a multispectral acquisition setup, in order to increase the recognition accuracy. In particular, the valleys between the fingers are used to coarsely align the images and extract the ROI. Then, the wavelet coefficients are merged in order to obtain a single image. A similar method is proposed in [412].

4.5.1.3 IMAGE ENHANCEMENT

Several methods are used in the preprocessing step, before the feature extraction process. In particular, the majority of the enhancement methods are based on derivative operators, Gabor filters, wavelet transforms, or Fourier transforms.

The Laplacian derivative operator, followed by a Gaussian low-pass filter, is used in [368] to enhance the details of the palm lines. The Sobel operator is used in [368, 363, 372, 420]. Other ad-hoc line detectors are used in [360, 405]. A local ridge enhancement method, based on a low-pass filter followed by a Laplacian operator, is used in [131] to enhance the palmprint and palm vein images.

Gabor filtering is used in [130, 369, 372, 375]. A circular Gabor filter is used in [370]. Gabor wavelets are used in [376].

Several wavelet transforms (Haar, Daubechies, Coiflets) are used in [361]. The Haar wavelet is used in [362]. The phase congruency of the wavelet response is used in [382] to enhance the edge and the lines of the palm. Wavelet-based enhancement methods are used in [366, 396, 367, 406, 400, 131].

The Discrete Fourier Transform is used in [364, 420, 419]. The DCT transform is used in [377, 421, 399, 392].

An enhancement method based on the combined use of Fourier Transform, Logarithm, DCT, and Wavelet transform is used in [383]. A regularization method based on Partial Differential Equations (PDE) is used in [371] to remove the noise in low-quality palmprint acquisitions. An adaptive histogram equalization technique, based on a Genetic Algorithm is proposed in [422]. A combination of wavelet transform and several Sobel operators with different orientations is used in [402].

A method for the correction of a non-uniform brightness in the acquisitions is proposed in [391]. The method is based on dividing the images into subregions, and computing the mean intensity value of each strip. The mean intensity map is interpolated in the entire image region in order to obtain a map of the reflections present. Then, the obtained map is subtracted from the original image.

A force field transformation is used in [393]. In particular, the force field transformation represents each pixel as exerting a force that is directly proportional to its intensity, and inversely proportional to the distance between the other pixels. Then, for each pixel the total force and orientation exerted by the remaining pixels is computed.

4.5.1.4 FEATURE EXTRACTION AND MATCHING

The methods used for the feature extraction and matching in two-dimensional contactless palmprint acquisitions can be divided using a classification similar to the one used in Section 4.4.1.4. In particular, five categories can be distinguished:

1. Line-based approaches;
2. Subspace-based approaches;
3. Statistical approaches;
4. Coding-based approaches;
5. Other approaches.

LINE-BASED APPROACHES The method proposed in [420] uses the Sobel operator to extract the palm lines, then the endpoints and cross points of the lines are computed and transformed in the frequency domain using the DFT. The resulting coefficients are matched using the Euclidean distance measure.

Four different line detectors are used in [360] to enhance and extract the palm lines, then the images are merged and the standard deviation of each subregion of the image is used to build the feature vector. The normalized correlation is used as a distance measure. A similar method, which uses the cosine similarity measure, is used in [405].

SUBSPACE-BASED APPROACHES The variance of each subregion of the images is used in [365], along with the response of the Haar wavelet. A PCA-based approach is used to reduce the dimensionality of the feature vector.

The DCT transform is used in [377] to enhance the image and extract the features, then the PCA is applied to reduce their dimensionality. A RBF Neural Network is used for classification.

Palm shape features, variance values of the subregions of the images, and the wavelet response are used in [366]. A Karhunen-Loève Transform (KLT) is used to reduce the dimensionality of the feature vector.

An approach based on Generalized Discriminant Analysis for feature extraction is used in [378].

A 2D PCA approach is used in [380] for the recognition of defocused palmprint acquisitions. A nearest neighbor classifier is used for matching.

A comparison between PCA, GDA, and LDA for palmprint recognition is proposed in [379].

LDA analysis is used in [410] to extract the features from palmprint, then a correlation-based approach is used to merge the palmprint features with features related to the finger geometry. The Euclidean distance is used for matching.

The 2D-DWT is used in [400] to enhance the image and extract the features, which are reduced using the PCA. The average sum of the squares of the distances between the feature vectors is used as the comparison measure.

STATISTICAL APPROACHES Local Binary Patterns are extracted from the Sobel-enhanced images in the method described in [368]. A Probabilistic Neural Network is used to classify the results.

A method based on the characteristic matrix as the distinctive feature for recognition is used in [423].

The energy values extracted from different wavelet transform applied to the image are used in [361] as the distinctive features. A neural network is used to compute the distance between different feature vectors.

In the method described in [371], a normalization approach is applied to each subregion of the image, then the intensity values of each region are used as features, and classified using a SVM-based method.

The energy values computed from the Haar wavelet transform of the image is used in [362]. The Euclidean distance is used to compare the features.

The entropy measure is used in [404] to characterize the statistical grayscale distribution of the images, and used as a distinctive feature. Both global and local entropy values for each subregion are computed. The Euclidean distance is used to measure the similarity between feature vectors.

The cohort information, obtained using multiple template comparisons per user, is used in [398] to enhance the recognition accuracy of the matching method based on ordinal features.

CODING-BASED APPROACHES A method based on matching the quantized responses of the Gabor filters, as proposed in [293], is often used in the literature [245, 238, 375] for matching contactless palmprint acquisitions.

The binarized response of different Sobel operators is used in [363] for representing the map of the dominant orientations of the palmprint images. The Hamming distance is used for comparing different samples. A similar method is applied in [131] for both palmprint and palm vein images, after decomposing the image using a wavelet transform. A SVM classifier is used for combining the match scores obtained with the two images.

The method described in [402] enhances the images using the wavelet transform, and uses the binarized response of the Sobel operator as the bit string used for matching.

A wavelet transform is used in [406] to enhance the details of the lines of the palmprint, then the response is encoded according to the local orientation. The Hamming distance is used for matching.

The use of Orthogonal Line Ordinal Features is described in [407]. In particular, orthogonal filters with different phase values are used to extract the orientation information of the palmprint. Then, the filter response is binarized and matched using the Hamming distance. Ordinal features are used in [411, 416] for the recognition of palmprints captured using an unconstrained, multispectral setup.

Steerable filters, that are based on a linear combination of oriented filters, are used in [388] to enhance the orientation of the palm lines. Then, the innovative distance measure proposed in [386] is used for matching palmprint acquisitions. In particular, it is shown that both the bitwise angular distance and the Hamming distance are particular cases of the proposed distance measure.

A symbolic representation of the palmprint images is proposed in [387] to efficiently encode the acquisitions. In particular, the proposed Symbolic Aggregate Approximation (SAX) converts a signal into a string of discrete symbols. The different symbols are generated with the same probability, by choosing threshold values that follow a Gaussian distribution. An ad-hoc distance measurement function is used to compare the resulting templates.

The method described in [391] segments the palmprint image in overlapping circular strips, which are averaged along their radial direction, in order to obtain a one-dimensional signal. Then, the Stockwell Transform is applied on the signal, and the phase differences between adjacent strips at the same location are extracted and binarized. The Hamming distance is used for matching.

The method proposed in [392] extracts overlapping rectangular blocks, with a particular orientation, from the palmprint images, then averages their intensities across the height in order to obtain a one-dimensional signal. The DCT transform is applied on each block, then the differences of the DCT coefficients in adjacent block are extracted and binarized. The Hamming distance is used as a measure of comparison.

A similar method, which uses the phase difference information computed from adjacent square blocks, is used in [394].

The Contourlet transform is used in [415] for palmprint recognition. In particular, the contourlet transform enhances the directional frequency information present in the image. Then, the dominant orientation at each image location is encoded. The templates are matched by counting the number of positive bits in common.

OTHER APPROACHES The method described in [383] enhances the images using a combination of Fourier Transform and logarithm operator, then uses the amplitudes of the DCT transform and the Haar wavelet transform as features. A neural approach is used to match the feature vectors from different acquisitions.

A feature extraction and matching method based on SIFT and Orthogonal Line Ordinal Features (OLOF) is used in [130]. The Euclidean distance is used to match the two sets of feature vectors, and a weighted sum is used to combine the two match scores. A similar method, which also compares different color spaces, is described in [424].

In the method described in [369], the Gabor-filtered image is convoluted with the features related to the shape of the hand. The result is binarized and the Hamming distance is used for matching.

A combination of Gabor Wavelet Networks (GWN) and Probabilistic Neural Networks is used in [376] for contactless palmprint recognition.

A string matching algorithm is used in [370] to match the palmprint acquisitions, after enhancing them with a Gabor filter.

The Fourier transform is used in [364] to enhance the images and extract the features of the palmprint. Then, a method based on RB K-Means and a hierarchical SVM classifier is used for classification.

The combination of wavelet features and Fuzzy features is used in [396]. In particular, the Fuzzy features are related to the cumulative difference between the intensity of the pixels in each subregion and the average intensity of each region.

The DCT transform is used in [421] to extract the features from several different color spaces. The Nearest Neighbor classifier is used for matching the feature vectors. A method based on 2D-DCT is used in [399].

The features extracted from several wavelet transform are concatenated in the method described in [367], and the Euclidean distance is used as a measure of comparison.

A set of three-value functions is used in [240, 244] to project the palmprint image onto the respective feature spaces. The dot product of each function and the palmprint is computed, and the results compose the feature vector. Different methods are used for the generation of the functions, in particular the random method, manual method, and PCA method are tested.

A comparison of subspace-based approaches (PCA, LDA), correlation approaches, and coding-based approaches (Ordinal Code, Competitive Code, and Line Orientation Code) is proposed in [228] for the recognition of palmprints captured using mobile devices.

SIFT features are used in the method described [389], which uses a matching procedure based on a KNN classifier, in order to compare the feature vectors.

A correlation-based method is used in [419] to match the phase information obtained by computing the DFT of the palmprint images.

A force field transformation is computed in [393] to enhance the details of the palmprint, then the orientation information of the force field is used as a distinctive feature. In particular, the Local Structure Tensor is used to describe the information related to the local orientation present in the image. A matching method based on the Euclidean distance is used to compare different acquisitions.

4.5.2 THREE-DIMENSIONAL CONTACTLESS PALMPRINT RECOGNITION

Currently, only few methods for the three-dimensional contactless palmprint recognition are proposed in the literature. In particular, methods that use three-dimensional laser scanners and methods based on structured light illumination are described. The advantages of three-dimensional contactless methods reside in the fact that they perform a more unconstrained recognition, since the position of the hand can be deter-

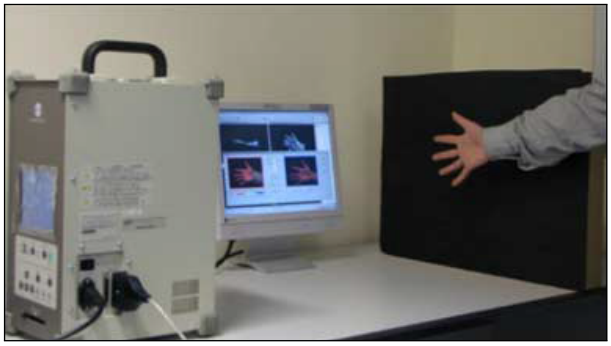

(a)

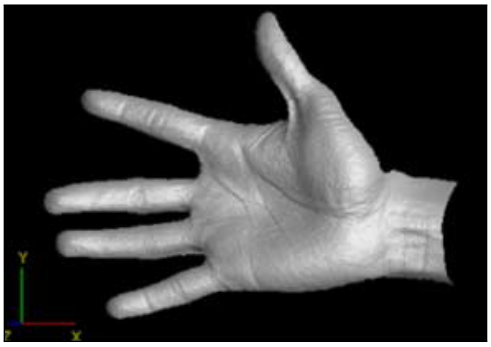

(b)

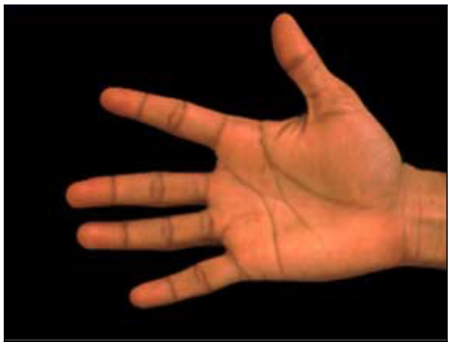

(c)

Figure 4.58: The three-dimensional contactless acquisition device used in [425]: (a) the device; (b) example of a three-dimensional model; (c) the corresponding color image.

mined in the metric space, and variations in the distance and orientation can be accurately measured. Moreover, a more accurate recognition is made possible with respect to two-dimensional contactless systems, because of the information related to the three-dimensional model of the hand. However, the acquisition setups are more complex and expensive, with respect to two-dimensional acquisition systems.

A framework for the contactless recognition using hand features is described in [425]. In particular, the method uses both two-dimensional and three-dimensional features are used, related to the palmprint, the hand geometry, and the finger geometry. The used acquisition device consists in a commercial 3-D digitizer, which is based on an illumination beam used to capture the light reflected from the surface. A triangulation procedure is used to compute the three-dimensional model, and a color image is simultaneously captured (Fig. 4.58).

The images and the models are captured with uncontrolled illumination conditions, and the position of the hand is unconstrained. However, subjects are asked to place the hand parallel to the image plane of the digitizer. A uniform background is used to facilitate the segmentation process. A size of 640×480 is used for both the color images and the three-dimensional models.

Then, the color image is binarized using the Otsu's threshold, and a contour tracking algorithm is used to extract the positions of the local minima and maxima of the boundary, corresponding respectively to the valleys and fingertips. Based on the posi-

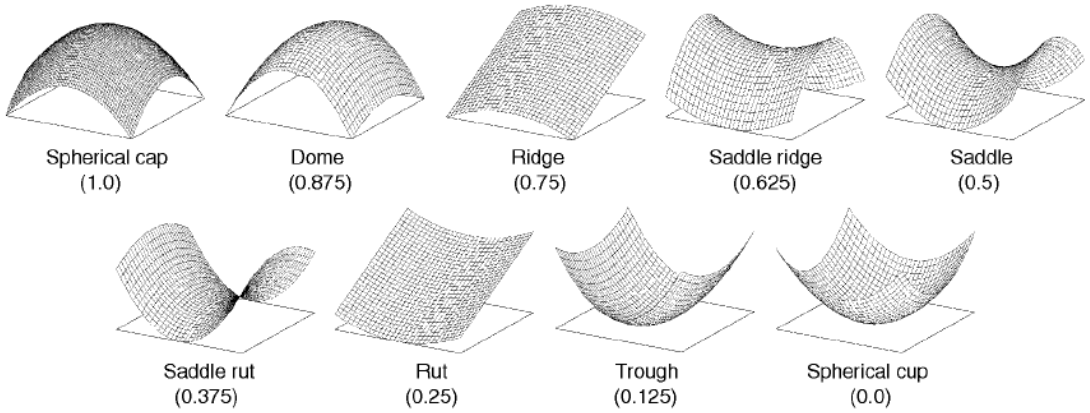

Figure 4.59: The nine possible shapes used in [425], and the corresponding Shape Index.

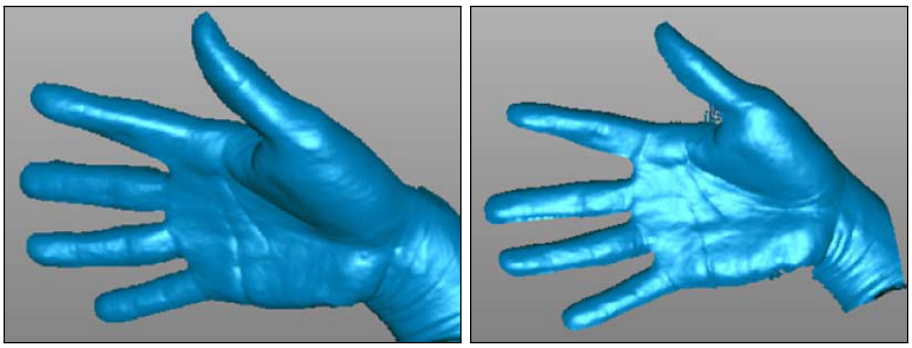

(a) **(b)**

Figure 4.60: The three-dimensional pose normalization method proposed in in [425]: (a) three-dimensional model of the hand before the normalization; (b) after the normalization.

tion of the valleys, a rectangular ROI of the palmprint is extracted from both the color image and the three-dimensional model.

Using the information of the three-dimensional shape of the palmprint, the principal curvature map of the palmprint is computed by fitting a surface over a local neighborhood of the image. The minimum and maximum values of the partial derivatives are computed, and used to construct a Shape Index (SI). According to the SI, nine possible surface categories can be defined (Fig. 4.59). Then, the SI relative to each pixel is encoded using a 4-bit string. This representation is called SurfaceCode, and a method based on the Hamming distance is used to compare different acquisitions.

The Competitive Code [295] feature extraction scheme is used for extracting the characteristics from the two-dimensional color image.

A similar acquisition and recognition method is proposed in [426], with the introduction of a technique for the normalization of the hand pose and orientation in the three-dimensional space. In particular, the center of the palm is located by computing the distance transform of the pixels of the segmented image, and a ROI with a fixed size is extracted. A plane is fitted using the position of the three-dimensional points of

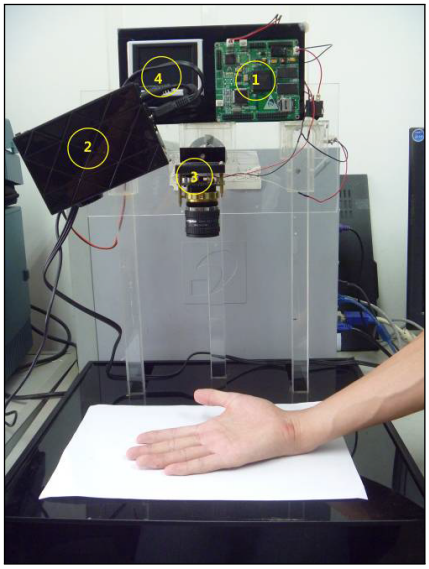

(a)

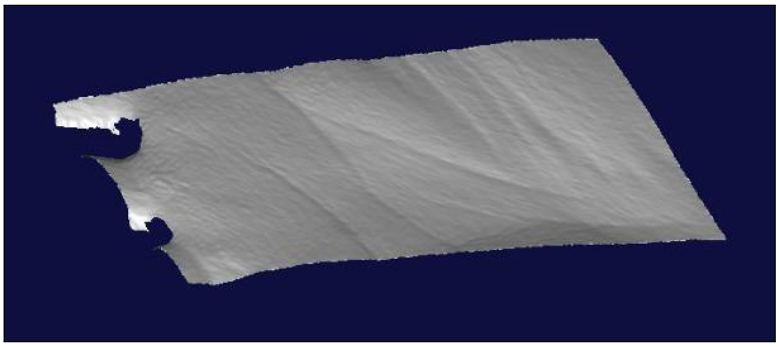

(b)

Figure 4.61: The three-dimensional contactless acquisition device used in [427]: (a) the device; (b) example of a three-dimensional model.

the ROI, and used to compute the orientation of the hand. Then, a rotation is applied to both the three-dimensional model and the image. An example of a model before and after the normalization of the hand pose is shown in Fig. 4.60.

An embedded three-dimensional surface measurement system is proposed in [427] for a contactless three-dimensional acquisition of the palmprint. In particular, the system uses a digital camera and a projector, and the reconstruction method is based on a structured light illumination technique. However, the hand of the user needs to be placed against a flat surface (Fig. 4.61).

4.6 QUALITY ESTIMATION OF PALMPRINT SAMPLES

Currently, only a few methods for the estimation of the quality of palmprint acquisitions are present in the literature.

The method described in [428] has the purpose of determining the least significant (fragile) bits in coding-based palmprint recognition approaches. In particular, fragile

Figure 4.62: The three regions of the palmprint defined in [429]: the region 3 near the thumb often has a lower quality.

bits occur when the inner product between the filter and the region of the image produces an output with a small magnitude. This can be caused by the particular structure of the palmprint region, by the used filtering scheme, by the quantization method, or by a combination of these factors. In particular, the method analyzes the recognition accuracy obtained using the Binary Co-occurrence Vector (BCOV) coding scheme [306], by removing the fragile bits corresponding to the filtered regions with low magnitude. It is demonstrated that, by removing the fragile bits, the recognition accuracy is increased.

A method for the quality estimation of palmprint samples, captured using inked impressions or using optical devices, is proposed in [429]. In particular, quality estimation techniques for contact-based palmprint samples are especially useful since very different pressures can be applied in the different parts of the palm. For example, the palm region near the thumb often presents a lower quality (Fig. 4.62).

The method divides the images into a set of blocks, and computes the quality indices for each block. In particular, the used indices are based on ridge continuity, ridge thickness uniformity, smudginess dryness, orientation certainty, ridge-valley frequency, and the special region index. The final quality value for each block is computed using a weighted sum, and the weights are computed using a linear regression technique.

4.7 PALMPRINT CLASSIFICATION

The classification of palmprint samples has the purpose of reducing the size of the database of samples that need to be compared in order to perform the recognition. In particular, efficient classification methods are useful for identification purposes. However, accurate classification methods can help in increasing the recognition accuracy also for applications that use authentication. In this section, the techniques for the classification of palmprint samples are reviewed.

The use of correlation filters for palmprint classification is proposed in [430]. In particular, correlation filters are a kind of filters that produces a sharp peak when correlated with a sample of the corresponding class, and a noisy output in the other cases.

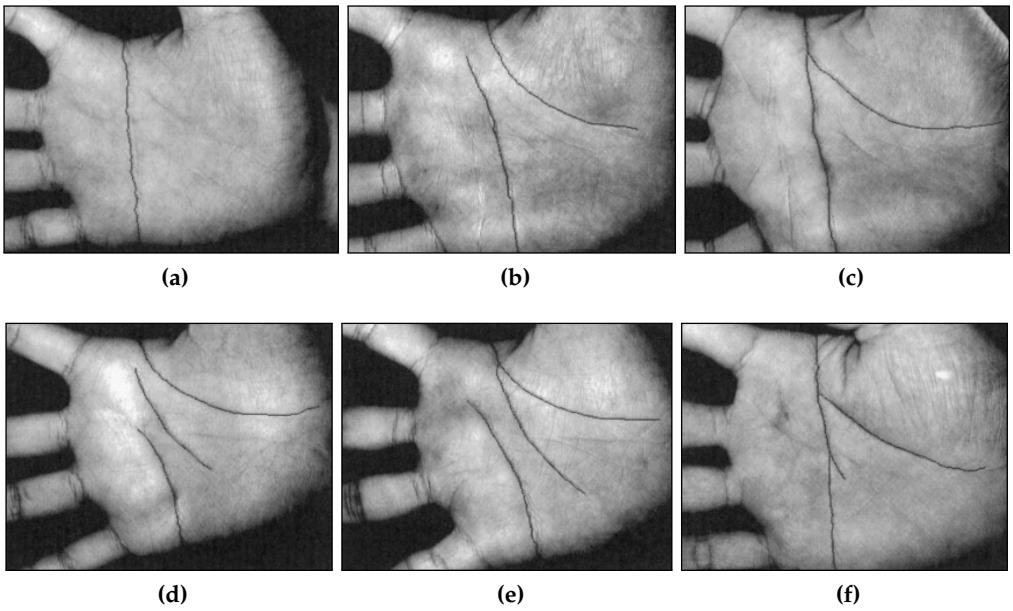

Figure 4.63: Examples of the six palmprint categories defined in [432]: (a) Category 1; (a) Category 2; (a) Category 3; (a) Category 4; (a) Category 5; (a) Category 6.

The method uses a line-based ROI extraction method, then extracts the lines of the palm using a phase-symmetry approach. Then, the energy output of the image containing the palm lines is computed, and the images with the highest energy are chosen for each class to train the correlation filters.

A classification method based on global features of three-dimensional palmprints is used in [431]. In particular, three global features are used for classification. The first feature is related to the maximum depth of the three-dimensional palmprint with respect to the reference plane, whose depth is computed as the mean depth of the three-dimensional palmprint. The second feature is computed by slicing the three-dimensional palmprint with horizontal planes at different depths. The area enclosed by each level curve is used as a feature. The third feature is computed by extracting the distance of each point lying on the contour of the level curve, and the corresponding centroid. This feature is used to describe the contour of each level curve. An LDA-based method is used to reduce the dimensionality of the feature vector, then an SVM-based method is used for the classification of the features.

An online palmprint classification scheme based on principal lines is described in [432]. First, the palmprint image is segmented and the main principal lines and their intersections are extracted using a method based on edge detectors. The number of the principal lines and the number of their intersections are used to classify the palmprints into six categories (Fig. 4.63). Since the category 5 is the most widespread, a method for the sub-classification of palmprints belonging to category 5 is proposed in [433].

A classification method based on the heart line (Fig. 4.4) is used in [434]. An edge detector based on the Sobel operator is used to extract the position of the heart line, then the palm image is divided into subregions, and the regions in which the heart

line is present are extracted and sorted. The set of regions crossed by the heart line is used as a feature vector for classification.

A method based on the curvature and the intersections of the heart and life lines is described in [435]. In particular, six categories are defined by considering three possible curvatures of the heart lines, and the presence or absence of an intersection between the heart and life lines.

The method proposed in [436] extracts the principal lines and a set of keypoints along the direction of the main lines. The position, direction, and energy of the keypoints are used for retrieving the set of similar palmprint samples. Moreover, a preliminary distinction between left and right palms is used to further reduce the set of possible matches.

A ridge-based method for palmprint classification is proposed in [437]. First, the palmprint image is registered according to a set of reference orientations, then the ridge orientation map and ridge density map are used for palmprint classification.

4.8 GENERATION OF SYNTHETIC PALMPRINT SAMPLES

In the literature, a preliminary study of a method for generating synthetic palmprint samples has been proposed in [438]. In particular, the generation of synthetic palmprint samples can reduce the time and cost needed for the collection of large databases.

The method is based on the extraction of the principal palm lines from a real palmprint image. Then, the wrinkles and ridges are synthetized, and combined with the principal lines in order to obtain the synthetic sample. Multiple images are generated starting from the obtained image, in order to compute several acquisition of the same individual.

First, a Canny edge detector is used to extract the principal lines from a real palmprint image. If the image has a low contrast or is too noisy, it is discarded. The real palmprint image is blurred in order to eliminate the principal lines, and a set of patches is extracted from the image. Then, the patches are combined in different ways to generate different synthetic images, and combined with the extracted principal lines.

In order to simulate different acquisitions of the same synthetic individual, with intra-class variations, deformation meshes are used to shift the position of the pixels in the image. A shifting of the grayscale values is used to simulate changes in the illumination, while Gaussian noise is used to simulate defects in the acquisition procedure.

4.9 SUMMARY

Palmprint recognition systems are a particular type of hand-based biometric systems, which have the advantages of featuring a good speed, a good accuracy, and a low intrusiveness. With respect to fingerprints, palmprint features can be extracted even from elderly people or manual workers. Moreover, palmprint recognition systems have a relatively big area usable for feature extraction, and can be realized with low-cost hardware.

Applications of palmprint recognition systems can be found in forensic and law enforcement scenarios, and in civil applications for access control, mobile authentication, or unconstrained recognition.

According to the level of detail, different features can be used for palmprint recognition, such as shape features, principal lines, wrinkles, singular points, or minutiae.

Palmprint recognition systems are usually based on five modules, which respectively perform the acquisition, the segmentation and registration, the enhancement, the feature extraction, and the matching.

According to the technique used in the feature extraction module, it is possible to divide the palmprint recognition methods in ridge-based approaches, line-based approaches, subspace-based approaches, statistical methods, and coding-based approaches.

Moreover, it is possible to classify the palmprint recognition methods according to the type of acquisition device. In particular, contact-based and contactless techniques can be distinguished, and each category can be divided according to the type of sample used. Both two-dimensional images and three-dimensional models can be used.

Two-dimensional contact-based acquisition methods can use ink-based acquisitions, latent palmprint lifting techniques, optical devices, digital scanners, or CCD-based acquisitions, both in visible and non-visible light. Structured light illumination systems, based on a CCD camera and a projector, are used for three-dimensional contact-based acquisitions. Contactless acquisition methods are based on CCD cameras, both using visible and IR light, while three-dimensional contactless acquisition methods are based on laser scanners. For each typology of acquisition device, the steps of segmentation, registration, enhancement, feature extraction and matching have been reviewed.

Quality estimation techniques are also present in the literature, based on the intensity of the Gabor filter response, or on the maps of the ridge orientation and frequency.

Methods for palmprint classification have been proposed in order to speed-up the recognition process, especially for identification scenarios. In particular, methods based on correlation filters, three-dimensional shape features, and the position and orientation of the principal lines are present in the literature.

A preliminary study on the generation of synthetic palmprint samples has also been proposed in the literature.

5

CONTACTLESS AND LESS-CONSTRAINED PALMPRINT RECOGNITION

In this chapter, innovative methods for a contactless and less-constrained palmprint recognition are described. In particular, the researched palmprint recognition system does not require the contact of the hand with any surface, nor the use of fixed positioning systems, and the only constraint imposed on the user requires that the hand is placed open facing the CCD cameras, and inside their field of view.

By not requiring a surface for the placement of the hand, it is possible to avoid the problems related to distortion, latent impressions, dirt, hygiene, or to cultural aspects. Moreover, the absence of a fixed required position for the hand increases the social acceptance and decreases the time needed for every acquisition. Differently from some methods in the literature, the users do not need to spread the fingers open in order to facilitate the segmentation process. The use of three-dimensional reconstruction techniques allows to compute a metric representation of the palmprint, independent of the distance and pose of the hand with respect to the camera.

Currently, both contact-based and contactless three-dimensional palmprint recognition methods are described in the literature. In particular, contact-based three-dimensional methods use a structured light illumination setup, composed by a CCD camera and a projector. Pegs are used to guide the hand in the correct position. Contactless three-dimensional methods are based on a laser scanner.

With respect to the contact-based three-dimensional palmprint recognition systems described in the literature, the researched methods use an original acquisition method, which does not use pegs to constrain the position of the hand, does not have the problems related to the contact of the palm with the sensor (distortion, dirt, latent impressions), is based on a simpler hardware setup with a lower cost (a projector is not required), and performs a faster capture of the image. With respect to contactless three-dimensional methods in the literature, the described methods require an acquisition setup with a lower cost (a laser scanner is not required), and perform a faster capture

of the image. The researched methods, in fact, perform a contactless three-dimensional acquisition using an innovative setup, which require only a two-view acquisition system and a led illumination.

Preliminary versions of the researched methods were studied for the design of a contactless fingerprint recognition system [103]. The research in the field of fingerprint recognition, in fact, is more advanced, and standard methods for the preprocessing, enhancement, quality estimation, and matching of fingerprint samples are available. Then, it was possible to use the available implementations of the standard methods in order to compare the samples, and focus the research on innovative methods for the contactless, less-constrained acquisition and processing of the fingerprints. Moreover, it was possible to compare the obtained results with the one obtained by using traditional contact-based fingerprint recognition systems, in order to evaluate the feasibility of the researched approaches. These methods, however, required a precise positioning of the finger, which needed to be placed on a flat surface in order to be correctly captured.

However, similar acquisition techniques and processing algorithms can be used in the case of fingerprints and palmprints, and the results obtained using the methods for the contactless fingerprint recognition enabled the extension of the implemented methods for the palmprint recognition: a feasibility study was conducted on samples captured by using a flat surface in order to control the acquisition distance from the camera. Subsequently, an innovative and less-constrained biometric system for the palmprint recognition was studied and implemented. In particular, the less-constrained approach does not need a flat surface and requires only that the palm is placed inside an acquisition volume. Moreover, the researched methods are more general, with respect to the ones researched for fingerprint recognition, and can be extended to include features related to fingerprints, finger knuckle, and hand shape. An outline of the performed research is shown in Fig. 5.1.

In this chapter, the preliminary methods for the contactless fingerprint recognition are introduced, then the palmprint recognition methods are presented. First, a feasibility study for a less-constrained recognition based on acquisitions performed at a fixed distance is described, then the innovative methods for the less-constrained recognition using acquisitions with uncontrolled distance are detailed. In particular, all the steps of the palmprint recognition systems are described, including the acquisition, the segmentation, the three-dimensional reconstruction, the three-dimensional model processing, the image enhancement, the feature extraction and matching.

5.1 PRELIMINARY RESEARCH IN CONTACTLESS FINGERPRINT RECOGNITION

Contactless less-constrained methods for fingerprint recognition were studied in the preliminary phases of the research, since standard implementations of the preprocessing, enhancement, and matching methods are available. Then, it was possible to compare the obtained results with standard contact-based methods, in order to evaluate the feasibility of the researched approaches.

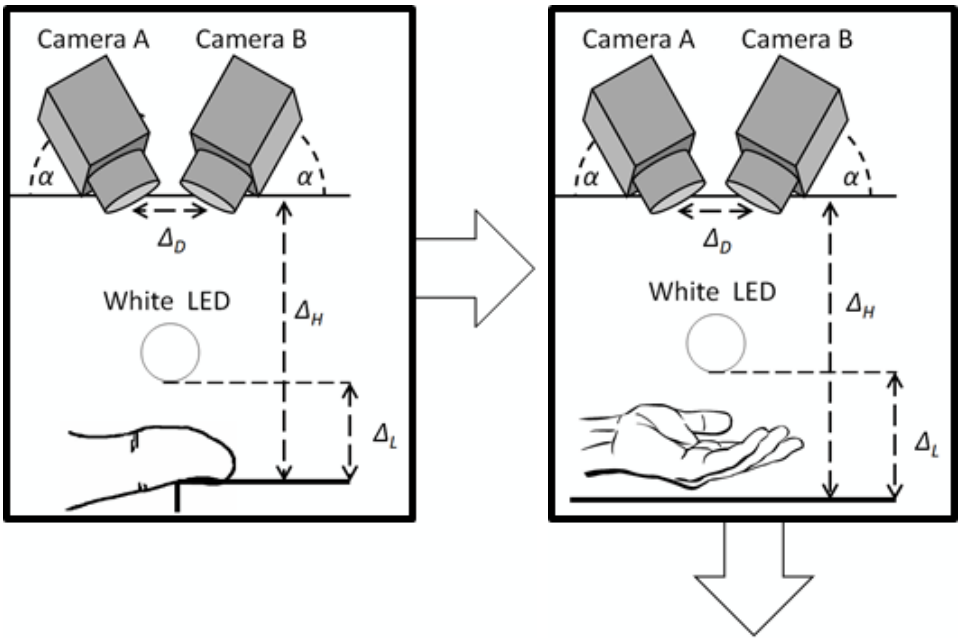

(a) (b)

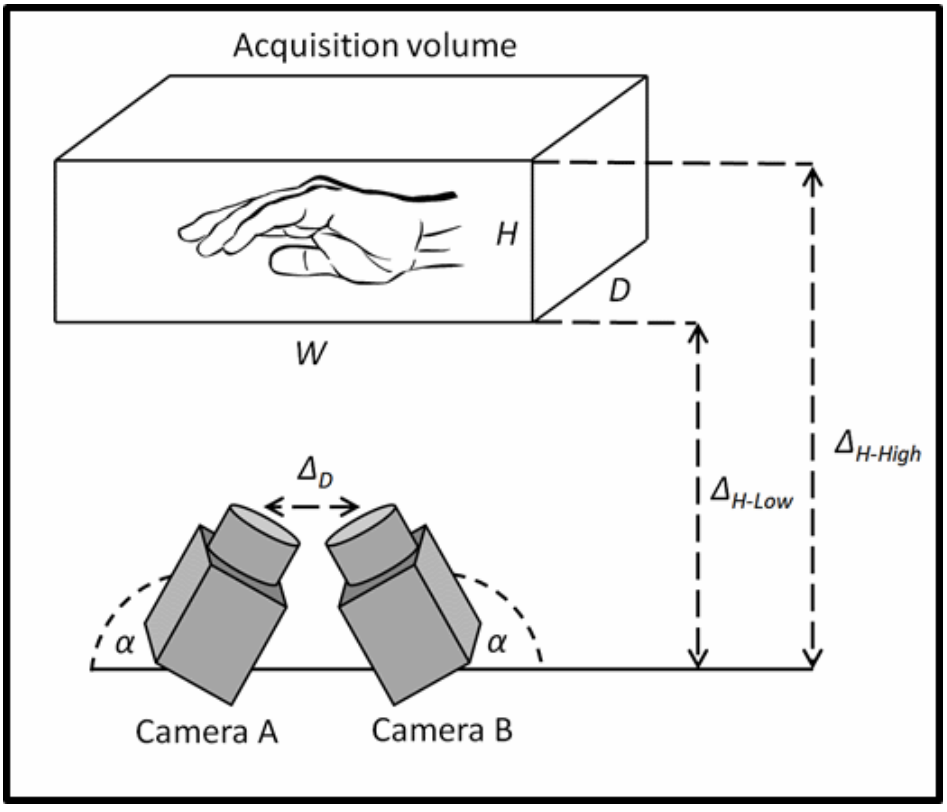

(c)

Figure 5.1: Outline of the performed research: the methods for the contactless fingerprint recognition (a) were extended to palmprint recognition using acquisitions performed at a fixed distance (b), then they enabled a less-constrained palmprint recognition with uncontrolled acquisition distance (c).

The researched method for the contactless fingerprint recognition consisted in the design and implementation of a fingerprint recognition system with absence of distortions, dust and dirt, without the possibility to extract latent impressions, and with a greater social acceptance. However, the researched methods left some problems open, such as the longer computational time needed, and the interoperability with traditional devices, which needed to be further studied.

The methods for the contactless fingerprint recognition can be divided into methods based on two-dimensional images, and methods based on three-dimensional models. The methods based on three-dimensional models can be further divided into methods that perform the recognition using three-dimensional templates, and methods that unwrap the three-dimensional model on a plane and perform the recognition using two-dimensional images. In particular, methods for every step of the biometric recognition were studied, including the acquisition, preprocessing, image enhancement, feature extraction and matching.

In this section, the preliminary methods for the contactless fingerprint recognition are described. First, the methods based on two-dimensional images are presented, then the methods based on three-dimensional models are described. Both the methods that use three-dimensional templates and the methods that perform the unwrapping of the model on a two-dimensional image are considered. The generation of synthetic three-dimensional fingerprint samples is also described, and a case study for the computation of the three-dimensional models of the fingerprints present on a clay artwork is presented.

5.1.1 CONTACTLESS TWO-DIMENSIONAL FINGERPRINT RECOGNITION

In this section, the methods for a contactless two-dimensional fingerprint reconstruction are presented. First, the contactless acquisition procedure is described, then the methods used for the enhancement of the image, the feature extraction and matching are described. Then, a method for the correction of the finger rotation is presented. An overview of the treated problems for the contactless two-dimensional fingerprint recognition is shown in Fig. 5.2.

5.1.1.1 ACQUISITION

The researched contactless two-dimensional acquisition setup is based on a CCD camera and led illuminator. For a correct acquisition, the finger must be placed on a flat surface at a distance to the camera equal to 220 mm. Different values for the camera angle were tested. No placement guides are needed, however a flat surface is necessary to place the finger at a fixed distance, since the depth of focus is narrow. In fact, the best results were obtained using lenses with a focal length of 25 mm, which resulted in a depth of focus equal to 6 mm.

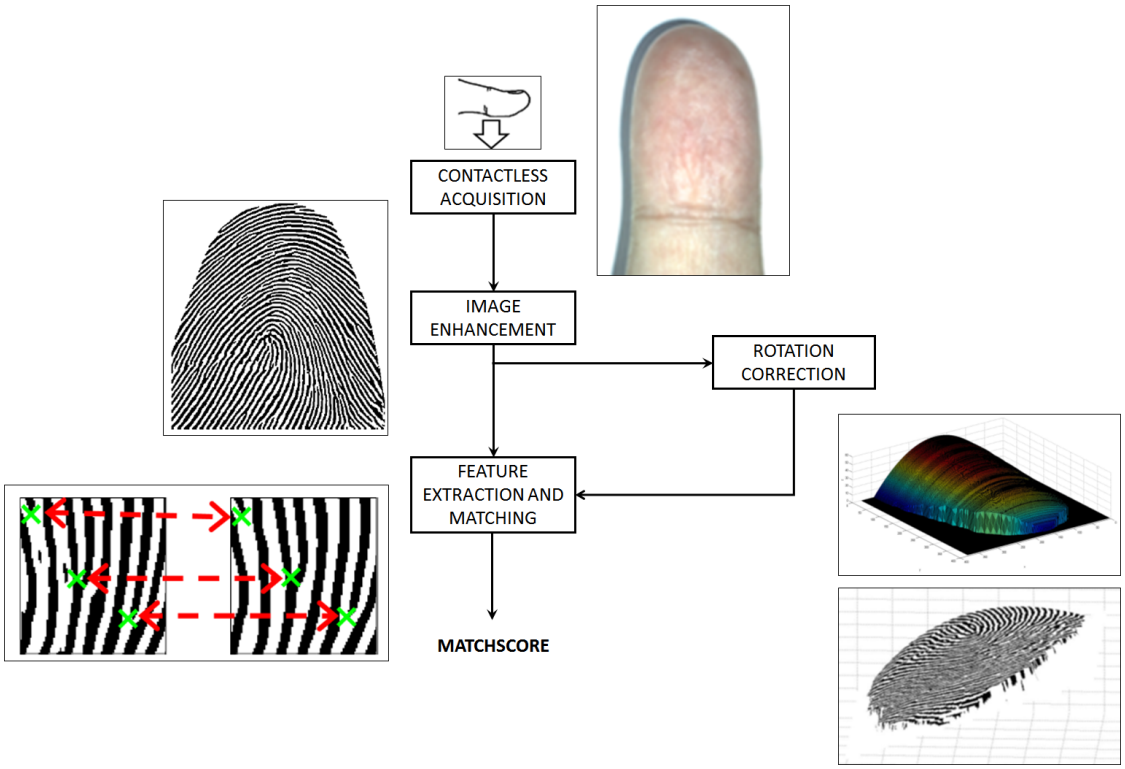

Figure 5.2: Overview of the treated problems for the contactless two-dimensional fingerprint recognition.

5.1.1.2 IMAGE ENHANCEMENT AND COMPUTATION OF THE CONTACT-EQUIVALENT IMAGE

The enhancement step has the purpose of increasing the contrast of the ridge pattern in order to compute an image that has the same high contrast between the ridges and the valleys, as the images captured using a contact-based sensor. In particular, two image enhancement methods were proposed, respectively for noisy and good quality acquisitions. Then, a resolution normalization step is applied.

IMAGE ENHANCEMENT FOR NOISY IMAGE ACQUISITIONS (E1) This method is based on the use of contextual filters and can be divided into four steps: ROI estimation, enhancement of the ridge visibility, enhancement of the ridge pattern, and image binarization.

The estimation of the ROI is performed using a method based on the local standard deviation of the image, then the shadow of the finger is removed using a thresholding operation. The ridge visibility is enhanced by first estimating the background I_B using a morphological operation, then removing it from the original image. The resulting image I_R is processed using a logarithm operator in order to reduce the noise.

The enhancement of the ridge pattern is performed by computing the ridge orientation and frequency map, then using a set of contextual Gabor filters, similarly to the method described in [439]. The obtained image is processed using a logarithm opera-

tion, obtaining the image I_I, then the histogram H is computed, and used to binarize the image, using the following equation:

$$I_B(x,y) = \begin{cases} 0 & \text{if } I_I(x,y) \leqslant \text{argmax}_i(H(i)) \\ 1 & \text{otherwise} \end{cases} , \tag{5.1}$$

where I_B is the resulting binarized image.

IMAGE ENHANCEMENT FOR GOOD QUALITY IMAGE ACQUISITIONS (E2) This enhancement method is based on ridge following and can be divided into three steps: ROI estimation, enhancement of the ridge visibility, enhancement and binarization of the ridge pattern.

The first two steps are the same used in the method E1, while the third step is performed using the enhancement and binarization method implemented in the NIST MINDTCT software [440]. This method is able to compute the binary image I_B from the image I_L by evaluating the shape of every ridge in the image.

RESOLUTION NORMALIZATION A normalization procedure is applied in order to obtain images with a 500 dpi resolution. Since the images are captured with a fixed distance to the camera, and the image plane is perpendicular to the camera optical axis, it is possible to compute the normalization factor n_f as:

$$n_f = \frac{i_x}{r_x \cdot 500} , \tag{5.2}$$

where i_x is the number of pixels in the image in the horizontal direction, corresponding to r_x inches in the horizontal direction of the captured area.

5.1.1.3 FEATURE EXTRACTION AND MATCHING

Different methods for the feature extraction and matching were researched. In particular, methods based on the analysis of the Level 1 features and Level 2 features, described in Section 2.3, were studied.

ANALYSIS OF LEVEL 1 FEATURES The detection of the principal singular point is crucial in fingerprint recognition methods based on a reference point, or for the methods that perform the fingerprint classification.

A method for the estimation of the position of the principal singular point in contactless fingerprint acquisitions, using computational intelligence techniques, was researched [147]. In particular, the method performs the estimation of the ROI and the image enhancement using the method E1 described in Section 5.1.1.2, then uses the Poincaré index [441] to compute a list of possible principal singular points. A set of features is extracted for every point, including the fingerprint class, the position of the point in different coordinate system, and the quantity of information contained in every corresponding region. A computational intelligence approach is used to clas-

sify the features and estimate the position of the principal singular point among the possible candidates.

ANALYSIS OF LEVEL 2 FEATURES The majority of contact-based fingerprint recognition systems perform the biometric recognition using Level 2 features, which consist in the position and orientation of the minutiae points. In particular, the NIST algorithm MINDTCT [440], is used for the extraction of minutiae points. Moreover, the MINDTCT algorithm can be applied also on contactless fingerprint acquisitions, after computing the contact-equivalent image using the image enhancement steps E1 or E2 described in Section 5.1.1.2. Then, the NIST BOZORTH3 [440] algorithm is used to match the extracted minutiae. The algorithm is based on searching a path linking the pairs of minutiae with corresponding distances and orientations in the two images.

5.1.1.4 CORRECTION OF FINGER ROTATIONS

A method for the correction of the finger rotations in two-dimensional contactless acquisitions was researched [79]. The method is based on the computation of an approximated three-dimensional shape of the finger and on computational intelligence techniques. The method can be divided into two phases: an enrollment phase, and a verification phase.

In the enrollment phase, a contactless acquisition is performed, then the image is enhanced and the contact-equivalent image is computed using the enhancement method E2 described in Section 5.1.1.2. Then, a general parametric three-dimensional model of the finger shape is computed and adapted to the silhouette of the captured finger. A set of rotated finger acquisitions is computed by rotating the three-dimensional model with different angles, and interpolating the pixel values in the new coordinates corresponding to the each rotated model. From each rotated image, a set of features is extracted. In particular, the used features are related to the asymmetry of the silhouette shape, and to the intensity of the Gabor filtered image.

During the verification phase, the captured image is processed using the enhancement method E2, then a set of features is extracted from the image. Combined feature sets are obtained by merging the feature set with every feature set obtained from the corresponding rotated templates computed in the enrollment phase. A neural approach is used to classify the combined feature set in order to estimate the rotation angle between the acquisitions. Then, the template with the corresponding rotation angle is used to perform the matching. In particular, the method based on the analysis of Level 2 features described in Section 5.1.1.3 is used to compare the templates.

5.1.2 CONTACTLESS FINGERPRINT RECOGNITION USING THREE-DIMENSIONAL TEMPLATES

In this section, the researched methods for the contactless fingerprint recognition using three-dimensional templates are described. First, the multiple-view setup calibration and acquisition procedure are introduced, then the preprocessing algorithms and the three-dimensional reconstruction method are presented. The method used for un-

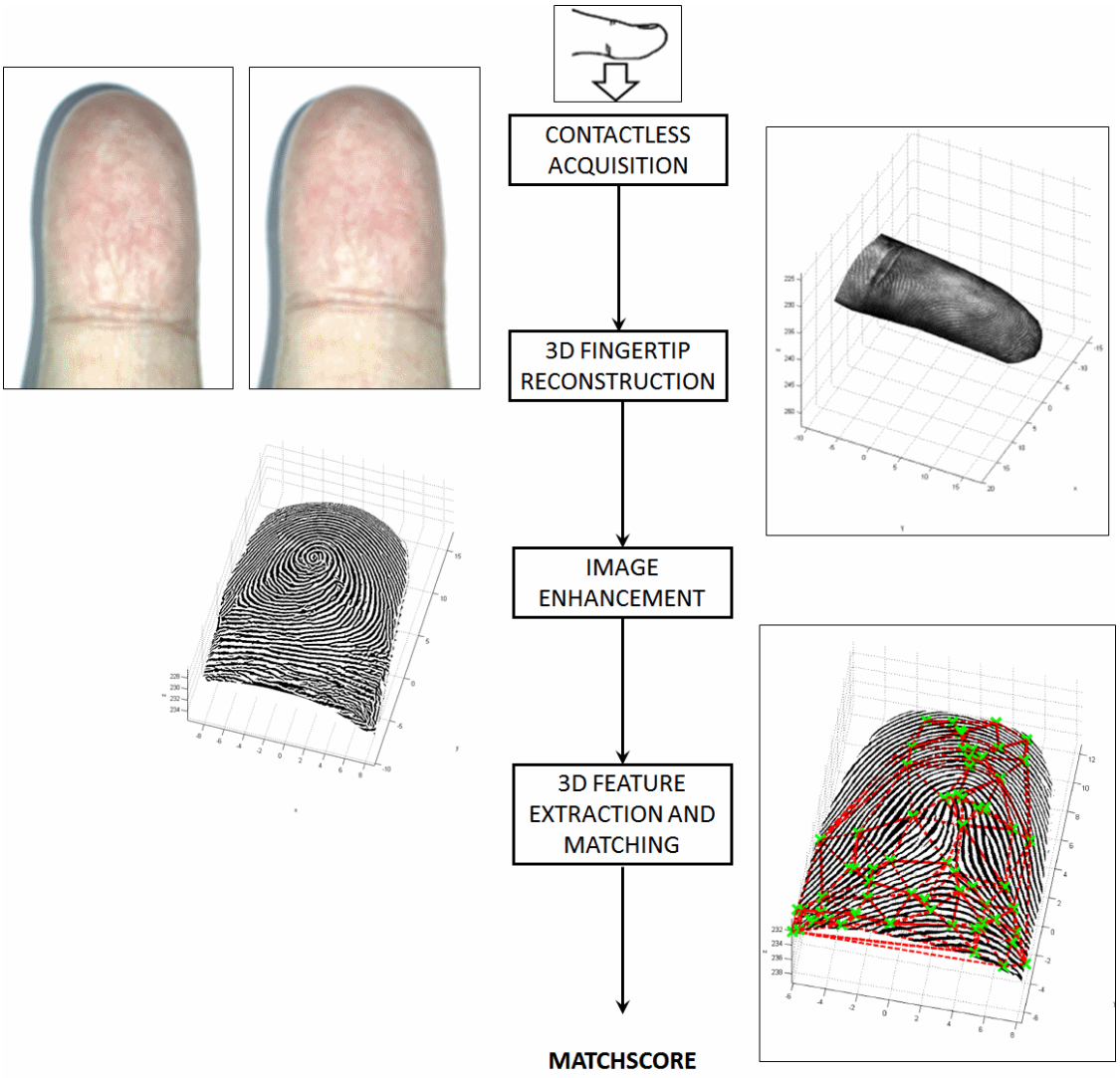

Figure 5.3: Overview of the treated problems for the contactless fingerprint recognition using three-dimensional templates.

wrapping the three-dimensional models is described, followed by the used image enhancement and feature extraction methods. An overview of the treated problems for the contactless fingerprint recognition using three-dimensional templates is shown in Fig. 5.3.

5.1.2.1 CAMERA CALIBRATION

The calibration of the multiple view setup is performed off-line once before the acquisition step. A plain chessboard was used as a calibration object, and captured with multiple orientations. A corner detection algorithm is used to extract the position of the corners in every acquisition, then the algorithms described in [442, 443] are used to compute the intrinsic and extrinsic parameters of the multiple view setup. A Direct Linear Transformation (DLT) method [444] is used to compute the homography matrix.

5.1.2.2 ACQUISITION

The acquisition setup is composed by two CCD cameras and an illuminator. The image acquisition procedure requires that the fingerprint is placed still on a flat surface, and in the overlapping field of view of the two cameras. No finger placement guides are needed, and uncontrolled yaw and roll orientations are possible. A synchronized two-view acquisition is used to capture the images.

In particular, three illumination methods were researched:

- *Method A*: an image with a regular pattern is projected on the finger, in order to simplify and speed up the reconstruction process. The pattern is composed by squares with alternate green and blue colors, computed starting from a uniform RGB image. The particularity of the pattern is that it is possible to recover both the squares and the original image from a single acquisition. This illumination scheme permits a fast and robust three-dimensional reconstruction. However, a DLP projector is needed [102].

- *Method B*: a white led light is used to illuminate the finger. This illumination scheme has a lower cost, but introduces the possibility of reflections and shadows in the acquisitions.

- *Method C*: a diffused blue led light is used to illuminate the finger. A blue wavelength is proved to better enhance the details of the fingerprint [445]. This illumination scheme is able to obtain good quality images, with a better visibility of the ridge pattern with respect to Method A and Method B.

5.1.2.3 IMAGE PREPROCESSING

Different preprocessing methods were studied according to the illumination method used in the acquisition step. In the case of Method A, the fingerprint image can be obtained by summing the G and B channels of the captured image, then two thresholds are used to segment the finger region.

The projected square pattern is obtained by subtracting the B channel from the G channel, then a thresholding operation and a morphological analysis are used to compute the centroids of the squares.

A similar segmentation method, based on two thresholds, is used to segment the images captured using the Method B, while a simpler Otsu's based thresholding is used to segment the images captured using Method C.

5.1.2.4 THREE-DIMENSIONAL FINGERTIP RECONSTRUCTION

The method used for the three-dimensional reconstruction is based on the extraction and matching of a set of equally spaced reference points. After a refinement step, the calibration information of the cameras is used to triangulate the matching points in the three-dimensional space. Linear interpolation techniques are used to compute a three-dimensional surface model describing the fingertip and the corresponding texture image [102, 446].

EXTRACTION AND MATCHING OF THE REFERENCE POINTS In the case of the acquisitions performed using Method A, only the centroids of the squares are considered and used as reference points, while in the case of Method B and Method C a downsampling procedure with a fixed step is used to extract the set of points in the left image F_A.

For each point x_A that belongs to the left image F_A, a preliminary matching point X_{BH}, belonging to the right image F_B, is computed in homogeneous coordinates by considering the homography matrix H:

$$X_{BH} = H X_B \ , \tag{5.3}$$

where X_{BH} is the preliminary matching point expressed in homogeneous coordinates:

$$X_{BH} = \begin{bmatrix} X & Y & W \end{bmatrix}^T \ . \tag{5.4}$$

The preliminary matching x_{BH} in Cartesian coordinates is computed as follows:

$$x_{BH} = \begin{bmatrix} \frac{X}{W} & \frac{Y}{W} \end{bmatrix}^T \ . \tag{5.5}$$

The preliminary matching points are refined by searching the best cross-correlation coefficient value between a $l \times l$ window centered in x_A and a $l \times l$ window sliding in a $H \times W$ rectangular region centered on x_B. The cross-correlation coefficient is computed as:

$$r = \frac{\sum_m \sum_n (A_{mn} - \bar{A})(B_{mn} - \bar{B})}{\sqrt{(\sum_m \sum_n (A_{mn} - \bar{A})^2)(\sum_m \sum_n (B_{mn} - \bar{B})^2)}} \ , \quad 1 < m < l, \ 1 < n < l \ , \tag{5.6}$$

where A and B are the two windows of size $l \times l$.

REFINEMENT OF THE MATCHED POINTS The matched points are refined in order to remove the outliers. In particular, different methods are used in the case of acquisitions performed using Method A, Method B, or Method C.

In the case of acquisitions performed using Method A, a RANSAC algorithm is used to fit a homography between the matching points [447]. Then, the pairs of points discarded by the RANSAC algorithms are eliminated.

The Euclidean distance between the pairs of matching points is computed, and the pairs for which their distance exceeds the mean global distance plus the global standard deviation of the distances, are discarded.

In the case of Method B, the pairs of matching points pertaining to the same column of F_A are stored in the vector V_C, which is interpolated using a third order polynomial. If the difference between the value in V_C and the interpolated value at the corresponding position exceeds a threshold, the pair of points is discarded. Then, the Euclidean

distance between the pairs of matching points is compared with the global mean and standard deviation values of the distances.

In the case of Method C, the Euclidean distance is compared with the global mean and standard deviation values of the distances, then a thin plate spline is applied to the set of corresponding points. This method performs a smooth and accurate filtering of the points. However, the amount of outliers must be low.

POINT TRIANGULATION AND SURFACE ESTIMATION The two-dimensional coordinates of the matching points are normalized using a rectification procedure, then the three-dimensional coordinate corresponding to each pair of matching points is computed using the triangulation formula [448]:

$$z = \frac{fT}{x_A - x_B} \tag{5.7}$$

where f is the focal length of the two cameras, T is the baseline distance between the two cameras and x_A and x_B are the two matched points.

A linear interpolation with a constant step s_{interp} is used to compute a dense three-dimensional surface model of the fingertip. Three-equispaced maps M_x, M_y, M_z are computed in order to describe the surface. The same interpolation is applied to the image F_A in order to compute the texture M_T of the three-dimensional model.

5.1.2.5 TEXTURE ENHANCEMENT AND COMPUTATION OF THE CONTACT-EQUIVALENT IMAGE

The texture M_T is processed using the image enhancement methods described in Section 5.1.1.2, in order to compute a contact-equivalent image. In particular, the textures of the models computed using the Method A and Method B are processed using the enhancement method E1. On the contrary, the textures of the models computed using the Method C, since they present a lower level of noise, are processed using the enhancement method E2.

5.1.2.6 FEATURE EXTRACTION AND MATCHING

The NIST software MINDTCT is used to extract the positions and orientations of the minutia points from the enhanced textures. Then, the maps used to describe the three-dimensional surface of the fingertip are used to compute the three-dimensional coordinates of the minutiae points, using the following formulas:

$$x = M_x(x_M, y_M) \;\; ; \;\; y = M_y(x_M, y_M) \;\; ; \;\; z = M_z(x_M, y_M). \tag{5.8}$$

Then, a six-element vector (i, x, y, z, θ, q) is used to describe each minutia, where i is an identifier, (x, y, z) are the three-dimensional coordinates, θ is the orientation, and q is the quality value. Since the areas near the borders of the fingertip models can be noisy, only the minutiae which have a quality q greater than a fixed threshold, and with the minor distance to the centroid of the fingertip, are considered.

Then, a two-dimensional Delaunay triangulation is computed using the positions of the minutiae, and the resulting set of triangles is used as template. In particular, each triangle of the computed triangulation is represented by a four-element set (I, L, θ_{max}, C) where I is a vector representing the coordinates of the three vertices, L contains the lengths of the facets, θ_{max} is the maximum angle of the triangle, and C contains the three-dimensional coordinates of the incenter of the triangle.

The matching of the three-dimensional templates is performed by first searching the pairs of similar triangles, then by using the corresponding triangles to align the minutiae. Finally, the minutiae are matched and the match score is computed.

The triangles pertaining to the two templates T_1 and T_2 to be matched are compared using the formula:

$$\begin{aligned} &|L_2(j) - L_1(i)| < s_L \ , \\ &\min(|\vartheta_2(j) - \vartheta_1(i)|, (360 - |\vartheta_2(j) - \vartheta_1(i)|) < s_O \ , \end{aligned} \tag{5.9}$$

where $L_1(i)$ and $L_2(j)$ represent respectively the lengths of the facets of the i-th triangle in template T_1, and of the j-th triangle in template T_2. The values $\vartheta_1(i)$ and $\vartheta_2(j)$ represent the orientations of the corresponding minutiae, and the thresholds s_L and s_O are empirically chosen.

Each pair of similar triangles is used to estimate the rototranslation between the three-dimensional coordinates of the two templates T_1 and T_2. In particular, for each pair of triangles the corresponding aligning rototranslation is performed, and the rotation coefficient is computed. The rotation coefficient is defined as the average difference between the orientations of the minutiae, after the rototranslation.

Then, the minutiae of the template T_2 are aligned according to the rotation coefficient, and translated according to the difference between the coordinates of the incenter of the triangles. For each rototranslation, the pairs of corresponding minutiae are searched by comparing their coordinates (x, y, z) and orientations Θ according to the formulas:

$$\begin{aligned} &\sqrt{(x_1(i) - x_2(j))^2 + \quad (y_1(i) - y_2(j))^2 + (z_1(i) - z_2(j))^2} \ < s_D \ , \\ &\min(|\Theta_1 - \Theta_2|, (360 - |\Theta_1 - \Theta_2|)) < s_\vartheta \ , \end{aligned} \tag{5.10}$$

where s_D and s_ϑ are threshold values empirically chosen.

The final match score m is computed based on the maximum number N_m of matching minutiae:

$$m = \frac{2N_m}{N \times M} \ , \tag{5.11}$$

where N and M are the numbers of minutiae respectively present in the templates T_1 and T_2.

5.1.3 CONTACTLESS FINGERPRINT RECOGNITION BASED ON UNWRAPPED THREE-DIMENSIONAL MODELS

In this section, the methods for the contactless fingerprint recognition based on the unwrapping of the three-dimensional models are described. In particular, the three-dimensional model and the corresponding texture are computed as described in Section 5.1.2, then an unwrapping procedure is used to map the three-dimensional model on a two-dimensional image. Image enhancement techniques are used to compute the contact-equivalent images, and computational intelligence techniques are used for the quality estimation of the enhanced images. Then, a feature extraction and matching method based on the analysis of Level 2 features is used. An overview of the treated problems for the contactless fingerprint recognition based on unwrapped three-dimensional models is shown in Fig. 5.4.

5.1.3.1 UNWRAPPING OF THE THREE-DIMENSIONAL FINGERTIP MODELS

The unwrapping procedure has the purpose of computing a two-dimensional image similar to rolled fingerprint acquisitions, in order to process it using state-of-the-art algorithms designed for two-dimensional contact-based images.

In particular, the researched unwrapping method is detailed in [102] and is similar to the one described in [153]. The method is based on the approximation of the finger shape with circles of different radii.

First, the maps M_x, M_y, M_z are used to compute a circular approximation for every y coordinate of the model by using the Newton method. The resulting vectors V_{x1}, V_{z1} are used to describe the center of the circles. The centers exceeding the median value by more of a fixed threshold are discarded, and a first order polynomial is used to approximate the resulting vectors, in order to obtain V_x, V_z.

The vector V_r describing the radii of the circles is computed by considering, for every y coordinate of the model, the average distance between the center of the corresponding circle, and the points belonging to the model with such y coordinate. A third order polynomial is used to approximate the vector V_z.

Then, for every column y, the intensity of the texture M_T is mapped into the approximated circle, resulting in the vector I_y. A linear interpolation is used to merge the vectors in the unwrapped image I_U. In particular, an interpolation step of 0.0508 mm is used to obtain a resolution of 500 dpi on the X axis. A 500 dpi resolution on the Y axis is obtained by sampling the approximating circle using a step equal to $(360/\text{perimeter}) \times 0.0508$.

5.1.3.2 TEXTURE ENHANCEMENT AND COMPUTATION OF THE CONTACT-EQUIVALENT IMAGE

The unwrapped image I_U is processed using the image enhancement methods described in Section 5.1.1.2, in order to compute a contact-equivalent image. Similarly to the enhancement method used for computing the contact-equivalent image from the texture M_T, as described in Section 5.1.2.5, the unwrapped images corresponding to

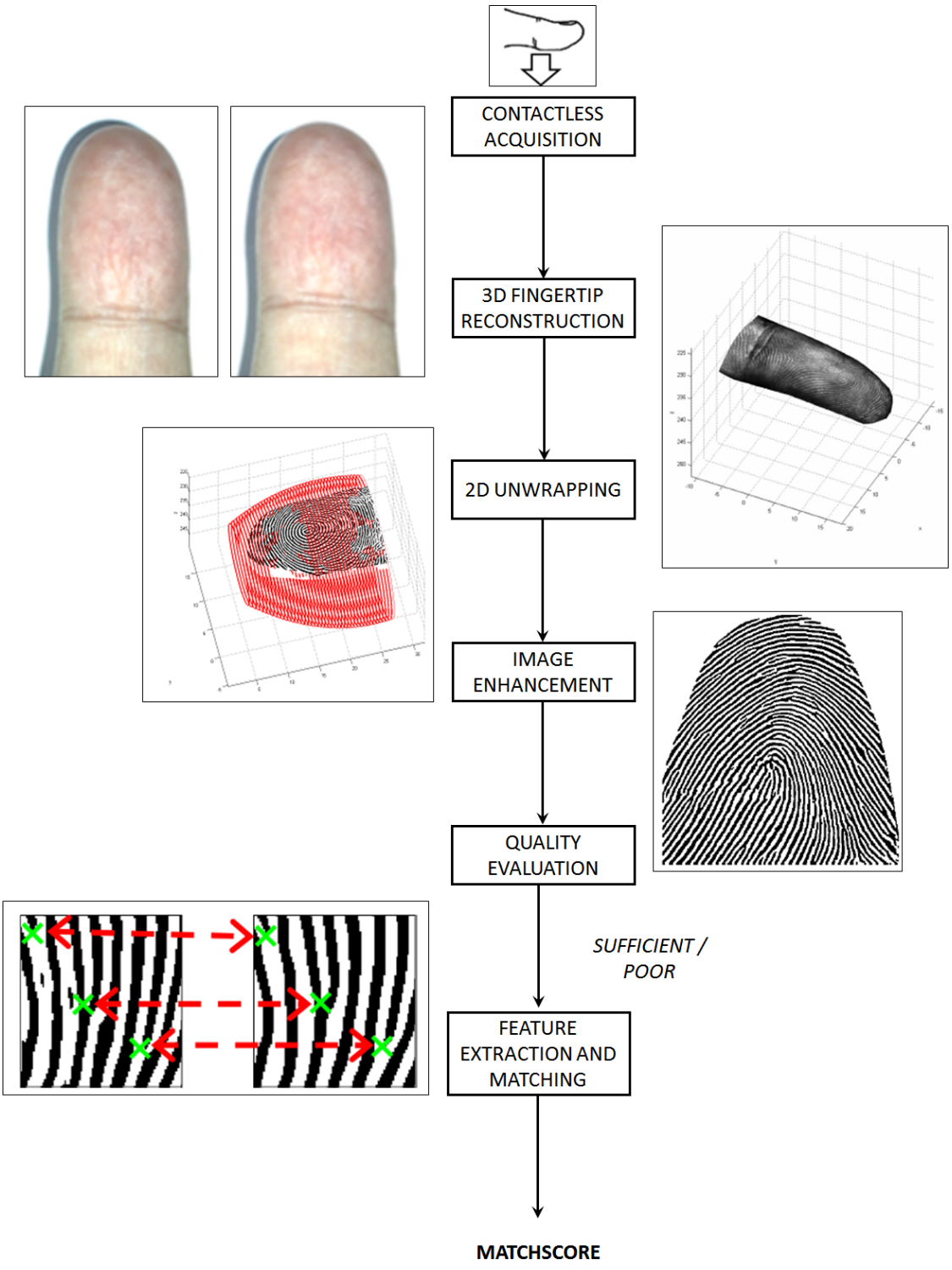

Figure 5.4: Overview of the treated problems for the contactless fingerprint recognition based on unwrapped three-dimensional models.

the acquisition Method A and Method B are processed using the enhancement method E1. The unwrapped images corresponding to the acquisition Method C are processed using the enhancement method E2.

5.1.3.3 QUALITY ASSESSMENT OF CONTACT-EQUIVALENT IMAGES COMPUTED FROM UNWRAPPED THREE-DIMENSIONAL MODELS

A method for the evaluation of the quality of contact-equivalent images computed from unwrapped three-dimensional models has been researched [449]. Contactless acquisitions, in fact, can present many non-idealities due to reflections, shadows, complex background, or motion blur. Moreover, errors in the three-dimensional reconstruction process can result in unwrapped images which present some regions with a lower quality. In particular, problems can be caused by regions of the three-dimensional model that are badly reconstructed (e.g., the matching points were not found), by spikes in the model (erroneous matching points), or by artifacts introduced during the computation of the contact-equivalent images.

The researched method for the quality estimation of contact-equivalent images obtained by unwrapping the three-dimensional models is based on computational intelligence techniques. In particular, the method extracts a set of features from the image and uses a neural classifier to classify the image as 'good', or 'not good'. The used features are related to the quality of the extracted minutiae, the shape of the ROI, the output of the Gabor filters, and the HOG features.

5.1.3.4 FEATURE EXTRACTION AND MATCHING

A feature extraction and matching method based on the analysis of Level 2 features, described in 5.1.1.3, is used to perform the recognition using the contact-equivalent images computed from the unwrapped three-dimensional models.

In particular, the NIST MINDTCT software is used to extract the minutiae, and the NIST BOZORTH3 algorithm is used to perform the matching of the extracted minutiae.

5.1.4 COMPUTATION OF SYNTHETIC THREE-DIMENSIONAL FINGERPRINT MODELS

A method for the computation of synthetic three-dimensional models of fingerprints has been researched [450]. In particular, the method extends the work described in [451] and considers a virtual environment for the simulation of the complete three-dimensional shape of the fingertip. Starting from real or synthetic images of contact-based acquisitions, the method permits to obtain realistic synthetic three-dimensional models of the finger shape and the fingeprints.

The method can be divided into several steps: first, the silhouette of the fingertip is computed and the three-dimensional finger shape is modeled. Then, the three-dimensional height of the ridges is computed and superimposed on the computed shape. The color information is introduced and illumination conditions are simulated. The virtual environment also allows to simulate a contactless biometric acquisition of the simulated three-dimensional models in a multiple view camera system.

5.1.4.1 COMPUTATION OF THE SILHOUETTE OF THE FINGERTIP

The method computes the three-dimensional finger shape based on the finger silhouette, which is particularly important for the computation of realistic models. In order to obtain realistic results, the method uses a silhouette modeled from real contactless acquisitions. The models are computed offline and are different for every finger class. In particular, the fingers were divided into three classes: thumb, little finger, and other fingers.

5.1.4.2 COMPUTATION OF THE THREE-DIMENSIONAL SHAPE OF THE FINGERTIP

This step computes the three-dimensional shape of the fingertip based on the silhouette obtained in the previous step. The method is based on the technique described in [79] and computes a parametric finger shape based on fourth-order polynomials. The parametric model has been designed by studying three-dimensional models computed from real acquisitions [102], and permits to create synthetic three-dimensional shapes in a simple and accurate manner.

5.1.4.3 COMPUTATION OF THE THREE-DIMENSIONAL HEIGHT OF THE RIDGES

This step computes the height of the ridges by analyzing the ridge pattern of a real or synthetic contact-based image with algorithms commonly used for biometric recognition. First, the three-dimensional height of the ridge pattern is estimated, and the camera focus is simulated. Then, the ridges are superimposed on the three-dimensional shape of the fingertip.

ESTIMATION ON THE HEIGHT OF THE RIDGE PATTERN First, the contact-based image is aligned with the two-dimensional silhouette computed by using the algorithm described in Section 5.1.4.1. Then, a first approximation of the three-dimensional ridge shape is performed by using a well-known enhancement method in the literature based on Gabor filters, and assuming that the result of the filtering procedure is proportional to the three-dimensional height of the ridges.

The height of the ridges is refined using a logarithm-based operator, and normalized according to the size of real human ridges. Then, an adaptive histogram equalization is performed. Salt and pepper noise is added in order to simulate incipient ridges and pores.

SIMULATION OF CAMERA FOCUS In order to simulate the out-of-focus on the peripheral regions of the images, the ridge pattern is smoothened progressively towards the borders. First, five regions are defined by subtracting from the mask the images obtained by eroding the mask using a structural element with increasing size. Each region of the ridge pattern is filtered according to its spatial position using a low-pass Gaussian filter. Filters with a greater area and standard deviation are used towards the borders.

SUPERIMPOSITION OF THE RIDGES First, the coordinates of both the ridge pattern and the fingertip shape are converted to millimeters by considering that the contact-based image presents a resolution of 500 dpi. Then, the height values of the ridges are adjusted to a mean value of 0.06 mm, corresponding to the mean height of human ridges.

The superimposition of the ridges on the fingertip surface is performed by summing the ridge height to the finger shape along the direction normal to its surface. A bilinear interpolation is applied in order to obtain a dense representation of the fingertip surface.

5.1.4.4 SIMULATION OF COLOR AND ILLUMINATION

The color information is computed from a real contactless image captured using a technique similar to the one described in [102]. The ridge pattern is removed by using a Gaussian low-pass filter, and the resulting image is superimposed on the fingerprint surface using a texture mapping procedure.

In order to simulate the ambient light, a light source placed at infinity is used to illuminate the scene. Then, a punctiform light source, radiating uniformly in all directions, is used to simulate a LED illumination. Specular features of the model are adjusted to match the ones of the human skin, and a Phong lighting algorithm is applied to compute the reflections.

5.1.4.5 SIMULATION OF A MULTIPLE VIEW ACQUISITION

The described method permits to compute images representing contactless biometric acquisitions of the simulated three-dimensional fingerprint model, performed with a multiple view system. In particular, the implemented method performs three-dimensional projections using calibration data obtained from real acquisition setups:

$$\begin{bmatrix} u & v & 1 \end{bmatrix}^T = K[R|t] \begin{bmatrix} X & Y & Z & 1 \end{bmatrix}^T , \tag{5.12}$$

where (u, v) are the projected pixel coordinates, K is the intrinsic camera matrix, R and t are the rotation matrix and translation vector. The images related to every view are computed using a linear interpolation.

5.1.5 COMPUTATION OF THE THREE-DIMENSIONAL MODELS OF THE FINGERPRINTS ON A CLAY ARTWORK

Clay artworks are often used by the artists to build a preliminary sketch of the sculptures. These artifacts are very important and valuable since they show the artistic path of the authors to the creation of the final artworks.

The authentication of clay artifacts is performed in order to distinguish the original artworks from the numerous forgeries often present in the market in the case of famous sculptors. This process can be made by using different techniques, like the microscope analysis and Carbon 14 dating. The authentication is usually performed by art histo-

rians in cooperation with forensic scientists. In this context, the analysis of the latent fingerprints present on the artifacts is an important recognition technique. In order to prove the authenticity of a sculpture, the fingerprints present on the artifact can be compared with other latent fingerprints attributed to a specific artist.

However, classical forensic techniques for the acquisition of latent fingerprints, involving the use of films, molds, or dusts, are often impossible to be applied to ancient artworks because of their value and fragility. Another important problem consists in the position of the latent fingerprints, which can be placed on a surface patch that is difficult to reach. For these reasons, contactless acquisition techniques and classical photographic techniques were used. However, in the case of clay artworks, the perspective distortion present in the captured images can be very high, due to the irregular shape of the object. Moreover, the aging of the artifacts can modify the color of the material, reducing the visibility of the ridge pattern.

In order to limit the presence of perspective deformations in the captured data, multiple view acquisition systems and three-dimensional reconstruction techniques can be used to compute a three-dimensional model of the artifact and the fingerprints. Then, the reconstructed models can be used to perform the authentication by applying algorithms based on two-dimensional or three-dimensional data.

The described method implements a low-cost, contactless, two-view acquisition system able to acquire the latent fingerprints left on a clay artwork, and to perform a three-dimensional metric reconstruction of the captured area. In this way, it is possible to obtain a less-distorted reconstruction of the fingerprint with respect to traditional methods. Moreover, the metric reconstruction permits to determine the size of the model in a view-independent manner. In particular, the researched method is focused on a specific clay artwork, attributed by experts to the Italian sculptor Antonio Canova (Italy, 1757–1822), which is probably a sketch of the well-known statue "Ninfa Dormiente" ("Sleeping Nymph") shown at the Victoria and Albert Museum, London.

The proposed method is based on image processing techniques and uses pairs of images captured using two synchronized color CCD cameras. First, an algorithm based on the cross-correlation is used in order to determine a series of matching points in the two images. Then, the points are triangulated and the three-dimensional model is completed with the wrapping of the interpolated texture computed from the original pair of images.

In particular, the method described in Section 5.1.2.4 is used to compute the three-dimensional models. Visual examinations on the computed models showed that the described method can perform a metric, view-independent reconstruction of the fingerprints present on the artwork, using a contactless acquisition which does not damage the artwork in any way.

5.2 FEASIBILITY STUDY FOR THE CONTACTLESS LESS-CONSTRAINED PALMPRINT RECOGNITION: A METHOD BASED ON A FIXED DISTANCE

Since the techniques for the acquisition and processing of fingerprint and palmprint samples are similar, the results obtained by the methods for the contactless fingerprint

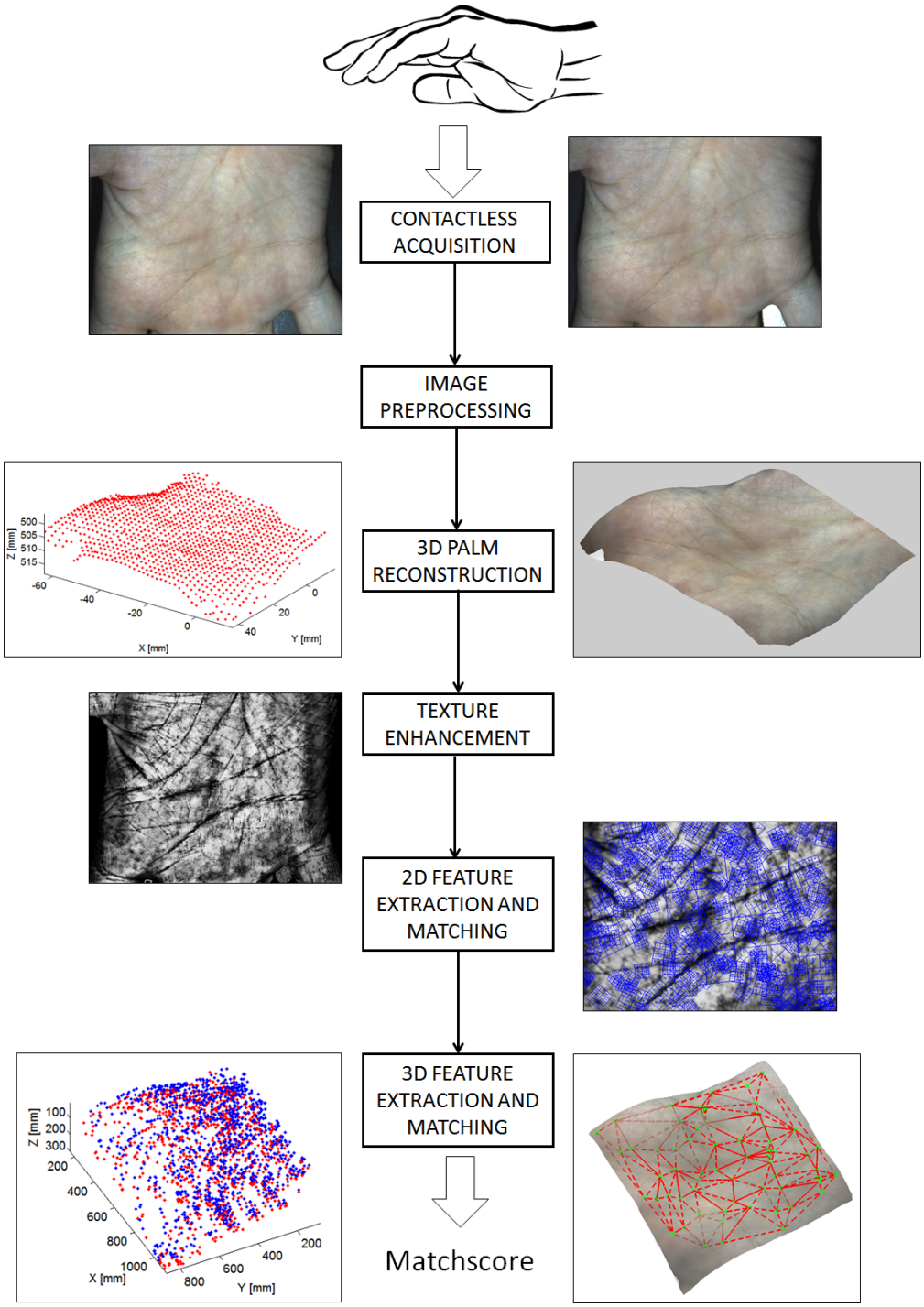

Figure 5.5: Schema of the palmprint recognition system using acquisitions performed with the hand positioned at a fixed distance.

recognition allowed to extend the researched method for the contactless palmprint recognition. In particular, a feasibility study for a less-constrained palmprint recognition was conducted by considering a similar setup for the acquisition, which use a flat surface in order to control the acquisition distance.

5.2.1 DIFFERENCES BETWEEN CONTACTLESS FINGERPRINT AND PALMPRINT RECOGNITION

Palmprints and fingerprints are biometric traits that present several differences, which required the development of ad-hoc methods for processing palmprint images. In particular, the acquisition of the palmprint images required a redesign of the optical hardware acquisition system, since the palm area which contains the distinctive information is significantly larger, with respect to a fingerprint, and the size of the palms can present large variations: for example, the hand of a male manual worker can be much larger with respect to the hand of a female. Moreover, the color and smoothness of the skin is different in every subject, causing the light to be absorbed and reflected by the skin in different ways, and so the shutter times needed to be adjusted accordingly.

In the palmprint images captured using the described methods, the ridges used for the fingerprint recognition are not always visible, and different methods for the image preprocessing and enhancement needed to be studied and implemented. For these reasons, new methods for the two-dimensional feature extraction and matching were also implemented for the palmprint recognition.

Moreover, while the method used for the computation of the three-dimensional model of the palmprint is similar to the one used in 5.1.2.4 for the contactless fingerprint recognition, the flatness of the palms prevented the use of the unwrapping method described in 5.1.3.1 for the computation of two-dimensional images of the fingerprint from the three-dimensional models. In fact, the curvature of the palmprint area is limited and the mapping of the three-dimensional model of the palmprint on a two-dimensional surface would not introduce significant improvements. For these reasons, new methods for the three-dimensional feature extraction and matching were studied and implemented for the palmprint recognition.

In this section, the methods for the contactless palmprint recognition using acquisitions performed at a fixed distance are described. These methods have a lower cost and hardware complexity, with respect to the methods designed in order to perform acquisitions with uncontrolled distance (described in Section 5.3). However, they require the positioning of the hand with a higher degree of precision and cooperation.

The researched method can be divided into several steps: first, the acquisition setup is calibrated, then a multiple-view contactless acquisition is performed. The images are preprocessed in order to segment the palm region, and a method based on the cross-correlation is used to compute the three-dimensional model of the palmprint. The corresponding texture images are enhanced, then the two-dimensional features are extracted and matched. A three-dimensional feature extraction and matching step is used to further increase the matching accuracy. An outline of the method is shown in Fig. 5.5.

5.2.2 CAMERA CALIBRATION

The calibration of the cameras of the multiple view setup is performed using the same procedure described in Section 5.1.2.1. The calibration is performed off-line once before

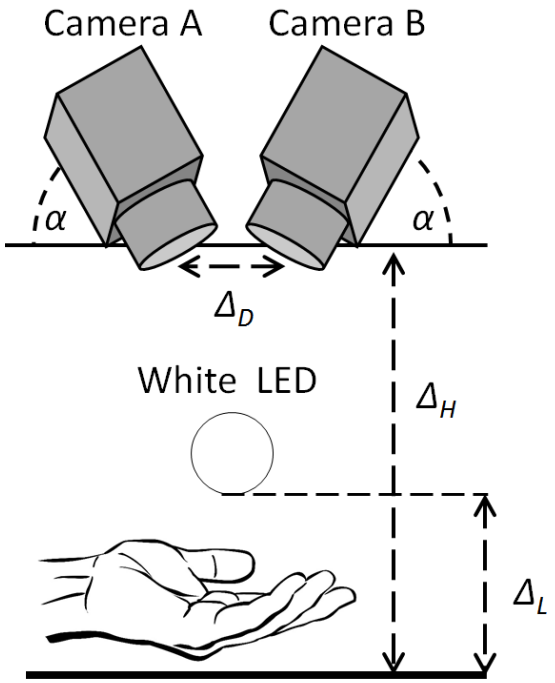

Figure 5.6: Schema of the contactless acquisition setup with the hand positioned at a fixed distance.

the acquisition. A chessboard captured in multiple orientations is used as a calibration objects, and a corner detector algorithm is used to extract the corners of the chessboards [448]. Then, the algorithms described in [442, 443] are used to compute the intrinsic and extrinsic parameters. A DLT method [444] is used to compute the homography matrix, and a RANSAC algorithm is used to compute the fundamental matrix [447].

5.2.3 ACQUISITION

The contactless acquisition setup is depicted in Fig. 5.6, and is composed by two CCD color cameras mounted at a fixed distance Δ_H from a flat surface with a dark uniform color, and a white led illuminator positioned at a distance Δ_L from the flat surface. The cameras are oriented with an angle α with respect to the surface, and placed with a distance Δ_D between the centers of the optics. The illuminator is placed so that the light is emitted almost perpendicularly to the surface to be captured.

The setup requires the user to place his hand on the flat surface at a fixed distance from the cameras, and position the palm of his hand in the overlapping fields of view of the two cameras. Then, a two-view acquisition is used to capture a pair of images I_A and I_B. A trigger mechanism is used to synchronize the cameras, and the used shutter time is fixed and chosen experimentally in order to enhance the details of the palm without saturating the image. An example of a pair of corresponding images is shown in Fig. 5.7.

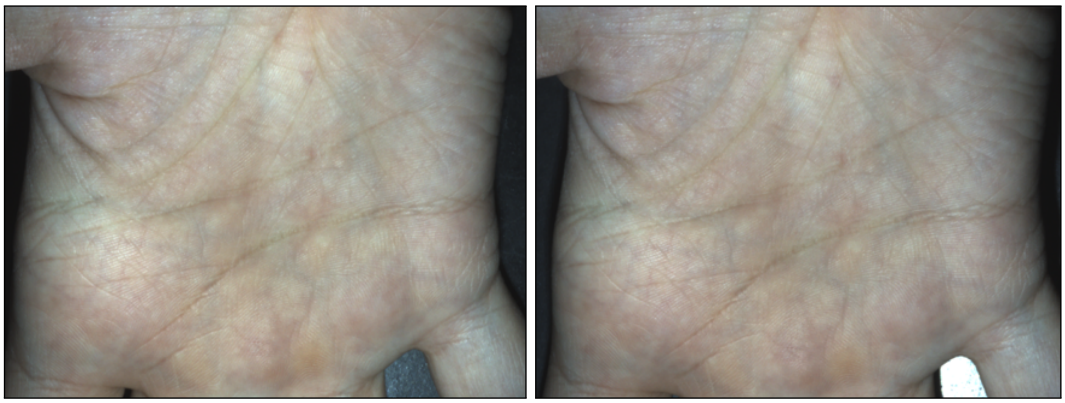

(a) (b)

Figure 5.7: Example of a pair of images captured at a fixed distance from the camera using the described setup: (a) left image I_A; (a) right image I_B.

5.2.4 IMAGE PREPROCESSING

The two images are segmented in order to remove the background. Since a surface with a uniform color is used, a thresholding operation is used to extract the foreground:

$$I_s(x,y) = \begin{cases} 1 & \text{if } I(x,y) > t_s \\ 0 & \text{otherwise} \end{cases}, \tag{5.13}$$

where $I_s(x,y)$ is the binary segmented mask, and t_s is an experimentally estimated threshold value. In order to eliminate possible points outside the boundary that can be segmented as foreground, a morphological opening operation is applied, followed by a closing operation. Then, only the largest connected component is extracted. An example of the segmentation operation is shown in Fig. 5.8.

5.2.5 THREE-DIMENSIONAL PALM RECONSTRUCTION

The method used for the computation of the three-dimensional model of the palm is similar to the method described in 5.1.2.4 for the three-dimensional reconstruction of the fingertip, and is based on the extraction of a set of equally spaced reference points, which are matched using a cross-correlation approach. A method based on the normalized cross-correlation was used since, as described in [452], the illumination can be considered as uniform in the two images captured using the two-view acquisition, and only small differences in the orientations of the cameras are present.

The calibration information of the cameras is used to triangulate the matching points in the three-dimensional space. A method for the refinement of the point cloud is applied, then linear interpolation techniques are used to compute a three-dimensional surface model describing the palm and the corresponding texture image. The outline of the used three-dimensional reconstruction technique is shown in Fig. 5.9.

The three-dimensional reconstruction method can be divided into several steps:

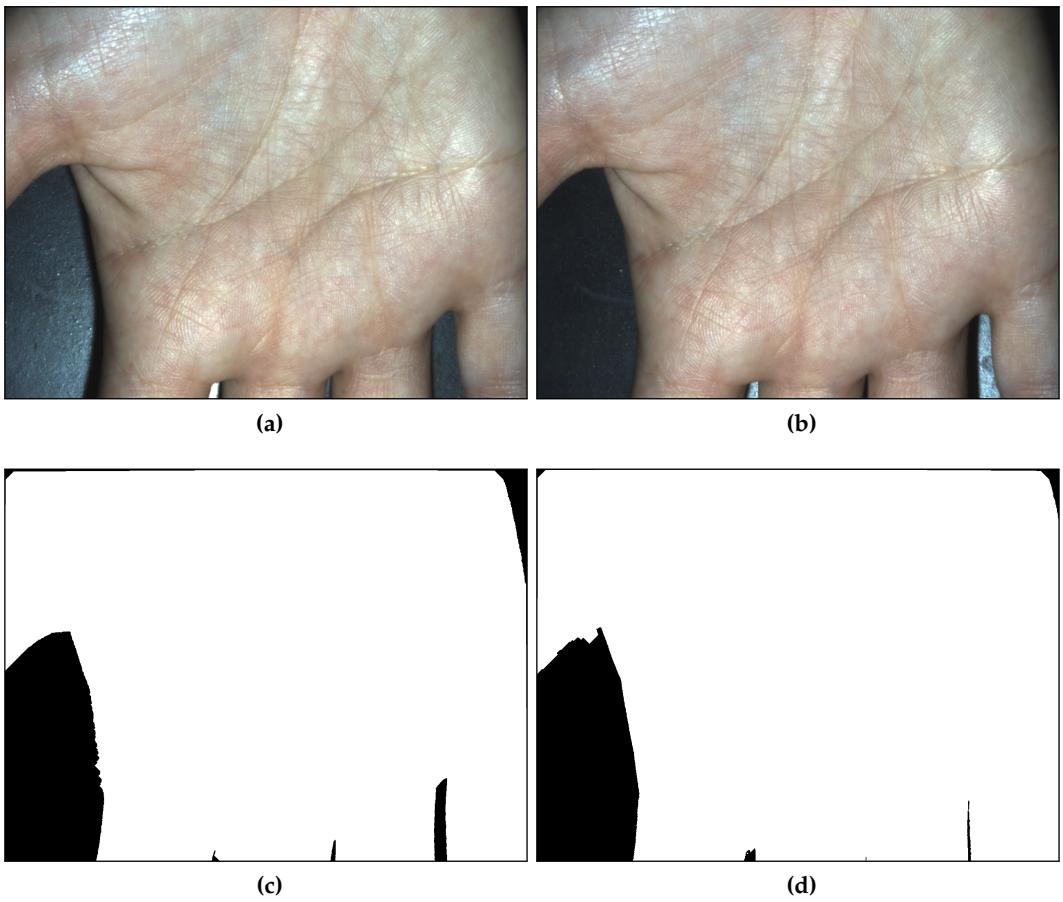

Figure 5.8: Example of the segmentation process: (a) original left image I_A; (b) original right image I_B; (c) segmented left image; (d) segmented right image.

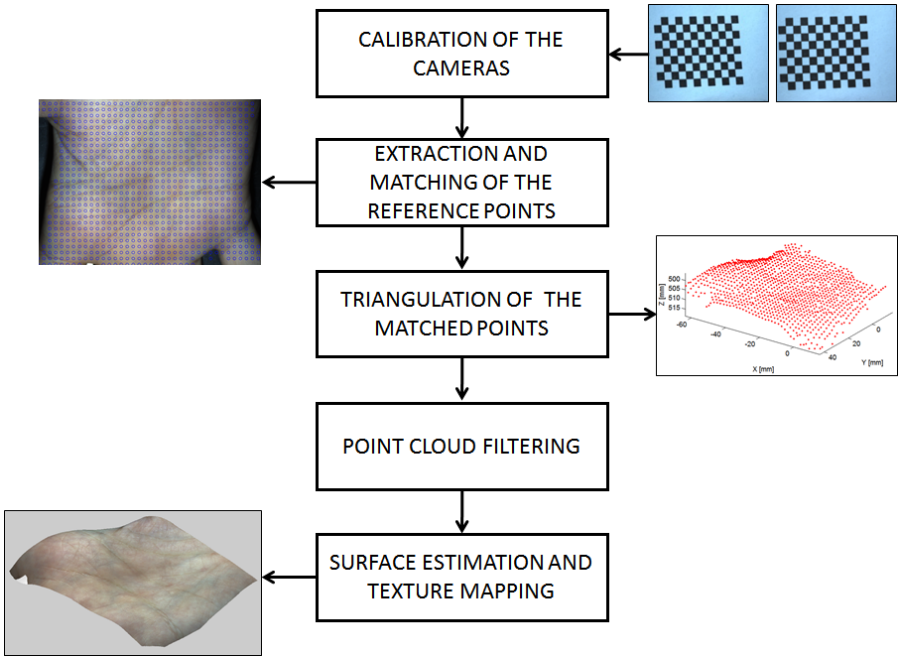

Figure 5.9: Outline of the researched three-dimensional reconstruction method.

1. Extraction and matching of the reference points;
2. Triangulation of the matched points;
3. Point cloud filtering;
4. Surface estimation and texture mapping.

5.2.5.1 EXTRACTION AND MATCHING OF THE REFERENCE POINTS

A downsampling procedure with a fixed step s_{ds} is used to extract a set of N_P reference points from the left image I_A. An adaptive procedure is used to compute the downsample step s_{ds} according to the desired number of points N_P to be matched.

Then, for each extracted point, a preliminary match is computed. In particular, for each point x_A pertaining to set of reference points extracted from I_A, the search for the matching point in the second image is performed by using the homography matrix:

$$X'_B = H X_A \ , \tag{5.14}$$

where H represents the 3×3 homography matrix, X_A is the point x_A converted in homogeneous coordinates:

$$X_A = \begin{bmatrix} x_A \\ y_A \\ 1 \end{bmatrix} \ , \tag{5.15}$$

and X'_B is the preliminary matching point expressed in homogeneous coordinates:

$$X'_B = \begin{bmatrix} X_B \\ Y_B \\ W_B \end{bmatrix} \ . \tag{5.16}$$

A Cartesian representation of the point X'_B is computed as:

$$x'_B = \begin{bmatrix} \frac{X_B}{W_B} \\ \frac{Y_B}{W_B} \end{bmatrix} \ . \tag{5.17}$$

A series of possible matching points adjacent to x'_B are extracted in a rectangular region centered in x'_B. The possible matching points are considered if:

$$\begin{aligned} d_x(x^i_B, x'_B) < \Delta_x \\ d_y(x^i_B, x'_B) < \Delta_y \ , \end{aligned} \tag{5.18}$$

where x^i_B is the i-th adjacent point, d_x and d_y represent the distances in the x and y directions, and Δ_x and Δ_y are the dimensions of the rectangular area.

For each point x_A, the set of possible matching points lies on the corresponding epipolar line in the image I_B. In particular, the distance of each possible matching point x_B^i from the corresponding epipolar line is computed as:

$$d_{ep}^i = \frac{(X_B^i)^T F X_A}{\sqrt{(l_1)^2 + (l_2)^2}} \ , \tag{5.19}$$

where d_{ep}^i is the epipolar distance, X_B^i is the i-th adjacent point expressed in homogeneous coordinates, F is the fundamental matrix, and l_1, l_2 are the first two components of the epipolar line l, which is computed using the equation:

$$l = F X_A \ . \tag{5.20}$$

The distance of the possible matching points from the corresponding epipolar line must be inferior to a threshold t_{ep}:

$$d_{ep}^i < t_{ep} \ . \tag{5.21}$$

The Canny edge detector is applied to the two images I_A and I_B and used as a check for the consistency of the possible matching points. Only the candidate matching points with corresponding values in the binary edge images are considered:

$$C_A(x_A) = C_B(x_B^i) \ , \tag{5.22}$$

where C_A, C_B are the images resulting from the application of Canny edge detector to I_A and I_B.

The set of the possible matching points x_B^i, corresponding to the point x_A, are inserted in the list V_B of the valid points to be checked if the aforementioned conditions are respected:

$$x_B^i \in V_B \text{ if } \begin{cases} d_{ep}^i < t_{ep} \ , \\ d_x(x_B^i, x_B') < \Delta_x \ , \\ d_y(x_B^i, x_B') < \Delta_y \ , \\ C_A(x_A) = C_B(x_B^i) \end{cases} . \tag{5.23}$$

The actual matching point is computed by performing the normalized cross-correlation of two $l \times l$ windows, one centered in x_A, and the other centered in every point of V_B (Fig. 5.10). The normalized cross-correlation coefficient of the two windows is computed as:

$$r = \frac{\sum_m \sum_n (A_{mn} - \bar{A})(B_{mn} - \bar{B})}{\sqrt{(\sum_m \sum_n (A_{mn} - \bar{A})^2)(\sum_m \sum_n (B_{mn} - \bar{B})^2)}} \ , \quad 1 < m < l, \ 1 < n < l \ , \tag{5.24}$$

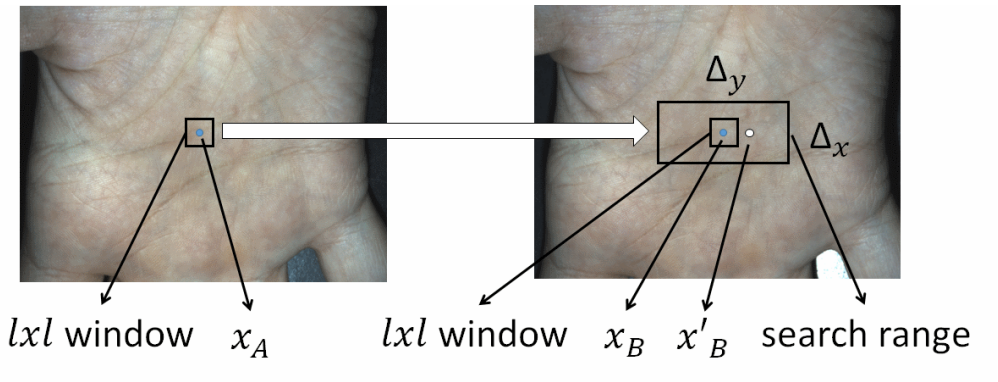

Figure 5.10: Graphical representation of the method used for searching the corresponding points.

where A and B are the two windows of size $l \times l$. The coefficient is computed on the Y, R, G, B channels separately, and the maximum coefficient is considered:

$$r_m = \max(r_Y, r_R, r_G, r_B) \ , \tag{5.25}$$

where r_m is the maximum cross-correlation coefficient, and r_Y, r_R, r_G, r_B are the cross-correlation coefficients computed respectively on the Y, R, G, B channels of the images.

The final matching point x_B is chosen as the point in V_B corresponding to the window that produces the highest cross-correlation coefficient r_m:

$$x_B = \underset{r_m}{\operatorname{argmax}}(x_B^i) \ . \tag{5.26}$$

The intensity maps for a sample pair of acquisitions, depicting the cross-correlation values along the epipolar line for different points, are shown in Fig. 5.11.

An example of a two-view acquisition and the computed matching points is shown in Fig. 5.12

5.2.5.2 TRIANGULATION OF THE MATCHED POINTS

The two-dimensional coordinates of the matching points are normalized using a rectification procedure, then the three-dimensional coordinates corresponding to each pair of matching points are computed using the triangulation formula [448]:

$$z = \frac{fT}{x_A - x_B} \tag{5.27}$$

where f is the focal length of the two cameras, T is the baseline distance between the rectified position of the two cameras and x_A and x_B are the two matched points. The three-dimensional coordinates of the points are adjusted using a common reference system. In particular, both the reference systems centered on the Camera A and the Camera B are considered, in order to obtain the two point clouds (X_A, Y_A, Z_A), (X_B, Y_B, Z_B).

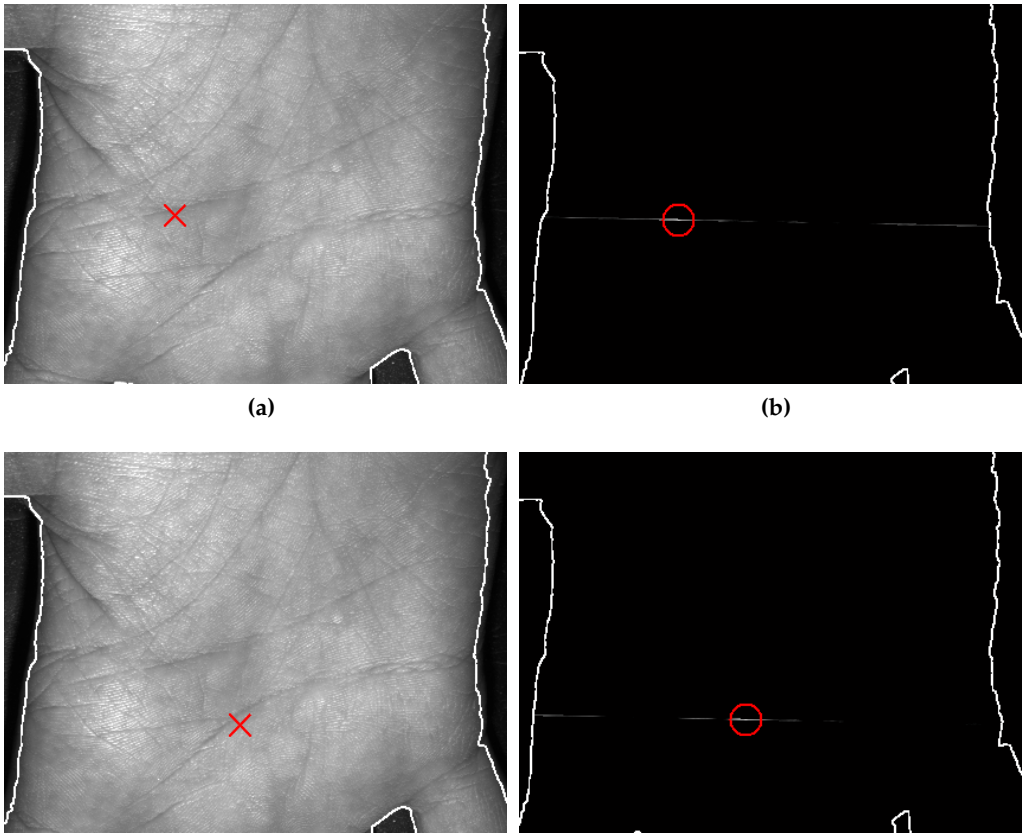

(a) (b)

(c) (d)

Figure 5.11: Example of intensity maps along the epipolar lines, corresponding to two different points of the same image: (a, c) image I_A and the point to be matched; (b, d) intensities along the corresponding epipolar line in the image I_B, and the matched point. The matched point is chosen as the point with the maximum intensity.

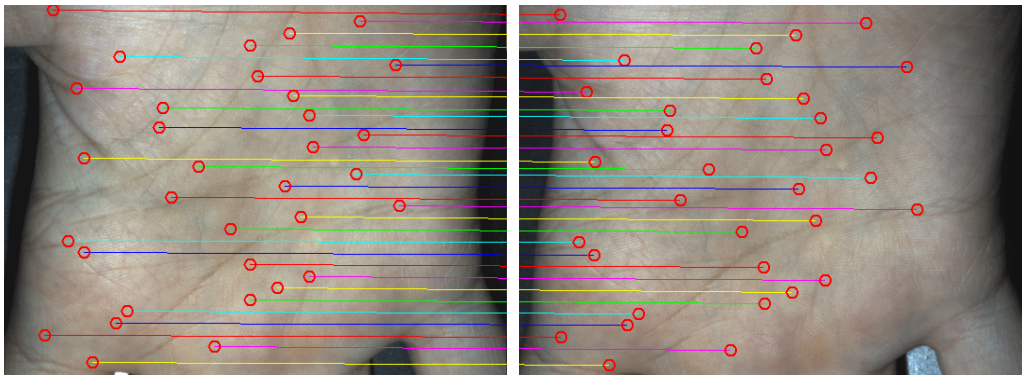

(a) (b)

Figure 5.12: Example of matched points in the two images: (a) left image I_A; (b) right image I_B.

Moreover, the point cloud (X_B, Y_B, Z_B) is related to the point cloud (X_A, Y_A, Z_A) by a rotation R and a translation t:

$$\begin{bmatrix} X_B \\ Y_B \\ Z_B \end{bmatrix} = R \begin{bmatrix} X_A \\ Y_A \\ Z_A \end{bmatrix} + t \ , \tag{5.28}$$

where R and t are computed in the calibration step, and describe the rotation and translation of the Camera B with respect to the Camera A.

5.2.5.3 POINT CLOUD FILTERING

Since the matched points are obtained using a downsampling method with a constant step s_{ds}, and the surface is sufficiently smooth, the three-dimensional point cloud of the reconstructed model should present a regular distribution of the points. The point cloud filtering procedure is applied separately on the point clouds (X_A, Y_A, Z_A) and (X_B, Y_B, Z_B).

A first check for outliers is performed by removing the points that are too distant from the mean Z coordinate of the point cloud:

$$(z_i - \overline{Z}) < (\sigma_Z \, t_s) \tag{5.29}$$

where z_i is the Z coordinate of the i-th three-dimensional point, $\overline{Z}$ is the mean Z coordinate of the point cloud, σ_Z is the standard deviation of the Z coordinate of the point cloud, and t_s is a fixed parameter.

A further check for outliers is performed by removing the three-dimensional points that are not close to any other point of the point cloud. The distance from each point to the points pertaining to its 4-neighborhood must be inferior to a threshold t_d:

$$\begin{aligned} d((x_i, y_i, z_i), (x_{i+j}, y_{i+j}, z_{i+j})) < t_d \\ 1 \leqslant j \leqslant 4 \ , \end{aligned} \tag{5.30}$$

where (x_i, y_i, z_i) is the i-th three-dimensional point, $(x_{i+j}, y_{i+j}, z_{i+j})$ are the points pertaining to its 4-neighborhood, and $d(\cdot)$ represents the Euclidean distance. The threshold t_d is computed as the double of the minimum distance between adjacent three-dimensional points:

$$t_d = 2 \min_{i=1 \ldots N} \left(d((x_i, y_i, z_i), (x_{i+1}, y_{i+1}, z_{i+1})) \right) \ , \tag{5.31}$$

where N is the number of three-dimensional points.

5.2.5.4 SURFACE ESTIMATION AND TEXTURE MAPPING

The intensity values of the original image I_A are stored in the vector C_A. Then, from the vectors X_A, Y_A, the maps S_{Ax} and S_{Ay} are computed as a mesh with a constant step s_{interp}. Then, the surface map S_{Az} and the texture intensity map S_{Ac} are obtained by

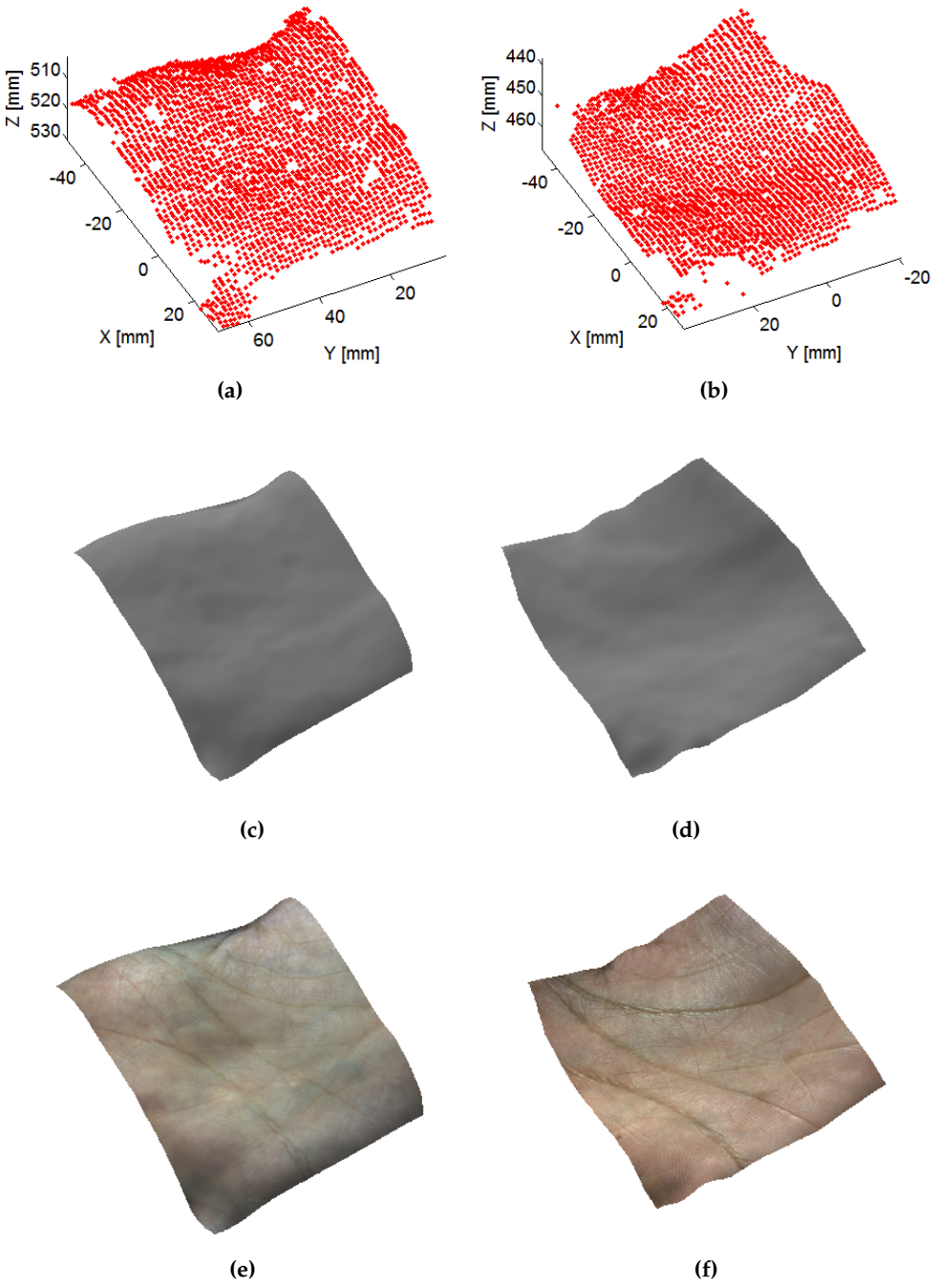

Figure 5.13: Example of reconstructed three-dimensional palmprint models: (a, b) filtered point clouds; (c, d) interpolated surfaces; (e, f) texture images.

applying a bilinear interpolation on the vectors Z_A and C_A at the coordinates described by the meshed maps S_{Ax} and S_{Ay}. The coordinates of the surface maps S_{Ax}, S_{Ay} are adjusted in order to match the coordinates of the image I_A.

Similarly, the surface estimation is performed considering the point cloud (X_B, Y_B, Z_B) computed using the reference system centered in the right Camera B, and the corresponding image I_B, in order to obtain the maps $S_{Bx}, S_{By}, S_{Bz}, S_{Bc}$. Then, the coordi-

nates of the surface maps S_{Bx}, S_{By} are adjusted in order to match the coordinates of the image I_B.

Examples of reconstructed point clouds with the relative estimated surfaces and textures are shown in Fig. 5.13.

5.2.6 TEXTURE ENHANCEMENT

In the performed experiments based on the captured samples, we found that the quality of the ridge pattern in the contactless acquisitions is very different in each individual, and in some people it is even hardly visible. For this reason, in the researched texture enhancement method, the details of the ridge pattern are not extracted.

An enhancement procedure similar to the enhancement method E1 described in Section 5.1.1.2 is used to enhance the details of the lines of the palm. However, differently from the method E1, we did not perform the enhancement of the ridge pattern, nor the image binarization.

The texture enhancement method can be divided into several steps. First, an adaptive histogram equalization procedure is used, then the background I_B containing the skin of the palm is estimated using a morphological operation, and removed it from the original image. The resulting image I_R is inverted and processed using a logarithm operator in order to reduce the noise:

$$I_L(x,y) = \log((1 - I_R(x,y)) + \epsilon) \ , \tag{5.32}$$

where a small value ϵ is needed to avoid the computation of the logarithm of 0. The resulting image is normalized by subtracting the minimum intensity value, and divided by its maximum value in order to adjust the intensity range in the interval $[0,1]$:

$$I_N(x,y) = \frac{I_L(x,y) - \min(I_L(x,y))}{\max(I_L(x,y))} \ . \tag{5.33}$$

Then, the inverse of the histogram equalized image is computed, obtaining the image I_E.

The same enhancement procedure is performed on the R and B channels of the image separately, and on both the images I_A and I_B. Examples of enhanced textures are shown in Fig. 5.14.

5.2.7 TWO-DIMENSIONAL FEATURE EXTRACTION AND MATCHING

For each palmprint sample, 8 images are considered in order to build the corresponding template. The used images are summarized in Table 5.1, and the notation I_A, I_B is used to indicate the images belonging to the first template, while the notation I'_A, I'_B is used to indicate the images belonging to the second template.

The two-dimensional feature extraction and matching procedure can be divided into several steps. First, the corresponding images in the two templates to be compared are aligned using an intensity-based transformation, then a method based on the use of

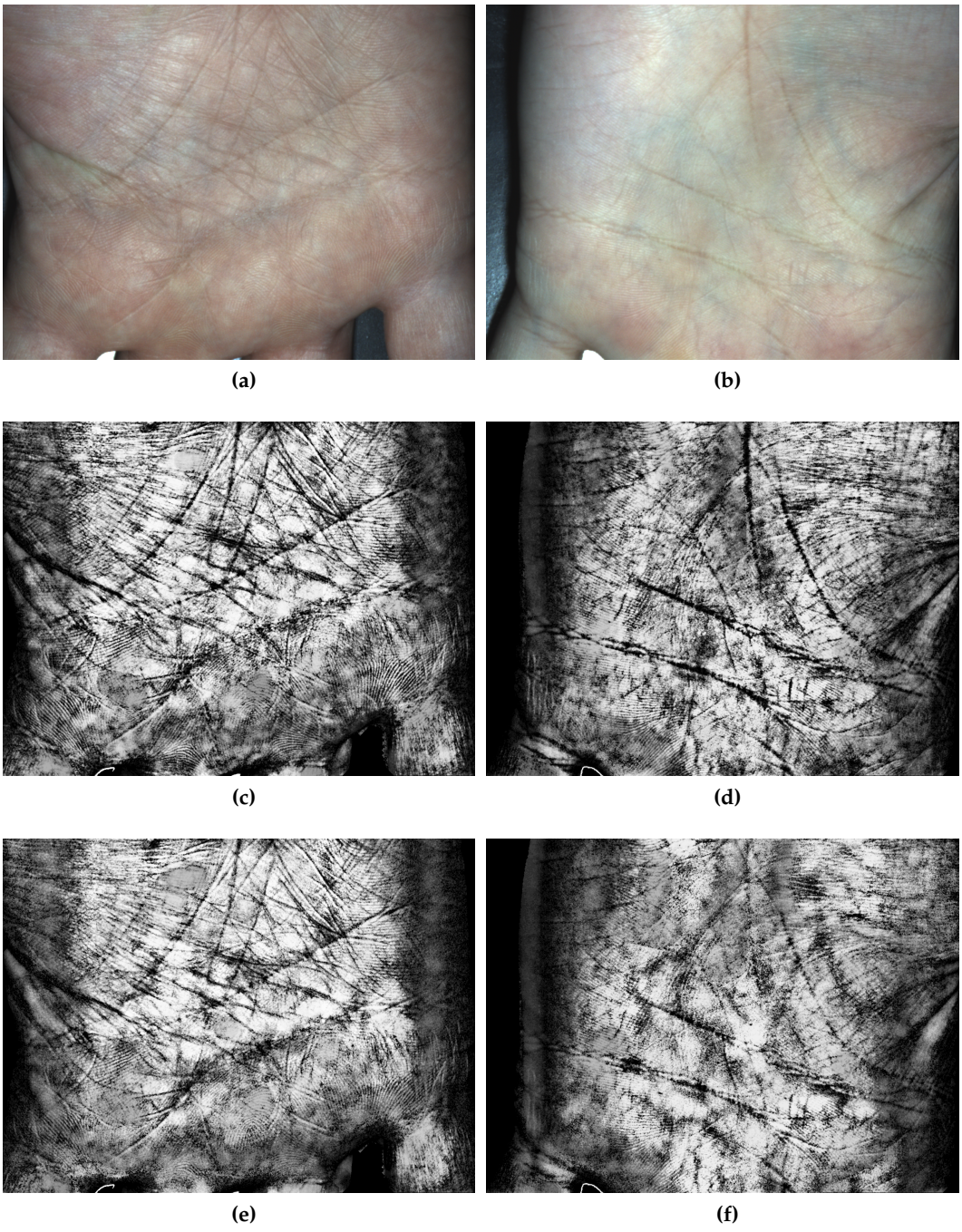

Figure 5.14: Example of enhanced texture images: (a, b) original left images from two different individuals; (c, d) enhanced textures obtained from the B channel; (e, f) enhanced textures obtained from the R channel.

SIFT features is used to extract and match the distinctive points. A procedure based on the point collinearity is used to refine the extracted points. An outline of the two-dimensional feature extraction and matching method is shown in Fig. 5.15.

Table 5.1: Summary of the images considered for each palmprint sample.

Notation	Description
I_{A_R}	R channel of the left texture image I_A
I_{A_B}	B channel of the left texture image I_A
I_{AE_R}	enhanced texture computed from the R channel of the left texture image I_A
I_{AE_B}	enhanced texture computed from the B channel of the left texture image I_A
I_{B_R}	R channel of the right texture image I_B
I_{B_B}	B channel of the right texture image I_B
I_{BE_R}	enhanced texture computed from the R channel of the right texture image I_B
I_{BE_B}	enhanced texture computed from the B channel of the right texture image I_B

5.2.7.1 IMAGE ALIGNMENT

Since the palms captured using the method described in Section 5.2.3, at a fixed distance and with the back of the hand placed on a flat surface, are almost flat, the three-dimensional models do not present sufficient information for a robust registration of the samples. For this reason, a two-dimensional alignment procedure is used. In particular, an intensity-based alignment procedure is used to register the corresponding images in the two templates to be compared. Only rigid transformations, consisting in a rotation and a translation, are considered. In particular, the transformation mapping the second image on the first is computed using a gradient descent algorithm. A linear interpolation is used to compute the intensity values in the rotated image.

An example of an aligned image is shown in Fig. 5.16.

5.2.7.2 POINT EXTRACTION AND MATCHING

The central region of the palm images, corresponding to the 3/4 of the image size, is extracted in order to discard possibly noisy regions including the bases and valleys of the fingers, and the border of the hand. The images are resized by a factor 1/2.

A Gaussian low-pass filter is applied to remove the high frequency information of the palm. Then, the SIFT feature points and descriptors [453] are extracted from the images to be compared [454]. In particular, the SIFT points are extracted from the 8 considered images of the first template to be compared, for a total of 8 sets of points $P_{1,\ldots,8}$.

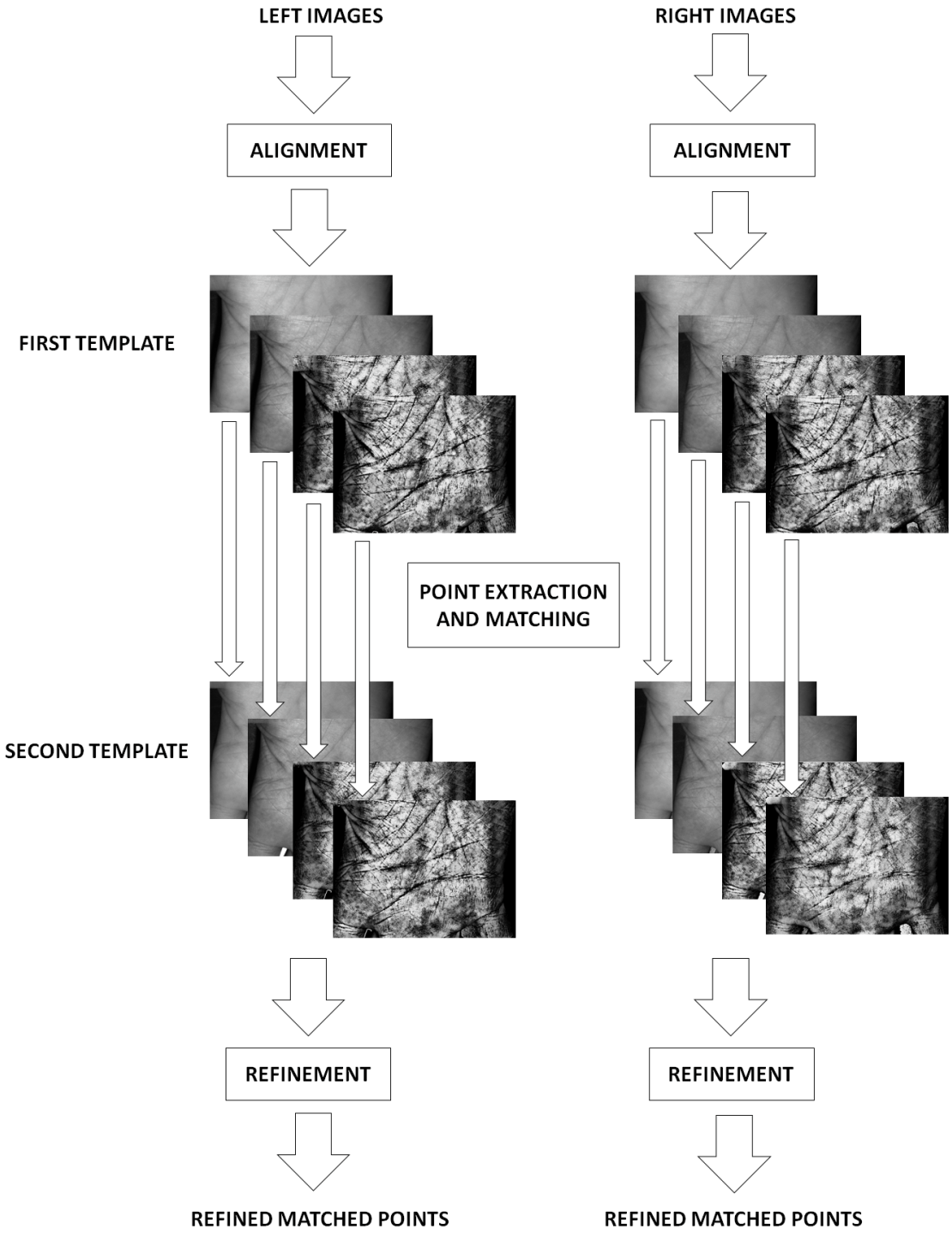

Figure 5.15: Outline of the two-dimensional feature extraction and matching method.

$$
\begin{aligned}
&I_{A_R} \rightarrow_{SIFT} P_1 \quad ; \quad I_{B_R} \rightarrow_{SIFT} P_5 \quad ; \\
&I_{AE_R} \rightarrow_{SIFT} P_2 \quad ; \quad I_{BE_R} \rightarrow_{SIFT} P_6 \quad ; \\
&I_{A_B} \rightarrow_{SIFT} P_3 \quad ; \quad I_{B_B} \rightarrow_{SIFT} P_7 \quad ; \\
&I_{AE_B} \rightarrow_{SIFT} P_4 \quad ; \quad I_{BE_B} \rightarrow_{SIFT} P_8 \quad ,
\end{aligned} \tag{5.34}
$$

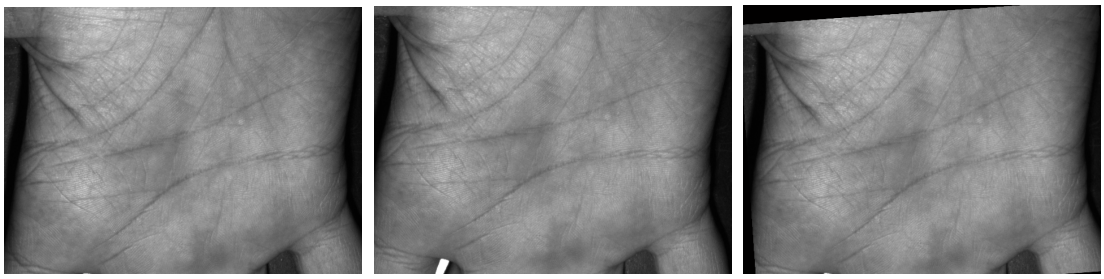

(a) (b) (c)

Figure 5.16: Example of the image alignment: (a) B channel extracted from the first image I_A; (b) B channel extracted from the second image I'_A; (c) second image aligned according to the first.

where $\rightarrow_{SIFT}$ to refers to the SIFT point extraction procedure.

The number of points in each set is variable. For each point, a descriptor $D(f_1, \ldots, f_{128})$, composed by 128 features, is computed. The same procedure is used to extract the sets of points $P'_{1,\ldots,8}$ and descriptors from the images pertaining to the second template.

The procedure described in [453], based on the Euclidean distance, is used to match the corresponding sets of descriptors obtained from the two templates. In particular, considering a set of points P_i corresponding to the first template, and the corresponding set of points P'_i corresponding to the second template, the Euclidean distance between each pair of descriptors is computed. Then, a descriptor D_m is considered as matched to a descriptor D'_n only if their distance, multiplied by a fixed threshold, is less than the maximum distance between D_m and the other descriptors:

$$d(D_m, D'_n) \cdot t_{SIFT} \leqslant \max_{p=1,\ldots,N'} (d(D_m, D'_p)) \tag{5.35}$$

where $d(\cdot)$ represent the Euclidean distance, t_{SIFT} is a fixed threshold, and N' is the number of points of the considered image to be compared in the second template. The obtained sets of matching points, corresponding to the matched descriptors, are referred as $M_{1,\ldots,8}$ and $M'_{1,\ldots,8}$.

5.2.7.3 REFINEMENT OF THE MATCHED POINTS

Since the palmprint images are captured in a horizontal position, the palm region of the hand can be considered as almost flat, and the images were previously aligned, the lines connecting the matched points must have all the same orientation. For this reason, a method based on the collinearity of the pairs of matched points is used to remove erroneous matchings.

First, the 8 sets of matching points $M_{1,\ldots,8}$ relative to the first template are merged in 2 sets, by distinguishing the matched points pertaining to the left images I_{A_R}, I_{A_B}, I_{AE_R}, I_{AE_B} and the matched points pertaining to the right images I_{B_R}, I_{B_B}, I_{BE_R}, I_{BE_B}, in order to obtain the sets M_{At}, M_{Bt}. Similarly, the sets of points relative to the images pertaining to the second template are merged in the sets M'_{At}, M'_{Bt}.

Then, the width W of the first image is summed to the X coordinates of the matched points belonging to M'_{At} and M'_{Bt}, in order to ideally translate them to the right of the corresponding points in the images of the first template.

The Euclidean distances between the pairs of matching points are computed, and only the pairs whose distance does not exceed a threshold are considered:

$$d(p(x,y), p'(x,y)) < t_f \ , \tag{5.36}$$

where $d(\cdot)$ represent the Euclidean distance, $(p(x,y), p'(x,y))$ is a pair of matching points, and the threshold t_f is defined as:

$$t_f = W + \frac{1}{10} W \tag{5.37}$$

where W is the width of the image.

Then, the derivative of the line connecting each pair of points is computed. First, the points belonging to M_{At} and M'_{At} are considered:

$$D_i = \frac{d_y(p_i(x,y), p'_i(x,y))}{d_x(p_i(x,y), p'_i(x,y))} \ , \tag{5.38}$$

where D_i represents the derivative of the line connecting the point $p_i(x,y)$, belonging to M_{At}, and the point $p'_i(x,y)$, belonging to M'_{At}. The values d_x and d_y represent respectively the Euclidean distance along the x and y axes. The pairs of points corresponding to the most diffused derivative value are considered as valid matching points. Similarly, the derivatives of the pairs of points in M_{Bt} and M'_{Bt} are computed, and only the pairs of points corresponding to the most diffused derivative value are considered as valid matching points.

The duplicate points are removed, and the resulting points are stored in the point sets M_{Af}, M'_{Af}, and M_{Bf}, M'_{Bf}. An example of the matched points before and after the refinement is shown in Fig. 5.17.

5.2.8 THREE-DIMENSIONAL FEATURE EXTRACTION AND MATCHING

The three-dimensional feature extraction and matching step can be divided into several steps. First, the three-dimensional coordinates of the refined matching points are computed, then the corresponding point clouds are registered using an ICP algorithm. A three-dimensional template based on the Delaunay triangulation is computed, then the number of similar triangles is extracted.

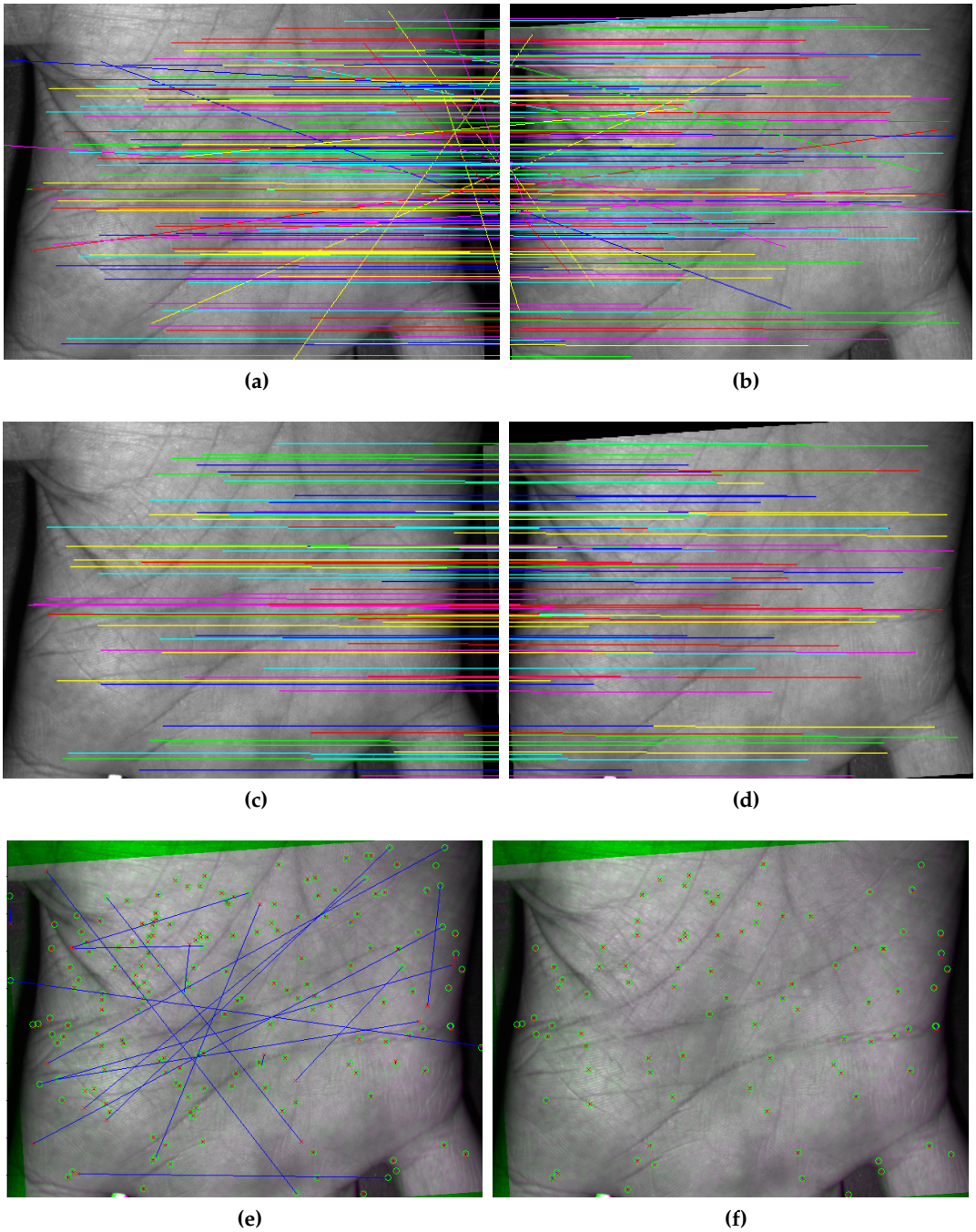

Figure 5.17: Example of the point refinement based on the collinearity: (a, b) matching points between the first and the second image, before the refinement; (c, d) matching points after the refinement; (e) superimposition of the first and the second image before the refinement. The matching points are connected using a blue line; (e) superimposition of the first and the second image after the refinement. The matching points are connected using a blue line.

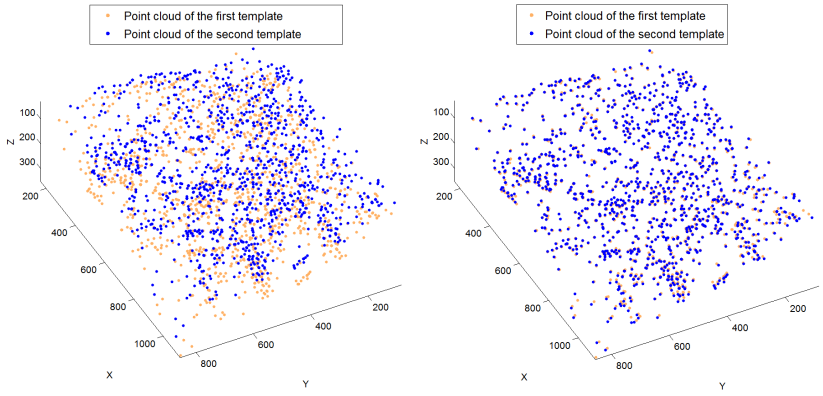

(a) **(b)**

Figure 5.18: Example of the three-dimensional point cloud registration based on the ICP algorithm: (a) point cloud (X_{Af}, Y_{Af}, Z_{Af}) (red) and $(X'_{Af}, Y'_{Af}, Z'_{Af})$ (blue) before registration; (b) point clouds after registration.

5.2.8.1 COMPUTATION OF THE THREE-DIMENSIONAL COORDINATES

The three-dimensional coordinates of the refined matching points M_{Af}, M_{Bf}, corresponding to the first template, are computed by using the surface maps S_{Ax}, S_{Ay}, S_{Az}, S_{Bx}, S_{By}, S_{Bz} estimated in the Section 5.2.5.4:

$$\begin{aligned} X_{Af} &= S_{Ax}(x_{Af}, y_{Af}) \;\; ; \;\; X_{Bf} = S_{Bx}(x_{Bf}, y_{Bf}) \;\; ; \\ Y_{Af} &= S_{Ay}(x_{Af}, y_{Af}) \;\; ; \;\; Y_{Bf} = S_{By}(x_{Bf}, y_{Bf}) \;\; ; \\ Z_{Af} &= S_{Az}(x_{Af}, y_{Af}) \;\; ; \;\; Z_{Bf} = S_{Bz}(x_{Bf}, y_{Bf}) \;\; , \end{aligned} \tag{5.39}$$

where (x_{Af}, y_{Af}) and (x_{Bf}, y_{Bf}) are the coordinates of the points belonging respectively to M_{Af} and M_{Bf}, while (X_{Af}, Y_{Af}, Z_{Af}) and (X_{Bf}, Y_{Bf}, Z_{Bf}) are the corresponding three-dimensional coordinates.

Similarly, the three-dimensional coordinates of the points belonging to M'_{Af} and M'_{Bf} are computed, in order to obtain the point clouds $(X'_{Af}, Y'_{Af}, Z'_{Af})$ and $(X'_{Bf}, Y'_{Bf}, Z'_{Bf})$.

5.2.8.2 REGISTRATION OF THE POINT CLOUDS

An ICP algorithm [455] is used to register the point clouds. In particular, the three-dimensional points (X_{Af}, Y_{Af}, Z_{Af}) and (X_{Bf}, Y_{Bf}, Z_{Bf}) are respectively registered with the points $(X'_{Af}, Y'_{Af}, Z'_{Af})$ and $(X'_{Bf}, Y'_{Bf}, Z'_{Bf})$.

An example of three-dimensional point clouds before and after the registration is shown in Fig. 5.18.

5.2.8.3 COMPUTATION OF THE THREE-DIMENSIONAL TEMPLATE

First, the two-dimensional Delaunay triangulation of the point clouds is computed by considering only the X and Y coordinates. Then, the Z coordinate is added to each

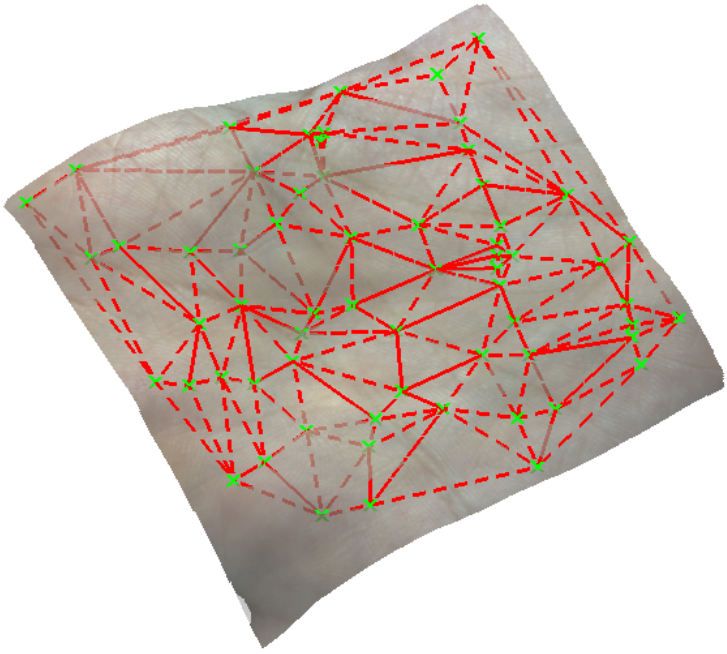

Figure 5.19: Example of a Delaunay triangulation.

vertex of the computed triangles (Fig. 5.19), and the lengths of the sides of the triangles in the three-dimensional space are computed:

$$\begin{aligned} L_{1i} &= \sqrt{(X_{1i} - X_{2i})^2 + (Y_{1i} - Y_{2i})^2 + (Z_{1i} - Z_{2i})^2} \ ; \\ L_{2i} &= \sqrt{(X_{2i} - X_{3i})^2 + (Y_{2i} - Y_{3i})^2 + (Z_{2i} - Z_{3i})^2} \ ; \\ L_{3i} &= \sqrt{(X_{1i} - X_{3i})^2 + (Y_{1i} - Y_{3i})^2 + (Z_{1i} - Z_{3i})^2} \ , \end{aligned} \tag{5.40}$$

where $(X_{1i}, Y_{1i}, Z_{1i}), (X_{2i}, Y_{2i}, Z_{2i}), (X_{3i}, Y_{3i}, Z_{3i})$ are the three-dimensional coordinates of the three vertices of the i-th triangle, and L_{1i}, L_{2i}, L_{3i} are the three lengths of the sides of the i-th triangle.

5.2.8.4 EXTRACTION OF THE SIMILAR TRIANGLES AND COMPUTATION OF THE MATCH SCORE

The triangles pertaining to the first and the second template are compared by analyzing the lengths of the sides of the triangles. Each triangle in the first template is compared to every triangle in the second template to determine if the three sides have a similar length:

$$\begin{aligned} L_{1i} - L'_{1j} &< (t_D \, L_{1i}) \ ; \\ L_{2i} - L'_{2j} &< (t_D \, L_{2i}) \ ; \\ L_{3i} - L'_{3j} &< (t_D \, L_{3i}) \ , \end{aligned} \tag{5.41}$$

where L_{1i}, L_{2i}, L_{3i} are the lengths of the three sides of the i-th triangle in the first template, $L'_{1j}, L'_{2j}, L'_{3j}$ are the lengths of the three sides of the j-th triangle in the second template, and t_D is a fixed threshold chosen experimentally.

The number of similar triangles, for which the differences of the corresponding three sides is less than the threshold, is used as the match score.

5.3 FULLY CONTACTLESS LESS-CONSTRAINED PALMPRINT RECOGNITION WITH UNCONTROLLED DISTANCE

The results obtained with the feasibility study for the contactless recognition based on acquisitions performed at a fixed distance allowed to extend the described methods using an innovative, fully contactless, and less-constrained acquisition.

In this section, the original researched methods based on acquisitions with uncontrolled distance are described. These methods are able to perform the contactless palmprint recognition with a reduced number of constraints with respect to the majority of the approaches in the literature. In particular, the hand does not touch any surface, and the user is required only to place his hand horizontally inside a volume, represented by the intersection of the field of views of the cameras, and the areas that are sufficiently close to the illumination. Moreover, the user is not required to spread his fingers or open his hand in a specific way. The use of three-dimensional reconstruction techniques permits a description of the palm that is invariant to the pose of the hand and the acquisition distance. With respect to the contactless three-dimensional palmprint recognition methods proposed in the literature [425, 426], the researched methods perform a faster acquisition, and are able to work using an innovative low-cost setup, composed of a two-view acquisition system and a led illumination.

The researched method for the palmprint recognition using acquisitions performed with uncontrolled distance can be divided into several steps. First, the acquisition setup is calibrated, then a multiple-view less-constrained contactless acquisition is performed, using a uniform led illumination. The images are preprocessed in order to segment the palm region. Then, the three-dimensional processing of the palmprint is performed: first, the three-dimensional model of the palmprint is reconstructed, then the model is registered in order to normalize the pose and the distance. A three-dimensional image registration is performed by reprojecting the models on the image plane using the calibration data. The corresponding texture images are enhanced, then the two-dimensional features are extracted and matched. A three-dimensional feature extraction and matching step is used to further refine the matching. An outline of the method is shown in Fig. 5.20.

5.3.1 CAMERA CALIBRATION

The method described in Section 5.2.2 is used for the calibration of the cameras. The intrinsic and extrinsic parameters of the cameras are computed, together with the homography matrix H and the fundamental matrix F.

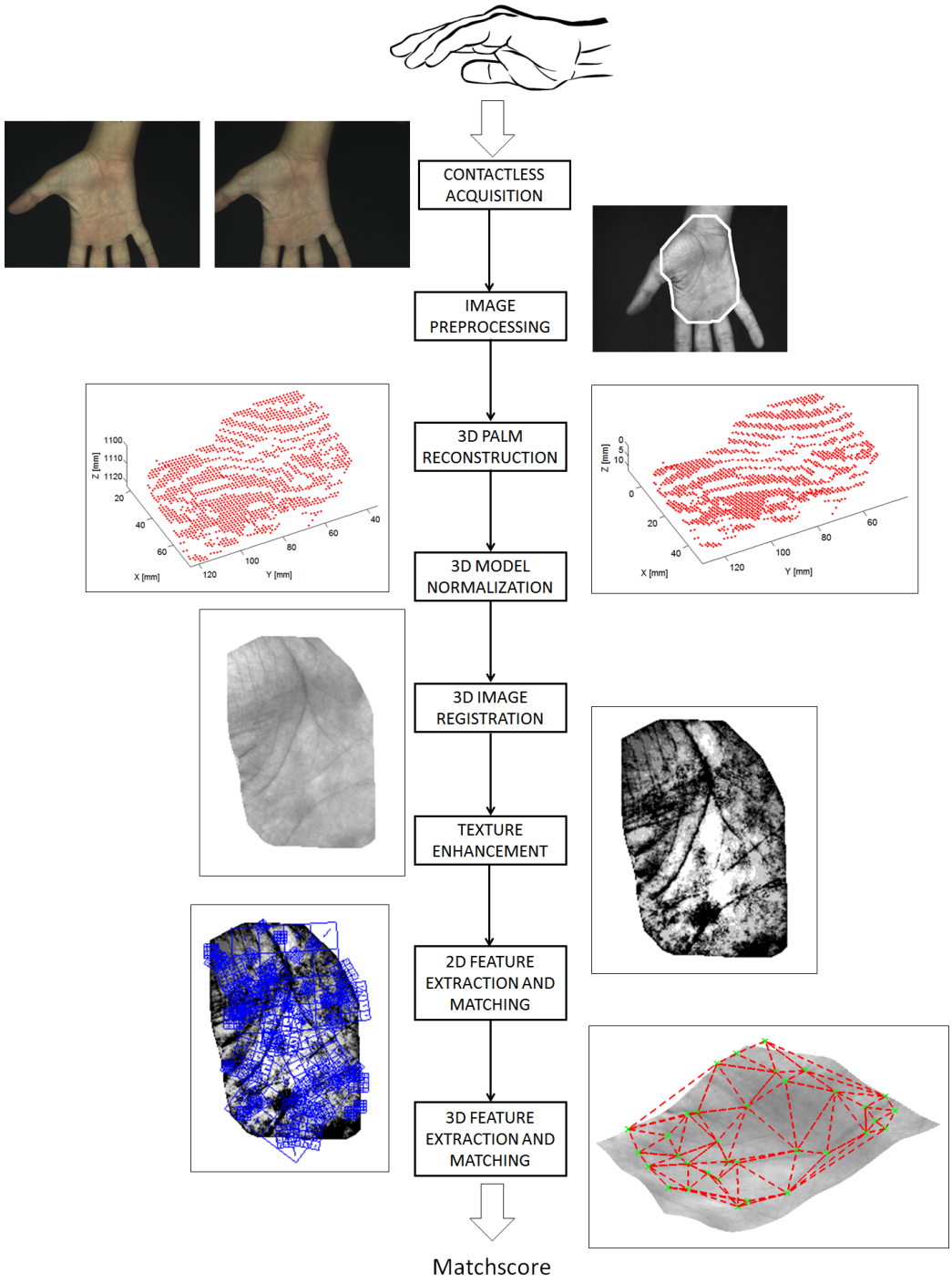

Figure 5.20: Schema of the palmprint recognition system using acquisitions performed with the hand positioned with uncontrolled distance.

5.3.2 ACQUISITION

The contactless acquisition setup used for capturing the palmprint images with an uncontrolled distance is depicted in Fig. 5.21, and consists of a two-view acquisition system and a led illumination. In particular, two CCD color cameras are used, and

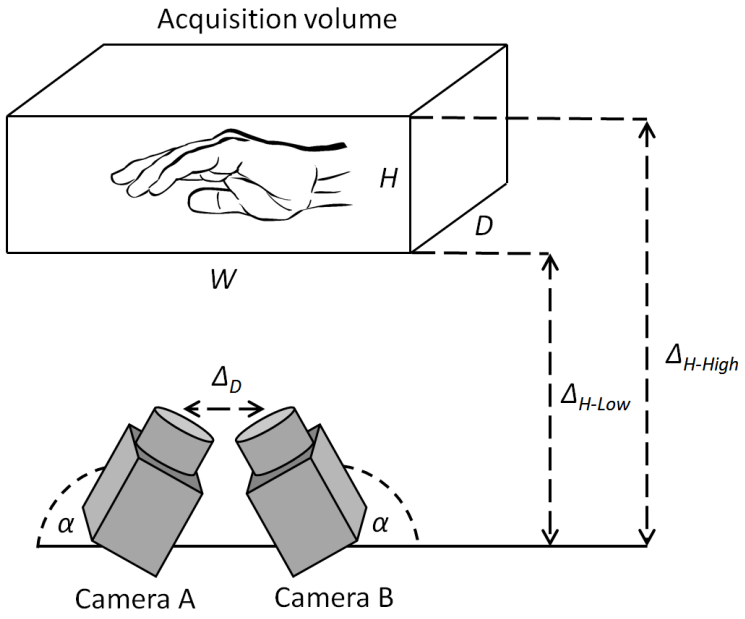

Figure 5.21: Acquisition volume.

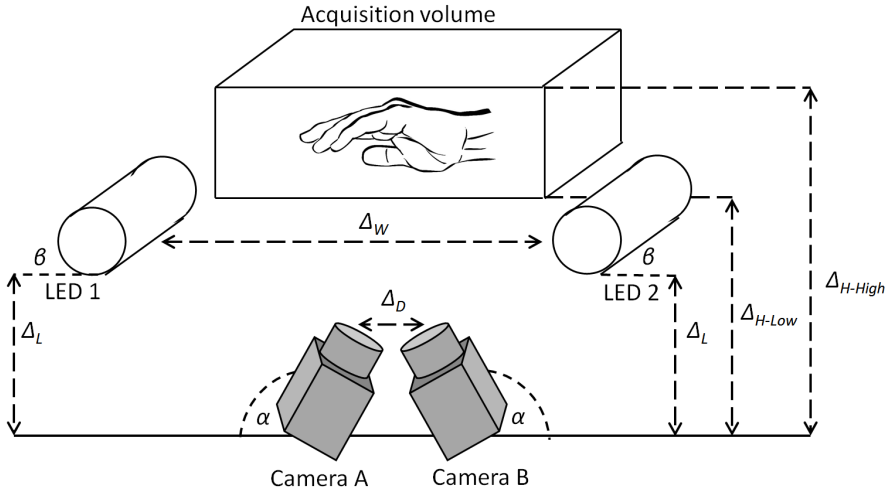

Figure 5.22: Schema of the illumination used in Method 1.

mounted facing upwards. The user's hand must only be placed inside an acquisition volume, which considers the field of view of the cameras, their depth of focus, and the region with uniform illumination. Moreover, the user is not required to spread the fingers in order to facilitate the segmentation process, and a relaxed position of the hand is sufficient to perform the recognition.

The acquisition volume, with size $W \times \mathrm{H} \times \mathrm{D}$, considers all the space in which the hand can be placed in order to perform a correct acquisition, and is placed at a distance $\Delta_{\mathrm{H-Low}}$ from the cameras. A surface with a uniform color is placed at a distance $\Delta_{\mathrm{H-High}}$ in order to delimit the superior part of the acquisition volume.

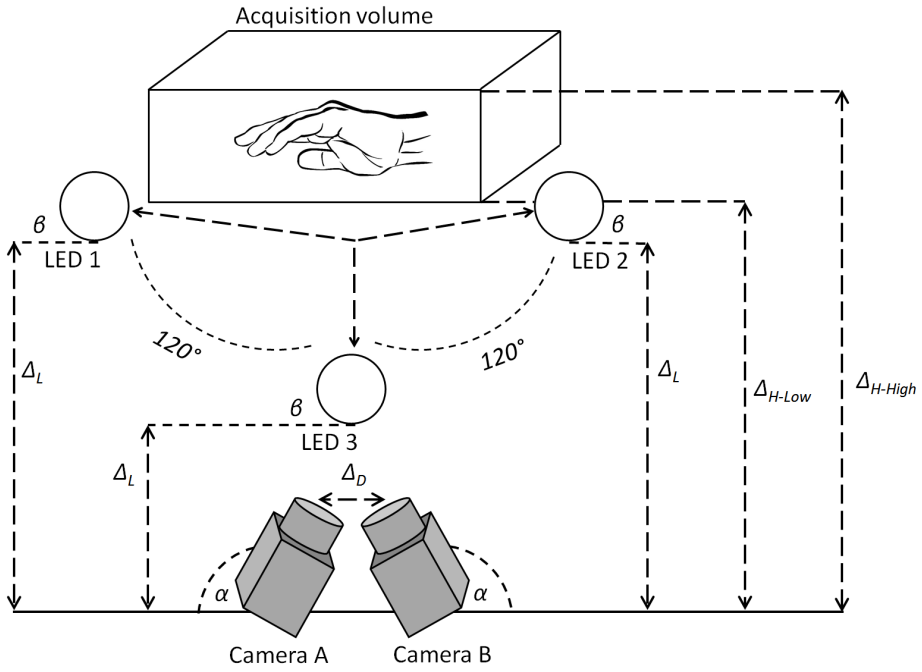

Figure 5.23: Schema of the illumination used in Method 2.

The illumination is designed in order to be uniform, and differences in the position, distance, and orientation of the hand inside the acquisition volume produce limited differences in the visibility of the details in different parts of the palm. However, the possible presence of regions with non-uniform illumination (e.g., reflections, or shadows) do not influence the position and the structure of palmprint details, and at most can partially reduce the usable area.

Moreover, three types of illuminations were considered, in order to achieve the most uniform illumination possible inside the acquisition volume, and are referred to as Method 1, Method 2, and Method 3:

- *Method 1*: two white led bars are mounted at the sides of the acquisition volume with a distance Δ_L from the cameras, and with a distance Δ_W between them. The bars are inclined towards the acquisition volume with an angle β (Fig. 5.22). This method provides a uniform illumination in the acquisition volume

- *Method 2*: three downlight illuminators with white leds are mounted with the same distance Δ_L from the cameras, and arranged equispaced in a circular fashion around the acquisition volume. The downlights are inclined towards the acquisition volume with an angle β (Fig. 5.23). With respect to Method 1, this method provides an illumination with more intensity.

- *Method 3*: four blue led bars are mounted with the distance Δ_L from the cameras, and arranged around the acquisition volume with a distance Δ_W between the lateral bars, and a distance Δ_D between the front and rear bars. The bars are inclined towards the acquisition volume with an angle β (Fig. 5.24). This method provides

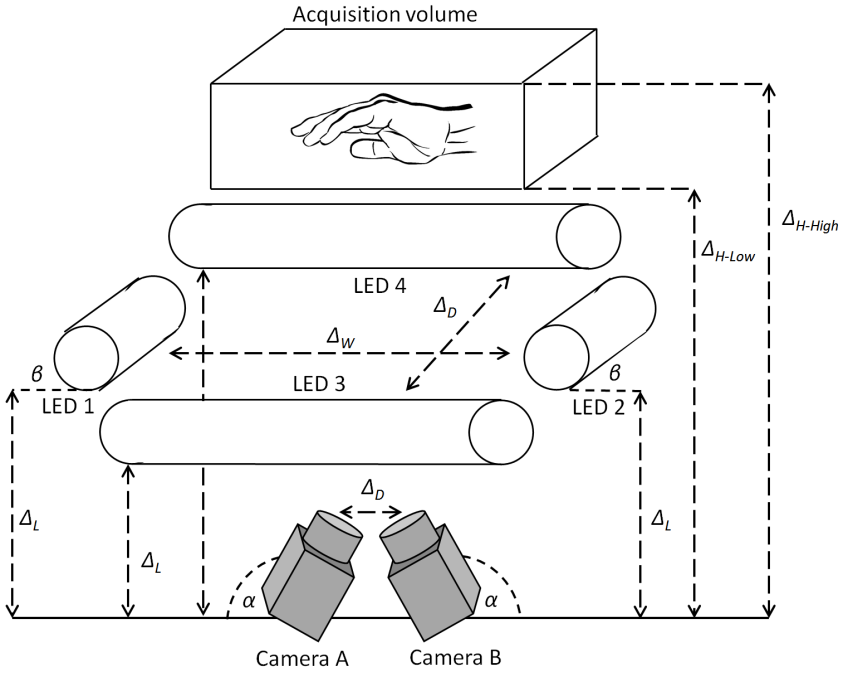

Figure 5.24: Schema of the illumination used in Method 3.

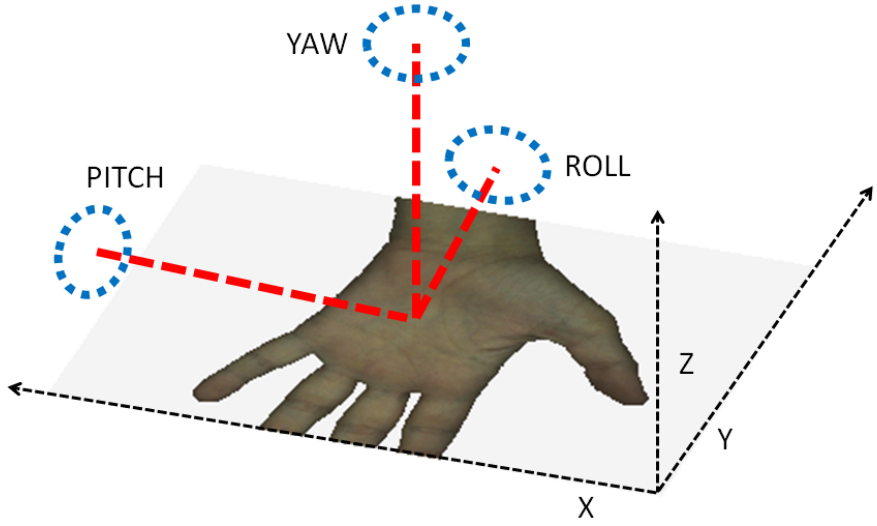

Figure 5.25: Schema of the three possible rotations.

a uniform illumination and the blue light enhances the details of the palmprint. However, the R channel of the captured images contains little information.

In order to capture a palmprint sample, the user is required to place his hand inside the acquisition volume, then a synchronized two-view acquisition is performed. The orientation and pose of the hand are not constrained, and the user is only required to place his hand in a way that makes the palmprint visible to the acquisition system. A

(a) (b)

Figure 5.26: Example of the user interface showing the live feed from the two-view camera setup.

relaxed position of the hand is possible, with uncontrolled yaw orientations (Fig. 5.25). However, small rotations along the pitch and roll angles can be tolerated.

An adaptive shutter adjustment scheme is used in order to capture images with a similar average brightness, in order to cope with changes in the ambient light, and with variations in the reflectivity of the skin of different persons:

$$t_{Shutter} = \begin{cases} t_{Shutter} + 1 & \text{if} \quad \overline{I(x,y)} < t_M \text{ and } \max I(x,y) < 250 \\ t_{Shutter} - 1 & \text{if} \quad \overline{I(x,y)} > t_M \\ t_{Shutter} & \text{if} \quad \overline{I(x,y)} = t_M \end{cases} , \tag{5.42}$$

where t_M is a value experimentally chosen, and the value 250 is used to avoid saturation effects.

In order to increase the ease of use of the acquisition device, a user interface is designed in order to show a live feed of the field of view of the cameras. Moreover, a circle is superimposed on the live image (Fig. 5.26), and when the palm of the user is placed over the circle, the acquisition is performed. In particular, in order to check for the palm inside the circle, a circular ROI mask $C(x,y)$ is defined and centered on the image. The live image is segmented using the equation:

$$I_s(x,y) = \begin{cases} 1 & \text{if } I(x,y) > t_s \\ 0 & \text{otherwise} \end{cases} , \tag{5.43}$$

where $I_s(x,y)$ is the binary segmented mask, and t_s is an experimentally estimated threshold value. The AND operator is used to combine the masks $I_s(x,y)$ and $C(x,y)$:

$$K(x,y) = I_s(x,y) \cap C(x,y) , \tag{5.44}$$

where $K(x,y)$ is the resulting image. If $K(x,y) = C(x,y)$ the central region of the hand, corresponding to the palm, is placed over the circle in the central area of the image. Then, a text is superimposed on the live feed, warning the user to remain steady.

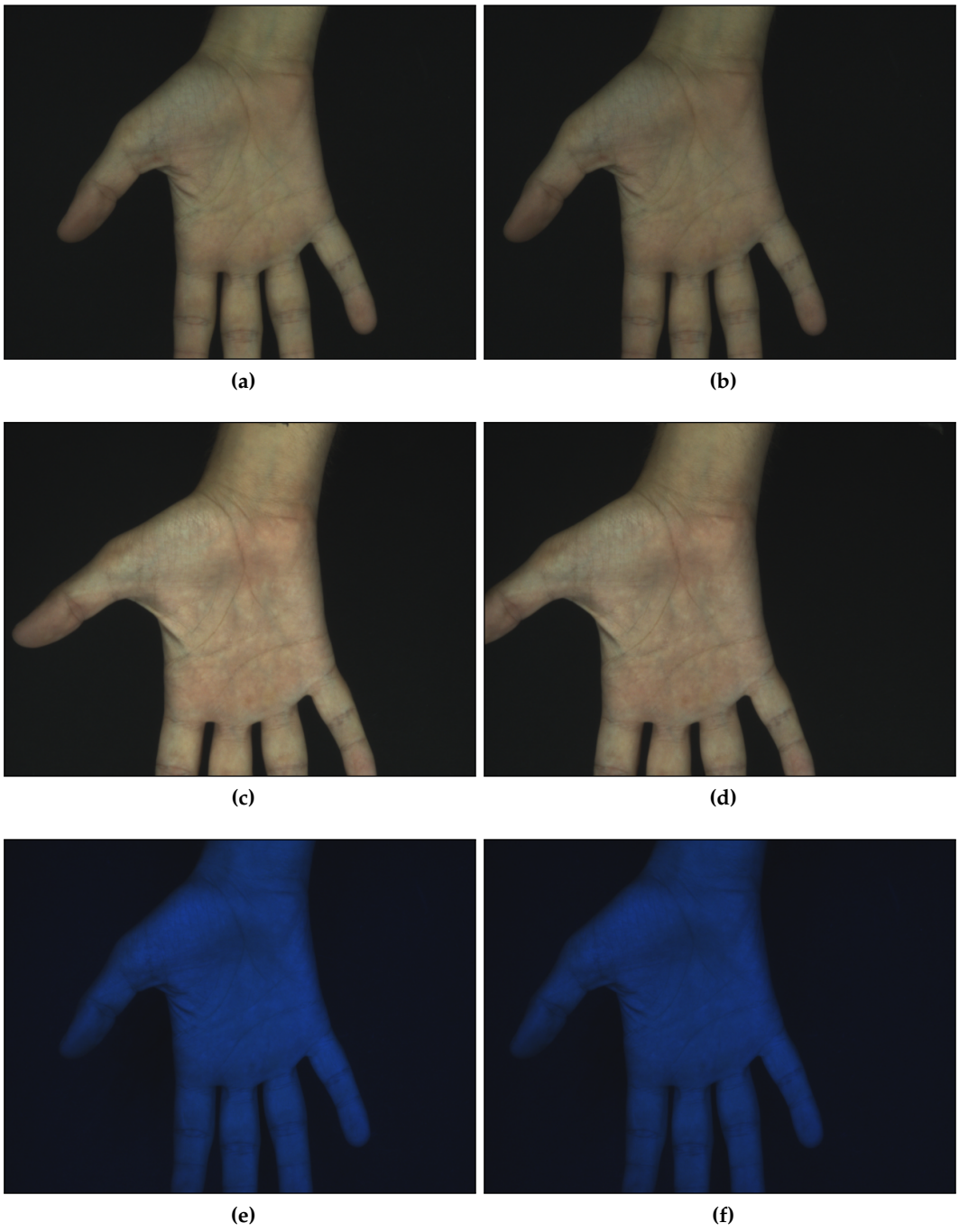

Figure 5.27: Example of the contactless two-view acquisition performed with uncontrolled hand distance: (a,b) acquisition performed using Method 1; (c,d) acquisition performed using Method 2; (e,f) acquisition performed using Method 3.

After a short period of time, needed in order to avoid motion blur, the acquisition is automatically performed.

Examples of acquisitions using the three described illumination methods are shown in Fig. 5.27.

5.3.3 IMAGE PREPROCESSING

The image preprocessing step has the purpose of segmenting the palm region of the hand in the acquisitions.

First, the two color images are converted to one-channel images. In the case of acquisitions performed using Method 1 and Method 2, the grayscale image is computed. In the case of acquisitions performed using Method 3, the blue B channel of the image is considered. Then, the images are segmented in order to remove the background. Since a surface with a uniform color is used, the thresholding operation described in Equation 5.43 is used to extract the foreground and obtain the image $I_s(x, y)$.

In order to eliminate possible points outside the boundary that can be segmented as foreground, a morphological opening operation is applied, followed by a closing operation. Then, only the largest connected component is extracted.

The fingers are removed by using a morphological open operation using a structural element with a circular shape and a fixed size, and the points lying on the computed boundary are extracted.

A two-dimensional ellipse is fitted on the extracted points, by solving a minimization problem:

$$\min\left(\log\left(\det A\right)\right) \ , \tag{5.45}$$

where A is the 2×2 matrix of the ellipse equation, expressed in the form:

$$(x - c_e)^T A (x - c_e) = 1 \ , \tag{5.46}$$

where c_e is the vector containing the coordinates of the center of the ellipse. The minimization problem is subject to the following constraints:

$$(p_i - c_e)^T A (p_i - c_e) \leqslant 1 \ , \tag{5.47}$$

where p_i is the i-th extracted point lying on the boundary.

Then, the singular value decomposition of the matrix A is computed:

$$[U \ Q \ V] = \mathrm{svd}(A) \ , \tag{5.48}$$

then the radii r_1, r_2 of the fitted ellipse are computed using the following equations:

$$r_1 = \frac{1}{\sqrt{Q_{(1,1)}}} \quad ; \quad r_2 = \frac{1}{\sqrt{Q_{(2,2)}}} \ . \tag{5.49}$$

A morphological open operation is performed in order to extract the central palm region, using a structural element with a circular shape and a size s_e, which is computed based on the radii of the fitted ellipse:

$$s_e = k_e \min\left(r_1, r_2\right) \ , \tag{5.50}$$

where k_e is a fixed parameter chosen experimentally.

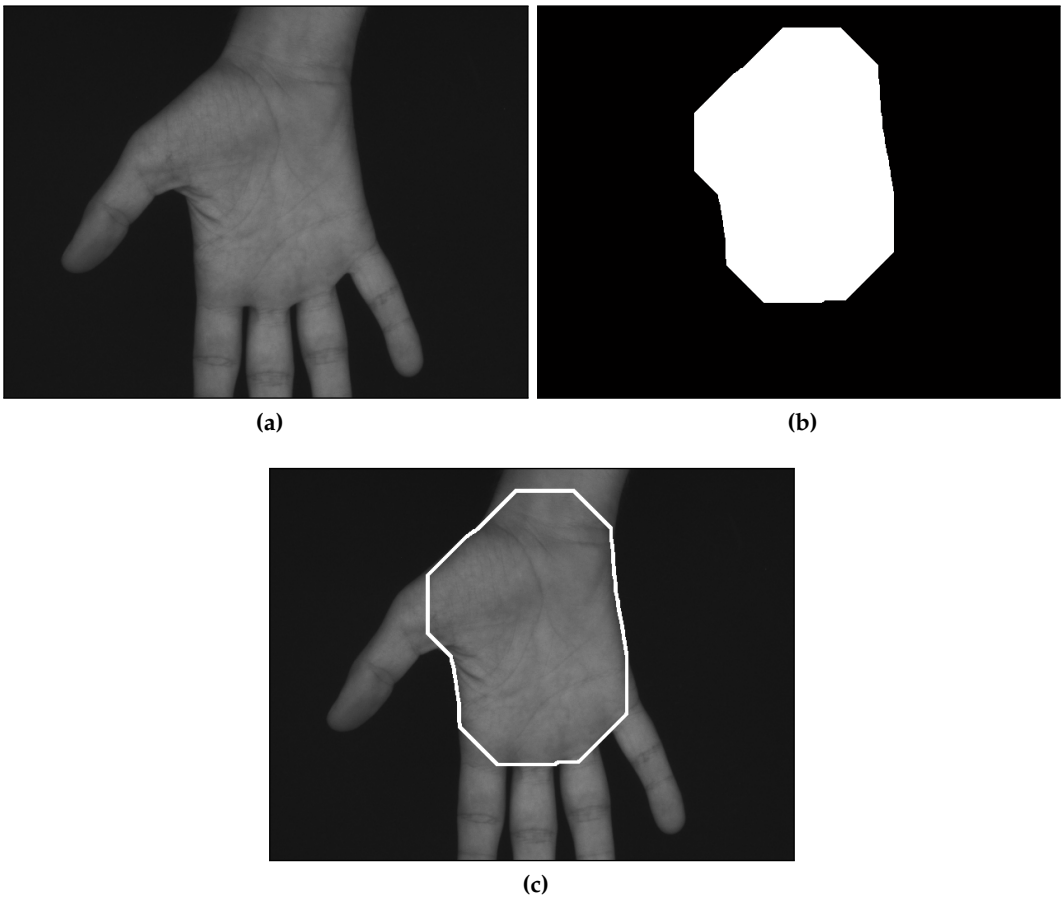

Figure 5.28: Example of the segmentation: (a) grayscale image captured using Method 1; (b) segmented image; (c) edge of the segmented image superimposed on the grayscale image.

An example of the segmentation operation is shown in Fig. 5.28.

5.3.4 THREE-DIMENSIONAL PALMPRINT PROCESSING

The three-dimensional processing of the palmprint can be divided into three steps. First, the three-dimensional model of the palm is reconstructed using the two-view acquisitions and the calibration data, then the model is normalized in the three-dimensional space. A three-dimensional image registration is performed by reprojecting the model on the image plane using the calibration data.

5.3.4.1 THREE-DIMENSIONAL PALMPRINT RECONSTRUCTION

The method described in Section 5.2.5, based on a cross-correlation approach, is used to compute the three-dimensional model of the palmprint, described by the point cloud (X_A, Y_A, Z_A). The corresponding surfaces and textures S_{Ax}, S_{Ay}, S_{Az}, S_{Ac} are obtained using a similar procedure for surface estimation and the texture mapping.

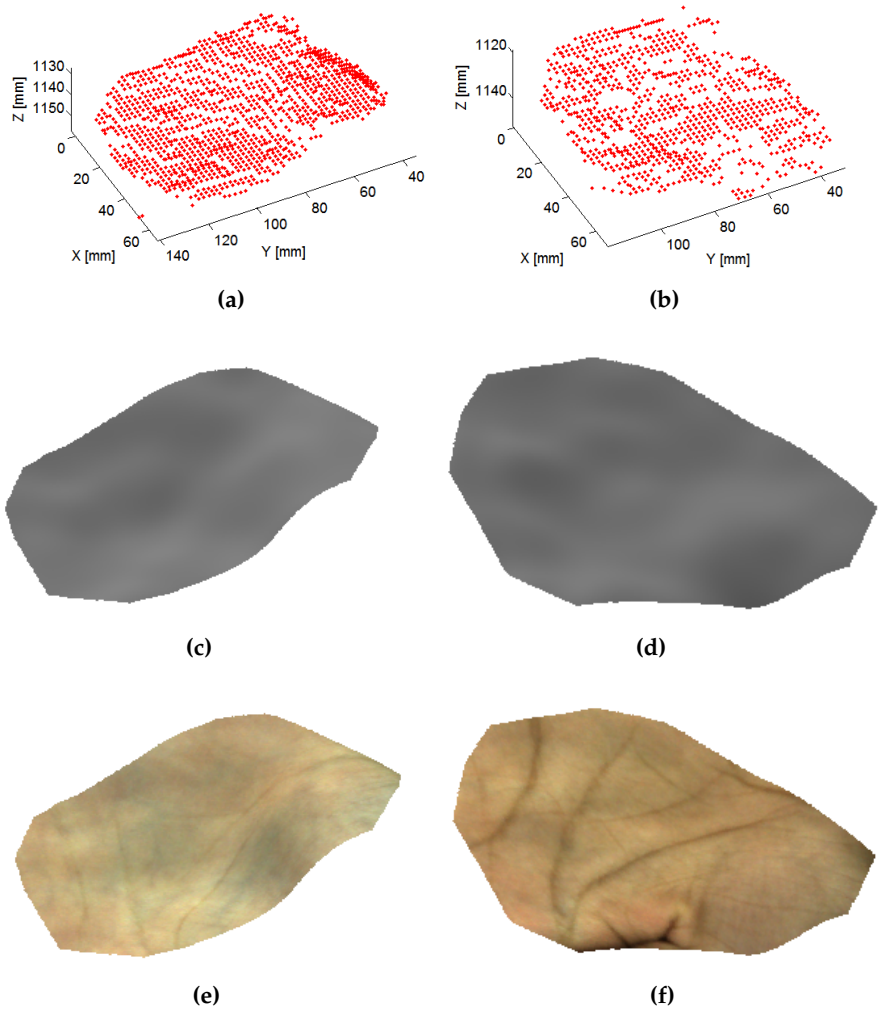

Figure 5.29: Example of reconstructed three-dimensional palmprint models: (a, b) filtered point clouds; (c, d) interpolated surfaces; (e, f) texture images.

Examples of reconstructed point clouds with the relative estimated surfaces and textures are shown in Fig. 5.29.

5.3.4.2 THREE-DIMENSIONAL MODEL NORMALIZATION

The three-dimensional point cloud (X_A, Y_A, Z_A) is registered in order to normalize its position and orientation in the three-dimensional space. In particular, the pitch and roll rotations are corrected (Fig. 5.25).

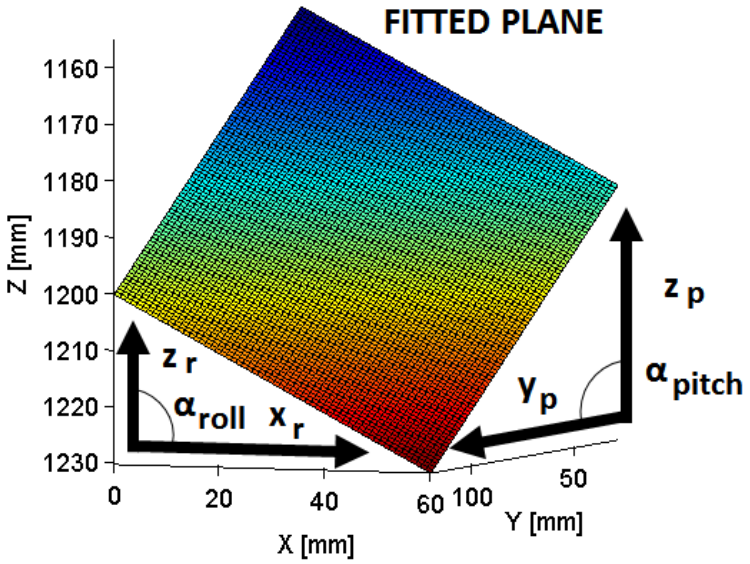

Figure 5.30: The computation of the roll and pitch angles using the fitted plane.

First, the point cloud is centered in the origin of the axes by subtracting from the point cloud the corresponding mean coordinates:

$$\begin{aligned} X_{Am} &= X_A - \frac{1}{N}\sum_{i=1}^{N} X_{A_i} \ ; \\ Y_{Am} &= Y_A - \frac{1}{N}\sum_{i=1}^{N} Y_{A_i} \ ; \\ Z_{Am} &= Z_A - \frac{1}{N}\sum_{i=1}^{N} Z_{A_i} \ , \end{aligned} \tag{5.51}$$

where N is the number of points in the point cloud. Then, a linear interpolation is used to fit a plane to the points, obtaining the point cloud (X_p, Y_p, Z_p). Then, the range of the values of the fitted plane on the X, Y, and Z axes are considered as the catheti of two right triangles, and trigonometric formulas are used to estimate the pitch and roll angles (Fig. 5.30).

First, the ranges of the values of the plane along the x and z directions are computed:

$$\begin{aligned} x_r &= \max X_p - \min X_p \ ; \\ z_r &= \max Z_p - \min Z_p \ ; \end{aligned} \tag{5.52}$$

where x_r is the range of the values of the fitted plane along the X axis, and z_r is the range of the values of the fitted plane along the Z axis. The ranges z_r, x_r are considered as the catheti of a right triangle, and the hypotenuse a_r is computed as:

$$a_r = \sqrt{x_r^2 + z_r^2} \ . \tag{5.53}$$

The roll angle α_{roll} is estimated using the trigonometric formula:

$$\alpha_{roll} = \sin^{-1} \frac{z_r}{a_r} \ . \tag{5.54}$$

The rotation matrix corresponding to α_{roll} is computed as:

$$R_{roll} = \begin{bmatrix} \cos(\alpha_{roll}) & 0 & \sin(\alpha_{roll}) \\ 0 & 1 & 0 \\ -\sin(\alpha_{roll}) & 0 & \cos(\alpha_{roll}) \end{bmatrix} \ , \tag{5.55}$$

then the rotation is applied to the points belonging to the reconstructed model of the palm:

$$\begin{bmatrix} X_{roll} \\ Y_{roll} \\ Z_{roll} \end{bmatrix} = R_{roll} \begin{bmatrix} X_{Am} \\ Y_{Am} \\ Z_{Am} \end{bmatrix} \ , \tag{5.56}$$

where $(X_{roll}, Y_{roll}, Z_{roll})$ is the point cloud after the compensation of the roll angle.

Similarly, the pitch angle is compensated by first estimating the ranges of the values of the fitted plane along the Y and Z axes:

$$\begin{aligned} y_p &= \max Y_p - \min Y_p \ ; \\ z_p &= \max Z_p - \min Z_p \ , \end{aligned} \tag{5.57}$$

where y_p is the range of the values of the fitted plane along the Y axis and z_p is the range of the values of the fitted plane along the Z axis. The hypotenuse a_p is computed as:

$$a_p = \sqrt{y_p^2 + z_p^2} \ , \tag{5.58}$$

and the pitch angle α_{pitch} is estimated using the trigonometric formula:

$$\alpha_{pitch} = \sin^{-1} \frac{z_p}{a_p} \ . \tag{5.59}$$

The rotation matrix corresponding to α_{pitch} is computed as:

$$R_{pitch} = \begin{bmatrix} \cos(\alpha_{pitch}) & 0 & \sin(\alpha_{pitch}) \\ 0 & 1 & 0 \\ -\sin(\alpha_{pitch}) & 0 & \cos(\alpha_{pitch}) \end{bmatrix} \ , \tag{5.60}$$

then the rotation is applied to the points obtained after the correction of the roll angle:

$$\begin{bmatrix} X_{pitch} \\ Y_{pitch} \\ Z_{pitch} \end{bmatrix} = R_{pitch} \begin{bmatrix} X_{roll} \\ Y_{roll} \\ Z_{roll} \end{bmatrix} , \tag{5.61}$$

where $(X_{pitch}, Y_{pitch}, Z_{pitch})$ is the point cloud after the compensation of the pitch angle.

The obtained point cloud is centered in the origin of the axes by subtracting the corresponding mean coordinates:

$$\begin{aligned} X_{norm} &= X_{pitch} - \frac{1}{N}\sum_{i=1}^{N} X_{pitch_i} \ ; \\ Y_{norm} &= Y_{pitch} - \frac{1}{N}\sum_{i=1}^{N} Y_{pitch_i} \ ; \\ Z_{norm} &= Z_{pitch} - \frac{1}{N}\sum_{i=1}^{N} Z_{pitch_i} \ , \end{aligned} \tag{5.62}$$

Examples of normalized point clouds are shown in Fig. 5.31.

5.3.4.3 THREE-DIMENSIONAL IMAGE REGISTRATION

The three-dimensional image registration step has the purpose of reprojecting the normalized models on the image plane using common parameters, in order to obtain two-dimensional images as captured in the same position and with the same orientation, even if the acquisitions of the hand were performed at different distances and with different orientations.

In particular, the calibration data computed using the method described in the Section 5.3.1 is used to project the normalized model on the image plane, using the method described in [450]:

$$\begin{bmatrix} u \\ v \\ 1 \end{bmatrix} = K[R|t] \begin{bmatrix} X_{norm} \\ Y_{norm} \\ Z_{norm} \\ 1 \end{bmatrix} , \tag{5.63}$$

where (u, v) are the projected pixel coordinates, K is the intrinsic camera matrix, R and t are the rotation matrix and translation vector that describe the position of the object with respect to the camera, and $(X_{norm}, Y_{norm}, Z_{norm})$ is the normalized three-dimensional point cloud.

In order to project every model in the same manner, fixed values for R, t were used. Moreover, two different values are used in order to project the model in two positions,

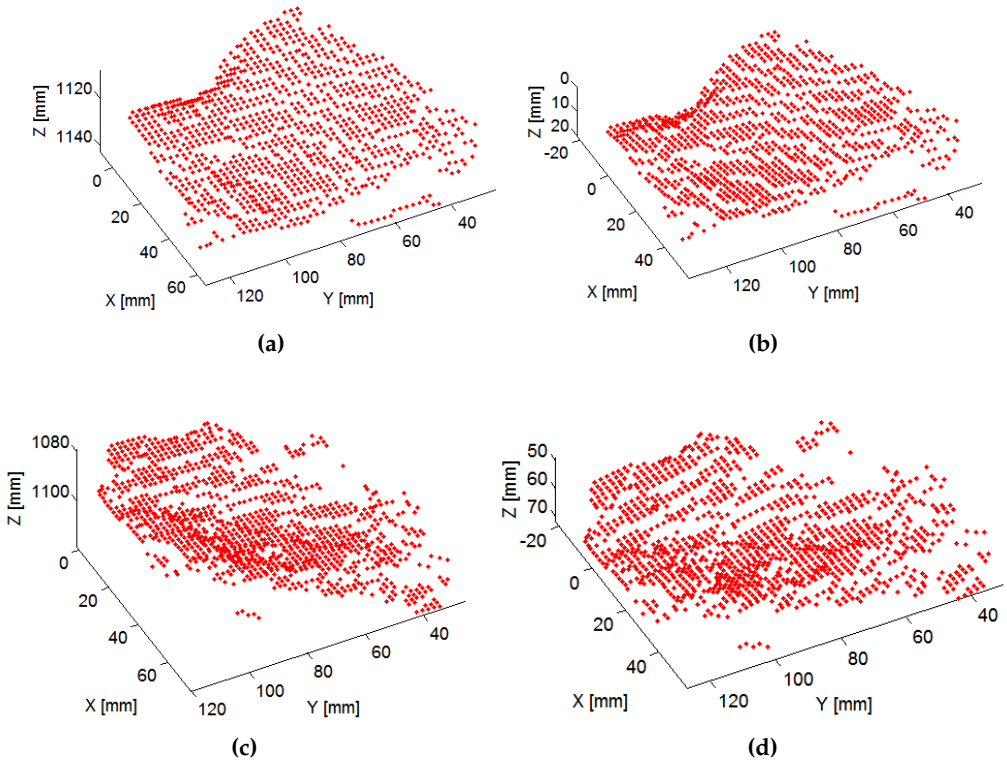

Figure 5.31: Example of three-dimensional normalized models, obtained from acquisitions performed using Method 1: (a, c) three-dimensional models before the normalization; (b, d) three-dimensional models after the normalization.

maintaining the same relative difference between the two registered acquisitions that is present in the original images I_A and I_B:

$$R_L = \begin{bmatrix} 1 & 0 & 0 \\ 0 & 1 & 0 \\ 0 & 0 & 1 \end{bmatrix} \; ; \; t_L = \begin{bmatrix} t_x \\ t_y \\ t_z \end{bmatrix} \; ;$$
$$R_R = R_c \; ; \; t_R = (R_R \, t_L) + t_C \; , \tag{5.64}$$

where R_L, t_L are the parameters used to project the model in the first position, R_R, t_R are the parameters used to project the model in the second position, t_x, t_y, t_z are fixed values, R_C, t_C are the parameters obtained from the calibration of the acquisition setup, which describe the relative position of the right Camera B with respect to the left Camera A.

The resulting images were computed using a linear interpolation of the images I_A and I_B at the new positions (u, v), obtaining the registered images I_{Ar} and I_{Br}.

The method described in the Section 5.2.5.4 is used to compute the surface maps S'_{Ax}, S'_{Ay}, S'_{Az} from the normalized point cloud $(X_{norm}, Y_{norm}, Z_{norm})$. The coordinates of the surface maps S'_{Ax}, S'_{Ay} are adjusted in order to match the coordinates of the image I_{Ar}.

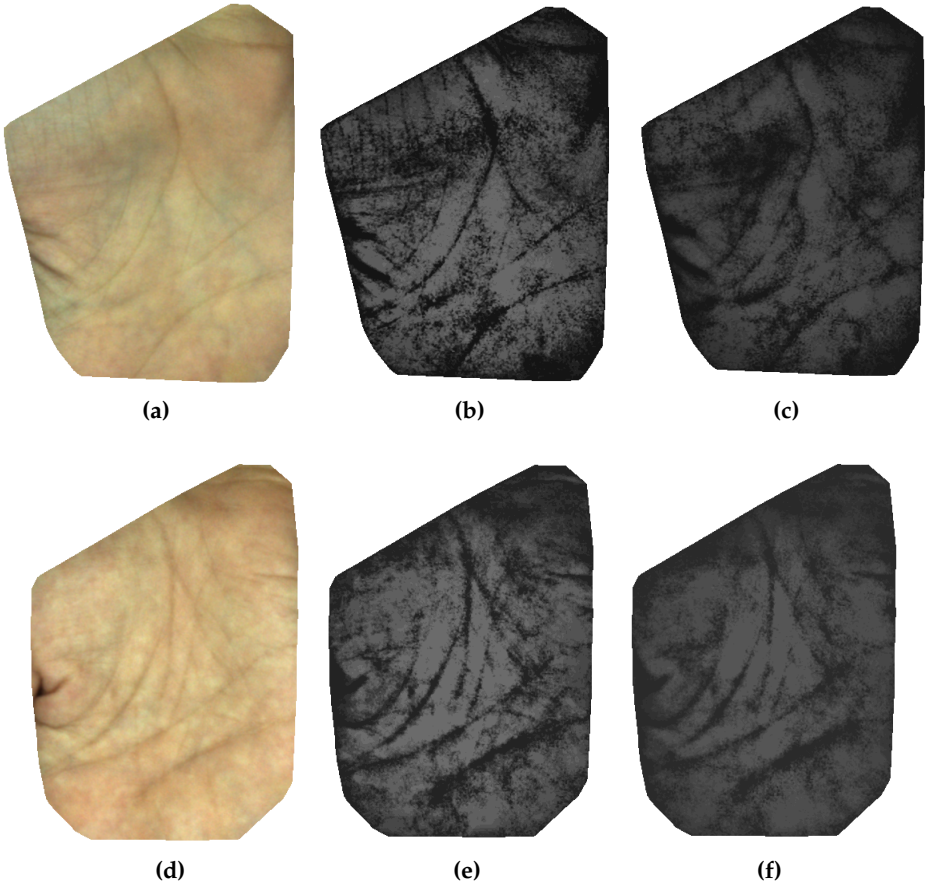

Figure 5.32: Example of enhanced texture images, captured using Method 1: (a, d) original left images from two different individuals; (b, e) enhanced textures obtained from the B channel; (c, f) enhanced textures obtained from the R channel.

Similarly, the surface maps S'_{Bx}, S'_{By}, S'_{Bz} are obtained by adjusting the coordinates of the computed surface maps, in order to match the coordinates of the image I_{Br}.

5.3.5 TEXTURE ENHANCEMENT

A texture enhancement procedure similar to the one described in Section 5.2.6 is used to enhance the images obtained after the three-dimensional registration. The method is based on a background subtraction, a logarithm operator, and a histogram equalization procedure.

In the case of palmprint samples captured using Method 1 or Method 2, the same enhancement procedure is performed on the R and B channels of the image separately, of both the left and right images I_{Ar} and I_{Br}. In the case of palmprint samples captured using Method 3, the enhancement procedure is performed only on the B channel of the left and right images. Examples of enhanced textures are shown in Fig. 5.32.

Table 5.2: Summary of the images considered for each palmprint sample captured using Method 1 or Method 2.

Notation	Description
I_{A_R}	R channel of the left texture image
I_{A_B}	B channel of the left texture image
I_{AE_R}	enhanced texture computed from the R channel of the left texture image
I_{AE_B}	enhanced texture computed from the B channel of the left texture image
I_{B_R}	R channel of the right texture image
I_{B_B}	B channel of the right texture image
I_{BE_R}	enhanced texture computed from the R channel of the right texture image
I_{BE_B}	enhanced texture computed from the B channel of the right texture image

Table 5.3: Summary of the images considered for each palmprint sample captured using Method 3.

Notation	Description
I_{A_B}	B channel of the left texture image
I_{AE_B}	enhanced texture computed from the B channel of the left texture image
I_{B_B}	B channel of the right texture image
I_{BE_B}	enhanced texture computed from the B channel of the right texture image

5.3.6 TWO-DIMENSIONAL FEATURE EXTRACTION AND MATCHING

For each palmprint sample captured using Method 1 or Method 2, 8 images are considered in order to build the corresponding template. Table 5.2 summarizes the considered images. In the case of palmprint samples captured using Method 3, only 4 images, summarized in Table 5.3, are used.

In this Section, the method used for extracting and matching the two-dimensional features of two templates is described. In particular, the notation I_A, I_B is used to indicate the images corresponding to the first template, while the notation I'_A, I'_B is used to indicate the images corresponding to the second template.

The two-dimensional feature extraction and matching method can be divided into several steps. First, the images to be compared are aligned, then a method similar to the one described in Section 5.2.7, based on the SIFT features, is used to extract and match the distinctive points. A procedure based on the point collinearity is used to refine the extracted points.

5.3.6.1 IMAGE ALIGNMENT

Since the region of interest of the palms captured using the method described in 5.3.2 is almost flat, the corresponding three-dimensional models present only little information for registering the models, and a correct alignment procedure would not be possible using only the three-dimensional information. For this reason, a two-dimensional alignment procedure is used. In particular, a SIFT-based method [454] is used to align the images pertaining to the templates to be compared. In the case of the samples captured using Method 1 and Method 2, the SIFT feature points are extracted from the enhanced images of the first template I_{AE_R}, I_{AE_B}, I_{BE_R}, I_{BE_B}:

$$\begin{aligned} &I_{AE_R} \rightarrow_{SIFT} S_1 \quad ; \quad I_{BE_R} \rightarrow_{SIFT} S_3 \quad ; \\ &I_{AE_B} \rightarrow_{SIFT} S_2 \quad ; \quad I_{BE_B} \rightarrow_{SIFT} S_4 \quad . \end{aligned} \tag{5.65}$$

Similarly, the SIFT feature points are extracted from the images I'_{AE_R}, I'_{AE_B}, I'_{BE_R}, I'_{BE_B} pertaining to the second template. In the case of samples captured using the Method 3, only the images I_{AE_B}, I_{BE_B} pertaining to the first template, and the images I'_{AE_B}, I'_{BE_B} pertaining to the second template are considered.

The number of points extracted from each image is variable, and for each point a descriptor $D(f_1, \ldots, f_{128})$, composed by 128 features, is computed.

A procedure based on the Euclidean distance is used to match the sets of descriptors extracted from the corresponding images of the two templates. In particular, a descriptor D_m is matched to a descriptor D'_n only if their distance, multiplied by a fixed threshold, is less than the maximum distance between D_m and the other descriptors:

$$d(D_m, D'_n) \times t_{SIFT} \leqslant \max_{p=1,\ldots,N'} (d(D_m, D'_p)) \ , \tag{5.66}$$

where $d(\cdot)$ represent the Euclidean distance, and N' is the number of points in the image to be compared in the second template. The locations of the matching points, corresponding to the matched descriptors, are referred as $M_{1,\ldots,4}$ and $M'_{1,\ldots,4}$.

Then, the sets of matching points $M_{1,\ldots,4}$ relative to the first template are merged in 2 sets, by distinguishing the matched points pertaining to the left images I_{AE_R}, I_{AE_B} and the matched points pertaining to the right images I_{BE_R}, I_{BE_B}, in order to obtain the sets M_{At}, M_{Bt}. Similarly, the sets of points relative to the images pertaining to the second template are merged in the sets M'_{At}, M'_{Bt}.

The sets of matched points M_{At}, M'_{At} are used to compute the non-reflective similarity transformation between the left images of the first template I_{A_R}, I_{A_B}, I_{AE_R}, I_{AE_B} and the left images of the second template I'_{A_R}, I'_{A_B}, I'_{AE_R}, I'_{AE_B}. A non-reflective similarity transformation is a subset of the affine transformations that may include a rotation, a translation, and a scaling. In non-reflective similarity transformations, shapes and angles are preserved, parallel lines remain parallel, and straight lines remain straight. In particular, A RANSAC-based algorithm is used to estimate the transformation T_A, described by a 3×2 matrix, which transforms the point locations M'_{At} in the locations M_{At}.

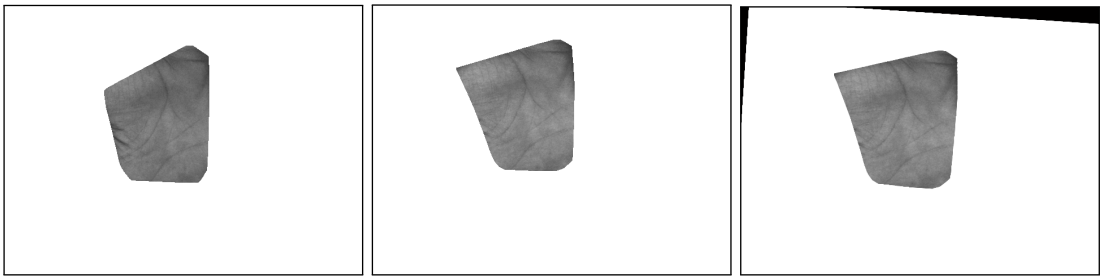

(a) (b) (c)

Figure 5.33: Example of the image alignment: (a) B channel extracted from the first image I_A; (b) B channel extracted from the second image I'_A; (c) second image aligned according to the first.

Similarly, the sets M_{Bt}, M'_{Bt} are used to compute the non-reflective similarity transformation between the right images of the first template I_{B_R}, I_{B_B}, I_{BE_R}, I_{BE_B} on the right images I'_{B_R}, I'_{B_B}, I'_{BE_R}, I'_{BE_B} of the second template. The transformation is described by the matrix T_B, which maps the points M'_{Bt} in the points M_{Bt}.

The computed transformation matrix T_A is applied to the left images of the second template I'_{A_R}, I'_{A_B}, I'_{AE_R}, I'_{AE_B}, in order to obtain the aligned images I''_{A_R}, I''_{A_B}, I''_{AE_R}, I''_{AE_B}. Similarly, the transformation T_B is applied to the right images of the second template I'_{B_R}, I'_{B_B}, I'_{BE_R}, I'_{BE_B}, in order to obtain the aligned images I''_{B_R}, I''_{B_B}, I''_{BE_R}, I''_{BE_B}.

An example of image alignment is shown in Fig. 5.33.

5.3.6.2 POINT EXTRACTION AND MATCHING

The method based on the SIFT feature points, similar to the method described in Section 5.2.7.2, is used to extract and match the points from the images pertaining to the two templates to be compared. In particular, with respect to the method described in Section 5.2.7.2, the entire image is considered, and the images are not resized.

5.3.6.3 REFINEMENT OF THE MATCHED POINTS

The method based on the collinearity of the matched points, described in Section 5.2.7.3, is used to refine the obtained sets of matching points. An example of the matched points before and after the refinement is shown in Fig. 5.34.

5.3.7 THREE-DIMENSIONAL FEATURE EXTRACTION AND MATCHING

The method described in Section 5.2.8 is used for the extraction and matching of the three-dimensional features. The method is based on the computation of the three-dimensional coordinates of the matching points using the surface maps computed in the Section 5.3.4.1, and on the use of the ICP algorithm to register the obtained point clouds. Then, a Delaunay triangulation is applied, and the number of similar triangles is used as the match score.

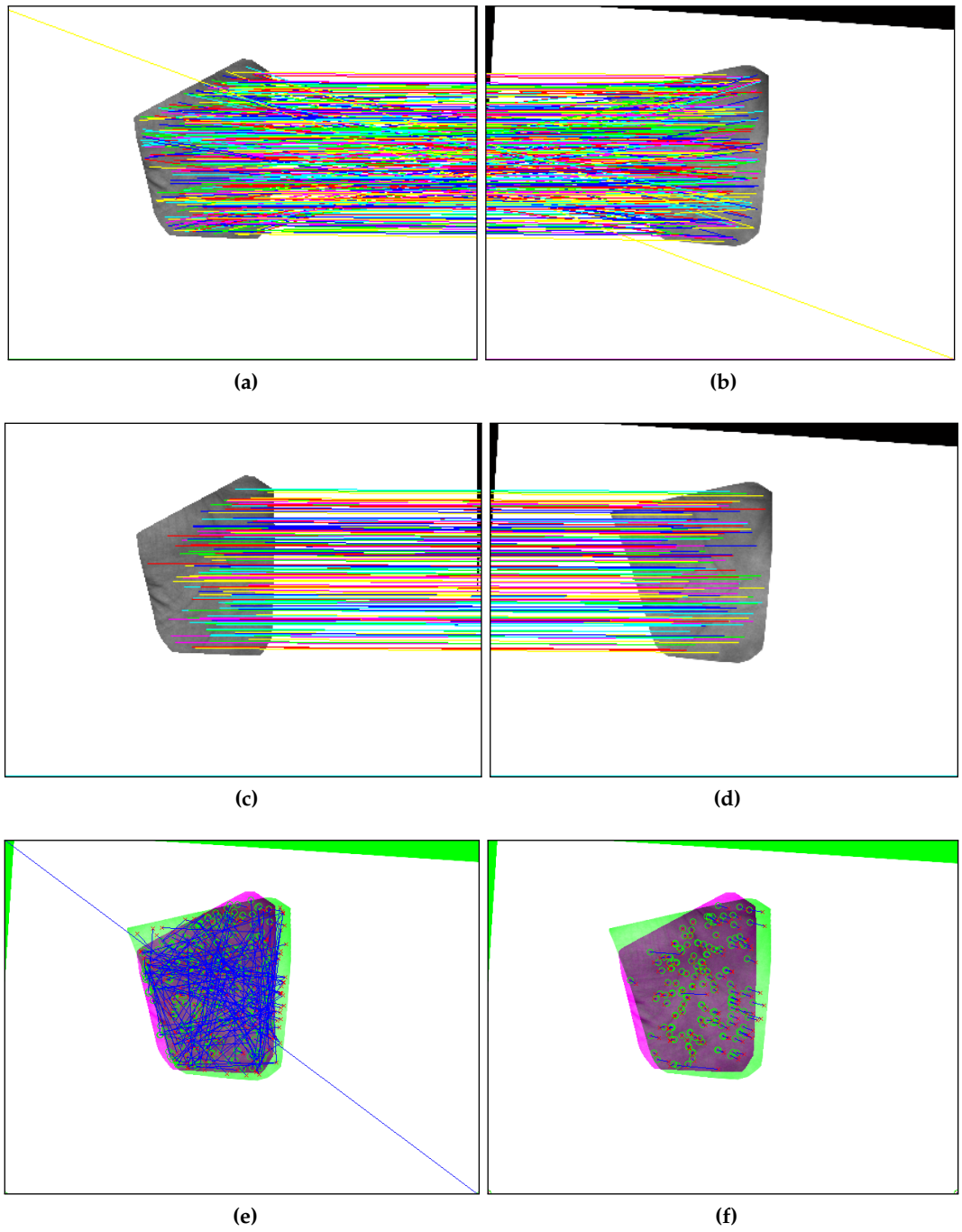

Figure 5.34: Example of the point refinement based on the collinearity: (a, b) matching points between the first and the second image, before the refinement; (c, d) matching points after the refinement; (e) superimposition of the first and the second image before the refinement. The matching points are connected using a blue line; (e) superimposition of the first and the second image after the refinement. The matching points are connected using a blue line.

5.4 SUMMARY

Innovative methods for a contactless and less-constrained palmprint recognition were described. The researched approaches do not require the user to place the palm on any surface, thus avoiding hygiene problems, increasing the acceptability, and decreasing the acquisition time. With respect to the methods in the literature based on contactless three-dimensional acquisition, the researched methods are original since they perform a fully contactless acquisition, with a shorter capture time, and with a lower cost.

A preliminary version of the researched palmprint recognition methods is described for the contactless fingerprint recognition. The research in the field of fingerprint recognition, in fact, is more advanced, and standard methods for the preprocessing, enhancement, and matching of fingerprints are available. The feasibility of the researched methods was evaluated using standard references. Moreover, similar techniques can be used to capture and process palmprint samples, and so the obtained results allowed to extend the researched methods for the palmprint recognition. The described methods for the palmprint recognition are more general and can be easily extended in order to integrate hand shape features, finger shape characteristics, and finger knuckle recognition.

Two versions of the contactless palmprint recognition methods were researched: the first method is a feasibility study and requires the hand to be placed against a fixed surface, while the second method is fully contactless and does not require a fixed position for the hand nor any kind of support. In fact, the three-dimensional metric reconstruction of the palm is a representation that is invariant to the pose and to the acquisition distance.

First, the method that requires a fixed position of the hand is described. The back of the hand must be placed on a fixed surface, and a two-view contactless acquisition is performed. A led illumination is used to enhance the visibility of the details. The captured images are segmented, then a method based on the cross-correlation is used to obtain a set of matching points, which are triangulated in the three-dimensional space using the information related to the camera calibration. A point cloud filtering procedure is applied, then the three-dimensional surface is computed, along with the corresponding texture. The texture is enhanced using a method based on background subtraction, logarithm, and adaptive histogram equalization.

A SIFT-based method is used to extract and match the distinctive points in the images. The points are subsequently refined, and the corresponding three-dimensional coordinates are computed. The ICP algorithm is used to register the three-dimensional points of different samples, then the Delaunay triangulation is computed. The number of similar triangles in the three-dimensional space is used as the match score.

Then, a fully contactless and less-constrained method is described: the method does not require a fixed position of the hand, and uses an original contactless acquisition procedure that defines an acquisition volume in which the hand is free to be positioned. The user is not required to spread the fingers in order to facilitate the segmentation process. Innovative illumination methods, based on leds with different colors and positions, are used in order to achieve an uniform illumination, and enhance the details of the palmprint.

The acquisitions are segmented using morphological operators and methods based on ellipse fitting, then the three-dimensional models are reconstructed. A normalization of the models in the three-dimensional space is performed in order to compensate for the differences in the orientation and the acquisition distance. The models are reprojected on the image plane using the same parameters, in order to obtain two-dimensional images as they were captured at the same position and with the same orientation.

Then, the resulting textures are enhanced, aligned, and a SIFT method is used to extract and match the distinctive points. A method based on ICP registration is used to register the point clouds, then the Delaunay triangulation is performed, and the number of similar triangles is used as the match score.

6

EXPERIMENTAL RESULTS

This chapter contains the experimental results relative to the innovative researched methods described in Chapter 5. The methods were tested in order to evaluate the different biometric aspects of the implemented techniques, consisting in the accuracy, robustness, speed, cost, interoperability, usability, acceptability, security, and privacy. However, a particular emphasis was given to the evaluation of the accuracy of the researched palmprint recognition systems, since it is commonly considered the most important factor. The used evaluation procedures and figures of merit are described in Section 2.4.

In this chapter, the results relative to the methods based on acquisitions at a fixed distance are presented, including a description of the acquisition of the test datasets, a summary of the used parameters, an evaluation of the three-dimensional models, and a description of the recognition accuracy performances. Then, the results of the methods based on acquisitions with uncontrolled distance are presented and described. In particular, the acquisition of the test datasets is described, the used parameters are summarized, and the three-dimensional models are evaluated. Then, the obtained recognition accuracy is described, the robustness to hand orientations and environmental illuminations is considered, and the other biometric aspects are analyzed. A comparison of the researched methods with the most recent approaches in the literature is presented. Some final considerations about the obtained results conclude the chapter.

6.1 RESULTS OF THE METHODS BASED ON ACQUISITIONS AT A FIXED DISTANCE

In this section, the experiments related to the methods based on acquisitions at a fixed distance, described in Section 5.2, are presented. First, the collection of the test datasets is described in detail, including the description of the hardware setup, and the procedure used for the collection of the samples. The used acquisition parameters, the

acquisitions conditions, and the types of samples captured are also described. The parameters used in the experimental tuning of the algorithms are reported, then an evaluation of the three-dimensional reconstruction step is presented, in order to determine the accuracy of the reconstruction method. Then, the recognition accuracy was evaluated, using the procedures and the figures of merit described in Section 2.4.

6.1.1 COLLECTION OF THE TEST DATASETS

The acquisition procedure described in Section 5.2.3 was used to collect the dataset. In particular, the used acquisition setup consists in two Sony XCD-SX90CR CCD color cameras with a 25 mm focal length, which capture images at 15 fps with a 1280×960 resolution. The cameras are synchronized using a trigger mechanism, and are oriented with an angle $\alpha = 85°$ with respect to the surface, and the distance between the center of the optics is $\Delta_D = 100$ mm. The distance from the optics to the surface is $\Delta_H = 485$ mm, and the distance of the illumination from the surface is $\Delta_H = 250$ mm.

The dataset PF, used in the evaluation of the researched method, was collected by capturing the 2 palms of 13 individuals, for a total of 26 different palms. For each palm, 8 two-view acquisitions were performed, for a total of 208 two-view acquisitions. Between different acquisitions, the user was required to remove his hand and place it again on the surface, in order to capture a different sample each time. The acquisitions corresponding to each user were performed in a single session. The volunteers were both male and female, with different ethnicities, and with ages ranging from 25 to 45 years. Some examples of acquisitions of different individuals are shown in Fig. 6.1.

In order to perform the calibration, we used a two-dimensional rigid chessboard composed by 12×9 squares, in which each square has a size of 2.8×2.8 mm. The chessboard was captured in 15 different positions, using synchronized two-view acquisitions performed using the described setup. We used these acquisitions in order to perform the calibration of the two-view acquisition system, and we computed a reconstruction error equal to 0.03 mm. In particular, we computed the reconstruction error by triangulating the positions of the corners of the squares in the three-dimensional space, using the formula described in Section 5.2.5.2, and fitting a plane through the points. The standard deviation of the distances between the points and the fitted plane is assumed as the measure of the reconstruction error, similarly to the method described in [456].

6.1.2 PARAMETERS USED

The threshold used in the segmentation step is $t_s = 50$. The number of extracted points is $N_P = 10,000$. In the three-dimensional reconstruction step, the size of the rectangular search area used is $\Delta_x = 150, \Delta_y = 10$, the epipolar distance threshold used is $t_{ep} = 2$, the size of the cross-correlation window is $l \times l = 15 \times 15$. The parameter used in the point cloud filtering step is $t_s = 5$. The threshold used in the two-dimensional feature extraction and matching step is $t_{SIFT} = 1.5$. The threshold used for comparing the triangles in the three-dimensional feature extraction and matching step is $t_D = 0.2$.

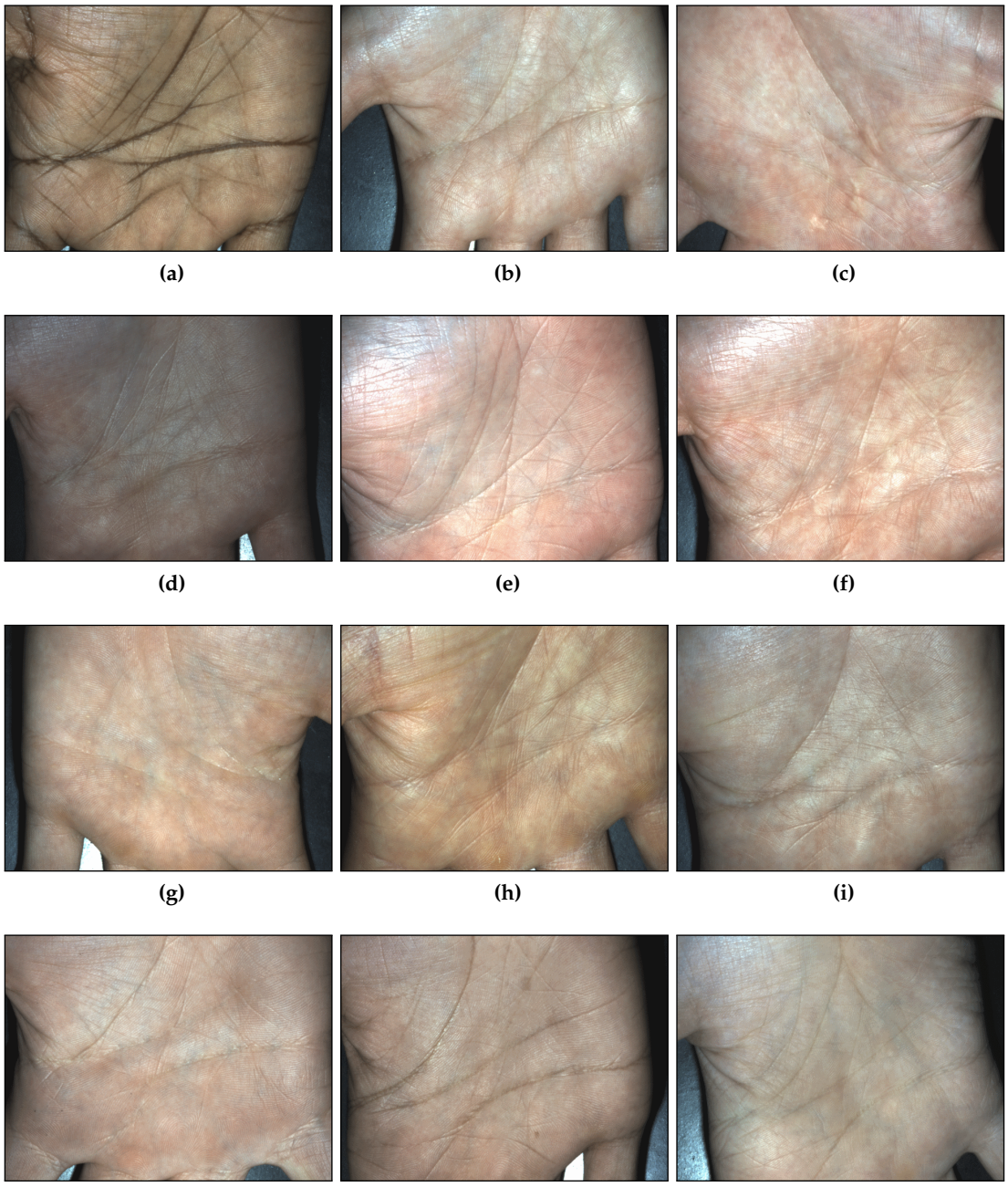

Figure 6.1: Examples of acquisitions of palmprints captured at a fixed distance.

6.1.3 EVALUATION OF THE THREE-DIMENSIONAL RECONSTRUCTION

In order to evaluate the accuracy of the three-dimensional reconstruction process, we considered the percentage of the correctly reconstructed points, by computing for each reconstructed model the ratio of the final number of points, obtained after the point cloud filtering step, to the number of extracted points from the image I_A. The mean ratio and its standard deviation, computed considering all the samples in the database,

Table 6.1: Percentage of the correctly reconstructed points, expressed as the ratio of the number of points after the point cloud filtering step, to the number of extracted points from the image I_A.

Dataset	Ratio	
	Mean	**Std**
PF	89.37 %	3.49 %

are reported in the Table 6.1. It is possible to observe that the majority of the extracted points were correctly matched.

The percentage and the spatial distribution of the matched points influence the accuracy of the computed template. In particular, a smaller percentage of matched points can result in a smaller area usable for the recognition, since some areas of the palmprint do not have their corresponding three-dimensional information. Moreover, areas with a smaller spatial distribution of matched points result in a smoother three-dimensional model, which conveys less information and can decrease the recognition accuracy. However, in our experiments, a correct three-dimensional model, with a sufficient number of points, was always reconstructed.

An example of the reconstructed three-dimensional models, computed using the method described in Section 5.2.5, is shown in Fig. 6.2, together with the corresponding interpolated surfaces and textures. It is possible to observe that the three-dimensional reconstruction method is able to compute accurate models, able to describe the shape of the depicted hand region. However, the resolution of the used imaging system is not sufficient for the computation of the information related to the three-dimensional depth of the palm lines. For these reason, accurate three-dimensional features cannot be used, and the three-dimensional feature extraction and matching method described in Section 5.2.8 is used as a refinement step, after the extraction and matching of the two-dimensional features.

6.1.4 RECOGNITION ACCURACY

The described feature extraction and matching method, composed by the two-dimensional and three-dimensional feature extraction and matching methods described in Section 5.2.7 and in Section 5.2.8, was applied to the computed three-dimensional models and the corresponding textures.

The ROC curve describing the recognition accuracy of the method is shown in Fig. 6.3, and Table 6.2 contains the obtained FMR and FNMR values in different points of the curve. In particular, the researched recognition method achieved an EER value equal to 0.25 %. It is possible to observe that the researched method was able to perform an accurate recognition, comparable to the techniques in the literature that perform the palmprint recognition based on contactless acquisition systems, as summarized in Section 6.2.7. Moreover, from the Table 6.2 it is possible to observe that the system obtained low percentages of false non-matches, similar to the EER value, with thresholds of the

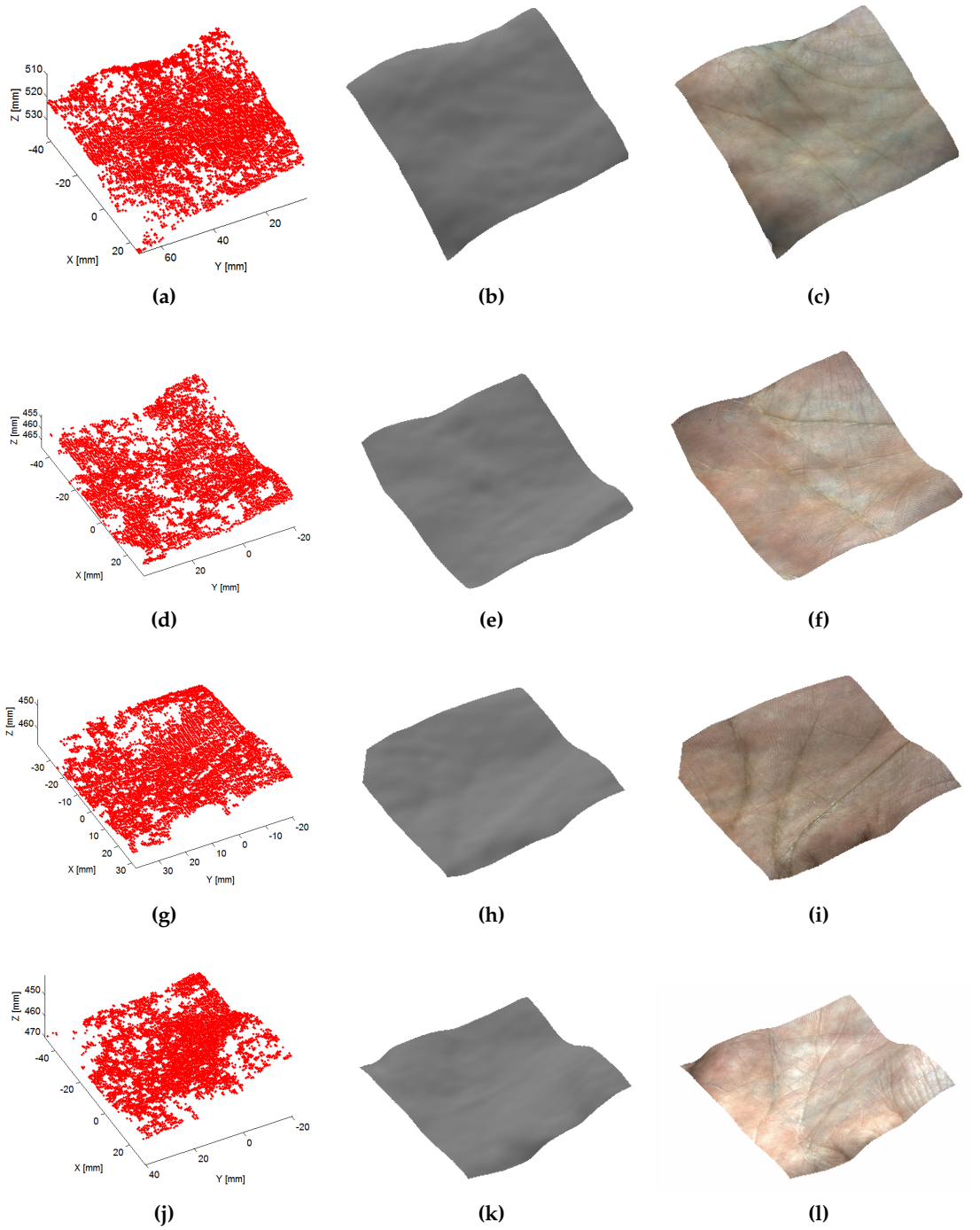

Figure 6.2: Example of three-dimensional palmprint models reconstructed using the method described in Section 5.2.5: (a, d, g, j) filtered point clouds; (b, e, h, j) interpolated surfaces; (c, f, i, l) corresponding textures.

matching scores that obtain small numbers of false matches, allowing to use the system in high security applications. Moreover, the system obtained low percentages of false matches, similar to the EER value, also with threshold values that obtain small

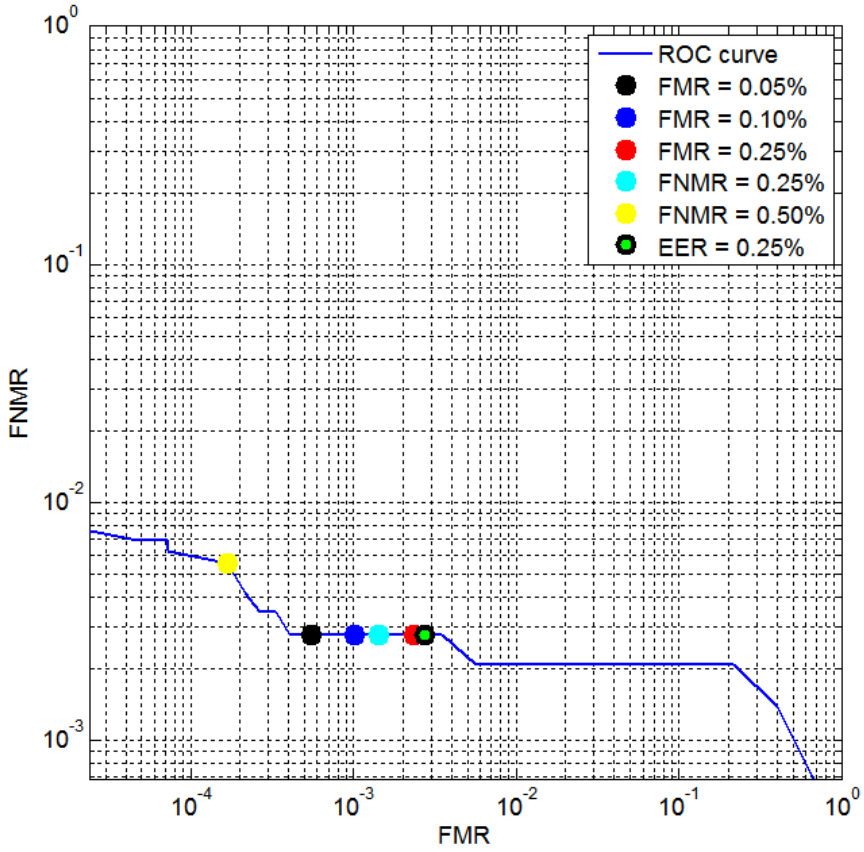

Figure 6.3: ROC curve of the researched palmprint recognition method based on acquisitions performed at a fixed distance.

Table 6.2: FMR and FNMR obtained by the researched palmprint recognition method based on acquisitions performed at a fixed distance.

	FNMR @FMR	FNMR @FMR	FNMR @FMR	FMR @FNMR	FMR @FNMR
EER %	**=0.05%**	**=0.10%**	**=0.25%**	**=0.25%**	**=0.50%**
0.25 %	0.27 %	0.27 %	0.27 %	0.14 %	0.02 %

numbers of false non-matches, allowing to use the system also for low and medium security applications.

The number of individuals in the tested dataset is not sufficient for more general considerations about the recognition accuracy. However, the obtained results allowed to extend the method in the case of acquisitions performed with uncontrolled distance.

6.2 RESULTS OF THE METHODS BASED ON ACQUISITIONS WITH UNCONTROLLED DISTANCE

In this section, the experiments related to the methods based on acquisitions with uncontrolled distance, described in Section 5.3, are described. First, the collection of the test datasets is described, including the description of the hardware setup and the procedure used for the collection of the used dataset. The used acquisition parameters, the acquisition conditions, and the types of samples captured is also described. The parameters used in the experimental tuning of the algorithms are reported, then an evaluation of the three-dimensional reconstruction step is presented, in order to determine the accuracy of the reconstruction method. The recognition accuracy is analyzed using the procedures and the figures of merit described in Section 2.4. Moreover, the obtained recognition accuracy using multiple comparisons is also presented. Then, the robustness of the method to hand orientations and environmental illumination situations is analyzed. The other biometric aspects, consisting in the speed, cost, interoperability, usability, acceptability, security, and privacy are analyzed using the most common practices. A comparison with the most recent approaches described in the literature is presented, then an overall summary of the results is described.

6.2.1 COLLECTION OF THE TEST DATASETS

The acquisition procedure described in Section 5.3.2 was used to collect the used datasets. In particular, the used acquisition setup consists in two Sony XCD-SX90CR CCD color cameras with a 25 mm focal length, which capture images at 15 fps with a 1280×960 resolution. The cameras are synchronized using a trigger mechanism. The cameras are oriented with an angle $\alpha = 87°$ with respect to the surface, and the distance between the center of the optics is $\Delta_D = 100\,mm$. The distances from the optics of the cameras to the lowest and highest points of the acquisition volume are respectively $\Delta_{H-Low} = 1080\,mm$ and $\Delta_{H-High} = 1380\,mm$. The size of the acquisition volume is $W = 225\,mm$, $H = 300\,mm$, $D = 155\,mm$. The value t_M is used for controlling the shutter time is $t_M = 100$.

The parameters used in the implementation of the illumination setups are the sequent:

- *Method 1*: The led bars are mounted with a distance $\Delta_L = 960\,mm$ from the cameras, and with a distance $\Delta_W = 240\,mm$ between them. The bars are inclined towards the acquisition volume with an angle $\beta = 45°$. Some examples of acquisitions captured using Method 1 are shown in Fig. 6.4.

- *Method 2*: The downlight illuminations with white leds are mounted with a distance $\Delta_L = 960\,mm$ from the cameras, and inclined towards the acquisition volume with an angle $\beta = 45°$. Some examples of acquisitions captured using Method 2 are shown in Fig. 6.5.

- *Method 3*: The blue led bars are mounted with a distance $\Delta_L = 960\,mm$ from the cameras, with a distance $\Delta_W = 290\,mm$ between the lateral bars, and a dis-

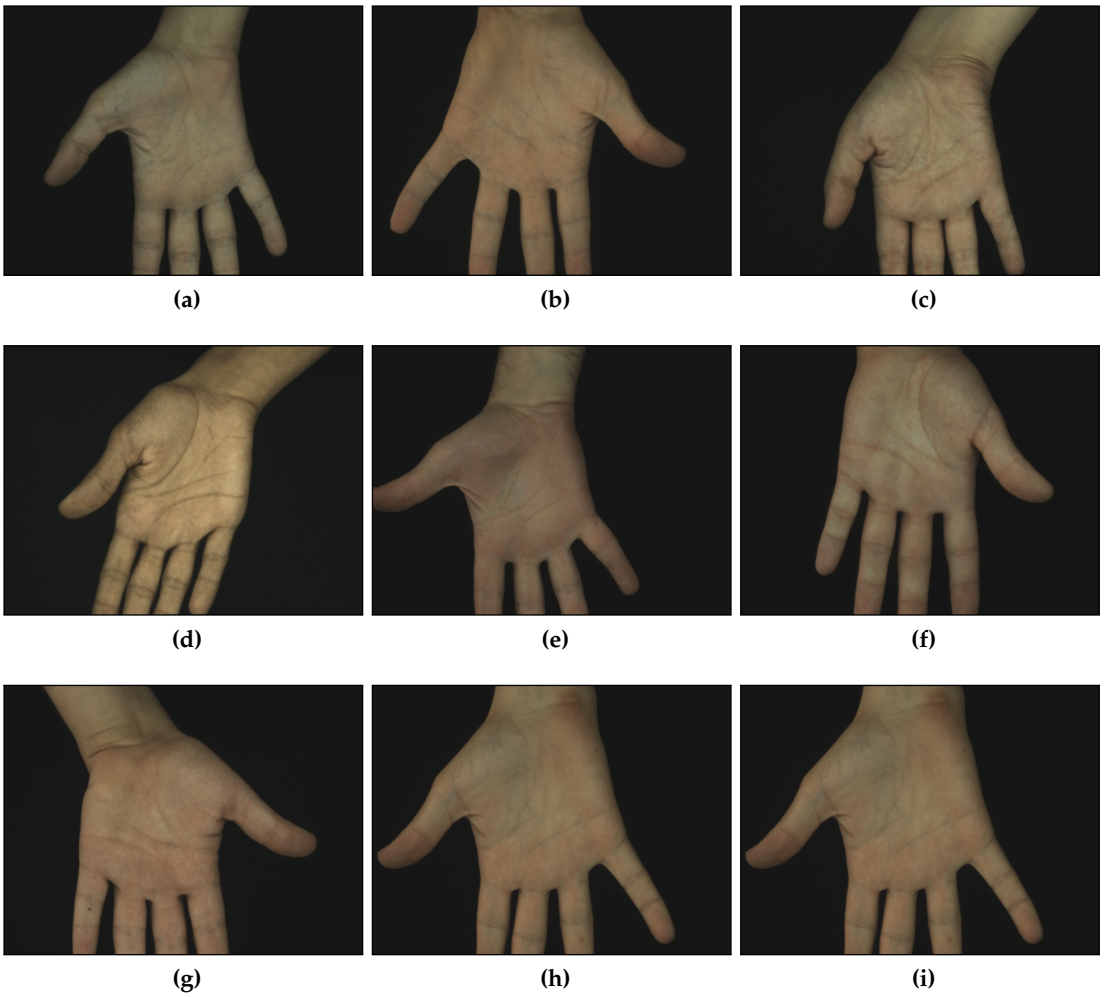

Figure 6.4: Examples of acquisitions of palmprints captured with uncontrolled distance using Method 1.

tance $\Delta_D = 300\,\text{mm}$ between the front and rear bars. The bars are positioned horizontally ($\beta = 0°$). Some examples of acquisitions captured using Method 1 are shown in Fig. 6.6.

We used the three different illumination methods in order to collect two datasets PA and PB. In particular, each dataset contains the samples of individuals captured using two different illumination methods. First, we collected the dataset PA, which contains the samples of individuals respectively captured using Method 1 and Method 3, in order to test the differences between a white illumination and a blue illumination. Then, the obtained results drove us to collect a second dataset PB, which contains the samples of individuals respectively captured using Method 2 and Method 3, in order to test the effectiveness of a white illumination with more intensity, against a blue illumination.

Two datasets had to be collected, since the illumination Method 1 and Method 2 were implemented at different times, and it was not possible to acquire again the same individuals for the collection of the samples.

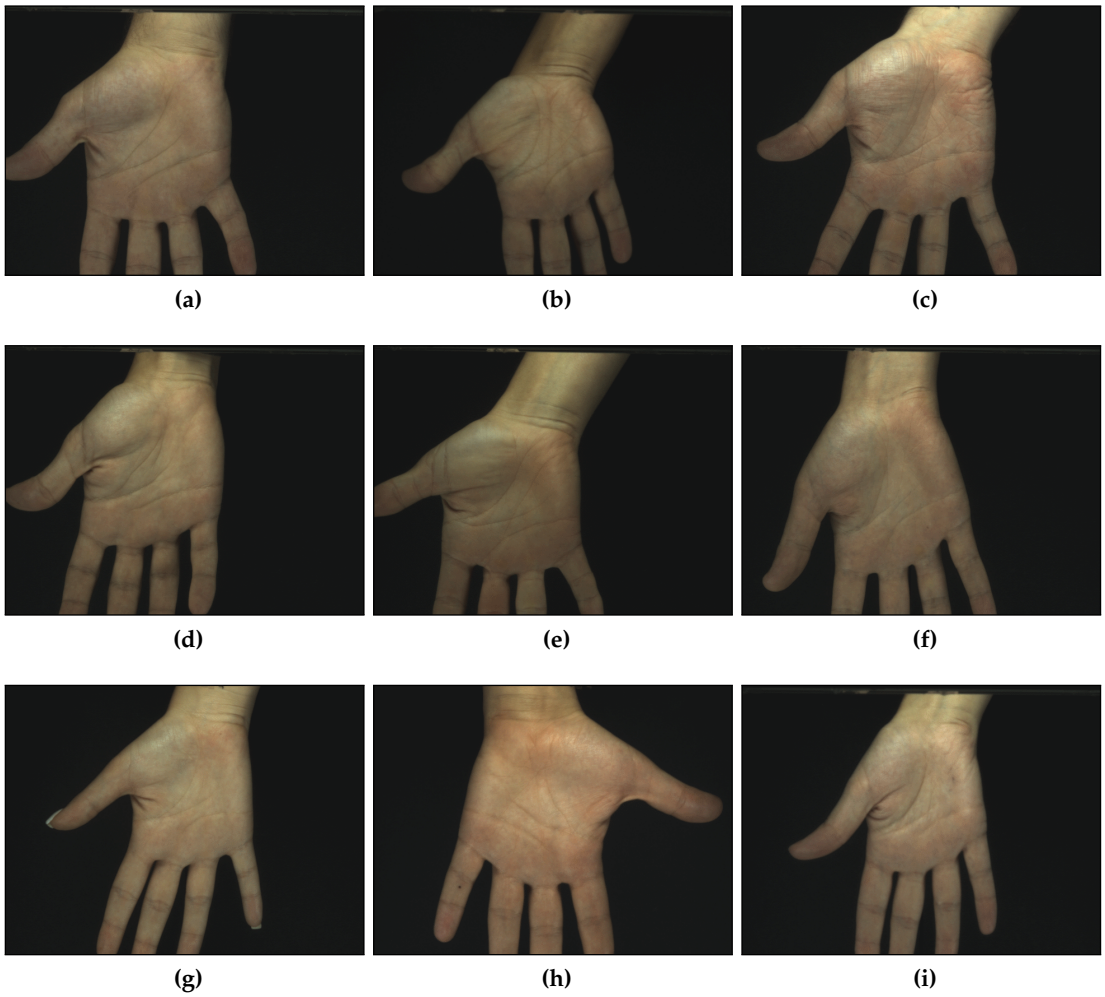

Figure 6.5: Examples of acquisitions of palmprints captured with uncontrolled distance using Method 2.

The two datasets PA and PB are summarized as follows:

- *Dataset* PA: this dataset was collected by using the Method 1 and the Method 3 for capturing the 2 palms of 9 individuals, for a total of 18 different palms. For each palm, 10 two-view acquisitions were performed, for a total of 180 two-view acquisitions.
- *Dataset* PB: this dataset was collected by using the Method 2 and the Method 3 for capturing the 2 palms of 32 individuals, for a total of 64 different palms. For each palm, 10 two-view acquisitions were performed, for a total of 640 two-view acquisitions.

Between different acquisitions, the user was required to remove his hand, and place it again on the surface, in order to capture a different sample each time. A minimum amount of instructions was given to the users, and they were only required to extend the open hand in a relaxed position inside the acquisition volume, and place the palm

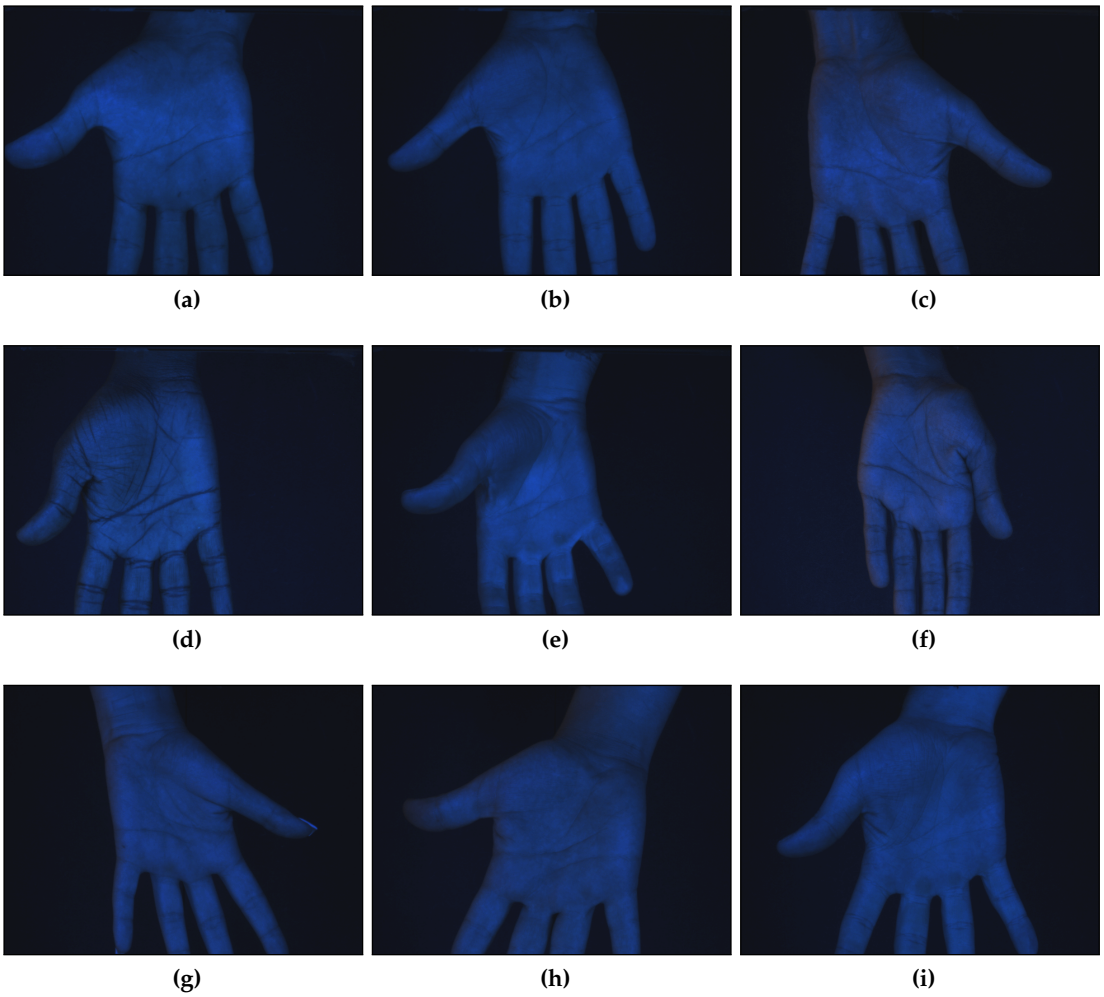

Figure 6.6: Examples of acquisitions of palmprints captured with uncontrolled distance using Method 3.

over the circle superimposed on the live feed (Fig. 5.26). The volunteers were both male and female, with different ethnicities, with ages ranging from 25 to 45 years.

The acquisitions corresponding to each user were performed in a single session. The entire acquisition procedure for each sample took approximately 5 s, including the time needed for positioning the hand, the time for the shutter duration to adapt, and the time that the system waits to make sure the hand is still (about 2 s). The actual capture of the image is performed almost instantly, with shutter times ranging from 0.02 s to 0.03 s.

In the performed experiments, a separate acquisition procedure was performed in order to capture the samples using the illumination Method 2 and Method 3. However, a method for the quasi-simultaneous capture of the images using both the illumination methods could be easily implemented using a small hardware circuit. In that case, the total capture time of the images is the sum of the two respective capture times, and would be at most 0.06 s.

Table 6.3: Percentage of the correctly reconstructed points, expressed as the ratio of the number of points after the point cloud filtering step, to the number of extracted points from the image I_A.

Dataset	Ratio	
	Mean	**Std**
PA - Method 1	66.72 %	13.71 %
PA - Method 3	74.44 %	15.23 %
PB - Method 2	70.50 %	12.99 %
PB - Method 3	70.94 %	15.25 %

In order to perform the calibration, we used a two-dimensional rigid chessboard composed by 12×9 squares, in which each square has a size of 7×7 mm. The chessboard was captured in 15 different positions, using synchronized two-view acquisitions performed using the described setup. We used these acquisitions in order to perform the calibration of the two-view acquisition system, and we computed a reconstruction error equal to 0.12 mm. In particular, we computed the reconstruction error by triangulating the positions of the corners of the squares in the three-dimensional space, using the formula described in Section 5.2.5.2, and fitting a plane through the points. The standard deviation of the distances between the points and the fitted plane is assumed as the reconstruction error measure, similarly to the method described in [456].

6.2.2 PARAMETERS USED

The threshold used in the segmentation step is $t_s = 50$, and the parameter used for extracting the central region of the palm is $k_e = 0.6$. The number of extracted points is $N_P = 2,000$. In the three-dimensional reconstruction step, the size of the rectangular search area is $\Delta_x = 90, \Delta_y = 2$, the epipolar distance threshold used is $t_{ep} = 2$, the size of the cross-correlation window is $l \times l = 30 \times 30$. The parameter used in the point cloud filtering step is $t_s = 1$. The threshold used in the alignment step, and in the two-dimensional feature extraction and matching step is $t_{SIFT} = 1.5$. The threshold used for comparing the triangles in the three-dimensional feature extraction and matching step, is $t_D = 0.2$.

6.2.3 EVALUATION OF THE THREE-DIMENSIONAL RECONSTRUCTION

In order to evaluate the accuracy of the three-dimensional reconstruction process, for each reconstructed model we analyzed the ratio of the final number of points, obtained after the point cloud filtering step, to the number of extracted points from the image I_A. The mean ratio and its standard deviation were computed for each dataset by considering all the samples, and are reported in the Table 6.3. It is possible to observe that about three quarters of the points were correctly matched.

As mentioned in Section 6.1.3, the percentage and the spatial distribution of the matched points influence the accuracy of the computed template. In particular, a smaller percentage of matched points can result in a smaller area usable for the recognition, since some areas of the palmprint do not have their corresponding three-dimensional information. Moreover, the normalization of the three-dimensional model, and the corresponding three-dimensional registration of the image could be performed with less precision. In our experiments, the thumb region of the hand (or the thenar region), which has a significant difference in terms of depth with respect to the other regions of the hand, is sometimes not reconstructed by the described three-dimensional reconstruction algorithm. However, the thenar area has a minor significance for the palmprint recognition, since only a small percentage of the details of the palmprint is contained in this region.

Areas with a smaller spatial distribution of matched points result in a smoother three-dimensional model, which conveys less information and can decrease the recognition accuracy. However, in our experiments, a redundant of points was extracted in order to have a sufficient number of points for describing the three-dimensional model correctly.

Examples of reconstructed three-dimensional models, computed using acquisitions performed with Method 1 described in Section 5.3.4.1, are shown in Fig. 6.7, together with the corresponding interpolated surfaces. Examples of reconstructed models, computed using acquisitions performed with Method 2, are shown in Fig. 6.8. Examples of reconstructed models, computed using acquisitions performed with Method 3, are shown in Fig. 6.9.

From the figures, it is possible to observe that the three-dimensional reconstruction method was able to compute accurate models, able to describe the shape of the considered hand region. However, the resolution of the used imaging system is not sufficient for the computation of the three-dimensional depth of the palm lines. For these reasons, pure three-dimensional features cannot be used, and the three-dimensional information is used to obtain a metric representation describing the distance, position, and orientation. Moreover, the feature extraction and matching method described in Section 5.3.7 is used as a refinement step, after the extraction and matching of the two-dimensional features.

6.2.4 RECOGNITION ACCURACY

We divided the tests for the measurement of the recognition accuracy according to the two datasets described in Section 6.2.1. First, we tested the recognition accuracy using the dataset PA in order to compare the acquisition Method 1 and Method 3. Then, we tested the redognition accuracy using the dataset PB, in order to compare the acquisition Method 2 and Method 3.

6.2.4.1 DATASET PA

First, we tested the accuracy of the described palmprint recognition method on the dataset PA, which contains samples of individuals captured using Method 1 and Me-

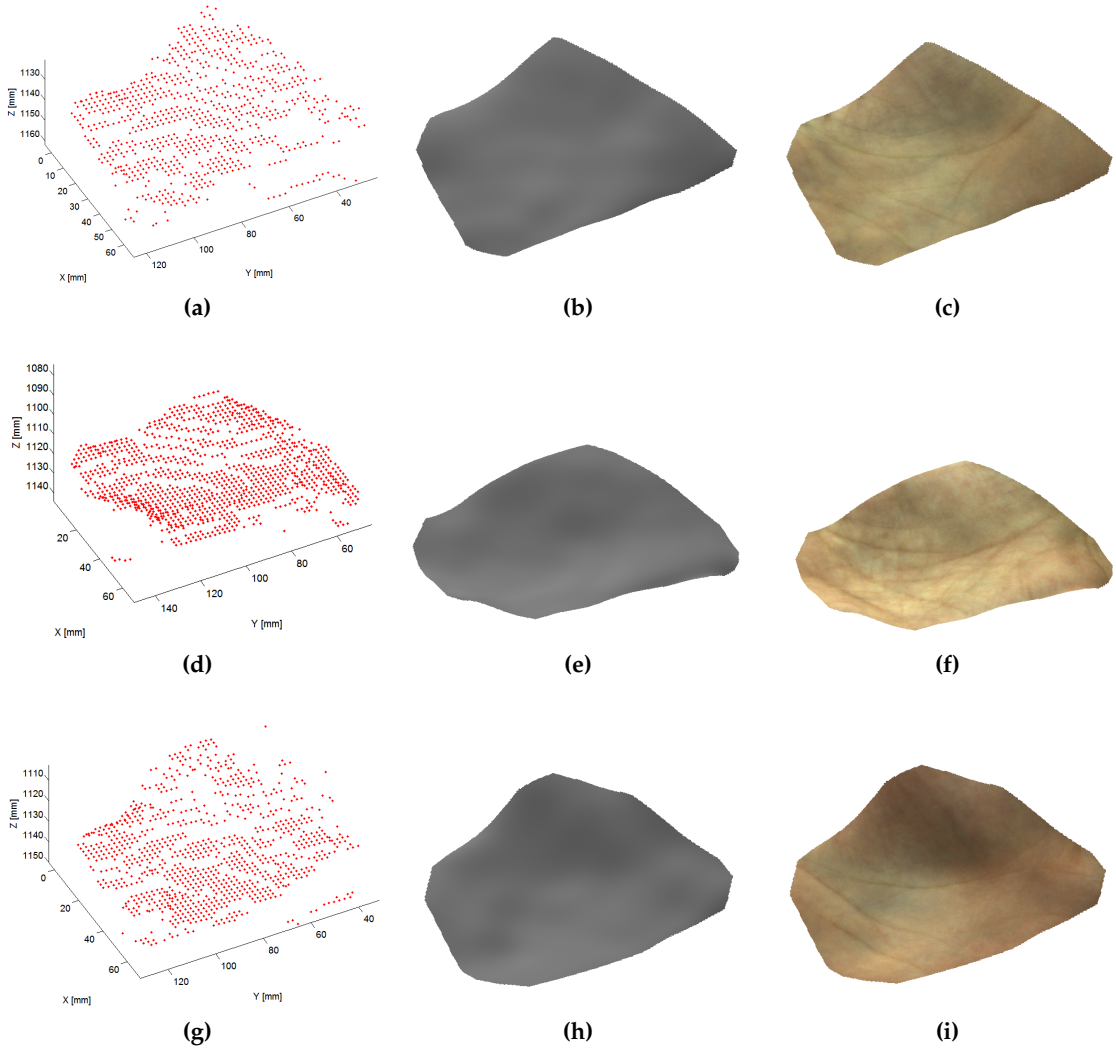

Figure 6.7: Example of three-dimensional palmprint models captured using Method 1, reconstructed using the method described in Section 5.2.5: (a, d, g) filtered point clouds; (b, e, h) interpolated surfaces; (c, f, i) corresponding textures.

thod 3. We compared the obtained results in order to determine which illumination method performed best. Moreover, we combined the obtained match scores corresponding to the two illumination methods using different fusion rules.

The ROC curves corresponding to the dataset PA are shown in Fig. 6.10. In particular, by using the samples captured with Method 1, the system achieved an EER value equal to 2.36 %, while by using the samples captured with Method 3 the system achieved an EER value equal to 1.71 %. It is possible to observe that using both methods it was possible to perform an accurate recognition. However, by using the samples captured using Method 1, it was possible to achieve a minor EER value, and the corresponding ROC curve shows better performances for almost the entire range of the curve.

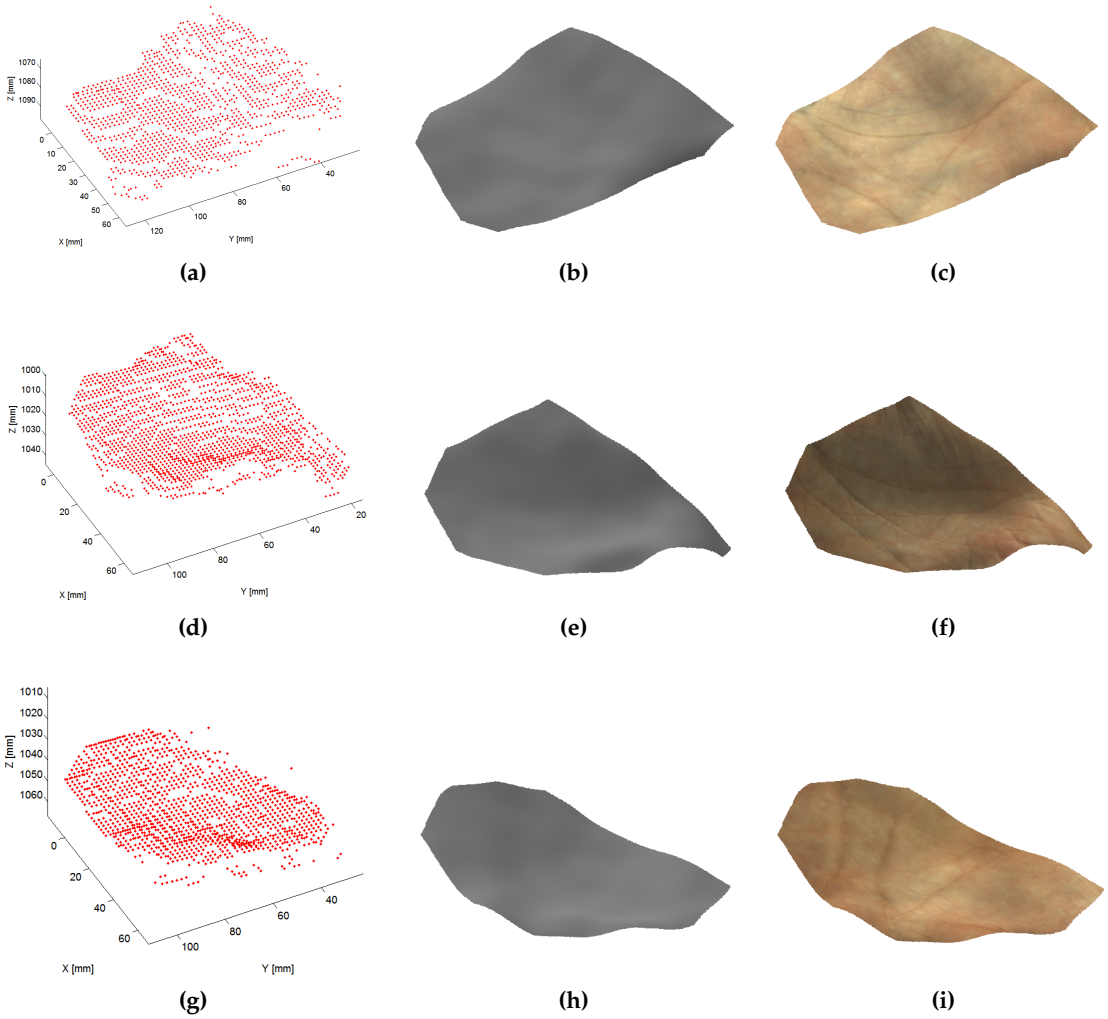

Figure 6.8: Example of three-dimensional palmprint models captured using Method 2, reconstructed using the method described in Section 5.2.5: (a, d, g) filtered point clouds; (b, e, h) interpolated surfaces; (c, f, i) corresponding textures.

Moreover, we tested the possibility of integrating Method 1 and Method 3, by using different fusion schemes at the match score level:

$$m_s(i,j) = \text{mean}\left(m_1(i,j), m_3(i,j)\right) \ ; \tag{6.1}$$

$$m_s(i,j) = \min\left(m_1(i,j), m_3(i,j)\right) \ ; \tag{6.2}$$

$$m_s(i,j) = \max\left(m_1(i,j), m_3(i,j)\right) \ , \tag{6.3}$$

where $m_1(i,j)$ is the match score corresponding to the comparison of the individuals i and j in the dataset PA, captured using Method 1, and $m_3(i,j)$ is the match score corresponding to the comparison of the individuals i and j in the dataset PA, captured using Method 3.

The corresponding ROC curves are reported in Fig. 6.11. In particular, the fusion scheme based on the computation of the mean match score using the Equation 6.1 obtained the best results, and permitted an increase of the recognition accuracy, corre-

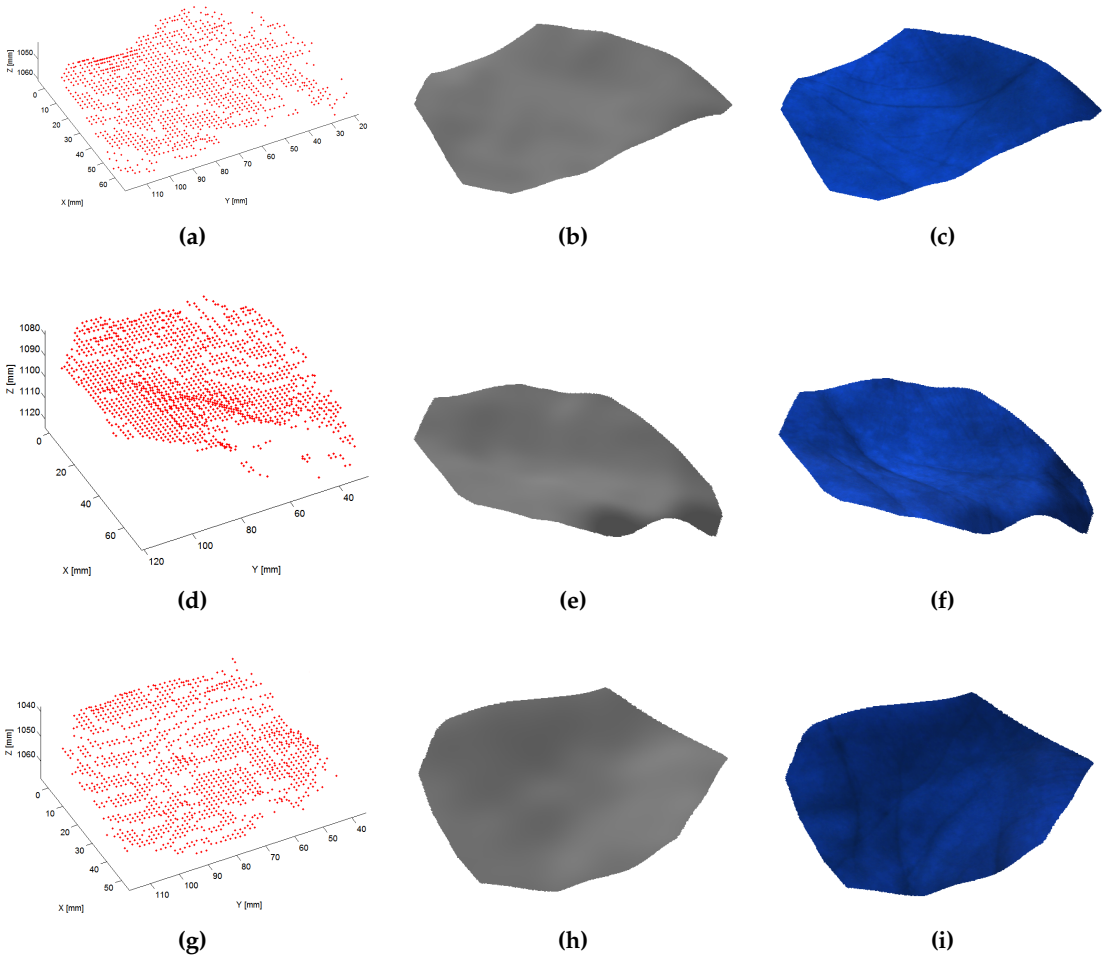

Figure 6.9: Example of three-dimensional palmprint models captured using Method 3, reconstructed using the method described in Section 5.2.5: (a, d, g) filtered point clouds; (b, e, h) interpolated surfaces; (c, f, i) corresponding textures.

Table 6.4: FMR and FNMR of the dataset PA, obtained by computing the mean of the results corresponding to the samples captured using Method 1 and Method 3.

Dataset	Fusion scheme	EER %	FNMR @FMR =0.25%	FNMR @FMR =0.50%	FNMR @FMR =0.75%	FMR @FNMR =0.50%	FMR @FNMR =0.75%
PA	Mean	0.42 %	0.49 %	0.43 %	0.38 %	0.18 %	0.06 %

sponding to an EER = 0.42 %. Moreover, the corresponding ROC curve shows better performances for almost the entire range of the curve.

The obtained FMR and FNMR values in different points of the curve, corresponding to the fusion scheme based on the computation of the mean match score, are reported in Table 6.4. It is possible to observe that by computing the average match score, the system exhibited low percentages of false non-matches, similar to the EER value, with

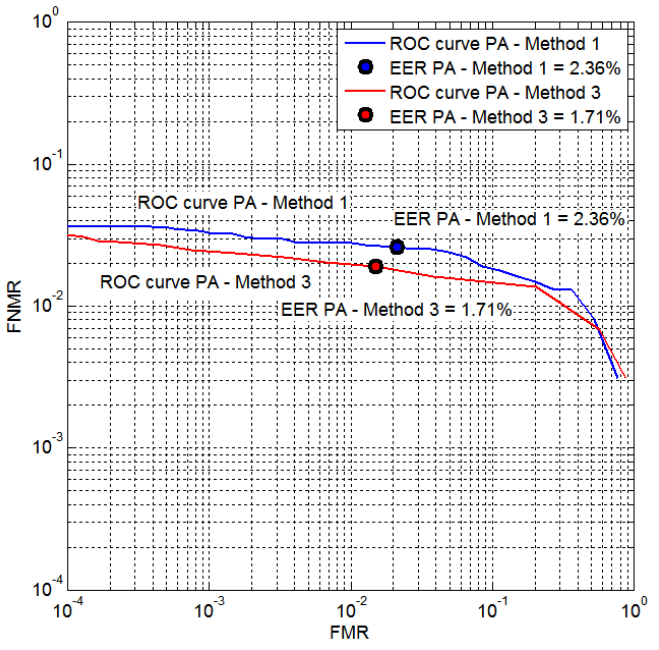

Figure 6.10: ROC curves of the dataset PA, corresponding to the samples captured using Method 1 and Method 3.

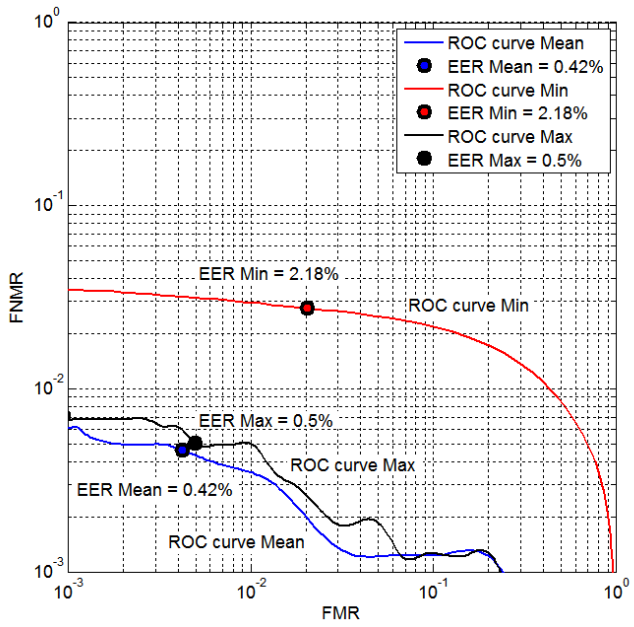

Figure 6.11: ROC curves of the dataset PA, corresponding to the different fusion schemes of the results corresponding to the samples captured using Method 1 and Method 3.

thresholds of the matching scores that obtain small numbers of false matches, allowing to use the system in high security applications. Moreover, the system obtained low percentages of false matches, similar to the EER value, also with threshold values that obtain small numbers of false non-matches, allowing to use the system also for low and medium security applications.

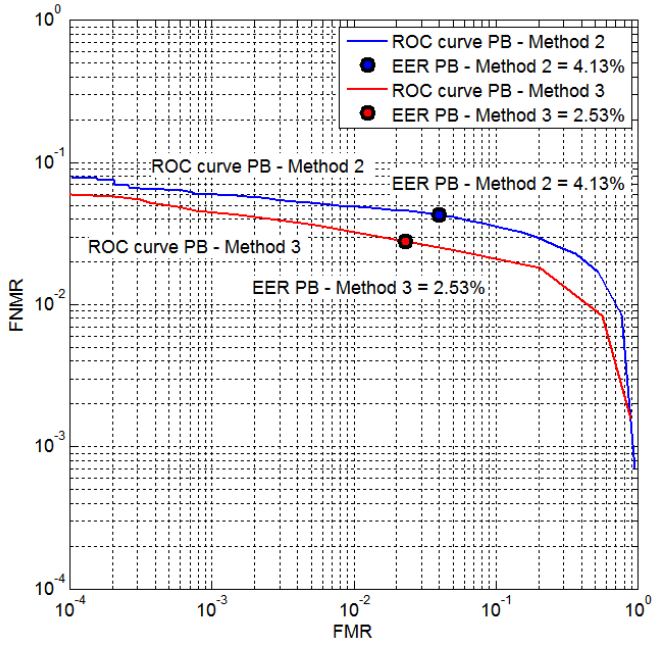

Figure 6.12: ROC curves of the dataset PB, corresponding to the samples captured using Method 2 and Method 3.

However, the illumination performed using Method 1 did not have a sufficient intensity for a real-time acquisition procedure, and could easily produce samples affected by motion blur. These aspects limited the usability of the system, and the supervision of an expert operator during the collection of the dataset PA was necessary. For this reason, a white illumination with more intensity was considered, and we collected the bigger dataset PB, using the illumination Method 2 and Method 3.

6.2.4.2 DATASET PB

We tested the accuracy of the described palmprint recognition method on the dataset PB, captured using illumination Method 2 and Method 3. We compared the obtained results in order to determine which illumination method performed best. We also computed the results obtained by comparing each biometric template with three templates, and considering the best result as the match score. Moreover, we combined the obtained match scores corresponding to the two illumination methods using different fusion rules, and estimated the corresponding confidence.

The ROC curves corresponding to the dataset PB are shown in Fig. 6.12. In particular, by using the samples captured with Method 2, the system achieved an EER value equal to 4.13 %, while by using the samples captured with Method 3 the system achieved an EER value equal to 2.53 %. It is possible to observe that by using the samples captured using Method 3 it was possible to obtain better results, and the corresponding ROC curve shows better performances for the entire range of the curve.

Moreover, we tested the possibility of integrating Method 2 and Method 3, by using the different fusion schemes at the match score level, computed using the Equations 6.1, 6.2, and 6.3.

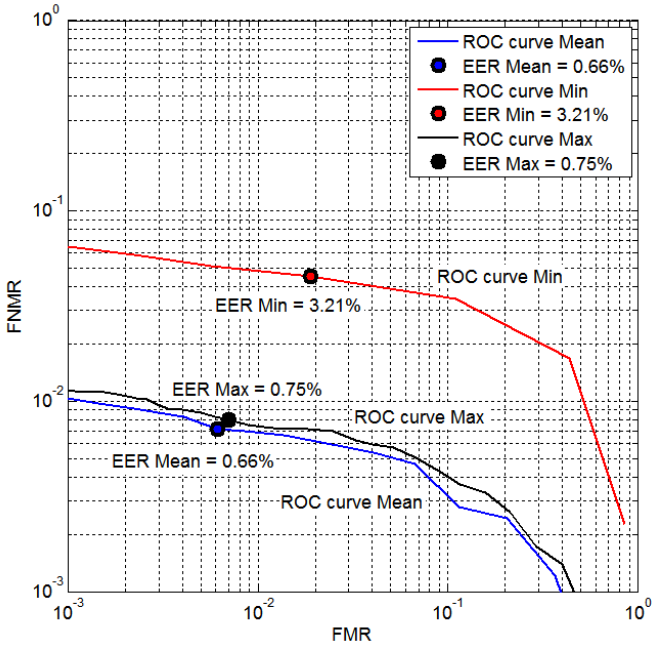

Figure 6.13: ROC curves of the dataset PB, corresponding to the different fusion schemes of the results corresponding to the samples captured using Method 2 and Method 3.

Table 6.5: FMR and FNMR of the dataset PB, obtained by computing the mean of the results corresponding to the samples captured using Method 2 and Method 3.

Dataset	Fusion scheme	EER %	FNMR @FMR =0.25%	FNMR @FMR =0.50%	FNMR @FMR =0.75%	FMR @FNMR =0.75%
PB	Mean	0.66 %	1.02 %	0.86 %	0.79 %	0.88 %

The corresponding ROC curves are reported in Fig. 6.13. It is possible to observe that the fusion scheme based on the computation of the mean match score obtained the best results and permitted an increase of the recognition accuracy with an EER = 0.66 %. Moreover, better performances were obtained, with respect to the other fusion methods, in the entire range of the ROC curve.

The obtained FMR and FNMR values in different points of the curve are reported in Table 6.5. From the table, it is possible to observe that the system exhibited low percentages of false non-matches, similar to the EER value, with thresholds of the matching scores that obtain small numbers of false matches, allowing to use the system in high security applications. Moreover, the system obtained low percentages of false matches, similar to the EER value, also with matching scores corresponding to small numbers of false non-matches.

By observing the genuine and impostor distributions of the dataset PB (Fig. 6.14), it is possible to observe that, while the distributions of the impostors are condensed in a limited range of values ($[0, \sim 20]$), the match scores of the genuine comparisons

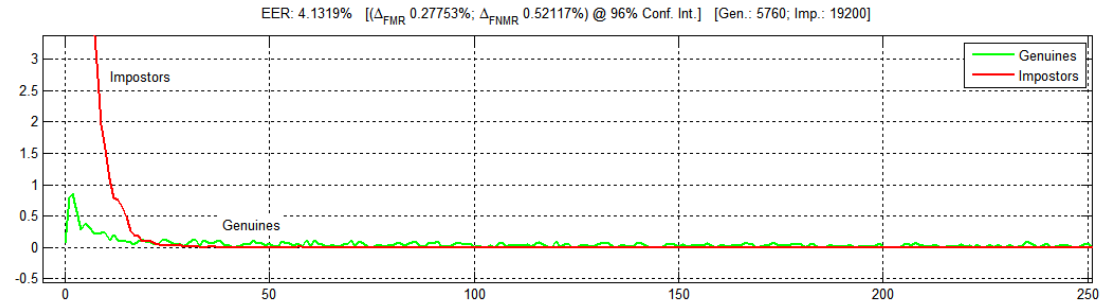

(a)

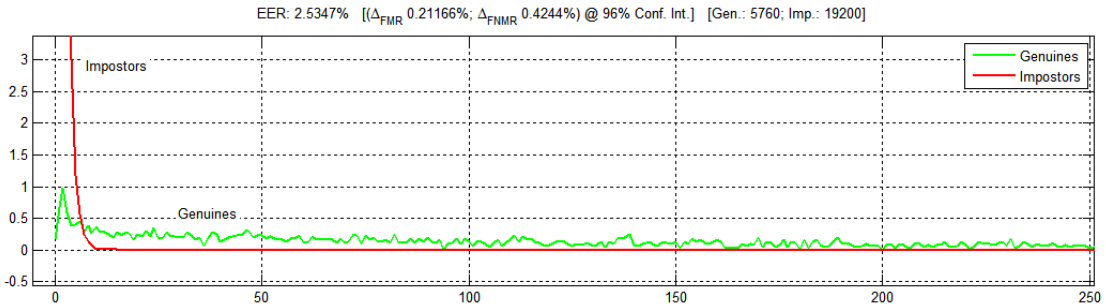

(b)

Figure 6.14: Genuine and impostor distributions of the dataset PB. The plots are zoomed in the overlapping areas of the distributions. (a) Genuine and impostor distributions corresponding to the samples captured using Method 2; (b) genuine and impostor distributions corresponding to the samples captured using Method 3.

are spread over a much wider range of values ($[0, \sim 7000]$). In particular, some genuine comparisons produced low match scores, which caused the distributions of the genuine comparisons to overlap with the impostor distributions. This is caused by the fact that the less-constrained acquisition procedure causes a variety in the quality of the samples and some less-quality samples were captured, which were not correctly matched to the other samples of the same individual.

In order to mitigate this problem, and increase the accuracy and robustness of the biometric system, it is possible to perform multiple comparisons for each recognition attempt and then select the best result, as stated in several documents describing the best practices for the evaluation of biometric recognition systems [73, 80].

We tested the accuracy of the described palmprint recognition method on the dataset PB, by performing 3 comparisons for each recognition attempt, and then selecting the maximum match score.

The ROC curves corresponding to the samples of the dataset PB captured using Method 2, both considering one comparison and 3 comparisons, are shown in Fig. 6.15. It is possible to observe that, by considering 3 comparisons, the recognition accuracy significantly increased. In particular, the EER was reduced from 4.13 % to 0.86 %.

The ROC curves corresponding to the samples of the dataset PB captured using Method 3, both considering one comparison and 3 comparisons, are shown in Fig. 6.16. It

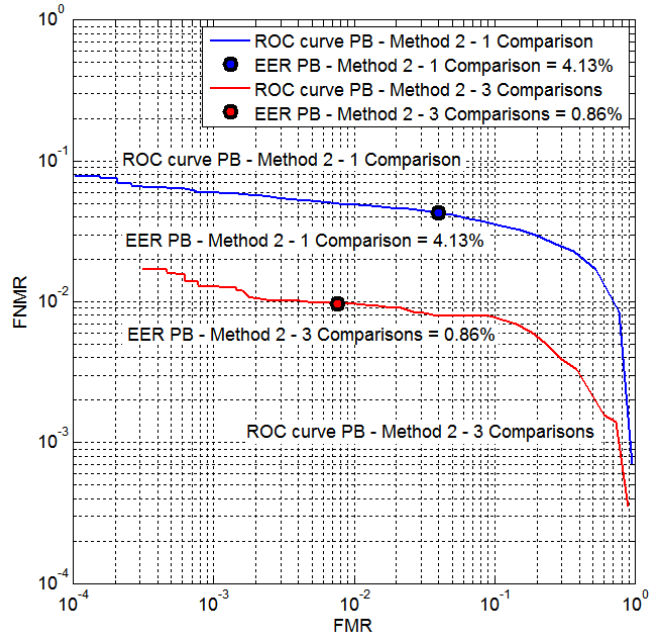

Figure 6.15: ROC curves of the dataset PB, corresponding to the samples captured using Method 2, both considering one comparison and with 3 comparisons.

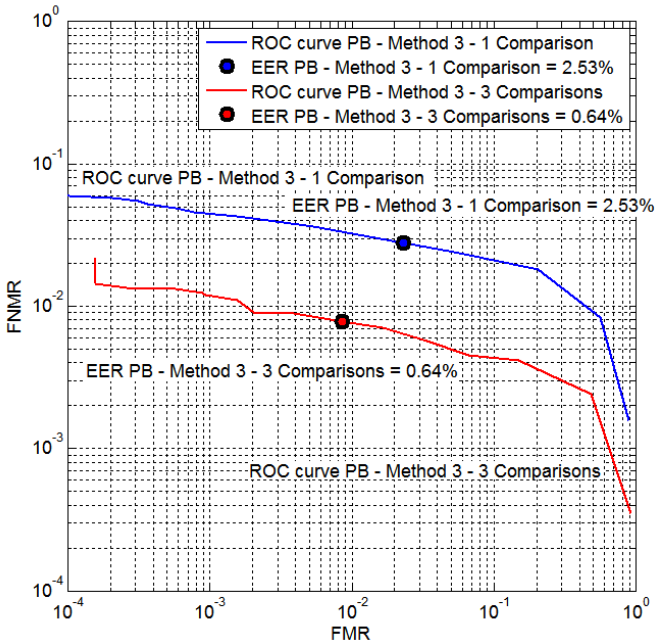

Figure 6.16: ROC curves of the dataset PB corresponding to the samples captured using Method 3, both considering one comparison and with 3 comparisons.

is possible to observe that also in this case, by considering 3 comparisons, the recognition accuracy increased. In particular, the EER was reduced from 2.53 % to 0.64 %.

Moreover, we combined the obtained match scores corresponding to the samples captured using Method 2 and Method 3, using the fusion rule based on the mean match score, described in the Equation 6.1. The corresponding ROC curve is shown in

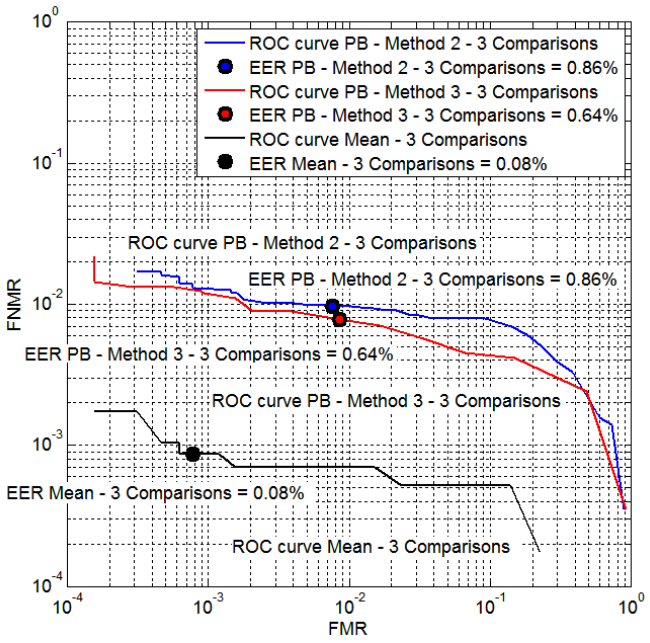

Figure 6.17: ROC curves of the dataset PB, obtained by computing the mean of the results corresponding to the samples captured using Method 2 and Method 3, and considering 3 comparisons.

Table 6.6: FMR and FNMR of the dataset PB, obtained by computing the mean of the results corresponding to the samples captured using Method 2 and Method 3, and considering 3 comparisons.

Dataset	Fusion scheme	EER %	FNMR @FMR =0.05%	FNMR @FMR =0.10%	FNMR @FMR =0.25%	FMR @FNMR =0.10%	FMR @FNMR =0.25%
PB	Mean	0.08 %	0.10 %	0.09 %	0.07 %	0.06 %	0.00 %

Notes: the average match score for 3 comparisons is considered.

Fig. 6.17. It is possible to observe that, by considering 3 comparisons and computing the average match score corresponding to the samples captured using Method 2 and Method 3, a lower EER = 0.08 % was obtained.

The obtained FMR and FNMR values in different points of the curve are reported in Table 6.6. From the table, it is possible to observe that the system exhibited low percentages of false non-matches, similar to the EER value, with thresholds of the matching scores that obtained small numbers of false matches, allowing to use the system in high security applications. Moreover, the system obtained low percentages of false matches, similar to the EER value, also with thresholds corresponding to small numbers of false non-matches.

Since it is not possible to collect databases of palmprints from the entire population, it is necessary to estimate the confidence of the performed accuracy measurements in order to test the applicability of the described biometric system in a real scenario.

In particular, the two techniques for the confidence estimation described in Section 2.4.3.4 were used: the first technique is based on the assumption that the obtained data follows a normal distribution, and the second technique is based on a bootstrap approach. Both the techniques use a confidence level equal to 90 %, and the bootstrap method is applied using 1000 iterations.

We computed the confidence boundaries of the accuracy of the dataset PB, obtained by computing the mean of the results corresponding to the samples captured using Method 2 and Method 3, and considering 3 comparisons. The obtained ROC curves, with the corresponding confidence boundaries, are shown in Fig. 6.18. It is possible to observe that the confidence boundaries of the proposed system are small, showing that the researched system could be effectively used in the case of a larger dataset.

6.2.5 ROBUSTNESS TO HAND ORIENTATION AND ENVIRONMENTAL ILLUMINATION

In order to test the robustness of the proposed method, the performance of the proposed method was tested by varying the hand orientation and the environmental illumination conditions during the acquisition.

The robustness to the hand orientation was tested by capturing a reduced dataset of palms in different roll orientations (Fig. 5.25), computing the biometric templates using the described method, and performing the biometric matching of the templates. The results were then analyzed in order to determine how the genuine and impostor match scores are modified according to the difference in the respective orientation of the samples.

In particular, 2 palms were captured in 20 different orientations each, ranging from $-90°$ to $+90°$ (Fig. 6.19) using both illumination Method 2 and Method 3. Examples of the captured palms are shown in Fig. 6.20 and Fig. 6.21.

Then, each sample pertaining to a palm was processed using the described method and compared with the other samples of the same palm. The resulting match scores corresponding to the samples captured using illumination Method 2 and Method 3 are reported respectively in the tables in Fig. 6.22 and Fig. 6.23.

The results show that the described method for the fully contactless and less-constrained palmprint recognition show a certain degree of tolerance in matching different samples pertaining to the same palm, if they are captured with a similar roll orientation. This is observable by analyzing the match scores near the main diagonal of the table in the Fig. 6.22, that in the majority of the cases are always greater than 58, which is the maximum impostor match score between samples pertaining to different palms. Similarly, the majority of the match scores near the main diagonal of the table in the Fig. 6.22 are greater than 28, which is the maximum impostor match score. However, excessive differences in the roll orientations used for capturing the samples can result in unrecognizable samples.

A similar experiment was performed in order to test the robustness of the proposed method in different environmental illumination conditions. In particular, we captured 10 samples from each of 2 palms in several illumination situations:

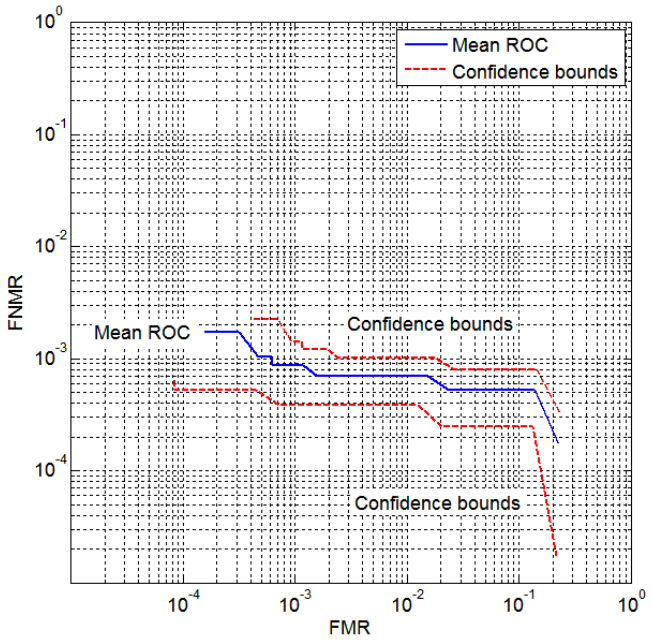

(a)

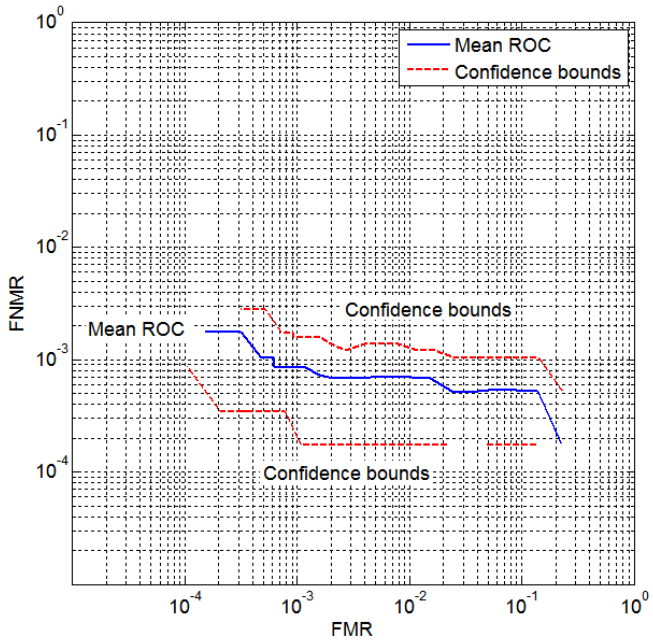

(b)

Figure 6.18: ROC curves of the dataset PB, and the relative confidence boundaries, obtained by computing the mean of the results corresponding to the samples captured using Method 2 and Method 3, and considering 3 comparisons: (a) confidence boundaries computed assuming a normal distribution of the data; (b) confidence boundaries computed using the bootstrap method.

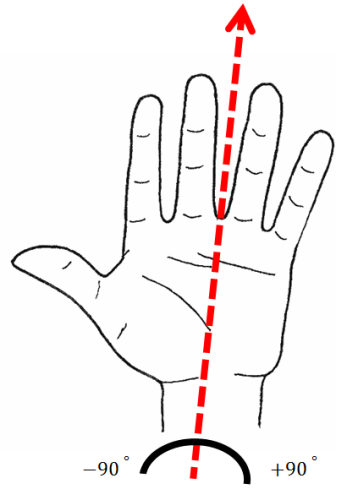

Figure 6.19: Palmprint captured in different orientations.

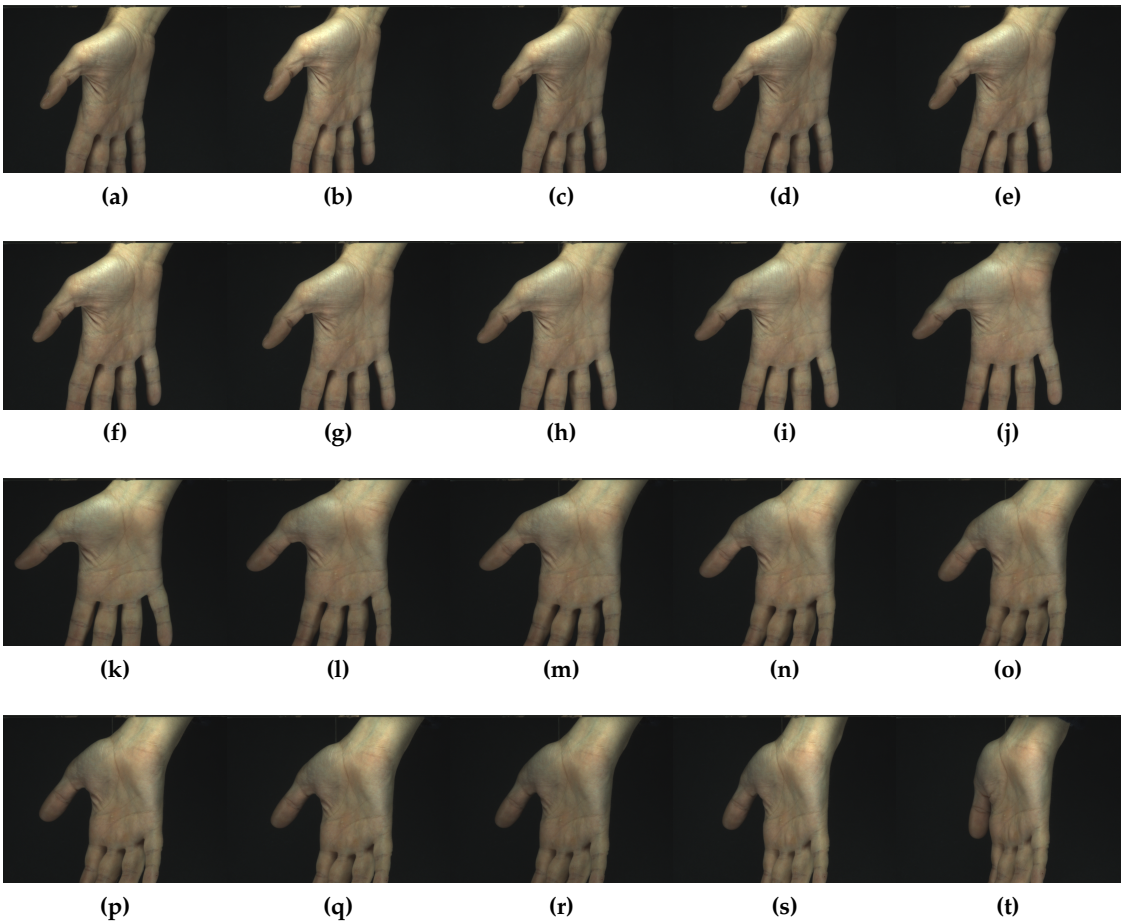

Figure 6.20: Examples of palmprints captured in different orientations using illumination Method 2.

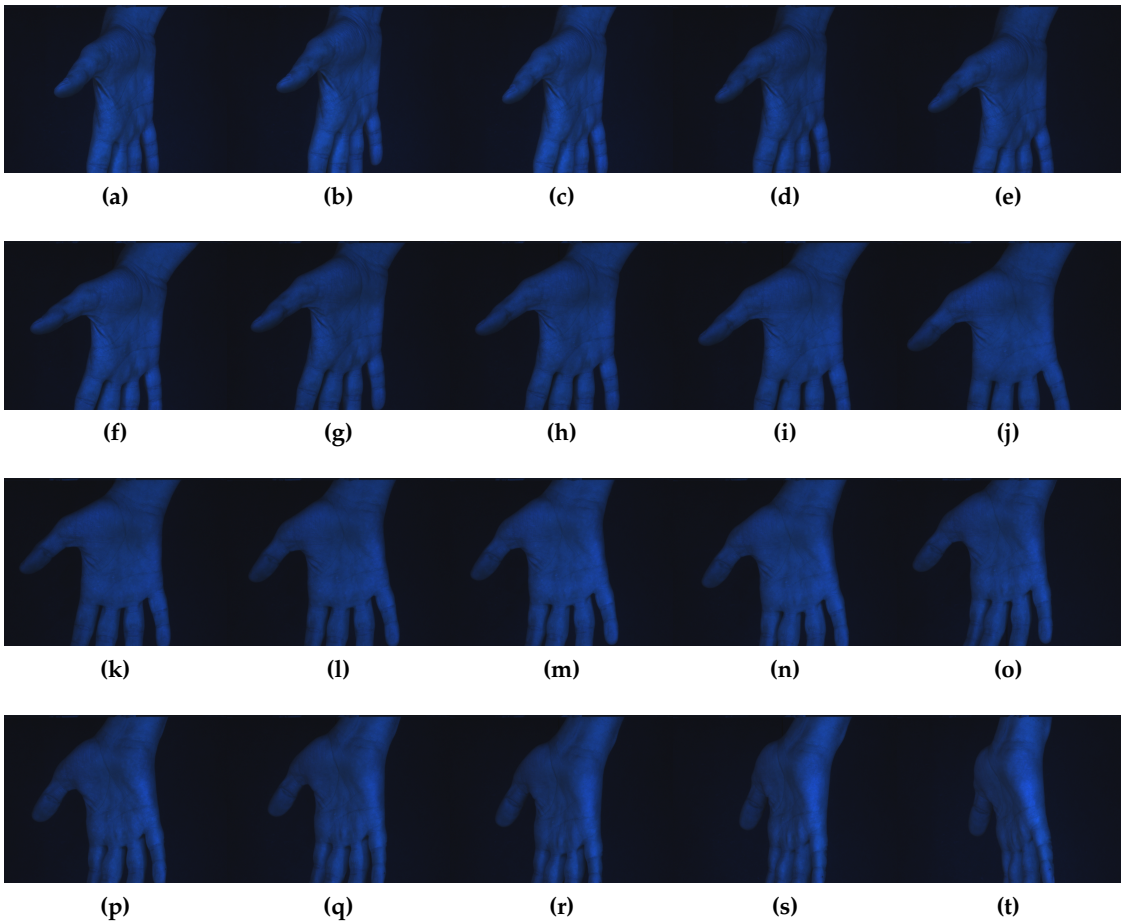

Figure 6.21: Examples of palmprints captured in different orientations using illumination Method 3.

Samples	01	02	03	04	05	06	07	08	09	10	11	12	13	14	15	16	17	18	19	20
01	-	1760.5	1563.5	1782.5	1410	955	538	231.5	29	2.5	2.5	1	2.5	2	1.5	2	1.5	2	2	3.5
02	1607.5	-	2165	863.5	1335.5	678.5	458	204.5	21.5	0.5	1.5	2	3	1	2	4	2.5	1	2.5	3.5
03	1394	1079	-	3360	1792.5	1287	1312	414	49	3	1.5	2	2.5	1.5	1.5	2	3	1.5	0.5	2.5
04	1375.5	1075	2754.5	-	4102.5	2325	1119.5	806	87	5	3	4	1.5	2.5	1.5	5	1	1.5	1.5	8
05	1365.5	1993	1973	3268.5	-	2943	2426.5	1422	305	1.5	1	2.5	8.5	3.5	2.5	2	5.5	2	3	0.5
06	895.5	1024.5	1970.5	2684.5	2189	-	3384.5	1967.5	954	1.5	1.5	1.5	2	0.5	4.5	3	4	3	2	2
07	342.5	1115	1265.5	1967.5	3601.5	4302	-	2823	1964	8	1.5	2	3	1	2.5	2.5	2.5	2	4	2
08	132.5	265.5	844.5	1411	1713.5	2295	2273.5	-	3059.5	106	3	1.5	2	3	3.5	2	3	6.5	1.5	4
09	5.5	1	75	169	317.5	609.5	2514.5	3503	-	637.5	3	1	3	1	1	2	1.5	1	1.5	1.5
10	2	3	4	5.5	2.5	7.5	19	27	441.5	-	1011.5	57	21.5	1.5	6	5.5	6.5	4	1	3.5
11	2.5	6.5	2.5	2	4.5	3	5.5	5.5	3	1490.5	-	893.5	422.5	41.5	2.5	5	2.5	4	4	3
12	2	5	2	1.5	3	7	2.5	2.5	0.5	88.5	574.5	-	2288	1037.5	210	642	24	21.5	18	3.5
13	2	1	3	2	4	4	5.5	4	9	37	79.5	2566	-	1086	531.5	789.5	115	98.5	17	7
14	1	8	4	2.5	5	2	3.5	2.5	1.5	4	39	1128	888	-	1412.5	1318.5	1056	7.5	84	2
15	0.5	2.5	4	2	7	2.5	4.5	3.5	3.5	2.5	4	192	355	1940	-	2050	4457.5	2477	701	23
16	3	3.5	2.5	3.5	2	2.5	13	2.5	3	5	11	469.5	876	1193.5	2911.5	-	3390.5	3493.5	1284	10.5
17	2	1	4	2	4.5	1.5	1	2	1.5	4.5	2	116	75.5	1524	3531	2744.5	-	3490	670.5	8
18	2.5	4.5	2	3	7	1.5	6	4.5	6.5	2.5	3.5	183.5	119.5	78	2297	2497	2205	-	3367	70.5
19	2	1.5	2.5	2	10.5	1.5	7	1	1.5	2	5.5	1	26	214	558.5	1138	884	2397.5	-	685
20	1	2.5	1.5	2	2.5	6.5	3	2	3	3	2	1.5	4	5	6	14	9	102	296.5	-

Figure 6.22: Match scores between samples captured using Method 2 with different roll orientations. The match scores greater than the maximum impostor match score are colored in green.

1. *Standard laboratory acquisition*: the room curtains are shut and the room illumination systems (neons or lamps) are turned off. This is the most controlled situation.

2. *Morning light*: the acquisitions are performed in the morning, the room curtains are open, and the sunlight enters the room. The windows of the laboratory face

Samples	01	02	03	04	05	06	07	08	09	10	11	12	13	14	15	16	17	18	19	20
01	-	1142	1888.5	1504	488	370.5	32	46	2.5	2	0.5	2.5	1.5	2	1	2	2	2	1.5	2.5
02	884	-	701	678	637	669	225	132	3.5	1	1	2	1.5	2	1	4	2	1	1	3
03	1233	932	-	3120	1608.5	447	173.5	26	2.5	2.5	1	2.5	2	2.5	0.5	2	1.5	1	2	1
04	1757	640.5	2604.5	-	2985	2017.5	671.5	86	2.5	1.5	1.5	2	2	2	1.5	1.5	2	3	1	2
05	359	887.5	2101	3199	-	4391.5	1889.5	390	35.5	2	2	2	2	2.5	2	1.5	0.5	0.5	1	2.5
06	292	491	474.5	1885	3036	-	2400.5	1720	134	2	2	1.5	2	1.5	2.5	1	0.5	1	2	1.5
07	90.5	341.5	189.5	521	1165	2484	-	2867.5	250.5	8.5	3	1.5	1	2	3	1	1.5	1.5	2.5	2
08	25.5	119	33.5	111	358	1376.5	3856	-	2866.5	16	21	2	3	2	1.5	1	1	2	3	1.5
09	5	3.5	3.5	20	47	189	391.5	2691	-	1009	281.5	3	2.5	2	2	2	2	1	1	1
10	1	1	2	0.5	1	2	5.5	38	1120	-	2086.5	67	37	22	4	2.5	2.5	1	1.5	1.5
11	2	0.5	1.5	1.5	1.5	1	6.5	23	400.5	1543.5	-	440.5	146.5	30.5	5	1	2.5	1.5	2	2
12	2	1.5	2	2.5	2	1	1.5	0.5	7.5	99	352.5	-	4122.5	1402.5	623.5	314	29.5	7	54.5	26.5
13	1	2	1.5	2	2.5	1.5	2.5	1	3.5	41.5	163	3250.5	-	2970	2104.5	799.5	144.5	26	287.5	141
14	0.5	2.5	2	2	2.5	2.5	2	2.5	2	13	15.5	1407	2426.5	-	1856	3432	343	342.5	854	221
15	1	4	1	2	1	2.5	1.5	1.5	2	4.5	4	969.5	1526.5	2403.5	-	3528.5	356.5	265	1137.5	470.5
16	1.5	2.5	1	1.5	1.5	2	1.5	1.5	1.5	1.5	8.5	226	864.5	3403.5	2411	-	1758.5	244.5	2657	2316.5
17	2.5	1.5	2.5	1.5	2.5	3	2	1	2	2.5	1	23	70	269	434.5	2442	-	2163.5	1167	144.5
18	0.5	1	2	1	1.5	2	2	1.5	2	4	0.5	15.5	22	151.5	262	208.5	3117.5	-	842.5	51.5
19	2	2	2	1.5	0.5	0	2	2.5	0.5	0.5	2	58	167.5	756	1049.5	2047	369	717	-	837
20	1.5	0.5	1	1	0.5	1.5	1.5	2	1.5	1.5	1	52.5	230	409.5	575	2898	193.5	186	1303.5	-

Figure 6.23: Match scores between samples captured using Method 3 with different roll orientations. The match scores greater than the maximum impostor match score are colored in green.

Illumination Situation	Match scores			
	Genuine comparisons		Impostor comparisons	
	Mean	Std	Mean	Std
Standard laboratory acquisition	3179.8	942.1	3.3	1.8
Morning light	2677.4	941.6	2	0.8
Afternoon light	2748.9	903.2	2	0.8
Artificial light	2770.9	876.8	2	0.8

Table 6.7: Average match scores of genuine and impostor comparisons, relative to the samples captured using Method 2, using different environmental illumination situations.

west so the sunlight do not hit directly the palm during the acquisition. The room illumination systems (neons or lamps) are turned off.

3. *Afternoon light*: the acquisitions are performed in the afternoon, the room curtains are open, and the sunlight enters the room. The windows of the laboratory face west so the sunlight hits directly the palm during the acquisition. The room illumination systems (neons or lamps) are turned off.

4. *Artificial light*: The acquisitions are performed in the evening, when there is no sunlight entering the room. The room illumination systems (neons or lamps) are turned on.

For each illumination situation, the acquisitions are performed using Method 2 and Method 3. Then, for each situation we performed the matching of the samples and computed the average match score of genuine and impostor comparisons. The results for Method 2 and Method 3 are depicted respectively in Table 6.7 and Table 6.8. From the table it is possible to observe that similar values for genuine and impostor match scores are obtained in the different illumination situations, indicating that the described method for the fully contactless and less-constrained palmprint recognition is robust to environmental illumination changes.

Illumination Situation	Match scores			
	Genuine comparisons		Impostor comparisons	
	Mean	Std	Mean	Std
Standard laboratory acquisition	2743.4	1405.7	1.6	0.9
Morning light	2566.3	1347.4	2.1	1.3
Afternoon light	3156.7	1141.5	1.4	1.3
Artificial light	2936.5	1212.2	1.4	1.3

Table 6.8: Average match scores of genuine and impostor comparisons, relative to the samples captured using Method 3, using different environmental illumination situations.

6.2.6 EVALUATION OF OTHER BIOMETRIC ASPECTS

In this Section, the evaluation of the other biometric aspects to be considered is described. In particular, the aspects related to the computational speed, cost, interoperability, usability, social acceptance, security, and privacy were evaluated.

6.2.6.1 COMPUTATIONAL SPEED

Two different times were considered separately in the evaluation of the computational speed of the described method. In particular, the acquisition time and the processing time were considered.

First, the acquisition time was considered in order to evaluate the usability of the proposed method. The acquisition time can be further divided into the time needed for positioning the hand, and the time needed for capturing the image. As mentioned in Section 6.2.1, about 5 s are necessary for positioning the hand, including the time needed by the user to place the hand inside the acquisition volume, the time needed for the shutter duration to adapt, and the time waited for making sure the hand is still (about 2 s). The actual capture of the image is performed almost instantly, in particular the time needed for capturing the image is related to the used shutter times, which are between 0.02 s and 0.03 s. If a system for the simultaneous acquisition of the images using both Method 2 and Method 3 was implemented, the corresponding capture time would be at most 0.06 s.

No study in the literature reports the complete acquisition times, and in particular the time needed for positioning the hand in the correct position. In fact, this time depends heavily on the type of used acquisition device, on the operational conditions, and on the familiarity of each user with the specific device, or with biometric systems in general. However, the time needed by our system for capturing the image is similar to other methods in the literature based on CCD acquisitions, and is considerably smaller than the other methods in the literature that use contact-based three-dimensional acquisitions [97] and contactless three-dimensional acquisitions, which require capture times up to 2.5 s [100, 457].

The processing time was evaluated by implementing the described methods using Matlab R2013a, and running them on an Intel Xeon 3.30 GHz processor with 8 GB RAM. The used operating system is Windows 7 Professional 64 bit. In particular, the

processing times include the time needed to create the biometric template from a sample (the three-dimensional model, and the enhanced texture), and the time needed for a biometric comparison (the feature extraction and matching step). In our experiments, the computational time needed to compute a template using the described method is about 200 s, while the computational time needed for one biometric comparison is about 10 s.

In any case, it must be noted the Matlab language is a prototypal development system and it is optimized for coding simplicity, rather than runtime speed. Studies in the literature have demonstrated an increase in computational speed up to 100 times using OpenCV libraries [458], written in C++, with respect to the corresponding Matlab implementations for image processing applications [459].

Moreover, many steps of the methods are highly parallelizable: for example the three-dimensional reconstruction step can be easily parallelized in order to compute several matching points at the same time, and the feature extraction and matching steps can be executed in parallel for the 8 images considered. For these reasons, the use of a multi-core parallel architecture, such as the CUDA architecture [460], could result in a great decrease of the computational time needed for the steps of the biometric recognition system. Studies in the literature have demonstrated an increase in computational speed up to 30 times using an OpenCV implementation which takes advantage of the CUDA architecture [461], with respect to a CPU-based OpenCV implementation.

For these reasons, a parallel C/C++ implementation using the OpenCV libraries and the CUDA architecture would greatly reduce the processing times, and allow with a high probability to use the researched methods in a real-time live biometric system.

A comparison of the times needed for the creation of the template with other methods in the literature is not presented, since those times are seldom reported. Moreover, the implementation of some of the most recent methods in the literature using Matlab would require a great amount of time, and the purchase and assembly of the used hardware. For these reasons, such a comparison would be out of the scope of this thesis. Similarly, a comparison of the times needed for a biometric comparison is not presented. However, optimized implementations of SIFT-based matching methods for image processing have been proved to operate in real-time [462].

6.2.6.2 COST

Currently, many methods in the literature for the palmprint recognition are oriented towards the use of low-cost sensors, such as flatbed scanners or low-resolution cameras (e.g., webcams). With respect to fingerprint recognition systems, which require 500 dpi, palmprint recognition systems can use lower resolutions, down to 75 dpi.

However, the systems in the literature based on a three-dimensional acquisition setup use complex and expensive setups. The methods based on contact-based three-dimensional acquisitions [227, 97] need a complex structured light illumination setup, while the methods that perform a contactless three-dimensional acquisition [425, 426] use an expensive three-dimensional laser scanner [457], which can cost several thousands of dollars.

In this context, the researched methods use a simpler two-view acquisition setup based on two CCD cameras and a led illumination. We used Sony XCD-SX90CR CCD cameras with 25 mm Tamron lenses, which cost about 1500 $. However, the captured images are resized and processed using a low-pass filter before the feature extraction step, showing that comparable results would be obtained by using cameras with a lower quality, resolution and, therefore, a lower cost.

Moreover, the illumination Method 2 uses four blue leds, with a total cost of about 150 $. The used illumination Method 1 uses three downlight leds, with a total cost of about 250 $. If a system which performs the quasi-simultaneous capture using both illumination is implemented, the total illumination cost would be about 400 $. However, the researched two-view acquisition setup is implemented using an open structure, with prototypal material. An implementation with a closed structure would results in a minor light dispersion and a stronger illumination on the palm. For this reason, leds with a minor intensity could be used in order to reduce the cost. Such acquisition setup would have a minor complexity and cost, with respect to three-dimensional palmprint recognition methods described in the literature.

6.2.6.3 INTEROPERABILITY

Currently, several different methods for the palmprint recognition are commercially available and described in the literature. However, the majority of the approaches in the literature use ad-hoc acquisition devices, and do not rely on standard methods for the acquisition of the samples, for their processing, for the exchange of palmprint data, or for the matching of palmprint samples.

Currently, only a standard exist for the exchange of palmprint data [254] in AFIS systems. However, the standard is typically used for forensic or investigative applications, and applies to palmprint samples captured from latent impressions or using optical-based devices.

For these reasons, the interoperability between palmprint recognition systems is currently limited and experiments using mixed databases, composed by samples captured using different acquisition techniques, were not performed.

6.2.6.4 USABILITY

We performed the evaluation of the usability during the collection of the dataset PB in order to evaluate the efficiency, effectiveness, and user satisfaction related to the acquisition procedure, similarly to the method described in [114]. As stated in the ISO 9241-11 [463], in fact, usability is defined as "*the extent to which a product can be used by specified users to achieve specified goals with effectiveness, efficiency and satisfaction in a specified context of use*". In particular, the three main aspects of the usability can be defined as such:

- *Effectiveness*: measures the accuracy and completeness with which the users achieve the specified goals. Aspects such as the completion rate and the number of errors influence this aspect.

Table 6.9: Effectiveness of the acquisition systems based on Method 2 and Method 3, evaluated considering the percentage of the images with quality "sufficient".

Dataset	t_{EER}	Percentage of images with quality "sufficient"	Percentage of images with quality "poor"
PB - Method 2	0.10	66.25 %	33.75 %
PB - Method 3	0.11	60.78 %	39.22 %

- *Efficiency*: measures the resources used in relation to the accuracy and completeness. It is usually measured in terms of time.
- *User satisfaction*: it is subjective and describes the way the technology is perceived by the users and meets their expectations. It is influenced by factors such as the ease of use and the usefulness of the technology.

A measure of the effectiveness can be defined by considering the quality of the captured images. In fact, the more high-quality images are acquired, the more likely it is that a correct recognition is performed. Since a standard tool for the measurement of contactless palmprint samples is not available, we used the normalized match score as a quality measure. In particular, the normalized match score defines the capability of a sample to be properly matched to other samples of the same individual, and is computed as:

$$o(x_i) = \frac{s_m(x_{ii}) + (\mu(s_m(x_{ij})) - s_m(x_{ii}))}{\sigma(s_m(x_{ij}))} \quad , \tag{6.4}$$

where x_i is the considered sample, $s_m(x_{ii})$ is the match-score obtained by comparing the sample x_i with x_i itself, $\mu(s_m(x_{ij}))$ and $\sigma(s_m(x_{ij}))$ are the mean and standard deviation of the match-scores obtained by comparing the sample x_i with the other samples pertaining to the same individual.

We defined the class of each sample x_i as

$$q(x_i) = \begin{cases} \text{"sufficient"} & \text{if } o(x_i) > t_{EER} \\ \text{"poor"} & \text{otherwise} \end{cases} \quad , \tag{6.5}$$

where the value t_{EER} was chosen as the lowest normalized match score for which, by discarding the images with quality "poor", the system obtained an EER $= 0$ %.

Table 6.9 reports the percentage of the images belonging to the two quality classes for each evaluated dataset, and the corresponding t_{EER} value. It can be observed that, by using a small value of t_{EER}, it is possible to obtain an EER $= 0$ %, and discard only a relatively small number of samples with quality "poor".

The evaluation of the efficiency was performed on the basis of qualitative measurements of the time needed for every biometric acquisition, as described in [114]. As described in Section 5.3.2, a user interface was designed in order to improve the ease of use of the system, by showing a live feed of the cameras, with a circle superimposed

over it (Fig. 5.26). When the palm of the user is placed over the circle, the acquisition is performed. A minimum amount of instructions was given to the users, and they were only required to extend the open hand in a relaxed position inside the acquisition volume, and place the palm over the circle superimposed on the live feed.

The guided acquisition procedure proved intuitive and easily usable, and in the majority of the cases it was sufficient in order to instruct people on how to perform the acquisition, and on where to put their hand for a correct placement. However, the acquisition device is still in a prototypal phase, and some supervision was required. If the device was enclosed in a structure the acquisition procedure would be almost completely intuitive, and complete unsupervised acquisitions would be possible.

As mentioned in Section 6.2.1, the time considered included the training time needed in order to describe to the volunteers how the acquisitions were performed, the time needed for the proper placement of the hand inside the acquisition volume, and the time needed to capture the image. The entire acquisition procedure for each sample took approximately 5 s, including the time needed for positioning the hand, the time for the shutter duration to adapt, and the time that the system waits to make sure the hand is still (about 2 s). The actual capture of the image is performed almost instantly, with shutter times ranging from 0.02 s to 0.03 s.

The user satisfaction was evaluated by asking each volunteer a series of questions about the performed acquisitions, in the form of a survey. Two questions were asked in order to evaluate the satisfaction regarding the usability of the system:

- *Q1*: Is the acquisition procedure comfortable?
- *Q2*: What do you think about the time needed for every acquisition?

Five answers were possible, both for Q1 and Q2:

- *A1*: Very poor;
- *A2*: Poor;
- *A3*: Sufficient;
- *A4*: Good;
- *A5*: Excellent;

The two questions Q1 and Q2 were asked both regarding the acquisition Method 2 and Method 3. Table 6.10 reports the mean values of the responses of the users to the survey. The histograms of the obtained answers are shown in Fig. 6.24.

The mean values relative to the question Q1 were 4.09 and 4.28, respectively regarding the acquisitions performed using Method 2 and Method 3. The results indicate that the volunteers whose samples were collected for the dataset consider both methods having a good acquisition comfort. Slightly better results were obtained by the acquisition Method 3, probably due to the minor illumination intensity, which resulted in a less invasive acquisition.

Table 6.10: Comparison of the usability of acquisition Method 2 and Method 3.

	Question	Mean vote	
		Method 2	Method 3
Q1	Is the acquisition procedure comfortable?	4.09	4.28
Q2	What do you think about the time needed for every acquisition?	4.16	4.22

Notes. The possible responses are: (1) very poor; (1) poor; (3) sufficient; (4) good; (5) excellent.

(a) **(b)**

Figure 6.24: Usability comparison of acquisition Method 2 and Method 3: (a) answers to the question Q1 "Is the acquisition procedure comfortable?"; (b) answers to the question Q2 "What do you think about the time needed for every acquisition?".

The mean values relative to the question Q2 were 4.16 and 4.22, respectively regarding the acquisitions performed using Method 2 and Method 3. The results indicate a good opinion of the users towards the required acquisition time.

It is possible to conclude that the performed usability evaluation obtained good results for the described palmprint acquisition method, both using Method 2 and Method 3.

6.2.6.5 SOCIAL ACCEPTANCE

We performed an evaluation of the social acceptance of the proposed system during the collection of the dataset PB, by asking the volunteers a set of questions in the form of a survey, as described in other works in the literature [115]. In particular, four questions were asked:

- *Q3*: Are you worried about hygiene issues?
- *Q4*: Are you worried about possible security lacks due to latent palmprints?
- *Q5*: Do you think that biometric data could be improperly used for police investigations?
- *Q6*: Do you feel that the system attacks your privacy?

Five answers were possible for each question:

Table 6.11: Comparison of the usability of acquisition Method 2 and Method 3.

	Question	Mean vote
Q3	Are you worried about hygiene issues?	4.38
Q4	Are you worried about possible security lacks due to latent palmprints?	4.23
Q5	Do you think that biometric data could be improperly used for police investigations?	3.87
Q6	Do you feel that the system attacks your privacy?	3.92

Notes. The possible responses are: (1) very worried; (2) worried; (3) normal; (4) not worried; (5) high trust.

- *A1*: Very worried;
- *A2*: Worried;
- *A3*: Normal;
- *A4*: Not worried;
- *A5*: High trust;

Table 6.11 reports the mean values of the responses of the users to the survey. The histograms of the obtained answers are shown in Fig. 6.25.

It is possible to observe that the users have a good attitude towards the considered biometric system, in particular regarding the aspects related to the hygiene (Q3), latent impressions (Q4), and the privacy (Q6). However, some people expressed less confidence about improper use of biometric data (Q5).

Then, we performed two more general final questions:

- *Q6*: Would you be willing to use the contactless fingerprint biometric system daily?
- *Q7*: Do you prefer contactless systems against contact-based systems?

All the volunteers responded that they prefer to use contactless biometric systems, with respect to contact-based biometric systems, and almost all the volunteers stated that they would be willing to use the described contactless system daily.

6.2.6.6 SECURITY

One of the improvements of contactless acquisition techniques over contact-based techniques is the absence of latent impressions left on the sensors, which can pose a security threat. The described methods do not allow to lifting a latent palmprint.

At the present stage, it would be possible to trick the acquisition sensor using a fake palmprint (e.g. a printed scan), since a module for checking the liveness of the palm is not present. However, simple palmprint liveness detection algorithms were implemented in the literature using a NIR illumination and a CCD camera [344].

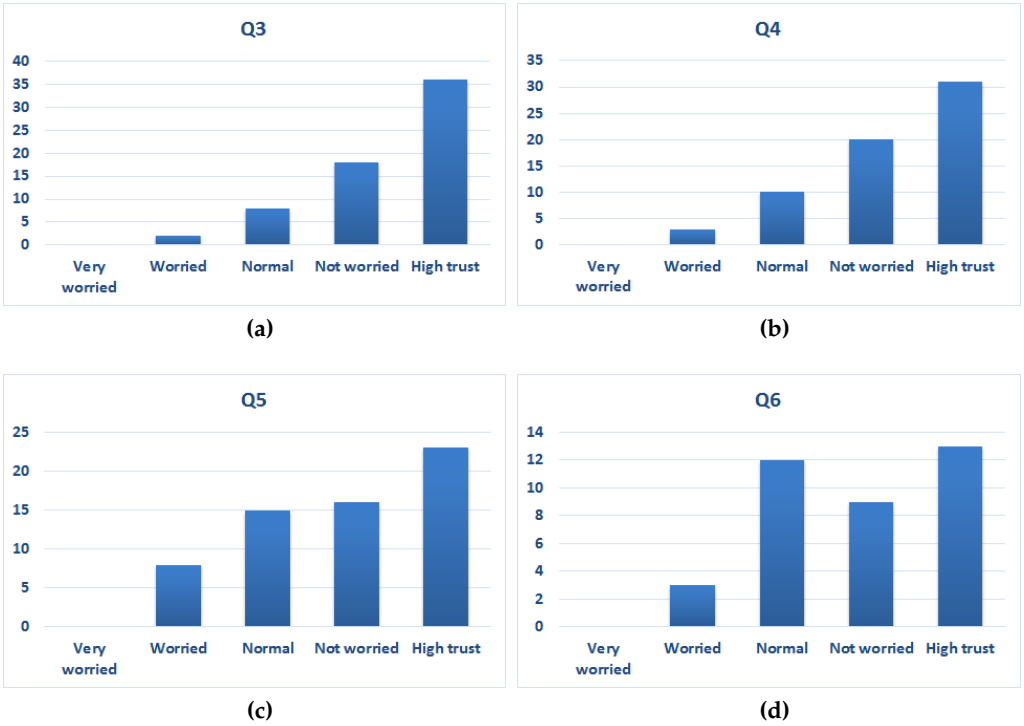

Figure 6.25: Comparison of the social acceptability of the acquisition using Method 2 and Method 3: (a) answers to the question Q3 "Are you worried about hygiene issues?"; (b) answers to the question Q4 "Are you worried about possible security lacks due to latent palmprints?" (c) answers to the question Q5 "Do you consider the system a hygienic solution?"; (d) answers to the question Q6 "Do you feel that the system attacks your privacy?".

6.2.6.7 PRIVACY

Techniques for the protection of the privacy of biometric data are necessary for the described contactless palmprint recognition method, as well for contact-based methods. In particular, palmprint samples can pose a threat to the users' privacy, since they can be used to diagnose diseases, genetic disorders, or even schizophrenia [16, 209].

At the present stage, techniques for the privacy protection are not implemented. However, there are several methods in the literature for the creation of encrypted template databases, or for the generation of cancelable biometrics [16].

6.2.7 COMPARISONS WITH OTHER METHODS IN THE LITERATURE

As mentioned in Section 4.1.3, it is possible to divide the methods for the palmprint recognition according to the type of acquisition performed. In particular, contact-based and contactless methods can be distinguished, and each category can be divided into methods based on two-dimensional images and methods based on three-dimensional models.

In order to test the validity of the proposed method, we compared the described methods with the other methods in the literature, according to the type of the acqui-

sition. In particular, two aspects are considered in the comparison: the advantages related to the type of the acquisition, and the obtained recognition accuracy.

6.2.7.1 COMPARISON RELATED TO THE TYPE OF THE ACQUISITION

It is possible to summarize the advantages of the researched methods over the methods in the literature, based on the different types of acquisitions:

- *Advantages over contact-based two-dimensional methods*: with respect to contact-based two-dimensional methods, the researched methods do not have the problems related to the contact of the palm with the sensor, such as distortion, dirt, sweat, or latent impressions. Moreover, the absence of contact increases the usability and acceptability of the system, especially since no pegs are used. The use of three-dimensional information allows to increase the accuracy, and to capture the palms without imposing a fixed position. With respect to the methods based on inked acquisitions, optical devices, or flatbed scanners, the researched method perform a faster acquisition.

- *Advantages over contact-based three-dimensional methods*: similarly to the case of contact-based two-dimensional methods, the researched methods do not have the problems related to the contact of the palm with the sensor. Moreover, the methods in the literature that perform the palmprint recognition using contact-based three-dimensional acquisitions use setups based on structured light illumination, which are complex and expensive. The researched methods require a simpler setup based on a two-view acquisition system, and a led illumination. Moreover, the researched method performs a faster capture of the image.

- *Advantages over contactless two-dimensional methods*: with respect to contactless two-dimensional palmprint recognition methods in the literature, the researched methods do not require the user to place the back of his hand on a fixed surface. By using a fully contactless acquisition, the researched methods avoid the problems related to dirt or to cultural aspects, also increasing the usability and acceptability of the system. Moreover, in the researched acquisition method the users are not required to place their hand perfectly horizontal, unnaturally spread their fingers, or use uncomfortable positions. The acquisition procedure is performed automatically, and by just requiring the volunteers to place their hand inside the acquisition volume. A greater acquisition distance is also used.

- *Advantages over contactless three-dimensional methods*: the other methods in the literature that perform a contactless three-dimensional palmprint recognition use expensive acquisition setups based on laser scanners, which require the user to hold the hand still during the computation of the three-dimensional model. The researched methods use a lower cost setup composed by a two-view acquisition system and a led illumination. Moreover, the capture of the image is performed faster and in an automatic way.

However, the described method presents some disadvantages, especially related to the lack of constraints. It is possible, in fact, to obtain acquisitions with a lower quality,

Table 6.12: Comparison of the obtained accuracy of the researched method (boldface) with the most recent approaches in the literature, classified according to the type of the acquisition.

Ref.	Type of acquisition	Device used	Size of dataset (palms)	EER (%)
[313]	Contact-based two-dimensional	CCD-based with pegs	250	0.10
[311]		CCD-based with pegs	386	0.02
[309]		CCD-based with pegs	386	0.14
[105]		Optical device	160	< 0.01
[281]		Flatbed scanner	80	0.60
[280]		Flatbed scanner	384	0.20
[97]	Contact-based three-dimensional	CCD-based and projector, with pegs	100	0.03
[228]	Contactless two-dimensional	Mobile device	200	0.14
[394]		Ad-hoc device	602	0.16
[393]		Ad-hoc device	602	0.06
[130]		Ad-hoc device	470	0.2
[388]		Ad-hoc device	602	0.41
[425]	Contactless three-dimensional	Laser scanner	354	0.22
[426]		Laser scanner	114	0.28
Described method		**Two-view CCD-based system**	64	0.08

with excessive rotations of the hand, or affected by motion blur. Moreover, the resolution of the three-dimensional models reconstructed using the described methods is inferior to the one obtained by using structured light illumination systems or laser scanners.

6.2.7.2 COMPARISON ACCORDING TO THE OBTAINED ACCURACY

We compared the accuracy of the researched methods with the most recent methods in the literature for palmprint recognition, classified according to the type of acquisition. In particular, we considered the size of the collected dataset, and the obtained EER value. The results are summarized in Table 6.12, and it is possible to observe that the accuracy of the researched method is comparable, or superior, to the accuracy of the most recent methods in the literature. Moreover, the researched method has the aforementioned advantages related to the fully contactless less-constrained acquisition, to the faster acquisition, and to the lower cost.

6.2.8 FINAL CONSIDERATIONS

The final considerations about the evaluated biometric aspects are summarized. In particular, we considered the evaluated accuracy, robustness, computational speed, cost, interoperability, usability, social acceptance, security, and privacy:

- *Accuracy*: the researched methods for a contactless less-constrained palmprint recognition obtained a good accuracy. In particular, by considering multiple comparisons and different illumination methods, it was possible to obtain a recognition accuracy comparable, or superior, to the most recent methods in the literature. Moreover, the obtained FMR and FNMR values proved that the method could be deployable in high-security scenarios.

- *Robustness*: the researched methods proved to be robust to small variations in the roll orientation of the hand during the acquisition. Moreover, the method proved to perform in a similar manner in all the tested environmental illumination situations.

- *Computational speed*: both the acquisition time and the processing time were considered in order to evaluate the computational speed.

  In particular, the acquisition time is composed by the time needed for positioning the hand inside the acquisition volume, the time spent in adapting the shutter duration, the time waited for the hand to be still, and the time for the actual capture of the image. The described system needs about 5 s for a complete acquisition, of which at most 0.06 s are needed for the actual capture.

  No study in the literature reports the complete acquisition times, since they depend on the type of used acquisition device, on the operational conditions, and on the familiarity of each user with the specific device. However, the time needed by the described system for capturing the image is considerably smaller than the other methods in the literature that use contact-based three-dimensional acquisitions, which require capture times up to 2.5 s.

  Regarding the processing times, at the present stage the described methods are not optimized, and a real-time use is not feasible. However, a parallel C/C++ implementation, for example based on the OpenCV libraries and the CUDA architecture, would dramatically reduce the computational times, and with a great probability a real-time use would be possible.

- *Cost*: the considered acquisition setup is composed by two CCD cameras and a led illumination, and is less expensive than the methods in the literature based on contactless three-dimensional acquisition. Moreover, the cost of the cameras can be reduced by using low-cost cameras with a lower resolution. A less expensive led illumination can be used by reducing the scale of the system, and using an enclosed structure.

- *Interoperability*: currently, the interoperability between palmprint recognition methods in the literature is very limited, and in general the different acquisition de-

vices are not compatible. There exists only a standard for the exchange of palmprint data in AFIS systems, which consider latent impressions, or acquisitions performed using an optical device.

- *Usability*: the described methods achieved a good effectiveness, evaluated by considering the ratio of the samples with good quality to the total number of samples. A good efficiency was also reached using an intuitive, automated, acquisition procedure. Moreover, we used a survey to estimate a positive user satisfaction towards the researched technology.

- *Social acceptance*: a survey was used to estimate a good social acceptance of the described technology, regarding the aspects of hygiene, security lacks, invasion of the privacy. However, some users have concerns regarding improper uses of the biometric data.

- *Security*: with respect to contact-based systems, no latent palmprint can be lifted from the researched palmprint recognition system, since it is based on contactless acquisitions. At the moment, a liveness detection module is not considered, however simple procedures described in the literature can be used.

- *Privacy*: at the moment, techniques for the privacy protection are not considered. However, several methods exist in the literature for the encryption of the templates, or for the generation of cancelable biometrics.

6.3 SUMMARY

In this chapter, the experimental results of the described palmprint recognition methods were introduced and described.

The method based on acquisitions at a fixed distance was able to compute realistic three-dimensional models, and to achieve a good accuracy recognition, comparable to the most recent contact-based methods in the literature for the palmprint recognition. However, the acquisition procedure imposes some constraints.

The method based on acquisitions with uncontrolled distance achieved a very good accuracy, in many cases superior to the most recent methods in the literature. In particular, the obtained FMR and FNMR values allow to use the method in high-security scenarios. Moreover, the acquisition procedure is almost unconstrained. A good robustness to variations in the hand orientation and differences in the environmental illumination situations was also obtained.

With regard to this method, the other biometric factors were evaluated, including the computational speed, cost, interoperability, usability, social acceptance, security, and privacy. In particular, the computational speed of the method can be optimized and easily parallelized, while the cost can be reduced using low-cost cameras and leds with a minor intensity.

The usability and social acceptance were evaluated by considering the quality of the samples, the time needed for the acquisitions, and by asking questions in the form of a survey. In these aspects, good results were obtained.

The system has a security advantage since it does not allow to lift a latent palmprint impression, however techniques for the security and privacy protection have still to be considered.

7

CONCLUSION AND FUTURE WORKS

In this chapter, a summary and conclusion of the described work is presented, along with a survey of the possible future works.

7.1 CONCLUSION

The work described in this thesis had the objective of researching innovative methods for the contactless, less-constrained palmprint recognition.

Preliminary methods for the contactless and less-constrained biometric recognition were studied for the recognition of the fingerprint, since the research in the field of fingerprint recognition is more advanced and standard methods for the processing and matching of the samples are available. The obtained results allowed to extend the developed algorithms in the more general case of hand-based biometrics, with a particular focus on the palmprint.

First, a feasibility study for a contactless palmprint recognition, based on acquisitions performed at a fixed distance, was studied and implemented. The method achieved a good recognition accuracy, comparable to the accuracy of the most recent contact-based methods in the literature, without the problems of distortions and dirt, typical of contact-based acquisitions. However, a fixed position of the hand was required.

The obtained results allowed to extend the implemented algorithms using a novel, fully contactless, and less-constrained palmprint acquisitions. In particular, the researched methods for the palmprint recognition performed an accurate recognition using a less-constrained, innovative acquisition setup with respect to the ones in the literature. In fact, the studied methods were able to perform the recognition without the need to place the hand on any surface, and without the need for the hand to be positioned in a specific position. In fact, the use of three-dimensional reconstructed models permitted to use a representation of biometric data independent from the position, the orientation, and the distance of the user's hand.

With respect to the methods in the literature that perform contact-based acquisitions, the researched method did not have the problems caused by the contact of the palm with the sensor, and had a greater usability and acceptability, also because no pegs were used. With respect to other methods in the literature that only use two-dimensional samples, the computation of the three-dimensional models realized a metric representation invariant to the acquisition position, orientation, and distance. In this manner, a less-constrained acquisition, with a relaxed position of the hand, could be performed. With respect to the other methods in the literature based on a contactless three-dimensional acquisition of the palmprint, the described approach used an innovative setup with a lower cost, and able to capture the samples considerably faster.

All the steps of the biometric systems were considered in the design and implementation of the palmprint recognition system, including the steps related to the acquisition, the segmentation and preprocessing, the image enhancement, the feature extraction and matching. The researched approaches make use of original optical acquisition systems, image processing techniques, three-dimensional reconstruction methods, and pattern recognition algorithms.

Biometric datasets of palms, containing a number of samples sufficient in order to produce significant results, were collected in order to test the described approaches, and the obtained results consisted in a good accuracy, in many cases superior to the accuracy of most recent methods in the literature. In particular, by combining different illumination methods, the palmprint recognition method achieved an EER equal to 0.08 % on a dataset with 640 samples. Moreover, low FMR values were obtained, showing that high-security applications of the described technology are possible.

Good results were also obtained regarding the robustness, usability and social acceptance. Moreover, the computational speed, cost, privacy, and security of the obtained methods were taken into consideration.

7.2 FUTURE WORKS

Different aspects of the researched methods could be considered for improvement, in order to increase the accuracy, usability, and social acceptance of the researched methods.

First, a simultaneous acquisition using illuminations with different wavelengths can be considered in order to improve the accuracy of the recognition. The obtained results, in fact, proved that the combination of the match scores obtained by comparing samples captured using different illuminations increased the recognition accuracy.

The design and implementation of more accurate reconstruction algorithm would allow to compute three-dimensional models with a greater resolution, which would make possible the design and development of more robust three-dimensional registration and matching methods, with the consequence of a greater recognition accuracy.

Moreover, if a larger acquisition area was used, the less-constrained biometric system based on the palmprint could be integrated using the information related to the fingerprint and the hand shape, in order to increase the accuracy.

The usability and social acceptance of the acquisition system could be improved by reducing the acquisition times, using an enclosed structure, and considering a real-time hand detection and quality estimation module.

In particular, a quicker acquisition with a lower shutter time could prove useful in allowing the users to be recognized just by passing their hand over the acquisition area. For this purpose, an enclosed structure containing the optical acquisition system would results in a stronger illumination on the palm, with the possibility of reducing the camera shutter time. Moreover, an enclosed structure would increase the usability of the system, by hiding the parts that do not concern the final user. The enclosure would also shield the used illumination systems, which can be perceived as too strong, unpleasant, or harmful, and increase the social acceptance of the device.

A real-time hand detector could be implemented in order to accurately detect when a hand is present in the acquisition area, and perform a faster acquisition as soon as the hand is inside the acquisition volume.

A quality detection module could be designed and implemented in order to improve the accuracy of the recognition by discarding the samples with a lower quality. A real-time implementation of the quality detection module would give the users a real-time feedback of the captured sample, and increase the intuitiveness and usability of the acquisition system.

[1] International Organization for Standards, "ISO/IEC JTC1 SC37 Standing Document 2, version 8, Harmonized Biometric Vocabulary," August 1997. *(Cited on pages 1 and 7)*

[2] A. K. Jain, P. J. Flynn, and A. A. Ross, *Handbook of Biometrics*. Springer Science + Business Media, LLC, 2008. *(Cited on pages 2 and 7)*

[3] RNCOS, "Biometric market forecast to 2014," 2012. *(Cited on page 7)*

[4] International Biometric Group, "Biometrics market and industry report, BMIR 2009-2014," 2009, http://www.ibgweb.com. *(Cited on page 7)*

[5] Biometric Research Group, Michigan State University, "Fingerprint reconstruction from minutiae," http://biometrics.cse.msu.edu/projects/fingerprint_reconstruct.html. *(Cited on pages XI and 11)*

[6] "Palmprint," *Popular Science Monthly*, vol. 63, 1903. *(Cited on pages XI and 11)*

[7] "Neurotechnology VeriEye," http://www.neurotechnology.com/verieye-technology.html. *(Cited on pages XI and 11)*

[8] "Biometric facial recognition: Using facial traits to identify people," http://www.questbiometrics.com/biometric-facial-recognition.html. *(Cited on pages XI and 11)*

[9] "Structure of life," http://lebbeuswoods.wordpress.com/2010/08/30/structure-of-life/. *(Cited on pages XI and 11)*

[10] "What is hand geometry?" http://360biometrics.com/faq/Hand-Geometry-Biometrics.php. *(Cited on pages XI, 11, and 15)*

[11] "Palm-reading devices get smart about security," http://www.scientificamerican.com/article.cfm?id=palm-reading-devices. *(Cited on pages XI and 11)*

[12] "Ear geometry," http://fingerchip.pagesperso-orange.fr/biometrics/types/ear.htm. *(Cited on pages XI and 11)*

[13] "Labview for ECG signal processing," http://fingerchip.pagesperso-orange.fr/biometrics/types/ear.htm. *(Cited on pages XI and 11)*

[14] D. Maltoni, D. Maio, and A. K. Jain, *Handbook of Fingerprint Recognition*, ser. Springer Professional Computing. Springer London, Limited, 2009. *(Cited on pages 10, 21, and 24)*

[15] R. Donida Labati and F. Scotti, "Fingerprint," in *Encyclopedia of Cryptography and Security (2nd ed.)*, H. C. A. van Tilborg and S. Jajodia, Eds. Springer, 2011, pp. 460–465. *(Cited on page 10)*

[16] A. Kong, D. Zhang, and M. Kamel, "A survey of palmprint recognition," *Pattern Recognition*, vol. 42, no. 7, pp. 1408–1418, Jul. 2009. *(Cited on pages 10, 14, 53, 55, 61, 62, and 202)*

[17] J. Daugman, "Iris recognition," in *Handbook of Biometrics*, A. K. Jain, P. Flynn, and A. A. Ross, Eds. Springer US, 2008, pp. 71–90. *(Cited on pages XI, 10, 13, 14, and 29)*

[18] R. Donida Labati, A. Genovese, V. Piuri, and F. Scotti, *Iris segmentation: state of the art and innovative methods*, ser. Intelligent Systems Reference Library, C. Liu and V. K. Mago, Eds. Springer, 2012, vol. 37. *(Cited on pages XII, 10, 43, and 44)*

[19] S. Z. Li and A. K. Jain, Eds., *Handbook of Face Recognition, 2nd Edition*. Springer, 2011. *(Cited on pages 10, 14, and 41)*

[20] D. P. Sidlauskas and S. Tamer, "Hand geometry recognition," in *Handbook of Biometrics*, A. K. Jain, P. Flynn, and A. A. Ross, Eds. Springer US, 2008, pp. 91–107. *(Cited on pages 10, 14, and 39)*

[21] A. H. Choi and C. N. Tran, "Hand vascular pattern technology," in *Handbook of Biometrics*, A. K. Jain, P. Flynn, and A. A. Ross, Eds. Springer US, 2008, pp. 253–270. *(Cited on pages 10 and 14)*

[22] D. J. Hurley, B. Arbab-Zavar, and M. S. Nixon, "The ear as a biometric," in *Handbook of Biometrics*, A. K. Jain, P. Flynn, and A. A. Ross, Eds. Springer US, 2008, pp. 131–150. *(Cited on pages 10, 15, 30, and 46)*

[23] T. Hicks and R. Coquoz, "Forensic DNA evidence," in *Encyclopedia of Biometrics*, S. Z. Li and A. K. Jain, Eds. Springer US, 2009, pp. 573–579. *(Cited on pages 10 and 15)*

[24] I. Odinaka, P.-H. Lai, A. D. Kaplan, J. O'Sullivan, E. J. Sirevaag, and J. W. Rohrbaugh, "ECG biometric recognition: A comparative analysis," *IEEE Transactions on Information Forensics and Security*, vol. 7, no. 6, pp. 1812–1824, 2012. *(Cited on pages 10 and 30)*

[25] J. González-Rodríguez, D. T. Toledano, and J. Ortega-García, "Voice biometrics," in *Handbook of Biometrics*, A. K. Jain, P. Flynn, and A. A. Ross, Eds. Springer US, 2008, pp. 151–170. *(Cited on pages 11 and 16)*

[26] R. Chellappa, A. Veeraraghavan, and N. Ramanathan, "Gait biometrics, overview," in *Encyclopedia of Biometrics*, S. Z. Li and A. K. Jain, Eds. Springer US, 2009, pp. 628–633. *(Cited on pages 11, 16, and 45)*

[27] D. Impedovo and G. Pirlo, "Automatic signature verification: The state of the art," *IEEE Transactions on Systems, Man, and Cybernetics, Part C: Applications and Reviews*, vol. 38, no. 5, pp. 609–635, 2008. *(Cited on pages 11 and 16)*

[28] D. Shanmugapriya and G. Padmavathi, "A survey of biometric keystroke dynamics: Approaches, security and challenges," *CoRR*, vol. abs/0910.0817, 2009. *(Cited on pages 11 and 16)*

[29] Biometry, "Permanent biometric voice recognition," http://biometry.com/perma-voice.html. *(Cited on pages XI and 11)*

[30] University of California Riverside, "Gait recognition," http://www.cris.ucr.edu/Biometric_Examples.php. *(Cited on pages XI and 11)*

[31] IIT's Visual Computing Lab, Illinois Institute of Technology, "Signature recognition," http://www.cs.iit.edu/~agam/vc/. *(Cited on pages XI and 11)*

[32] Deepnet Security, "Typesense," http://www.deepnetsecurity.com/tokens/bio/typesense/. *(Cited on pages XI and 11)*

[33] A. K. Jain, A. Ross, and S. Prabhakar, "An introduction to biometric recognition," *IEEE Transactions on Circuits and Systems for Video Technology*, vol. 14, no. 1, pp. 4–20, 2004. *(Cited on pages 11 and 20)*

[34] A. A. Ross, K. Nandakumar, and A. K. Jain, *Handbook of Multibiometrics (International Series on Biometrics)*. Secaucus, NJ, USA: Springer-Verlag New York, Inc., 2006. *(Cited on pages 12, 17, 29, and 46)*

[35] A. K. Jain, S. C. Dass, and K. Nandakumar, "Soft biometric traits for personal recognition systems," in *Proceedings of the International Conference on Biometric Authentication, Hong Kong*, 2004, pp. 731–738. *(Cited on pages 12, 16, and 46)*

[36] S. Denman, A. Bialkowski, C. Fookes, and S. Sridharan, "Determining operational measures from multi-camera surveillance systems using soft biometrics," in *Proceedings of the 2011 8th IEEE International Conference on Advanced Video and Signal-Based Surveillance (AVSS)*, 2011, pp. 462–467. *(Cited on pages 12 and 47)*

[37] C. Velardo and J. Dugelay, "Weight estimation from visual body appearance," in *Proceedings of the 2010 Fourth IEEE International Conference on Biometrics: Theory Applications and Systems (BTAS)*, 2010, pp. 1–6. *(Cited on page 12)*

[38] R. Donida Labati, A. Genovese, V. Piuri, and F. Scotti, "Weight estimation from frame sequences using computational intelligence techniques," in *Proceedings of the 2012 IEEE International Conference on Computational Intelligence for Measurement Systems and Applications (CIMSA)*, 2012, pp. 29–34. *(Cited on pages 12 and 47)*

[39] S. Denman, C. Fookes, A. Bialkowski, and S. Sridharan, "Soft-biometrics: Unconstrained authentication in a surveillance environment," in *Digital Image Computing: Techniques and Applications (DICTA)*, 2009, pp. 196–203. *(Cited on pages 12, 36, 46, and 47)*

[40] M. Demirkus, K. Garg, and S. Guler, "Automated person categorization for video surveillance using soft biometrics," in *Biometric Technology for Human Identification*, vol. VII, 2010. *(Cited on pages 12 and 47)*

[41] A. Dantcheva, N. Erdogmus, and J. Dugelay, "On the reliability of eye color as a soft biometric trait," in *Proceedings of the 2011 IEEE Workshop on Applications of Computer Vision (WACV)*, 2011, pp. 227–231. *(Cited on page 12)*

[42] Crossmatch, "Verifier 300 LC 2.0," http://www.crossmatch.com/verifier-300-lc-2.php. *(Cited on pages XI and 12)*

[43] "Ibm thinkpad t42 gets updated with biometric security," http://www.notebookreview.com/default.asp?newsID=2027. *(Cited on pages XI and 12)*

[44] P. Komarinski, *Automated Fingerprint Identification Systems (AFIS)*. Elsevier Science, 2005. *(Cited on page 12)*

[45] Nitgen, "Fingkey access," http://www.nitgen.com/eng/product/fingkeyaccess.html. *(Cited on pages XI and 13)*

[46] B. Alms, "Finger print dusting 2," http://it.photos.com/immagini-royalty-free/finger-print-dusting-2/121239594. *(Cited on pages XI and 13)*

[47] ZKTeco, "What is fingerprint identification?" http://eu.zksoftware.com/view.do?id=51. *(Cited on pages XI and 13)*

[48] IFSR, "Face / iris recognition based system," http://www.ifsr.in/Biometrics_products.html. *(Cited on pages XI and 14)*

[49] U.S. Department of Defense, "Handheld iris scanner," http://www.biometrics.org/bc2007/presentations/Thu_Sep_13/Session_I/13_Dee_DOD.pdf. *(Cited on pages XI and 14)*

[50] Brunel University, London, http://www.brunel.ac.uk/sed/ece/research/cesr/student-profiles/kazimali-m-khaki. *(Cited on pages XI and 15)*

[51] "FBI to install nationwide facial recognition system," http://nation.foxnews.com/fbi/2012/09/10/fbi-install-nationwide-facial-recognition-system. *(Cited on pages XI, XII, 15, and 43)*

[52] L. qing Zhu, "2D finger shape recognition based on local zero-order moment features," in *Proceedings of the 2nd International Congress on Image and Signal Processing (CISP)*, 2009, pp. 1–4. *(Cited on page 14)*

[53] H.-S. Kim and B. Bae, "Finger pattern identification for authentication purpose," in *Proceedings of the IEEE International Symposium on Industrial Electronics (ISIE)*, 2009, pp. 1674–1678. *(Cited on page 14)*

[54] D. L. Woodard and P. J. Flynn, "3D finger biometrics," in *Biometric Authentication*, ser. Lecture Notes in Computer Science, D. Maltoni and A. K. Jain, Eds. Springer Berlin Heidelberg, 2004, vol. 3087, pp. 238–247. *(Cited on page 14)*

[55] S. Malassiotis, N. Aifanti, and M. G. Strintzis, "Personal authentication using 3-D finger geometry," *IEEE Transactions on Information Forensics and Security*, vol. 1, no. 1, pp. 12–21, 2006. *(Cited on pages 14, 29, and 40)*

[56] A. Kumar and C. Ravikanth, "Personal authentication using finger knuckle surface," *IEEE Transactions on Information Forensics and Security*, vol. 4, no. 1, pp. 98–110, 2009. *(Cited on page 14)*

[57] K. Cheng and A. Kumar, "Contactless finger knuckle identification using smartphones," in *BIOSIG*, A. Brömme and C. Busch, Eds. IEEE, 2012, pp. 1–6. *(Cited on page 14)*

[58] Crossmatch, "L SCAN©1000PX," http://www.crossmatch.com/l-scan-1000px.php. *(Cited on pages XI, XIII, 16, 53, 57, 61, and 65)*

[59] "Epson perfection V33," http://www.epson.com.sg/epson_singapore/scanners/product.page?product_name=Epson_Perfection_V33. *(Cited on pages XI, XIII, 16, and 58)*

[60] Signal and Image Processing Lab, Technion, Israeli Institute of Technology, "Palmprint recognition," http://sipl.technion.ac.il/Info/News&Events_1_e.php?id=465. *(Cited on pages XI, XIII, 16, and 62)*

[61] FD, "Warwick palm reader 2000," http://www.fd.com.my/products/PalmReader/warwick.htm. *(Cited on pages XI and 16)*

[62] A. Ross and A. Abaza, "Human ear recognition," *Computer*, vol. 44, no. 11, pp. 79–81, 2011. *(Cited on pages XI and 17)*

[63] M. Sadowitz, S. Latifi, and D. Walker, "An overview of iris and retina scans and their fusion in a biometric system," in *Proceedings of the International Conference on Image Processing, Computer Vision and Pattern Recognition (IPCV)*, 2008, pp. 119–123. *(Cited on page 15)*

[64] S.-Y. Cho, L. Wang, and W. J. Ong, "Thermal imprint feature analysis for face recognition," in *Proceedings of the IEEE International Symposium on Industrial Electronics (ISIE)*, 2009, pp. 1875–1880. *(Cited on page 15)*

[65] K. Niinuma, U. Park, and A. K. Jain, "Soft biometric traits for continuous user authentication," *IEEE Transactions on Information Forensics and Security*, vol. 5, no. 4, pp. 771–780, 2010. *(Cited on pages 17 and 47)*

[66] A. Azzini, S. Marrara, R. Sassi, and F. Scotti, "A fuzzy approach to multimodal biometric continuous authentication," *Fuzzy Optimization and Decision Making*, vol. 7, no. 3, pp. 215–302, November 2008. *(Cited on pages 17 and 29)*

[67] S. Cimato, M. Gamassi, V. Piuri, D. Sana, R. Sassi, and F. Scotti, "Personal identification and verification using multimodal biometric data," in *Proceedings of the 2006 IEEE International Conference on Computational Intelligence for Homeland Security and Personal Safety (CIHSPS)*, Alexandria, VA, USA, October 2006, pp. 41–45. *(Cited on pages 17 and 29)*

[68] M. Gamassi, V. Piuri, D. Sana, O. Scotti, and F. Scotti, "A multi-modal multi-paradigm agent-based approach to design scalable distributed biometric systems," in *Proceedings of the 2005 IEEE International Conference on Computational Intelligence for Homeland Security and Personal Safety (CIHSPS)*, Orlando, FL, USA, April 2005, pp. 65–70. *(Cited on page 17)*

[69] M. Theofanos, B. Stanton, C. Sheppard, R. Micheals, N. Zhang, W. Wydler, L. Nadel, and R. Rubin, "Usability Testing of Height and Angles of Ten-Print Fingerprint Capture," NISTIR, Tech. Rep., Jun. 2008. *(Cited on page 19)*

[70] M. El-Abed, R. Giot, B. Hemery, and C. Rosenberger, "A study of users' acceptance and satisfaction of biometric systems," in *Proceedings of the IEEE International Carnahan Conference on Security Technology*, October 2010, pp. 170–178. *(Cited on page 19)*

[71] R. Ryan, "The importance of biometric standards," *Biometric Technology Today*, vol. 2009, no. 7, pp. 7–10, 2009. *(Cited on page 19)*

[72] "The first ICB competition on iris recognition (ICIR 2013)," 2013, http://iris.idealtest.org/2013/ICIR2013.jsp. *(Cited on page 20)*

[73] T. Mansfield, G. Kelly, D. Chandler, and J. Kane, "Biometric Product Testing Final Report V1.0," *Contract*, vol. 92, 2001. *(Cited on pages 20 and 187)*

[74] P. Flynn, "Voice biometrics," in *Handbook of Biometrics*, A. K. Jain, P. Flynn, and A. A. Ross, Eds. Springer US, 2008, pp. 529–548. *(Cited on page 20)*

[75] A. K. Jain, R. M. Bolle, and S. Pankanti, *Biometrics: Personal Identification in Networked Society*, ser. The Kluwer international series in engineering and computer science. Kluwer Academic Publishers, 1999. *(Cited on page 21)*

[76] M. Gamassi, M. Lazzaroni, M. Misino, V. Piuri, D. Sana, and F. Scotti, "Quality assessment of biometric systems: a comprehensive perspective based on accuracy and performance measurement," *IEEE Transactions on Instrumentation and Measurement*, vol. 54, no. 4, pp. 1489–1496, August 2005. *(Cited on page 21)*

[77] J. L. Wayman, A. K. Jain, D. Maltoni, and D. Maio, *Biometric Systems: Technology, Design and Performance Evaluation*. Springer-Verlag London Limited, 2005. *(Cited on page 21)*

[78] V. Piuri and F. Scotti, "Fingerprint biometrics via low-cost sensors and webcams," in *Proceedings of the 2008 IEEE International Conference on Biometrics: Theory, Applications and Systems (BTAS)*, Washington, D.C., USA, October 2008, pp. 1–6. *(Cited on pages XII, 24, and 37)*

[79] R. Donida Labati, A. Genovese, V. Piuri, and F. Scotti, "Contactless fingerprint recognition: a neural approach for perspective and rotation effects reduction," in *Proceedings of the IEEE Workshop on Computational Intelligence in Biometrics and Identity Management (CIBIM)*, Singapore, Singapore, April 2013. *(Cited on pages XII, 24, 37, 115, and 124)*

[80] A. J. Mansfield and J. L. Wayman, *Best Practices in Testing and Reporting Performance of Biometric Devices: Version 2.01*, ser. NPL report. Centre for Mathematics and Scientific Computing, National Physical Laboratory, 2002. *(Cited on pages 25, 26, and 187)*

[81] T. A. Louis, "Confidence intervals for a binomial parameter after observing no successes," *The American Statistician*, vol. 35, no. 3, pp. 154–154, 1981. *(Cited on page 25)*

[82] B. D. Jovanovic and P. S. Levy, "A look at the rule of three," *The American Statistician*, vol. 51, no. 2, pp. 137–139, 1997. *(Cited on page 25)*

[83] G. R. Doddington, M. A. Przybocki, A. F. Martin, and D. A. Reynolds, "The NIST speaker recognition evaluation - overview, methodology, systems, results, perspective," *Speech Communication*, vol. 31, no. 2-3, pp. 225–254, 2000. *(Cited on page 25)*

[84] G. W. Snedecor and W. G. Cochran, *Statistical Methods, Seventh Edition*. Iowa State University, 1980. *(Cited on page 26)*

[85] R. M. Bolle, N. K. Ratha, and S. Pankanti, "Confidence interval measurement in performance analysis of biometrics systems using the bootstrap," in *Proceedings of the IEEE Workshop on Empirical Evaluation Methods in Computer Vision*, 2001. *(Cited on page 26)*

[86] N. Poh and S. Bengio, "Estimating the confidence interval of expected performance curve in biometric authentication using joint bootstrap," in *Proceedings of the IEEE International Conference on Acoustics, Speech and Signal Processing*, vol. 2, April 2007, pp. 137–140. *(Cited on page 26)*

[87] R. Li, D. Tang, W. Li, and D. Zhang, "Second-level partition for estimating FAR confidence intervals in biometric systems," in *Computer Analysis of Images and Patterns*, ser. Lecture Notes in Computer Science, X. Jiang and N. Petkov, Eds. Springer Berlin Heidelberg, 2009, vol. 5702, pp. 58–65. *(Cited on page 26)*

[88] R. Li, B. Huang, R. Li, and W. Li, "Test sample size determination for biometric systems based on confidence elasticity," in *Proceedings of the International Joint Conference on Neural Networks (IJCNN)*, June 2012, pp. 1–7. *(Cited on page 26)*

[89] R. M. Bolle, N. K. Ratha, and S. Pankanti, "Error analysis of pattern recognition systems - the subsets bootstrap," *Computer Vision and Image Understanding*, vol. 93, no. 1, pp. 1–33, 2004. *(Cited on page 26)*

[90] S. C. Dass, Y. Zhu, and A. K. Jain, "Validating a biometric authentication system: Sample size requirements," *IEEE Transactions on Pattern Analysis and Machine Intelligence*, vol. 28, no. 12, pp. 1902–1319, December 2006. *(Cited on page 26)*

[91] N. Poh, A. Martin, and S. Bengio, "Performance generalization in biometric authentication using joint user-specific and sample bootstraps," *IEEE Transactions*

on Pattern Analysis and Machine Intelligence, vol. 29, no. 3, pp. 492–498, March 2007. *(Cited on page 27)*

[92] S. Cimato, R. Sassi, and F. Scotti, "Biometrics and privacy," *Recent Patents on Computer Science*, vol. 1, pp. 98–109, June 2008. *(Cited on page 27)*

[93] S. Cimato, M. U. de Las Palmas de Gran Canaria, V. Piuri, R. Sassi, and F. Scotti, *Privacy in biometrics*, ser. IEEE Press Series on Computational Intelligence, N. V. Boulgouris, K. N. Plataniotis, and E. Micheli-Tzanakou, Eds. Wiley-IEEE Press, 2009. *(Cited on page 27)*

[94] S. Cimato, M. Gamassi, V. Piuri, R. Sassi, and F. Scotti, *Privacy Issues in Biometric Identification*, ser. Touch Briefings. Business Briefings LtD, 2006. *(Cited on page 27)*

[95] S. Cimato, R. Sassi, and F. Scotti, "Biometric privacy," in *Encyclopedia of Cryptography and Security (2nd ed.)*, H. C. A. van Tilborg and S. Jajodia, Eds. Springer, 2011, pp. 101–104. *(Cited on page 27)*

[96] International Biometric Group, "Bioprivacy initiative," 2003, http://www.bioprivacy.org/. *(Cited on page 28)*

[97] W. Li, D. Zhang, G. Lu, and N. Luo, "A novel 3-D palmprint acquisition system," *IEEE Transactions on Systems, Man and Cybernetics, Part A: Systems and Humans*, vol. 42, no. 2, pp. 443–452, 2012. *(Cited on pages 29, 30, 59, 82, 83, 84, 195, 196, and 204)*

[98] Y. Wang, L. G. Hassebrook, and D. L. Lau, "Noncontact, depth-detailed 3D fingerprinting," *SPIE Newsroom*, November 2009. *(Cited on pages 29, 30, and 37)*

[99] V. Kanhangad, A. Kumar, and D. Zhang, "Combining 2D and 3D hand geometry features for biometric verification," in *Proceedings of the IEEE Computer Society Conference on Computer Vision and Pattern Recognition Workshops (CVPR)*, 2009, pp. 39–44. *(Cited on pages XII, 29, and 40)*

[100] ——, "A unified framework for contactless hand verification," *IEEE Transactions on Information Forensics and Security*, vol. 6, no. 3, pp. 1014–1027, 2011. *(Cited on pages XII, XIII, 29, 30, 40, 59, 60, 61, and 195)*

[101] H. Drira, B. Ben Amor, A. Srivastava, M. Daoudi, and R. Slama, "3D face recognition under expressions, occlusions, and pose variations," *IEEE Transactions on Pattern Analysis and Machine Intelligence*, vol. 35, no. 9, pp. 2270–2283, 2013. *(Cited on pages 29 and 30)*

[102] R. Donida Labati, A. Genovese, V. Piuri, and F. Scotti, "Fast 3-D fingertip reconstruction using a single two-view structured light acquisition," in *Proceedings of the 2011 IEEE Workshop on Biometric Measurements and Systems for Security and Medical Applications (BioMS)*, September 2011, pp. 1–8. *(Cited on pages XII, 29, 37, 38, 117, 121, 124, and 125)*

[103] R. Donida Labati, "Contactless fingerprint biometrics: Acquisition, processing, and privacy protection," Ph.D. dissertation, Università degli Studi di Milano, 2013. *(Cited on pages XII, 29, 30, 36, 37, 38, and 110)*

[104] R. Cappelli, M. Ferrara, and D. Maltoni, "Minutia Cylinder-Code: A new representation and matching technique for fingerprint recognition," *IEEE Transactions on Pattern Analysis and Machine Intelligence*, vol. 32, no. 12, pp. 2128–2141, 2010. *(Cited on page 29)*

[105] R. Cappelli, M. Ferrara, and D. Maio, "A fast and accurate palmprint recognition system based on minutiae," *IEEE Transactions on Systems, Man, and Cybernetics, Part B: Cybernetics*, vol. 42, no. 3, pp. 956–962, 2012. *(Cited on pages 29, 65, 71, 72, 77, and 204)*

[106] W. Li, D. Zhang, D. Zhang, G. Lu, and J. Yan, "3-D palmprint recognition with joint line and orientation features," *IEEE Transactions on Systems, Man, and Cybernetics, Part C: Applications and Reviews*, vol. 41, no. 2, pp. 274–279, 2011. *(Cited on pages 29, 82, 83, and 84)*

[107] Y. Si, J. Mei, and H. Gao, "Novel approaches to improve robustness, accuracy and rapidity of iris recognition systems," *IEEE Transactions on Industrial Informatics*, vol. 8, no. 1, pp. 110–117, 2012. *(Cited on page 29)*

[108] R. Donida Labati and F. Scotti, "Noisy iris segmentation with boundary regularization and reflections removal," *Image and Vision Computing, Iris Images Segmentation Special Issue*, vol. 28, no. 2, pp. 270–277, February 2010. *(Cited on pages 29 and 43)*

[109] R. Donida Labati, V. Piuri, and F. Scotti, "Agent-based image iris segmentation and multiple views boundary refining," in *Proceedings of the IEEE Third International Conference on Biometrics: Theory, Applications and Systems (BTAS)*, November 2009, pp. 1–7. *(Cited on page 29)*

[110] R. Donida Labati, V. Piuri, and F. Scotti, "Neural-based iterative approach for iris detection in iris recognition systems," in *Proceedings of the IEEE Symposium on Computational Intelligence for Security and Defence Applications*, December 2009, pp. 1–6. *(Cited on page 29)*

[111] K. W. Bowyer, "The results of the NICE.II iris biometrics competition," *Pattern Recognition Letters*, vol. 33, no. 8, pp. 965–969, June 2012. *(Cited on pages 29 and 44)*

[112] B. Kamgar-Parsi, W. Lawson, and B. Kamgar-Parsi, "Toward development of a face recognition system for watchlist surveillance," *IEEE Transactions on Pattern Analysis and Machine Intelligence*, vol. 33, no. 10, pp. 1925–1937, October 2011. *(Cited on pages 29 and 42)*

[113] J. R. Matey, O. Naroditsky, K. Hanna, R. Kolczynski, D. J. LoIacono, S. Mangru, M. Tinker, T. M. Zappia, and W. Y. Zhao, "Iris on the move: Acquisition of images for iris recognition in less constrained environments," *Proceedings of the IEEE*, vol. 94, no. 11, pp. 1936–1947, November 2006. *(Cited on pages XII, 30, 45, and 46)*

[114] M. Theofanos, B. Stanton, C. Sheppard, R. Micheals, N. Zhang, W. Wydler, L. Nadel, and R. Rubin, "Usability testing of height and angles of ten-print fingerprint capture," NISTIR, June 2008. *(Cited on pages 30, 197, and 198)*

[115] M. El-Abed, R. Giot, B. Hemery, and C. Rosenberger, "A study of users' acceptance and satisfaction of biometric systems," in *Proceedings of the IEEE International Carnahan Conference on Security Technology*, October 2010, pp. 170–178. *(Cited on pages 30 and 200)*

[116] D. Zhang and G. Lu, *3D Biometrics*. Springer Science + Business Media, New York, 2013. *(Cited on page 30)*

[117] A. Scheenstra, A. Ruifrok, and R. C. Veltkamp, "A survey of 3D face recognition methods," in *Lecture Notes in Computer Science*. SpringerVerlag, 2005, pp. 891–899. *(Cited on pages 30 and 41)*

[118] A. Adler, "Biometric system security," in *Handbook of Biometrics*, A. K. Jain, P. Flynn, and A. A. Ross, Eds. Springer US, 2008, pp. 381–402. *(Cited on page 30)*

[119] R. Donida Labati, V. Piuri, and F. Scotti, "Biometric privacy protection: Guidelines and technologies," in *E-Business and Telecommunications*, ser. Communications in Computer and Information Science, M. S. Obaidat, J. L. Sevillano, and J. Filipe, Eds. Springer Berlin Heidelberg, 2012, vol. 314, pp. 3–19. *(Cited on page 30)*

[120] K. N. Plataniotis, D. Hatzinakos, and J. K. M. Lee, "ECG biometric recognition without fiducial detection," in *Proceedings of the Biometrics Symposium: Special Session on Research at the Biometric Consortium Conference*, August 2006, pp. 1–6. *(Cited on page 30)*

[121] R. Donida Labati, R. Sassi, and F. Scotti, "ECG biometric recognition: Permanence analysis of QRS signals for 24 hours continuous authentication," in *Proceedings of the IEEE International Workshop on Information Forensics and Security (WIFS)*, Guangzhou, China, 11 2013. *(Cited on page 30)*

[122] A. Bonissi, R. Donida Labati, L. Perico, R. Sassi, F. Scotti, and L. Sparagino, "A preliminary study on continuous authentication methods for photoplethysmographic biometrics," in *Proceedings of the 2013 IEEE Workshop on Biometric Measurements and Systems for Security and Medical Applications (BioMS)*, September 2013, pp. 28–33. *(Cited on page 30)*

[123] M. Tistarelli, S. Z. Li, and R. Chellappa, *Handbook of Remote Biometrics: for Surveillance and Security*, 1st ed. Springer Publishing Company, Incorporated, 2009. *(Cited on pages 34 and 35)*

[124] F. Han, J. Hu, M. Alkhathami, and K. Xi, "Compatibility of photographed images with touch-based fingerprint verification software," in *Proceedings of the 2011 6th IEEE Conference on Industrial Electronics and Applications (ICIEA)*, 2011, pp. 1034–1039. *(Cited on pages XII and 35)*

[125] J. Doublet, M. Revenu, and O. Lepetit, "Robust grayscale distribution estimation for contactless palmprint recognition," in *Proceedings of the First IEEE International Conference on Biometrics: Theory, Applications, and Systems (BTAS)*, 2007, pp. 1–6. *(Cited on pages XII and 35)*

[126] G. K. O. Michael, T. Connie, L. S. Hoe, and A. T. B. Jin, "Locating geometrical descriptors for hand biometrics in a contactless environment," in *Proceedings of the 2010 International Symposium in Information Technology (ITSim)*, vol. 1, 2010, pp. 1–6. *(Cited on pages XII, 35, and 40)*

[127] I. Fujitsu, "PalmSecure-SL," 2012, http://pr.fujitsu.com/en/news/2003/03/31.html. *(Cited on pages XII, 35, 36, 38, and 39)*

[128] H. Proença, E. Y. Du, and J. Scharcanski, "Introduction to the special issue on unconstrained biometrics: advances and trends," *Signal, Image and Video Processing*, vol. 5, no. 4, pp. 399–400, 2011. *(Cited on page 35)*

[129] G. Parziale and Y. Chen, "Advanced technologies for touchless fingerprint recognition," *Handbook of Remote Biometrics*, pp. 83–109, 2009. *(Cited on pages 36 and 37)*

[130] A. Morales, M. A. Ferrer, and A. Kumar, "Towards contactless palmprint authentication," *IET Computer Vision*, vol. 5, no. 6, pp. 407–416, 2011. *(Cited on pages 36, 91, 97, 100, and 204)*

[131] G. K. O. Michael, T. Connie, and A. B. J. Teoh, "A contactless biometric system using palm print and palm vein features," in *Advanced Biometric Technologies*, D. G. Chetty, Ed., 2011. *(Cited on pages XII, XVI, 36, 37, 38, 39, 94, 97, and 99)*

[132] A. Santos Sierra, C. Sánchez-Àvila, A. Mendaza Ormaza, and J. Guerra Casanova, "An approach to hand biometrics in mobile devices," *Signal, Image and Video Processing*, vol. 5, no. 4, pp. 469–475, 2011. *(Cited on pages 36 and 40)*

[133] J. R. Matey and L. R. Kennell, "Iris recognition - beyond one meter," in *Handbook of Remote Biometrics*, ser. Advances in Pattern Recognition, M. Tistarelli, S. Z. Li, and R. Chellappa, Eds. Springer London, 2009, pp. 23–59. *(Cited on page 36)*

[134] M. Ao, D. Yi, Z. Lei, and S. Z. Li, "Face recognition at a distance: System issues," in *Handbook of Remote Biometrics*, ser. Advances in Pattern Recognition, M. Tistarelli, S. Li, and R. Chellappa, Eds. Springer London, 2009, pp. 155–167. *(Cited on pages XII, 36, and 41)*

[135] R. D. Seely, M. Goffredo, J. N. Carter, and M. S. Nixon, "View invariant gait recognition," in *Handbook of Remote Biometrics*, ser. Advances in Pattern Recognition, M. Tistarelli, S. Z. Li, and R. Chellappa, Eds. Springer London, 2009, pp. 61–81. *(Cited on pages XII, 36, and 46)*

[136] J. D. Bustard and M. S. Nixon, "Toward unconstrained ear recognition from two-dimensional images," *IEEE Transactions on Systems, Man and Cybernetics, Part A: Systems and Humans*, vol. 40, no. 3, pp. 486–494, May 2010. *(Cited on pages XII, 36, and 46)*

[137] R. Donida Labati, A. Genovese, V. Piuri, and F. Scotti, "Touchless fingerprint biometrics: a survey on 2D and 3D technologies," *Journal of Internet Technology*, 2014, to appear. *(Cited on page 36)*

[138] M. O. Derawi, B. Yang, and C. Busch, "Fingerprint recognition with embedded cameras on mobile phones," in *Security and Privacy in Mobile Information and Communication Systems*, ser. Lecture Notes of the Institute for Computer Sciences, Social Informatics and Telecommunications Engineering, R. Prasad, K. Farkas, A. U. Schmidt, A. Lioy, G. Russello, and F. L. Luccio, Eds. Springer Berlin Heidelberg, 2012, vol. 94, pp. 136–147. *(Cited on page 37)*

[139] F. Han, J. Hu, M. Alkhathami, and K. Xi, "Compatibility of photographed images with touch-based fingerprint verification software," in *Proceedings of the 2011 6th IEEE Conference on Industrial Electronics and Applications (ICIEA)*, 2011, pp. 1034–1039. *(Cited on page 37)*

[140] B. Y. Hiew, A. B. J. Teoh, and D. C. L. Ngo, "Automatic digital camera based fingerprint image preprocessing," in *Proceedings of the 2006 International Conference on Computer Graphics, Imaging and Visualisation*, 2006, pp. 182–189. *(Cited on page 37)*

[141] B. Y. Hiew, A. B. J. Teoh, and Y. H. Pang, "Digital camera based fingerprint recognition," in *Proceedings of the IEEE International Conference on Telecommunications and Malaysia International Conference on Communications (ICT-MICC)*, 2007, pp. 676–681. *(Cited on page 37)*

[142] B. Y. Hiew, A. B. J. Teoh, and D. C. L. Ngo, "Preprocessing of fingerprint images captured with a digital camera," in *Proceedings of the 9th International Conference on Control, Automation, Robotics and Vision (ICARCV)*, 2006, pp. 1–6. *(Cited on page 37)*

[143] Y. Song, C. Lee, and J. Kim, "A new scheme for touchless fingerprint recognition system," in *Proceedings of 2004 International Symposium on Intelligent Signal Processing and Communication Systems (ISPACS)*, 2004, pp. 524–527. *(Cited on page 37)*

[144] C. Lee, S. Lee, and J. Kim, "A study of touchless fingerprint recognition system," in *Structural, Syntactic, and Statistical Pattern Recognition*, ser. Lecture Notes in Computer Science, D.-Y. Yeung, J. T. Kwok, A. Fred, F. Roli, and D. Ridder, Eds. Springer Berlin Heidelberg, 2006, vol. 4109, pp. 358–365. *(Cited on page 37)*

[145] R. Donida Labati, V. Piuri, and F. Scotti, "A neural-based minutiae pair identification method for touch-less fingerprint images," in *Proceedings of the 2011 IEEE Workshop on Computational Intelligence in Biometrics and Identity Management (CIBIM)*, 2011, pp. 96–102. *(Cited on page 37)*

[146] ——, "Neural-based quality measurement of fingerprint images in contactless biometric systems," in *Proceedings of the 2010 International Joint Conference on Neural Networks (IJCNN)*, 2010, pp. 1–8. *(Cited on page 37)*

[147] R. Donida Labati, A. Genovese, V. Piuri, and F. Scotti, "Measurement of the principal singular point in contact and contactless fingerprint images by using computational intelligence techniques," in *Proceedings of the 2010 IEEE International Conference on Computational Intelligence for Measurement Systems and Applications (CIMSA)*, 2010, pp. 18–23. *(Cited on pages 37 and 114)*

[148] H. Choi, K. Choi, and J. Kim, "Mosaicing touchless and mirror-reflected fingerprint images," *IEEE Transactions on Information Forensics and Security*, vol. 5, no. 1, pp. 52–61, 2010. *(Cited on page 37)*

[149] L. Wang, R. H. A. El-Maksoud, J. M. Sasian, W. P. Kuhn, K. Gee, and V. S. Valencia, "A novel contactless aliveness-testing (CAT) fingerprint sensor," in *Novel Optical Systems Design and Optimization XII*, R. J. Koshel and G. G. Gregory, Eds., vol. 7429, no. 1. SPIE, 2009. *(Cited on page 37)*

[150] G. Parziale, E. Diaz-Santana, and R. Hauke, "The surround imager: A multi-camera touchless device to acquire 3D rolled-equivalent fingerprints." in *Proceedings of the International Conference of Biometrics (ICB)*, 2006, pp. 244–250. *(Cited on pages XII, 37, and 38)*

[151] G. Paar, M. d. Perucha, A. Bauer, and B. Nauschnegg, "Photogrammetric fingerprint unwrapping," *Journal of Applied Geodesy*, vol. 2, pp. 13–20, 2008. *(Cited on page 37)*

[152] X. Pang, Z. Song, and W. Xie, "Extraction of valley-ridge lines from the point cloud-based 3D fingerprint model," *IEEE Computer Graphics and Applications*, 2012. *(Cited on page 37)*

[153] Y. Wang, L. G. Hassebrook, and D. L. Lau, "Data acquisition and processing of 3-D fingerprints," *IEEE Transactions on Information Forensics and Security*, vol. 5, no. 4, pp. 750–760, December 2010. *(Cited on pages XII, 37, 38, and 121)*

[154] D. Koller, L. Walchshäusl, G. Eggers, F. Neudel, U. Kursawe, P. Kühmstedt, M. Heinze, R. Ramm, C. Bräuer-Burchardt, G. Notni, R. Kafka, R. Neubert, H. Seibert, M. C. Neves, and A. Nouak, "3D capturing of fingerprints - on the way to a contactless certified sensor," in *BIOSIG*, 2011, pp. 33–44. *(Cited on page 37)*

[155] F. Han, J. Hu, M. Alkhathami, and K. Xi, "Compatibility of photographed images with touch-based fingerprint verification software," in *Proceedings of the IEEE Conference on Industrial Electronics and Applications*, June 2011, pp. 1034–1039. *(Cited on page 37)*

[156] Y. Wang, D. L. Lau, and L. G. Hassebrook, "Fit-sphere unwrapping and performance analysis of 3d fingerprints," *Applied Optics*, vol. 49, no. 4, pp. 592–600, February 2010. *(Cited on page 37)*

[157] S. Shafaei, T. Inanc, and L. G. Hassebrook, "A new approach to unwrap a 3-D fingerprint to a 2-D rolled equivalent fingerprint," in *Proceedings of the IEEE 3rd*

International Conference on Biometrics: Theory, Applications, and Systems, September 2009, pp. 1–5. *(Cited on page 37)*

[158] Q. Zhao, A. K. Jain, and G. Abramovich, "3D to 2D fingerprints: Unrolling and distortion correction," in *Proceedings of the 2011 International Joint Conference on Biometrics (IJCB)*, October 2011, pp. 1–8. *(Cited on page 37)*

[159] A. Pillai and S. Mil'shtein, "Can contactless fingerprints be compared to existing database?" in *Proceedings of the 2012 IEEE Conference on Technologies for Homeland Security (HST)*, 2012, pp. 390–394. *(Cited on page 37)*

[160] B. Y. Hiew, A. B. J. Teoh, and D. C. L. Ngo, "Automatic digital camera based fingerprint image preprocessing," in *Proceedings of the International Conference on Computer Graphics, Imaging and Visualisation*, July 2006, pp. 182–189. *(Cited on page 37)*

[161] B. Y. Hiew, B. J. Andrew, and Y. H. Pang, "Digital camera based fingerprint recognition," in *Proceedings of the IEEE International Conference on Telecommunications and Malaysia International Conference on Communications*, May 2007, pp. 676–681. *(Cited on page 37)*

[162] B. Y. Hiew, A. B. J. Teoh, and D. C. L. Ngo, "Preprocessing of fingerprint images captured with a digital camera," in *Proceedings of the International Conference on Control, Automation, Robotics and Vision*, December 2006, pp. 1–6. *(Cited on page 37)*

[163] C. Lee, S. Lee, J. Kim, and S.-J. Kim, "Preprocessing of a fingerprint image captured with a mobile camera," in *Advances in Biometrics*, ser. Lecture Notes in Computer Science, D. Zhang and A. K. Jain, Eds. Springer Berlin / Heidelberg, 2005, vol. 3832, pp. 348–355. *(Cited on page 37)*

[164] G. K. O. Michael, T. Connie, and A. T. B. Jin, "Design and implementation of a contactless palm print and palm vein sensor," in *Proceedings of the 2010 11th International Conference on Control Automation Robotics Vision (ICARCV)*, 2010, pp. 1268–1273. *(Cited on page 38)*

[165] Y. Hao, Z. Sun, T. Tan, and C. Ren, "Multispectral palm image fusion for accurate contact-free palmprint recognition," in *Proceedings of the 15th IEEE International Conference on Image Processing (ICIP)*, 2008, pp. 281–284. *(Cited on pages 38 and 95)*

[166] Y. Zhou and A. Kumar, "Contactless palm vein identification using multiple representations," in *Proceedings of the 2010 Fourth IEEE International Conference on Biometrics: Theory Applications and Systems (BTAS)*, 2010, pp. 1–6. *(Cited on page 38)*

[167] ——, "Human identification using palm-vein images," *IEEE Transactions on Information Forensics and Security*, vol. 6, no. 4, pp. 1259–1274, 2011. *(Cited on page 38)*

[168] V. Kanhangad, A. Kumar, and D. Zhang, "Contactless and pose invariant biometric identification using hand surface," *IEEE Transactions on Image Processing*, vol. 20, no. 5, pp. 1415–1424, 2011. *(Cited on pages XII, 39, and 40)*

[169] R. Sanchez-Reillo, C. Sanchez-Avila, and A. Gonzalez-Marcos, "Biometric identification through hand geometry measurements," *IEEE Transactions on Pattern Analysis and Machine Intelligence*, vol. 22, no. 10, pp. 1168–1171, October 2000. *(Cited on page 39)*

[170] A. K. Jain, A. A. Ross, and S. Pankanti, "A prototype hand geometry-based verification system," in *Proceedings of the 2nd Int'l Conference on Audio- and Video-based Biometric Person Authentication, Washington D.C.*, 1999. *(Cited on page 39)*

[171] W. Xiong, K.-A. Toh, W.-Y. Yau, and X. Jiang, "Model-guided deformable hand shape recognition without positioning aids," *Pattern Recognition*, vol. 38, no. 10, pp. 1651–1664, 2005. *(Cited on page 39)*

[172] A. Morales, M. A. Ferrer, F. DÃaz, J. B. Alonso, and C. M. Travieso, "Contact-free hand biometric system for real environments," in *Proceedings of the 16th European Signal Processing Conference, Laussane, Switzerland*, September 2008. *(Cited on page 40)*

[173] W. Bu, Q. Zhao, X. Wu, Y. Tang, and K. Wang, "A novel contactless multimodal biometric system based on multiple hand features," in *Proceedings of the 2011 International Conference on Hand-Based Biometrics (ICHB)*, 2011, pp. 1–6. *(Cited on page 40)*

[174] C. Xin, X. Wu, Z. Qiushi, and T. Youbao, "A contactless hand shape identification system," in *Proceedings of the 2011 3rd International Conference on Advanced Computer Control (ICACC)*, 2011, pp. 561–565. *(Cited on page 40)*

[175] J. Doublet, O. Lepetit, and M. Revenu, "Contactless hand recognition based on distribution estimation," in *Proceedings of the Biometrics Symposium, 2007*, 2007, pp. 1–6. *(Cited on page 40)*

[176] M. A. Ferrer, F. Vargas, and A. Morales, "BiSpectral contactless hand based biometric system," in *Proceedings of the 2011 2nd National Conference on Telecommunications (CONATEL)*, 2011, pp. 1–6. *(Cited on page 40)*

[177] A. Morales, M. A. Ferrer, J. B. Alonso, and C. M. Travieso, "Comparing infrared and visible illumination for contactless hand based biometric scheme," in *Proceedings of the 42nd Annual IEEE International Carnahan Conference on Security Technology (ICCST)*, 2008, pp. 191–197. *(Cited on page 40)*

[178] F. Tsalakanidou, S. Malassiotis, and M. G. Strintzis, "A 3D face and hand biometric system for robust user-friendly authentication," *Pattern Recognition Letters*, vol. 28, no. 16, pp. 2238–2249, 2007. *(Cited on page 40)*

[179] S. K. Zhou, R. Chellappa, and W. Zhao, *Unconstrained Face Recognition*, ser. International Series on Biometrics. Boston, MA: Springer US, 2006. *(Cited on page 41)*

[180] M. Turk and A. Pentland, "Eigenfaces for recognition," *Journal of Cognitive Neuroscience*, vol. 3, no. 1, pp. 71–86, January 1991. *(Cited on page 41)*

[181] R. Basri and D. W. Jacobs, "Lambertian reflectance and linear subspaces," *IEEE Transactions on Pattern Analysis and Machine Intelligence*, vol. 25, no. 2, pp. 218–233, February 2003. *(Cited on page 41)*

[182] J. J. Atick, P. A. Griffin, and A. N. Redlich, "Statistical approach to shape from shading: Reconstruction of three-dimensional face surfaces from single two-dimensional images," *Neural Computation*, vol. 8, no. 6, pp. 1321–1340, August 1996. *(Cited on page 41)*

[183] V. Blanz and T. Vetter, "Face recognition based on fitting a 3D morphable model," *IEEE Transactions on Pattern Analysis and Machine Intelligence*, vol. 25, no. 9, pp. 1063–1074, September 2003. *(Cited on page 41)*

[184] X. Zhang and Y. Gao, "Face recognition across pose: A review," *Pattern Recognition*, vol. 42, no. 11, pp. 2876–2896, 2009. *(Cited on page 41)*

[185] U. Park, Y. Tong, and A. K. Jain, "Age-invariant face recognition," *IEEE Transactions on Pattern Analysis and Machine Intelligence*, vol. 32, no. 5, pp. 947–954, May 2010. *(Cited on page 41)*

[186] H. Ling, S. Soatto, N. Ramanathan, and D. W. Jacobs, "Face verification across age progression using discriminative methods," *IEEE Transactions on Information Forensics and Security*, vol. 5, no. 1, pp. 82–91, March 2010. *(Cited on page 41)*

[187] S. Zhou, V. Krueger, and R. Chellappa, "Probabilistic recognition of human faces from video," *Computer Vision and Image Understanding*, vol. 91, no. 1-2, pp. 214–245, 2003. *(Cited on page 42)*

[188] F. W. Wheeler, R. L. Weiss, and P. H. Tu, "Face recognition at a distance system for surveillance applications," in *Proceedings of the Fourth IEEE International Conference on Biometrics: Theory Applications and Systems (BTAS)*, September 2010, pp. 1–8. *(Cited on page 42)*

[189] J. Y. Choi, W. De Neve, and Y. M. Ro, "Towards an automatic face indexing system for actor-based video services in an iptv environment," *IEEE Transactions on Consumer Electronics*, vol. 56, no. 1, pp. 147–155, February 2010. *(Cited on page 42)*

[190] B. Chen, J. Shen, and H. Sun, "A fast face recognition system on mobile phone," in *Proceedings of the International Conference on Systems and Informatics*, May 2012, pp. 1783–1786. *(Cited on page 42)*

[191] A. Pentland and T. Choudhury, "Face recognition for smart environments," *Computer*, vol. 33, no. 2, pp. 50–55, February 2000. *(Cited on page 42)*

[192] T. Leyvand, C. Meekhof, Y.-C. Wei, J. Sun, and B. Guo, "Kinect identity: Technology and experience," *Computer*, vol. 44, no. 4, pp. 94–96, April 2011. *(Cited on page 42)*

[193] "Okao vision face recognition sensor," http://asia.cnet.com/okao-vision-face-recognition-sensor-62100202.htm. *(Cited on pages XII and 43)*

[194] "Kinect-powered motion capture mimics your facial movements in real time," http://www.theverge.com/2012/11/17/3658966/watch-this-faceshift-motion-capture-kinect. *(Cited on pages XII and 43)*

[195] H. Proença, "Iris recognition: On the segmentation of degraded images acquired in the visible wavelength," *IEEE Transaction on Pattern Analysis and Machine Intelligence*, vol. 32, no. 8, pp. 1502–1516, August 2010. *(Cited on page 43)*

[196] S. Shah and A. Ross, "Iris segmentation using geodesic active contours," *IEEE Transaction on Information Forensics Security*, vol. 4, no. 4, pp. 824–836, December 2009. *(Cited on page 43)*

[197] F. Scotti and V. Piuri, "Adaptive reflection detection and location in iris biometric images by using computational intelligence techniques," *IEEE Transactions of Instrumentation and Measurement*, vol. 59, no. 7, pp. 1825–1833, July 2010. *(Cited on page 43)*

[198] F. Scotti, "Computational intelligence techniques for reflections identification in iris biometric images," in *Proceedings of the IEEE International Conference on Computational Intelligence for Measurement Systems and Applications (CIMSA*, June 2007, pp. 84–88. *(Cited on page 43)*

[199] S. A. C. Schuckers, N. A. Schmid, A. Abhyankar, V. Dorairaj, C. K. Boyce, and L. A. Hornak, "On techniques for angle compensation in nonideal iris recognition," *IEEE Transactions on Systems, Man, and Cybernetics, Part B: Cybernetics*, vol. 37, no. 5, pp. 1176–1190, October 2007. *(Cited on page 43)*

[200] C.-T. Chou, S.-W. Shih, W.-S. Chen, V. W. Cheng, and D.-Y. Chen, "Non-orthogonal view iris recognition system," *IEEE Transactions on Circuits and Systems for Video Technology*, vol. 20, no. 3, pp. 417–430, March 2010. *(Cited on page 43)*

[201] K. Nguyen, C. Fookes, S. Sridharan, and S. Denman, "Quality-driven super-resolution for less constrained iris recognition at a distance and on the move," *IEEE Transactions on Information Forensics and Security*, vol. 6, no. 4, pp. 1248–1258, December 2011. *(Cited on page 44)*

[202] Z. Sun, W. Dong, and T. Tan, "Technology roadmap for smart iris recognition," in *Proceedings of the International Conference on Computer Graphics & Vision*, 2008, pp. 12–19. *(Cited on pages XII and 44)*

[203] W. Dong, Z. Sun, T. Tan, and X. Qiu, "Self-adaptive iris image acquisition system," in *Proceedings of SPIE*, 2008. *(Cited on pages XII, 45, and 46)*

[204] C. L. Fancourt, L. Bogoni, K. J. Hanna, Y. Guo, R. P. Wildes, N. Takahashi, and U. Jain, "Iris recognition at a distance," in *Proceedings of Audio and Video Based Person Authentication*, 2005, pp. 1–13. *(Cited on pages XII, 45, and 46)*

[205] W. Dong, Z. Sun, and T. Tan, "A design of iris recognition system at a distance," in *Proceedings of the Chinese Conference on Pattern Recognition*, November 2009, pp. 1–5. *(Cited on pages XII, 45, and 46)*

[206] J. Zhang, Y. Cheng, and C. Chen, "Low resolution gait recognition with high frequency super resolution," in *PRICAI 2008: Trends in Artificial Intelligence*, ser. Lecture Notes in Computer Science, T.-B. Ho and Z.-H. Zhou, Eds. Springer Berlin / Heidelberg, 2008, vol. 5351, pp. 533–543. *(Cited on page 46)*

[207] R. Raposo, E. Hoyle, A. Peixinho, and H. Proenca, "UBEAR: A dataset of ear images captured on-the-move in uncontrolled conditions," in *Proceedings of the IEEE Workshop on Computational Intelligence in Biometrics and Identity Management*, April 2011, pp. 84–90. *(Cited on page 46)*

[208] Y. Ran, G. Rosenbush, and Q. Zheng, "Computational approaches for real-time extraction of soft biometrics," in *Proceedings of the 19th International Conference on Pattern Recognition*, 2008, pp. 1–4. *(Cited on page 47)*

[209] M. Cannon, M. Byrne, D. Cotter, P. Sham, C. Larkin, and E. O'Callaghan, "Further evidence for anomalies in the hand-prints of patients with schizophrenia: a study of secondary creases," *Schizophrenia Research*, vol. 13, no. 2, pp. 179–184, September 1994. *(Cited on pages 50 and 202)*

[210] A. W.-K. Kong, D. Zhang, and G. Lu, "A study of identical twins' palmprints for personal verification," *Pattern Recognition*, vol. 39, no. 11, pp. 2149–2156, 2006. *(Cited on page 50)*

[211] Y. Zhou, Y. Zeng, Lizhen, and W. Hu, "Application and development of palm print research," *Technology and Health Care*, vol. 10, no. 5, pp. 383–390, November 2002. *(Cited on page 50)*

[212] A. K. Jain and J. Feng, "Latent palmprint matching," *IEEE Transactions on Pattern Analysis and Machine Intelligence*, vol. 31, no. 6, pp. 1032–1047, 2009. *(Cited on pages XIII, XIV, 51, 57, 61, 64, 76, 77, and 78)*

[213] Q. Zhang and X. Zhu, "Study of the thinning algorithm for thenar palmprint," in *Proceedings of the 2010 First ACIS International Symposium on Cryptography and Network Security, Data Mining and Knowledge Discovery, E-Commerce Its Applications and Embedded Systems (CDEE)*, 2010, pp. 179–182. *(Cited on page 51)*

[214] X. Zhu and D. Liu, "Analysis of divisibility in thenar palmprint with texture features," in *2010 First ACIS International Symposium on Cryptography and Network Security, Data Mining and Knowledge Discovery, E-Commerce Its Applications and Embedded Systems (CDEE)*, 2010, pp. 183–186. *(Cited on page 51)*

[215] X. Zhu, Q. Zhang, D. Liu, and W. Lv, "An edge extraction algorithm of thenar palmprint image based on wavelet multi-scale," in *Proceedings of the 2010 Third International Symposium on Information Processing (ISIP)*, 2010, pp. 555–558. *(Cited on page 51)*

[216] "Palm reading guide," http://www.md-health.com/Palm-Reading-Guide.html. *(Cited on pages XII and 53)*

[217] G. Lu, D. Zhang, W. K. Kong, and M. Wong, "A palmprint authentication system," in *Handbook of Biometrics*, A. K. Jain, P. Flynn, and A. A. Ross, Eds. Springer US, 2008, pp. 171–187. *(Cited on pages XIII, 51, 54, 58, and 62)*

[218] W. Shu and D. Zhang, "Automated personal identification by palmprint," *Optical Engineering*, vol. 37, no. 8, pp. 2359–2362, 1998. *(Cited on page 53)*

[219] N. Duta, A. K. Jain, and K. V. Mardia, "Matching of palmprints," *Pattern Recognition Letters*, vol. 23, no. 4, pp. 477–485, 2002. *(Cited on page 53)*

[220] "NEC Automated Palmprint Identification System," http://nz.nec.com/en_NZ/solutions/public_safety/fingerprint_identification.html. *(Cited on pages 53 and 61)*

[221] D. Zhang, W. Zuo, and F. Yue, "A comparative study of palmprint recognition algorithms," *ACM Computing Surveys (CSUR)*, vol. 44, no. 1, pp. 2:1–2:37, January 2012. *(Cited on pages XXI, 53, and 54)*

[222] Konica Minolta Sensing, Inc., "Konica Minolta 3D Laser Scanners | VIVID 9i | VIVID 910," http://www.3dscanco.com/products/3d-scanners/3d-laserscanners/konica-minolta/. *(Cited on pages XII and 54)*

[223] J. You, W.-K. Kong, D. Zhang, and K.-H. Cheung, "On hierarchical palmprint coding with multiple features for personal identification in large databases," *IEEE Transactions on Circuits and Systems for Video Technology*, vol. 14, no. 2, pp. 234–243, 2004. *(Cited on pages 54, 66, and 81)*

[224] F. Yue, W. Zuo, D. Zhang, and B. Li, "Fast palmprint identification with multiple templates per subject," *Pattern Recognition Letters*, vol. 32, no. 8, pp. 1108–1118, 2011. *(Cited on pages 54 and 66)*

[225] D. D. Zhang, *Palmprint Authentication*, ser. International Series on Biometrics. Springer, 2004. *(Cited on pages XII, XIII, 56, 58, 61, and 64)*

[226] X. Pan and Q.-Q. Ruan, "Palmprint recognition with improved two-dimensional locality preserving projections," *Image and Vision Computing*, vol. 26, no. 9, pp. 1261–1268, 2008. *(Cited on pages XIII, 58, 65, 66, 77, and 79)*

[227] D. Zhang, G. Lu, W. Li, D. Zhang, and N. Luo, "Palmprint recognition using 3-D information," *IEEE Transactions on Systems, Man, and Cybernetics, Part C: Applications and Reviews*, vol. 39, no. 5, pp. 505–519, 2009. *(Cited on pages XIII, XIV, 59, 82, 83, 84, and 196)*

[228] W. Jia, R.-X. Hu, J. Gui, Y. Zhao, and X.-M. Ren, "Palmprint recognition across different devices," *Sensors*, vol. 12, no. 6, pp. 7938–7964, 2012. *(Cited on pages XIII, 59, 62, 91, 96, 101, and 204)*

[229] A. Kumar, M. Hanmandlu, V. K. Madasu, and S. Vasikarla, "A palm print authentication system using quantized phase feature representation," in *Proceedings of the 2011 IEEE Applied Imagery Pattern Recognition Workshop (AIPR)*, 2011, pp. 1–8. *(Cited on pages XIII, 58, 67, and 68)*

[230] X. Pan and Q.-Q. Ruan, "Palmprint recognition using Gabor feature-based (2D)^{2}PCA," *Neurocomputing*, vol. 71, no. 13-15, pp. 3032–3036, 2008. *(Cited on pages 58, 65, and 77)*

[231] Y. Han, Z. Sun, F. Wang, and T. Tan, "Palmprint recognition under unconstrained scenes," in *Computer Vision - ACCV 2007*, ser. Lecture Notes in Computer Science, Y. Yagi, S. Kang, I. Kweon, and H. Zha, Eds. Springer Berlin Heidelberg, 2007, vol. 4844, pp. 1–11. *(Cited on pages 59 and 62)*

[232] "Identix tp3800 livescan," http://www.azafis.gov/equipment/indentix.asp. *(Cited on pages XIII and 62)*

[233] "Biometrics: Contactless capture," http://latanyasweeney.org/work/hand.html. *(Cited on pages XIII and 62)*

[234] Business Wire, "El Paso police installs Sagem Morpho Palmprint System," 2002, http://www.businesswire.com. *(Cited on page 61)*

[235] E. Liu, A. K. Jain, and J. Tian, "A coarse to fine minutiae-based latent palmprint matching," *IEEE Transactions on Pattern Analysis and Machine Intelligence*, 2013. *(Cited on pages 61, 64, and 78)*

[236] S. K. Dewan, "Elementary, watson: Scan a palm, find a clue," *The New York Times*, November 2003. *(Cited on page 61)*

[237] D. Zhang, Z. Guo, G. Lu, D. Zhang, and W. Zuo, "An online system of multispectral palmprint verification," *IEEE Transactions on Instrumentation and Measurement*, vol. 59, no. 2, pp. 480–490, 2010. *(Cited on pages XIV, 62, 69, and 70)*

[238] C. Methani and A. M. Namboodiri, "Video based palmprint recognition," in *Proceedings of the 2010 20th International Conference on Pattern Recognition (ICPR)*, 2010, pp. 1352–1355. *(Cited on pages 62 and 99)*

[239] Y. Feng, J. Li, L. Huang, and C. Liu, "Real-time ROI acquisition for unsupervised and touch-less palmprint," *World Academy of science, Engineering and Technology*, vol. 78, pp. 823–827, 2011. *(Cited on page 62)*

[240] C. Michal and R. Kozik, "Contactless palmprint and knuckle biometrics for mobile devices," *Pattern Analysis & Applications*, vol. 15, no. 1, pp. 73–85, February 2012. *(Cited on pages 62, 91, 96, and 101)*

[241] M. Franzgrote, C. Borg, B. J. Tobias Ries, S. Bussemaker, X. Jiang, M. Fieleser, and D. Zhang, "Palmprint verification on mobile phones using accelerated competitive code," in *Proceedings of the 2011 International Conference on Hand-Based Biometrics (ICHB)*, 2011, pp. 1–6. *(Cited on pages 62, 91, and 96)*

[242] F. Li, M. K. H. Leung, and C. S. Chian, "Making palm print matching mobile," *CoRR*, vol. abs/0912.0578, 2009. *(Cited on pages 62 and 91)*

[243] Y. Han, T. Tan, Z. Sun, and Y. Hao, "Embedded palmprint recognition system on mobile devices," in *Advances in Biometrics*, ser. Lecture Notes in Computer Science, S.-W. Lee and S. Z. Li, Eds. Springer Berlin Heidelberg, 2007, vol. 4642, pp. 1184–1193. *(Cited on pages 62 and 91)*

[244] M. Choraś and R. Kozik, "Feature extraction method for contactless palmprint biometrics," in *Advanced Intelligent Computing Theories and Applications*, ser. Communications in Computer and Information Science, D.-S. Huang, M. McGinnity, L. Heutte, and X.-P. Zhang, Eds. Springer Berlin Heidelberg, 2010, vol. 93, pp. 435–442. *(Cited on pages 62, 91, and 101)*

[245] C. Methani and A. M. Namboodiri, "Pose invariant palmprint recognition," in *Advances in Biometrics*, ser. Lecture Notes in Computer Science, M. Tistarelli and M. Nixon, Eds. Springer Berlin Heidelberg, 2009, vol. 5558, pp. 577–586. *(Cited on pages 62, 96, and 99)*

[246] W. Shu and D. Zhang, "Automated personal identification by palmprint," *Optical Engineering*, vol. 37, no. 8, pp. 2359–2362, 1998. *(Cited on page 63)*

[247] D. Zhang and W. Shu, "Two novel characteristics in palmprint verification: datum point invariance and line feature matching," *Pattern Recognition*, vol. 32, no. 4, pp. 691–702, 1999. *(Cited on pages 63 and 79)*

[248] J. Li, G. Shi, Y. Zheng, and Y. Liu, "The research on offline palmprint identification," in *Proceedings of the 2009 WRI World Congress on Computer Science and Information Engineering*, vol. 1, 2009, pp. 587–590. *(Cited on pages XIV, 63, 76, 77, and 78)*

[249] J. Li and G. Shi, "A novel palmprint feature processing method based on skeleton image," in *Proceedings of the IEEE International Conference on Signal Image Technology and Internet Based Systems (SITIS)*, 2008, pp. 221–228. *(Cited on page 63)*

[250] Y. Zheng, Y. Liu, G. Shi, J. Li, and Q. Wang, "Segmentation of offline palmprint," in *Proceedings of the Third International IEEE Conference on Signal-Image Technologies and Internet-Based System (SITIS)*, 2007, pp. 804–811. *(Cited on pages 63 and 71)*

[251] Y. Zheng, G. Shi, Q. Wang, and L. Zhang, "Location of special areas on palmprint," in *Proceedings of the Congress on Image and Signal Processing (CISP)*, vol. 2, 2008, pp. 786–791. *(Cited on page 63)*

[252] N. Duta, A. K. Jain, and K. V. Mardia, "Matching of palmprints," *Pattern recognition letters*, vol. 23, pp. 477–485, 2002. *(Cited on pages 63 and 79)*

[253] FBI, "A practical guide for palm print capture - document overview," https://www.fbibiospecs.org/docs/PalmGuidance%20v1.0.pdf. *(Cited on page 64)*

[254] National Science and Technology Council (NSTC), "Palmprint recognition," http://www.biometrics.gov/documents/palmprintrec.pdf. *(Cited on pages 64 and 197)*

[255] M. Laadjel, A. Bouridane, F. Kurugollu, O. Nibouche, and W. Yan, "Partial palmprint matching using invariant local minutiae descriptors," in *Transactions on Data Hiding and Multimedia Security V*, ser. Lecture Notes in Computer Science, Y. Shi, Ed. Springer Berlin Heidelberg, 2010, vol. 6010, pp. 1–17. *(Cited on pages 64 and 78)*

[256] S. Singh, M. Ramalho, P. L. Correia, and L. D. Soares, "PP-RIDER: A rotation-invariant degraded partial palmprint recognition technique," in *2012 Proceedings of the 20th European Signal Processing Conference (EUSIPCO)*, 2012, pp. 1499–1503. *(Cited on pages 64, 78, and 81)*

[257] R. Wang, D. Ramos, and J. FiÃ©rrez, "Improving radial triangulation-based forensic palmprint recognition according to point pattern comparison by relaxation." in *ICB*, A. K. Jain, A. A. Ross, S. Prabhakar, and J. Kim, Eds. IEEE, 2012, pp. 427–432. *(Cited on pages 64 and 78)*

[258] Y. Zhou, T. Guo, M. Wu, and T. Zhao, "Latent palmprint image segmentation based on dissimilarity tolerance," in *Proceedings of the 2010 International Conference on Multimedia Communications (Mediacom)*, 2010, pp. 83–86. *(Cited on pages 64 and 71)*

[259] M. Laadjel, F. Kurugollu, A. Bouridane, and S. Boussakta, "Degraded partial palmprint recognition for forensic investigations," in *Proceedings of the 2009 16th IEEE International Conference on Image Processing (ICIP)*, 2009, pp. 1513–1516. *(Cited on page 64)*

[260] Z. Tan, J. Yang, Z. Shang, G. Shi, and S. Chang, "Minutiae-based offline palmprint identification system," in *Proceedings of the WRI Global Congress on Intelligent Systems (GCIS)*, vol. 4, 2009, pp. 466–471. *(Cited on page 64)*

[261] A. K. Jain and M. Demirkus, "On latent palmprint matching," Department of Computer Science, Michigan State University, East Lansing, Michigan, Tech. Rep. MSU-CSE-08-8, May 2008. *(Cited on pages 64, 71, 72, 77, and 79)*

[262] FBI, "The Science of Fingerprints. Classification and Uses," U.S. Department of Justice, FBI. Superintendent of Documents, U.S. Government Printing Office, Washington, D.C., 2006. *(Cited on page 64)*

[263] A. Gupta, M. Sachdeva, and U. Garg, "OPMAOP: Opposite Pair Matching Approach in Offline Palmprint," in *Proceedings of the IEEE International Advance Computing Conference (IACC)*, 2009, pp. 519–524. *(Cited on pages 65 and 79)*

[264] J. Dai and J. Zhou, "Multifeature-based high-resolution palmprint recognition," *IEEE Transactions on Pattern Analysis and Machine Intelligence*, vol. 33, no. 5, pp. 945–957, 2011. *(Cited on pages XIII, 65, and 77)*

[265] J. Dai, J. Feng, and J. Zhou, "Robust and efficient ridge-based palmprint matching," *IEEE Transactions on Pattern Analysis and Machine Intelligence*, vol. 34, no. 8, pp. 1618–1632, 2012. *(Cited on pages 65 and 76)*

[266] W. Huang, X. Lin, and X. Dai, "A novel approach for palmprint ridges features extraction," in *Proceedings of the 2nd International Congress on Image and Signal Processing (CISP)*, 2009, pp. 1–5. *(Cited on page 65)*

[267] T. Connie, A. T. B. Jin, M. G. K. Ong, and D. N. C. Ling, "An automated palmprint recognition system," *Image and Vision Computing*, vol. 23, no. 5, pp. 501–515, 2005. *(Cited on pages XIV, 65, 73, 74, 75, 77, and 79)*

[268] W. li Yang and L. li Wang, "Research of palmprint identification method using Zernike moment and neural network," in *Proceedings of the 2010 Sixth International Conference on Natural Computation (ICNC)*, vol. 3, 2010, pp. 1310–1313. *(Cited on pages 65 and 80)*

[269] H. Masood, M. Asim, M. Mumtaz, and A. B. Mansoor, "Combined contourlet and non-subsampled contourlet transforms based approach for personal identification using palmprint," in *Digital Image Computing: Techniques and Applications (DICTA)*, 2009, pp. 408–415. *(Cited on pages XIV, 65, 72, 74, 78, and 81)*

[270] X. Pan, Q. Ruan, and Y. Wang, "Palmprint recognition using contourlets-based local fractal dimensions," in *Proceedings of the 9th International Conference on Signal Processing (ICSP)*, 2008, pp. 2108–2111. *(Cited on pages 65, 78, and 81)*

[271] I. Fratric and S. Ribaric, "Colour-based palmprint verification - an experiment," in *Proceedings of the 14th IEEE Mediterranean Electrotechnical Conference (MELECON)*, 2008, pp. 890–895. *(Cited on pages 65 and 80)*

[272] W. Yang, S. Wang, L. Jie, and G. Shao, "A new palmprint identification technique based on a two-stage neural network classifier," in *Proceedings of the Fourth International Conference on Natural Computation (ICNC)*, vol. 5, 2008, pp. 18–23. *(Cited on page 65)*

[273] X. Pan, Q. Ruan, and Y. Wang, "Palmprint recognition using fusion of local and global features," in *Proceedings of the International Symposium on Intelligent Signal Processing and Communication Systems (ISPACS)*, 2007, pp. 642–645. *(Cited on pages 65 and 80)*

[274] Y. Wang, Q. Ruan, and X. Pan, "Palmprint recognition method using dual-tree complex wavelet transform and local binary pattern histogram," in *Proceedings of the International Symposium on Intelligent Signal Processing and Communication Systems (ISPACS)*, 2007, pp. 646–649. *(Cited on pages 65 and 78)*

[275] X. Pan, Q.-Q. Ruan, and Y.-X. Wang, "An improved 2DLPP method on Gabor features for palmprint recognition," in *Proceedings of the IEEE International Conference on Image Processing (ICIP)*, vol. 2, 2007, pp. 413–416. *(Cited on pages 65 and 77)*

[276] A. K. Qin, P. N. Suganthan, C. H. Tay, and H. S. Pa, "Personal identification system based on multiple palmprint features," in *Proceedings of the 9th International Conference on Control, Automation, Robotics and Vision (ICARCV)*, 2006, pp. 1–6. *(Cited on pages XIV, 65, 73, 75, and 77)*

[277] M. Wang and Q. Ruan, "Palmprint recognition based on two-dimensional methods," in *Proceedings of the 2006 8th International Conference on Signal Processing*, vol. 4, 2006. *(Cited on pages 65 and 80)*

[278] Y. Wang and Q. Ruan, "Kernel fisher discriminant analysis for palmprint recognition," in *Proceedings of the 18th International Conference on Pattern Recognition (ICPR)*, vol. 4, 2006, pp. 457–460. *(Cited on pages 65 and 80)*

[279] M. Mu, Q. Ruan, and Y. Ming, "Shape parameters of Gaussian as descriptor for palmprint recognition based on dual-tree complex wavelet transform," in *Proceedings of the 2010 IEEE 10th International Conference on Signal Processing (ICSP)*, 2010, pp. 1406–1409. *(Cited on pages 65, 77, and 80)*

[280] Y.-X. Wang and G.-H. Sun, "Palmprint recognition using palm-line direction field texture feature," in *Proceedings of the 2012 International Conference on Machine Learning and Cybernetics (ICMLC)*, vol. 3, 2012, pp. 1130–1134. *(Cited on pages 65, 77, 80, and 204)*

[281] S. Ribaric and M. Marcetic, "Personal recognition based on the Gabor features of colour palmprint images," in *Proceedings of the 2012 Proceedings of the 35th International Convention MIPRO*, 2012, pp. 967–972. *(Cited on pages 65, 77, 79, and 204)*

[282] S. Kanchana and G. Balakrishnan, "Quadtree decomposition for palm print feature representation in palmprint recognition system," in *Proceedings of the 2012 IEEE International Conference on Advanced Communication Control and Computing Technologies (ICACCCT)*, 2012, pp. 291–294. *(Cited on pages 65, 77, and 81)*

[283] X. Pan and Q.-Q. Ruan, "A modified preprocessing method for palmprint recognition," in *Proceedings of the 2006 8th International Conference on Signal Processing*, vol. 2, 2006. *(Cited on page 65)*

[284] Y. Wang and Q. Ruan, "An improved unsharp masking method for palmprint image enhancement," in *Proceedings of the First International Conference on Innovative Computing, Information and Control (ICICIC)*, vol. 2, 2006, pp. 669–672. *(Cited on pages 65 and 77)*

[285] ——, "Palm-line extraction using steerable filters," in *Proceedings of the 2006 8th International Conference on Signal Processing*, vol. 3, 2006, pp. –. *(Cited on pages 65 and 77)*

[286] S. Shekhar, B. S. Kumar, and S. Ramesh, "Robust approach for palm (ROI) extraction in palmprint recognition system," in *Proceedings of the 2012 IEEE International Conference on Engineering Education: Innovative Practices and Future Trends (AICERA)*, 2012, pp. 1–6. *(Cited on pages 65, 72, and 77)*

[287] Y. Wang, Q. Ruan, and X. Pan, "An improved square-based palmprint segmentation method," in *Proceedings of the International Symposium on Intelligent Signal Processing and Communication Systems (ISPACS)*, 2007, pp. 316–319. *(Cited on pages XIV, 65, 72, 73, and 75)*

[288] S. Ribaric, I. Fratric, and K. Kis, "A biometric verification system based on the fusion of palmprint and face features," in *Proceedings of the 4th International Symposium on Image and Signal Processing and Analysis (ISPA)*, 2005, pp. 12–17. *(Cited on pages 65 and 77)*

[289] W. Xiao-yong, X. Dan, and C.-W. Ngo, "Multibiometrics based on palmprint and handgeometry," in *Proceedings of the Fourth Annual ACIS International Conference on Computer and Information Science*, 2005, pp. 495–500. *(Cited on pages 65 and 78)*

[290] R. S. Choras and M. Choras, "Hand shape geometry and palmprint features for the personal identification," in *Proceedings of the Sixth International Conference on Intelligent Systems Design and Applications (ISDA)*, vol. 2, 2006, pp. 1085–1090. *(Cited on pages 65 and 77)*

[291] J. J. Fuertes, C. M. Travieso, M. A. Ferrer, and J. B. Alonso, "Intra-modal biometric system using hand-geometry and palmprint texture," in *Proceedings of the 2010 IEEE International Carnahan Conference on Security Technology (ICCST)*, 2010, pp. 318–322. *(Cited on pages 65, 77, and 78)*

[292] H. B. Kekre and V. A. Bharadi, "Fingerprint & palmprint segmentation by automatic thresholding of Gabor magnitude," in *Proceedings of the 2009 2nd International Conference on Emerging Trends in Engineering and Technology (ICETET)*, 2009, pp. 235–241. *(Cited on pages 65 and 72)*

[293] D. Zhang, W.-K. Kong, J. You, and M. Wong, "Online palmprint identification," *IEEE Transactions on Pattern Analysis and Machine Intelligence*, vol. 25, no. 9, pp. 1041–1050, 2003. *(Cited on pages XIII, XIV, 66, 67, 74, 75, 76, 77, 80, 83, and 99)*

[294] W. Li, D. Zhang, and Z. Xu, "Palmprint identification by Fourier transform," *International Journal of Pattern Recognition and Artificial Intelligence*, vol. 16, no. 04, pp. 417–432, 2002. *(Cited on pages 66, 78, and 81)*

[295] A. W. K. Kong and D. Zhang, "Competitive coding scheme for palmprint verification," in *Proceedings of the 17th International Conference on Pattern Recognition (ICPR)*, vol. 1, 2004, pp. 520–523. *(Cited on pages 66, 81, 83, and 103)*

[296] X. Wu, K. Wang, and D. Zhang, "HMMs based palmprint identification," in *Biometric Authentication*, ser. Lecture Notes in Computer Science, D. Zhang and A. K. Jain, Eds. Springer Berlin Heidelberg, 2004, vol. 3072, pp. 775–781. *(Cited on pages 66, 77, and 79)*

[297] M. Wong, D. Zhang, W.-K. Kong, and G. Lu, "Real-time palmprint acquisition system design," *IEE Proceedings - Vision, Image and Signal Processing*, vol. 152, no. 5, pp. 527–534, 2005. *(Cited on page 66)*

[298] M. Ekinci and M. Aykut, "Gabor-based kernel PCA for palmprint recognition," *Electronics Letters*, vol. 43, no. 20, pp. 1077–1079, 2007. *(Cited on pages 66 and 77)*

[299] W. Jia, B. Ling, K.-W. Chau, and L. Heutte, "Palmprint identification using restricted fusion," *Applied Mathematics and Computation*, vol. 205, no. 2, pp. 927–934, 2008. *(Cited on pages 66, 78, and 79)*

[300] D.-S. Huang, W. Jia, and D. Zhang, "Palmprint verification based on principal lines," *Pattern Recognition*, vol. 41, no. 4, pp. 1316–1328, 2008. *(Cited on pages 66, 78, and 79)*

[301] W. Jia, D.-S. Huang, and D. Zhang, "Palmprint verification based on robust line orientation code," *Pattern Recognition*, vol. 41, no. 5, pp. 1504–1513, 2008. *(Cited on pages 66, 78, and 81)*

[302] A. Kong, D. Zhang, and M. Kamel, "Three measures for secure palmprint identification," *Pattern Recognition*, vol. 41, no. 4, pp. 1329–1337, April 2008. *(Cited on pages 66 and 77)*

[303] J. Lu, Y. Zhao, and J. Hu, "Enhanced Gabor-based region covariance matrices for palmprint recognition," *Electronics Letters*, vol. 45, no. 17, pp. 880–881, 2009. *(Cited on pages 66, 77, and 81)*

[304] P. Shang and T. Li, "Multifractal characteristics of palmprint and its extracted algorithm," *Applied Mathematical Modelling*, vol. 33, no. 12, pp. 4378–4387, 2009. *(Cited on pages XIV, 66, 74, 75, and 81)*

[305] F. Yue, W. Zuo, D. Zhang, and K. Wang, "Orientation selection using modified FCM for competitive code-based palmprint recognition," *Pattern Recognition*, vol. 42, no. 11, pp. 2841–2849, 2009. *(Cited on pages 66, 77, and 81)*

[306] Z. Guo, D. Zhang, L. Zhang, and W. Zuo, "Palmprint verification using binary orientation co-occurrence vector," *Pattern Recognition Letters*, pp. 1219–1227, 2009. *(Cited on pages 66, 77, 81, and 105)*

[307] M. Mu, Q. Ruan, and S. Guo, "Shift and gray scale invariant features for palmprint identification using complex directional wavelet and local binary pattern," *Neurocomputing*, vol. 74, no. 17, pp. 3351–3360, 2011. *(Cited on pages 66, 78, and 80)*

[308] O. Nibouche, J. Jiang, and P. Trundle, "Analysis of performance of palmprint matching with enforced sparsity," *Digital Signal Processing*, vol. 22, no. 2, pp. 348–355, 2012. *(Cited on pages 66 and 80)*

[309] S. M. Prasad, V. Govindan, and P. S. Sathidevi, "Image quality augmented intramodal palmprint authentication," *IET Image Processing*, vol. 6, no. 6, pp. 668–676, 2012. *(Cited on pages 66, 78, 81, and 204)*

[310] X. Wang, L. Lei, and M. Wang, "Palmprint verification based on 2D - Gabor wavelet and pulse-coupled neural network," *Knowledge-Based Systems*, vol. 27, no. 0, pp. 451–455, 2012. *(Cited on pages 66, 77, and 82)*

[311] W. Li, B. Zhang, L. Zhang, and J. Yan, "Principal line-based alignment refinement for palmprint recognition," *IEEE Transactions on Systems, Man, and Cybernetics, Part C: Applications and Reviews*, vol. 42, no. 6, pp. 1491–1499, 2012. *(Cited on pages 66, 76, and 204)*

[312] X. Wang, J. Liang, and M. Wang, "On-line fast palmprint identification based on adaptive lifting wavelet scheme," *Knowledge-Based Systems*, vol. 42, pp. 68–73, 2013. *(Cited on pages 66, 78, and 82)*

[313] O. Nibouche and J. Jiang, "Palmprint matching using feature points and SVD factorisation," *Digital Signal Processing*, vol. 23, no. 4, pp. 1154–1162, 2013. *(Cited on pages 66, 79, and 204)*

[314] G. S. Badrinath and P. Gupta, "<," in *Proceedings of the First Workshops on Image Processing Theory, Tools and Applications (IPTA)*, 2008, pp. 1–8. *(Cited on pages 66, 74, 75, and 82)*

[315] A. B. Mansoor, H. Masood, M. Mumtaz, and S. A. Khan, "A feature level multimodal approach for palmprint identification using directional subband energies," *Journal of Network and Computer Applications*, vol. 34, no. 1, pp. 159–171, 2011. *(Cited on pages 66 and 78)*

[316] The Hong Kong Polytechnic University, "PolyU palmprint database," http://www4.comp.polyu.edu.hk/~biometrics/polyudb.htm. *(Cited on page 67)*

[317] X.-Y. Jing and D. Zhang, "A face and palmprint recognition approach based on discriminant DCT feature extraction," *IEEE Transactions on Systems, Man, and Cybernetics, Part B: Cybernetics*, vol. 34, no. 6, pp. 2405–2415, 2004. *(Cited on pages 67 and 78)*

[318] Y. Yan and Y.-J. Zhang, "Discriminant projection embedding for face and palmprint recognition," *Neurocomputing*, vol. 71, no. 16-18, pp. 3534–3543, 2008. *(Cited on page 67)*

[319] M. Wan, Z. Lai, J. Shao, and Z. Jin, "Two-dimensional local graph embedding discriminant analysis (2DLGEDA) with its application to face and palm biometrics," *Neurocomputing*, vol. 73, no. 1-3, pp. 197–203, 2009. *(Cited on page 67)*

[320] J. Gui, W. Jia, L. Zhu, S.-L. Wang, and D.-S. Huang, "Locality preserving discriminant projections for face and palmprint recognition," *Neurocomputing*, vol. 73, no. 13-15, pp. 2696–2707, 2010. *(Cited on page 67)*

[321] W. Zuo, H. Zhang, D. Zhang, and K. Wang, "Post-processed LDA for face and palmprint recognition: What is the rationale," *Signal Processing*, vol. 90, no. 8, pp. 2344–2352, 2010. *(Cited on page 67)*

[322] R. Raghavendra, B. Dorizzi, A. Rao, and G. H. Kumar, "Designing efficient fusion schemes for multimodal biometric systems using face and palmprint," *Pattern Recognition*, vol. 44, no. 5, pp. 1076–1088, 2011. *(Cited on pages 67 and 77)*

[323] J. Lu and Y.-P. Tan, "Improved discriminant locality preserving projections for face and palmprint recognition," *Neurocomputing*, vol. 74, no. 18, pp. 3760–3767, 2011. *(Cited on page 67)*

[324] X. Jing, S. Li, D. Zhang, C. Lan, and J. Yang, "Optimal subset-division based discrimination and its kernelization for face and palmprint recognition," *Pattern Recognition*, vol. 45, no. 10, pp. 3590–3602, 2012. *(Cited on page 67)*

[325] L. Zhang and H. Li, "Encoding local image patterns using Riesz transforms: With applications to palmprint and finger-knuckle-print recognition," *Image and Vision Computing*, vol. 30, no. 12, pp. 1043–1051, 2012. *(Cited on pages 67 and 78)*

[326] Z. Li-cong, X.-M. Ding, Z. Yan-qiang, L. Qiang, and W. Cheng-qi, "Embedded online palmprint verification system based on Ethernet," in *Proceedings of the 2nd International Congress on Image and Signal Processing (CISP)*, 2009, pp. 1–5. *(Cited on pages XIII, XIV, 67, 68, and 76)*

[327] H. Zhang and D. Hu, "Palmprint verification system using Moiré pattern," in *Proceedings of the 2009 IEEE International Conference on Robotics and Biomimetics (ROBIO)*, 2009, pp. 1224–1229. *(Cited on pages XIII, 67, and 68)*

[328] M. Aykut and M. Ekinci, "AAM-based palm segmentation in unrestricted backgrounds and various postures for palmprint recognition," *Pattern Recognition Letters*, vol. 34, no. 9, pp. 955–962, 2013. *(Cited on pages XIII, 67, 69, 72, and 75)*

[329] Z. Guo, D. Zhang, L. Zhang, W. Zuo, and G. Lu, "Empirical study of light source selection for palmprint recognition," *Pattern Recognition Letters*, vol. 32, no. 2, pp. 120–126, 2011. *(Cited on page 69)*

[330] Z. Guo, D. Zhang, L. Zhang, and W. Liu, "Feature band selection for online multispectral palmprint recognition," *IEEE Transactions on Information Forensics and Security*, vol. 7, no. 3, pp. 1094–1099, 2012. *(Cited on page 69)*

[331] J. Cui, "Multispectral fusion for palmprint recognition," *Optik - International Journal for Light and Electron Optics*, 2012. *(Cited on page 69)*

[332] S. Zhang and X. Gu, "Palmprint recognition method based on score level fusion," *Optik - International Journal for Light and Electron Optics*, 2012. *(Cited on page 69)*

[333] C.-W. Lu, I. Fan, C.-C. Han, J.-C. Chang, K.-C. Fan, and H. Y. M. Liao, "Palmprint verification using gradient maps and support vector machines," in *Proceedings of the 2012 Asia-Pacific Signal Information Processing Association Annual Summit and Conference (APSIPA ASC)*, 2012, pp. 1–4. *(Cited on page 69)*

[334] K. P. Shashikala and K. B. Raja, "Palmprint identification using transform domain and spatial domain techniques," in *Proceedings of the 2012 International Conference on Computing Sciences (ICCS)*, 2012, pp. 105–109. *(Cited on page 69)*

[335] D. Kostadinov and S. Bogdanova, "Logistic regression classifier for palmprint verification," in *Proceedings of the 2012 19th International Conference on Systems, Signals and Image Processing (IWSSIP)*, 2012, pp. 413–416. *(Cited on page 69)*

[336] S. Valarmathy, M. A. Kumar, and M. Sudha, "Improvement in palmprint recognition rate using fusion of multispectral palmprint images," in *Proceedings of the 2012 International Conference on Computing, Communication and Applications (ICCCA)*, 2012, pp. 1–5. *(Cited on page 69)*

[337] H. B. Kekre, T. Sarode, R. Vig, A. Pranay, I. Aashita, and B. Saurabh, "Palmprint identification using Kronecker product of DCT and Walsh transforms for multispectral images," in *Proceedings of the 2011 International Conference on Hand-Based Biometrics (ICHB)*, 2011, pp. 1–7. *(Cited on page 69)*

[338] A. Meraoumia, S. Chitroub, and A. Bouridane, "Fusion of multispectral palmprint images for automatic person identification," in *Proceedings of the 2011 Saudi International Electronics, Communications and Photonics Conference (SIECPC)*, 2011, pp. 1–6. *(Cited on page 69)*

[339] X. Xu and Z. Guo, "Multispectral palmprint recognition using quaternion principal component analysis," in *Proceedings of the 2010 International Workshop on Emerging Techniques and Challenges for Hand-Based Biometrics (ETCHB)*, 2010, pp. 1–5. *(Cited on page 69)*

[340] D. Han, Z. Guo, and D. Zhang, "Multispectral palmprint recognition using wavelet-based image fusion," in *Proceedings of the 9th International Conference on Signal Processing (ICSP)*, 2008, pp. 2074–2077. *(Cited on page 69)*

[341] The Hong Kong Polytechnic University, "PolyU multispectral palmprint database," http://www4.comp.polyu.edu.hk/~biometrics/MultispectralPalmprint/MSP.htm. *(Cited on page 69)*

[342] Z. Guo, D. Zhang, L. Zhang, and W. Liu, "Feature band selection for online multispectral palmprint recognition," *IEEE Transactions on Information Forensics and Security*, vol. 7, no. 3, pp. 1094–1099, 2012. *(Cited on page 69)*

[343] The Hong Kong Polytechnic University, "PolyU hyperspectral palmprint database," http://www4.comp.polyu.edu.hk/~biometrics/HyperspectralPalmprint/HSP.htm. *(Cited on page 69)*

[344] D. Zhang, Z. Guo, G. Lu, L. Zhang, Y. Liu, and W. Zuo, "Online joint palmprint and palmvein verification," *Expert Systems with Applications*, vol. 38, no. 3, pp. 2621–2631, 2011. *(Cited on pages XIV, 69, 71, and 201)*

[345] N. Luo, Z. Guo, G. Wu, and C. Song, "Joint palmprint and palmvein verification by dual competitive coding," in *Proceedings of the 2011 3rd International Conference on Advanced Computer Control (ICACC)*, 2011, pp. 538–542. *(Cited on page 69)*

[346] R. Cai and D. Hu, "Image fusion of palmprint and palm vein: Multispectral palm image fusion," in *Proceedings of the 2010 3rd International Congress on Image and Signal Processing (CISP)*, vol. 6, 2010, pp. 2778–2781. *(Cited on pages 69 and 70)*

[347] J.-G. Wang, W.-Y. Yau, and A. Suwandy, "Feature-level fusion of palmprint and palm vein for person identification based on a "Junction Point" representation," in *Proceedings of the 15th IEEE International Conference on Image Processing (ICIP)*, 2008, pp. 253–256. *(Cited on pages 69 and 70)*

[348] J.-G. Wang, W.-Y. Yau, A. Suwandy, and E. Sung, "Fusion of palmprint and palm vein images for person recognition based on "Laplacianpalm" feature," in *Proceedings of the IEEE Conference on Computer Vision and Pattern Recognition (CVPR)*, 2007, pp. 1–8. *(Cited on pages 69 and 70)*

[349] G. S. Badrinath and P. Gupta, "An efficient multi-algorithmic fusion system based on palmprint for personnel identification," in *Proceedings of the International Conference on Advanced Computing and Communications (ADCOM)*, 2007, pp. 759–764. *(Cited on page 78)*

[350] A. Kong, D. Zhang, and M. Kamel, "Palmprint identification using feature-level fusion," *Pattern Recognition*, vol. 39, no. 3, pp. 478–487, 2006. *(Cited on page 81)*

[351] D. Zhang, V. Kanhangad, N. Luo, and A. Kumar, "Robust palmprint verification using 2D and 3D features," *Pattern Recognition*, vol. 43, no. 1, pp. 358–368, 2010. *(Cited on pages 82, 83, and 84)*

[352] J. Cui, "2D and 3D palmprint fusion and recognition using PCA plus TPTSR method," *Neural Computing and Applications*, pp. 1–6, 2012. *(Cited on pages 82 and 84)*

[353] Y. Xu, Z. Fan, M. Qiu, D. Zhang, and J.-Y. Yang, "A sparse representation method of bimodal biometrics and palmprint recognition experiments," *Neurocomputing*, vol. 103, pp. 164–171, 2013. *(Cited on page 82)*

[354] The Hong Kong Polytechnic University, "PolyU 2D + 3D palmprint database," http://www4.comp.polyu.edu.hk/~biometrics/2D_3D_Palmprint.htm. *(Cited on page 83)*

[355] W. Li, D. Zhang, D. Zhang, G. Lu, and J. Yan, "Efficient joint 2D and 3D palmprint matching with alignment refinement," in *Proceedings of the 2010 IEEE Conference on Computer Vision and Pattern Recognition (CVPR)*, 2010, pp. 795–801. *(Cited on pages 83 and 84)*

[356] M. Liu and L. Li, "Cross-correlation based binary image registration for 3D palmprint recognition," in *Proceedings of the 2012 IEEE 11th International Conference on Signal Processing (ICSP)*, vol. 3, 2012, pp. 1597–1600. *(Cited on page 83)*

[357] W. Li, D. Zhang, and D. Zhang, "Three dimensional palmprint recognition," in *Proceedings of the IEEE International Conference on Systems, Man and Cybernetics (SMC)*, 2009, pp. 4847–4852. *(Cited on pages 83 and 84)*

[358] A. Meraoumia, S. Chitroub, and A. Bouridane, "2D and 3D palmprint information and Hidden Markov Model for improved identification performance," in *Proceedings of the 2011 11th International Conference on Intelligent Systems Design and Applications (ISDA)*, 2011, pp. 648–653. *(Cited on page 84)*

[359] J. Cui and Y. Xu, "Three dimensional palmprint recognition using linear discriminant analysis method," in *Proceedings of the 2011 Second International Conference on Innovations in Bio-inspired Computing and Applications (IBICA)*, 2011, pp. 107–111. *(Cited on page 84)*

[360] A. Kumar, D. C. M. Wong, H. C. Shen, and A. K. Jain, "Personal verification using palmprint and hand geometry biometric," in *Audio- and Video-Based Biometric Person Authentication*, ser. Lecture Notes in Computer Science, J. Kittler and M. Nixon, Eds. Springer Berlin Heidelberg, 2003, vol. 2688, pp. 668–678. *(Cited on pages XIV, 85, 91, 94, 97, and 98)*

[361] K. Y. E. Wong, G. Sainarayanan, and A. Chekima, "Palmprint identification using wavelet energy," in *Proceedings of the International Conference on Intelligent and Advanced Systems (ICIAS)*, 2007, pp. 714–719. *(Cited on pages XIV, 85, 86, 95, 97, and 99)*

[362] E. W. K. Yih, G. Sainarayanan, A. Chekima, and G. Narendra, "Palmprint identification using sequential modified Haar wavelet energy," in *Proceedings of the International Conference on Signal Processing, Communications and Networking (ICSCN)*, 2008, pp. 411–416. *(Cited on pages 85, 97, and 99)*

[363] K. Y. E. Wong, A. Chekima, J. A. Dargham, and G. Sainarayanan, "Palmprint identification using Sobel operator," in *Proceedings of the 10th International Conference on Control, Automation, Robotics and Vision (ICARCV)*, 2008, pp. 1338–1341. *(Cited on pages 85, 97, and 99)*

[364] Y.-P. Wu, J.-W. Tian, D. Xu, and X.-J. Zhang, "Palmprint recognition based on RB K-means and hierarchical SVM," in *Proceedings of the 2007 International Conference on Machine Learning and Cybernetics*, vol. 6, 2007, pp. 3641–3647. *(Cited on pages XIV, 85, 86, 95, 97, and 101)*

[365] M. Choras, R. Kozik, and A. Zelek, "A novel shape-texture approach to palmprint detection and identification," in *Proceedings of the Eighth International Conference on Intelligent Systems Design and Applications (ISDA)*, vol. 3, 2008, pp. 638–643. *(Cited on pages XV, 86, 87, and 98)*

[366] R. Kozik, A. Zelek, and M. Choras, "Palmprint recognition enhanced by the shape features," in *Proceedings of the 7th Computer Information Systems and Industrial Management Applications (CISIM)*, 2008, pp. 214–215. *(Cited on pages 86, 97, and 98)*

[367] H. Masood, M. Mumtaz, M. A. A. Butt, A. B. Mansoor, and S. A. Khan, "Wavelet based palmprint authentication system," in *Proceedings of the International Symposium on Biometrics and Security Technologies (ISBAST)*, 2008, pp. 1–7. *(Cited on pages XV, 86, 87, 95, 97, and 101)*

[368] G. K. O. Michael, T. Connie, and A. B. J. Teoh, "Touch-less palm print biometrics: Novel design and implementation," *Image and Vision Computing*, vol. 26, no. 12, pp. 1551–1560, 2008. *(Cited on pages XV, 86, 87, 95, 97, and 99)*

[369] J. Doublet, O. Lepetit, and M. Revenu, "Contact less hand recognition using shape and texture features," in *Proceedings of the 2006 8th International Conference on Signal Processing*, vol. 3, 2006, pp. –. *(Cited on pages XV, 88, 96, 97, and 101)*

[370] ——, "Contactless palmprint authentication using circular Gabor filter and approximated string matching," in *Proceedings of the Ninth IASTED International Conference on Signal and Image Processing*, ser. SIP. Anaheim, CA, USA: ACTA Press, 2007, pp. 511–516. *(Cited on pages 88, 97, and 101)*

[371] J. Doublet, M. Revenu, and O. Lepetit, "Robust grayscale distribution estimation for contactless palmprint recognition," in *Proceedings of the First IEEE International Conference on Biometrics: Theory, Applications, and Systems (BTAS)*, 2007, pp. 1–6. *(Cited on pages 88, 97, and 99)*

[372] C. Methani and A. M. Namboodiri, "Video based palmprint recognition," in *Proceedings of the 2010 20th International Conference on Pattern Recognition*, ser. ICPR. Washington, DC, USA: IEEE Computer Society, 2010, pp. 1352–1355. *(Cited on pages 88 and 97)*

[373] Y. Feng, J. Li, L. Huang, and C. Li, "Real-time ROI acquisition for unsupervised and touch-less palmprint," *World Academy of science, Engineering and Technology*, vol. 78, pp. 823–827, 2011. *(Cited on pages XV, 88, and 96)*

[374] S. Ben Jemaa, M. Frikha, I. Moalla, M. Hammami, and H. Ben-Abdallah, "Sfax-Miracl hand database for contactless hand biometrics applications," in *Image and Signal Processing*, ser. Lecture Notes in Computer Science, A. Elmoataz, D. Mammass, O. Lezoray, F. Nouboud, and D. Aboutajdine, Eds. Springer Berlin Heidelberg, 2012, vol. 7340, pp. 226–234. *(Cited on pages 88 and 96)*

[375] A. Poinsot, F. Yang, and M. Paindavoine, "Small sample biometric recognition based on palmprint and face fusion," in *Proceedings of the Fourth International Multi-Conference on Computing in the Global Information Technology (ICCGI)*, 2009, pp. 118–122. *(Cited on pages XV, 88, 89, 92, 95, 97, and 99)*

[376] D. Sun, Z. Qiu, and L. Qiang, "Palmprint identification using Gabor wavelet probabilistic neural networks," in *Proceedings of the 2006 8th International Conference on Signal Processing*, vol. 4, 2006, pp. –. *(Cited on pages XV, 89, 97, and 101)*

[377] P.-F. Yu and D. Xu, "Palmprint recognition based on modified DCT features and RBF neural network," in *Proceedings of the 2008 International Conference on Machine Learning and Cybernetics*, vol. 5, 2008, pp. 2982–2986. *(Cited on pages XV, 89, 90, 97, and 98)*

[378] P. Yu and D. Xu, "Palmprint recognition using generalized discriminant analysis," in *Proceedings of the International Conference on Audio, Language and Image Processing (ICALIP)*, 2008, pp. 1517–1521. *(Cited on pages 90 and 98)*

[379] P. Yu, P. Yu, and D. Xu, "Comparison of PCA, LDA and GDA for palmprint verification," in *Proceedings of the 2010 International Conference on Information Networking and Automation (ICINA)*, vol. 1, 2010, pp. V1–148–V1–152. *(Cited on pages 90 and 99)*

[380] H. Sang and F. Liu, "Defocused palmprint recognition using 2DPCA," in *Proceedings of the International Conference on Artificial Intelligence and Computational Intelligence (AICI)*, vol. 1, 2009, pp. 611–615. *(Cited on pages XV, 90, and 99)*

[381] Institute of Automation, Chinese Academy of Sciences, "Casia palmprint image database," http://biometrics.idealtest.org/dbDetailForUser.do?id=5. *(Cited on pages XV and 90)*

[382] Y. Punsawad and Y. Wongsawat, "Palmprint image enhancement using phase congruency," in *Proceedings of the IEEE International Conference on Robotics and Biomimetics (ROBIO)*, 2009, pp. 1643–1646. *(Cited on pages 90 and 97)*

[383] M. M. M. Fahmy, "Palmprint recognition based on Mel frequency Cepstral coefficients feature extraction," *Ain Shams Engineering Journal*, vol. 1, no. 1, pp. 39–47, 2010. *(Cited on pages 90, 97, and 100)*

[384] G. Yashodha and R. Bremananlh, "Rotation invariant palmprint recognition: An overview and implementation," in *Proceedings of the 2012 International Conference on Machine Vision and Image Processing (MVIP)*, 2012, pp. 145–148. *(Cited on page 90)*

[385] J. Wang, D. Li, M. Li, and Y. Lin, "Research on the extraction to the region of interest area in palmprint," in *Proceedings of the 2012 24th Chinese Control and Decision Conference (CCDC)*, 2012, pp. 3714–3718. *(Cited on page 90)*

[386] Z. Guo, W. Zuo, L. Zhang, and D. Zhang, "A unified distance measurement for orientation coding in palmprint verification," *Neurocomputing*, vol. 73, no. 4-6, pp. 944–950, January 2010. *(Cited on pages 90 and 100)*

[387] J. Chen, Y.-S. Moon, M.-F. Wong, and G. Su, "Palmprint authentication using a symbolic representation of image," *Image and Vision Computing*, vol. 28, no. 3, pp. 343–351, 2010. *(Cited on pages 90 and 100)*

[388] W. Zuo, F. Yue, and D. Zhang, "On accurate orientation extraction and appropriate distance measure for low-resolution palmprint recognition," *Pattern Recognition*, vol. 44, no. 4, pp. 964–972, 2011. *(Cited on pages 90, 100, and 204)*

[389] H. P. Abeysundera and M. T. Eskil, "Palmprint verification using sift majority voting," in *Computer and Information Sciences II*, E. Gelenbe, R. Lent, and G. Sakellari, Eds. Springer London, 2012, pp. 291–297. *(Cited on pages 90 and 101)*

[390] G. S. Badrinath and P. Gupta, "Palmprint based verification system robust to rotation, scale and occlusion," in *Proceedings of the 12th International Conference on Computers and Information Technology (ICCIT)*, 2009, pp. 408–413. *(Cited on page 90)*

[391] ——, "Stockwell transform based palm-print recognition," *Applied Soft Computing*, vol. 11, no. 7, pp. 4267–4281, 2011. *(Cited on pages 90, 98, and 100)*

[392] G. S. Badrinath, K. Tiwari, and P. Gupta, "An efficient palmprint based recognition system using 1D-DCT features," in *Intelligent Computing Technology*, ser. Lecture Notes in Computer Science, D.-S. Huang, C. Jiang, V. Bevilacqua, and J. Figueroa, Eds. Springer Berlin Heidelberg, 2012, vol. 7389, pp. 594–601. *(Cited on pages 90, 97, and 100)*

[393] K. Tiwari, D. K. Arya, G. S. Badrinath, and P. Gupta, "Designing palmprint based recognition system using local structure tensor and force field transformation for human identification," *Neurocomputing*, vol. 116, no. 0, pp. 222–230, 2013. *(Cited on pages 90, 98, 101, and 204)*

[394] G. S. Badrinath and P. Gupta, "Palmprint based recognition system using phase-difference information," *Future Generation Computer Systems*, vol. 28, no. 1, pp. 287–305, 2012. *(Cited on pages 90, 100, and 204)*

[395] Indian Institute of Technology Delhi, "IIT Delhi Touchless Palmprint Database (Version 1.0)," http://www4.comp.polyu.edu.hk/~csajaykr/IITD/Database_Palm.htm. *(Cited on pages XV, 90, and 91)*

[396] H. Madasu, H. M. Gupta, N. Mittal, and S. Vasikarla, "An authentication system based on palmprint," in *Proceedings of the Sixth International Conference on Information Technology: New Generations (ITNG)*, 2009, pp. 399–404. *(Cited on pages 91, 95, 97, and 101)*

[397] A. Morales, M. A. Ferrer, and A. Kumar, "Improved palmprint authentication using contactless imaging," in *Proceedings of the 2010 Fourth IEEE International Conference on Biometrics: Theory Applications and Systems (BTAS)*, 2010, pp. 1–6. *(Cited on page 91)*

[398] A. Kumar, "Incorporating cohort information for reliable palmprint authentication," in *Proceedings of the Sixth Indian Conference on Computer Vision, Graphics Image Processing (ICVGIP)*, 2008, pp. 583–590. *(Cited on pages 91 and 99)*

[399] H. Imtiaz and S. A. Fattah, "A DCT-based feature extraction algorithm for palmprint recognition," in *Proceedings of the 2010 IEEE International Conference on Communication Control and Computing Technologies (ICCCCT)*, 2010, pp. 657–660. *(Cited on pages 91, 97, and 101)*

[400] ——, "A histogram-based dominant wavelet domain feature selection algorithm for palm-print recognition," *Computers & Electrical Engineering*, vol. 39, no. 4, pp. 1114–1128, 2013. *(Cited on pages 91, 97, and 99)*

[401] ——, "A wavelet-based dominant feature extraction algorithm for palm-print recognition," *Digital Signal Processing*, vol. 23, no. 1, pp. 244–258, 2013. *(Cited on page 91)*

[402] G. K. O. Michael, T. Connie, and A. T. B. Jin, "An innovative contactless palm print and knuckle print recognition system," *Pattern Recognition Letters*, vol. 31, no. 12, pp. 1708–1719, Sep. 2010. *(Cited on pages XV, 91, 97, and 99)*

[403] ——, "Robust palm print and knuckle print recognition system using a contactless approach," in *Proceedings of the 2010 the 5th IEEE Conference on Industrial Electronics and Applications (ICIEA)*, 2010, pp. 323–329. *(Cited on page 91)*

[404] J. Wu and Z. Qiu, "A hierarchical palmprint identification method using hand geometry and grayscale distribution features," in *Proceedings of the 18th International Conference on Pattern Recognition (ICPR)*, vol. 4, 2006, pp. 409–412. *(Cited on pages 91, 95, and 99)*

[405] A. Kumar and D. Zhang, "Combining fingerprint, palmprint and hand-shape for user authentication," in *Proceedings of the 18th International Conference on Pattern Recognition (ICPR)*, vol. 4, 2006, pp. 549–552. *(Cited on pages 91, 92, 97, and 98)*

[406] W.-S. Chen, Y.-S. Chiang, and Y.-H. Chiu, "Biometric verification by fusing hand geometry and palmprint," in *Proceedings of the Third International Conference on Intelligent Information Hiding and Multimedia Signal Processing (IIHMSP)*, vol. 2, 2007, pp. 403–406. *(Cited on pages XV, 91, 92, 95, 97, and 100)*

[407] A. Morales, M. A. Ferrer, C. M. Travieso, and J. B. Alonso, "Multisampling approach applied to contactless hand biometrics," in *Proceedings of the 2012 IEEE International Carnahan Conference on Security Technology (ICCST)*, 2012, pp. 224–229. *(Cited on pages XV, 92, 95, and 100)*

[408] R. Chu, S. Liao, Y. Han, Z. Sun, S. Z. Li, and T. Tan, "Fusion of face and palmprint for personal identification based on ordinal features," in *Proceedings of the IEEE Conference on Computer Vision and Pattern Recognition (CVPR).*, 2007, pp. 1–2. *(Cited on page 92)*

[409] Y. J. Chin, T.-S. Ong, M. K. O. Goh, and B. Y. Hiew, "Integrating palmprint and fingerprint for identity verification," in *Proceedings of the Third International Conference on Network and System Security (NSS)*, 2009, pp. 437–442. *(Cited on page 92)*

[410] P. Yu, D. Xu, and H. Zhou, "Feature level fusion using palmprint and finger geometry based on Canonical Correlation Analysis," in *Proceedings of the 2010 3rd International Conference on Advanced Computer Theory and Engineering (ICACTE)*, vol. 5, 2010, pp. V5–260–V5–264. *(Cited on pages 92 and 99)*

[411] Y. Han, Z. Sun, F. Wang, and T. Tan, "Palmprint recognition under unconstrained scenes," in *Computer Vision - ACCV 2007*, ser. Lecture Notes in Computer Science, Y. Yagi, S. Kang, I. Kweon, and H. Zha, Eds. Springer Berlin Heidelberg, 2007, vol. 4844, pp. 1–11. *(Cited on pages XV, 92, 93, 97, and 100)*

[412] Y. Hao, Z. Sun, T. Tan, and C. Ren, "Multispectral palm image fusion for accurate contact-free palmprint recognition," in *Proceedings of the 15th IEEE International Conference on Image Processing (ICIP)*, 2008, pp. 281–284. *(Cited on pages 92 and 97)*

[413] Institute of Automation, Chinese Academy of Sciences, "CASIA Multispectral Palmprint database," http://www.idealtest.org/dbDetailForUser.do?id=6. *(Cited on page 93)*

[414] D. R. Kisku, P. Gupta, J. K. Sing, and C. J. Hwang, "Multispectral palm image fusion for person authentication using ant colony optimization," in *Proceedings of the 2010 International Workshop on Emerging Techniques and Challenges for Hand-Based Biometrics (ETCHB)*, 2010, pp. 1–7. *(Cited on pages 93 and 97)*

[415] Z. Khan, A. Mian, and Y. Hu, "Contour Code: Robust and efficient multispectral palmprint encoding for human recognition," in *Proceedings of the 2011 IEEE International Conference on Computer Vision (ICCV)*, 2011, pp. 1935–1942. *(Cited on pages 93, 95, and 100)*

[416] M. A. Ferrer, F. Vargas, and A. Morales, "BiSpectral contactless hand based biometric system," in *Proceedings of the 2011 2nd National Conference on Telecommunications (CONATEL)*, 2011, pp. 1–6. *(Cited on pages XV, 93, and 100)*

[417] Universidad de Las Palmas de Gran Canaria, "GPDS 100 Contactless hands 2Band database," http://www.gpds.ulpgc.es/download/. *(Cited on page 94)*

[418] M. O. Rotinwa-Akinbile, A. M. Aibinu, and M. J. E. Salami, "A novel palmprint segmentation technique," in *Proceedings of the 2011 First International Conference on Informatics and Computational Intelligence (ICI)*, 2011, pp. 235–239. *(Cited on page 96)*

[419] K. Ito, T. Aoki, H. Nakajima, K. Kobayashi, and T. Higuchi, "A phase-based palmprint recognition algorithm and its experimental evaluation," in *Proceedings of the International Symposium on Intelligent Signal Processing and Communications (ISPACS)*, 2006, pp. 215–218. *(Cited on pages 97 and 101)*

[420] M. O. Rotinwa-Akinbile, A. M. Aibinu, and M. J. E. Salami, "Palmprint recognition using principal lines characterization," in *Proceedings of the 2011 First International Conference on Informatics and Computational Intelligence (ICI)*, 2011, pp. 278–282. *(Cited on pages 97 and 98)*

[421] J. Zhou, D. Sun, Z. Qiu, K. Xiong, D. Liu, and Y. Zhang, "Palmprint recognition by fusion of multi-color components," in *Proceedings of the International Conference on Cyber-Enabled Distributed Computing and Knowledge Discovery (CyberC)*, 2009, pp. 273–278. *(Cited on pages 97 and 101)*

[422] S. Palanikumar, M. Sasikumar, and J. Rajeesh, "Palmprint enhancement using GA-AIVHE method," in *Proceedings of the 2010 IEEE International Conference on Communication Control and Computing Technologies (ICCCCT)*, 2010, pp. 637–642. *(Cited on page 97)*

[423] C.-L. Su, "Palm-print recognition by matrix discriminator," *Expert Systems and Applications*, vol. 36, no. 7, pp. 10 259–10 265, September 2009. *(Cited on page 99)*

[424] A. Morales, A. Kumar, and M. A. Ferrer, "Incorporating color information for reliable palmprint authentication," in *Proceedings of the 2011 18th IEEE International Conference on Image Processing (ICIP)*, 2011, pp. 3193–3196. *(Cited on page 100)*

[425] V. Kanhangad, A. Kumar, and D. Zhang, "A unified framework for contactless hand verification," *IEEE Transactions on Information Forensics and Security*, vol. 6, no. 3, pp. 1014–1027, 2011. *(Cited on pages XVI, 102, 103, 147, 196, and 204)*

[426] ——, "Contactless and pose invariant biometric identification using hand surface," *IEEE Transactions on Image Processing*, vol. 20, no. 5, pp. 1415–1424, 2011. *(Cited on pages 103, 147, 196, and 204)*

[427] S. Ma, G. Wu, N. Zhang, H. Li, N. Luo, and Q. Chen, "Embedded three-dimensional surface measurement system for palmprint," in *Proceedings of the 2011 International Conference on Hand-Based Biometrics (ICHB)*, 2011, pp. 1–5. *(Cited on pages XVI and 104)*

[428] L. Zhang, H. Li, and J. Niu, "Fragile bits in palmprint recognition," *IEEE Signal Processing Letters*, vol. 19, no. 10, pp. 663–666, 2012. *(Cited on page 104)*

[429] Y. Zheng, G. Shi, Q. Wang, and L. Zhang, "Palmprint image quality measures in minutiae-based recognition," in *Proceedings of the 14th International Workshop on Systems, Signals and Image Processing, 2007 and 6th EURASIP Conference focused on Speech and Image Processing, Multimedia Communications and Services*, 2007, pp. 140–143. *(Cited on pages XVI and 105)*

[430] P. H. Hennings-Yeomans, B. V. K. V. Kumar, and M. Savvides, "Palmprint classification using multiple advanced correlation filters and palm-specific segmentation," *IEEE Transactions on Information Forensics and Security*, vol. 2, no. 3, pp. 613–622, 2007. *(Cited on page 105)*

[431] B. Zhang, W. Li, P. Qing, and D. Zhang, "Palm-print classification by global features," *IEEE Transactions on Systems, Man, and Cybernetics: Systems*, vol. 43, no. 2, pp. 370–378, 2013. *(Cited on page 106)*

[432] D. Zhang, "Online palmprint classification," in *Palmprint Authentication*, ser. International Series on Biometrics. Springer US, 2004, vol. 3, pp. 155–167. *(Cited on pages XVI and 106)*

[433] L. Fang, M. K. H. Leung, T. Shikhare, V. Chan, and K. F. Choon, "Palmprint classification," in *Proceedings of the IEEE International Conference on Systems, Man and Cybernetics (SMC)*, vol. 4, 2006, pp. 2965–2969. *(Cited on page 106)*

[434] A. Negi, B. Panigrahi, M. V. N. Prasad, and M. Das, "A palmprint classification scheme using heart line feature extraction," in *Proceedings of the 9th International Conference on Information Technology (ICIT)*, 2006, pp. 180–181. *(Cited on page 106)*

[435] M. Sakdanupab and N. Covavisaruch, "An efficient approach for automatic palmprint classification," in *Proceedings of the IEEE International Conference on Signal Image Technology and Internet Based Systems (SITIS)*, 2008, pp. 229–234. *(Cited on page 107)*

[436] W. Jia, Y.-H. Zhu, L.-F. Liu, and D.-S. Huang, "Fast palmprint retrieval using principal lines," in *Proceedings of the IEEE International Conference on Systems, Man and Cybernetics (SMC)*, 2009, pp. 4118–4123. *(Cited on page 107)*

[437] X. Yang, J. Feng, and J. Zhou, "Palmprint indexing based on ridge features," in *Proceedings of the 2011 International Joint Conference on Biometrics*, ser. IJCB. Washington, DC, USA: IEEE Computer Society, 2011, pp. 1–8. *(Cited on page 107)*

[438] Z. Wei, Y. Han, Z. Sun, and T. Tan, "Palmprint image synthesis: A preliminary study," in *Proceedings of the 15th IEEE International Conference on Image Processing (ICIP)*, 2008, pp. 285–288. *(Cited on page 107)*

[439] L. Hong, Y. Wan, and A. K. Jain, "Fingerprint image enhancement: algorithm and performance evaluation," *IEEE Transactions on Pattern Analysis and Machine Intelligence*, vol. 20, no. 8, pp. 777–789, 1998. *(Cited on page 113)*

[440] C. I. Watson, M. D. Garris, E. Tabassi, C. L. Wilson, R. M. McCabe, S. Janet, and K. Ko, "User's guide to NIST biometric image software (NBIS)," 2007. *(Cited on pages 114 and 115)*

[441] M. Kawagoe and A. Tojo, "Fingerprint pattern classification," *Pattern Recognition*, vol. 17, no. 3, pp. 295–303, June 1984. *(Cited on page 114)*

[442] Z. Zhang, "A flexible new technique for camera calibration," *IEEE Transactions on Pattern Analysis and Machine Intelligence*, vol. 22, no. 11, pp. 1330–1334, 2000. *(Cited on pages 116 and 129)*

[443] J. Heikkila and O. Silvén, "A four-step camera calibration procedure with implicit image correction," *Proceedings of the IEEE Computer Society Conference on Computer Vision and Pattern Recognition (CVPR'97)*, pp. 1106–1112, 1997. *(Cited on pages 116 and 129)*

[444] R. I. Hartley and A. Zisserman, *Multiple View Geometry in Computer Vision*, 2nd ed. Cambridge University Press, 2004. *(Cited on pages 116 and 129)*

[445] L. Wang, R. H. A. El-Maksoud, J. M. Sasian, and V. S. Valencia, "Illumination scheme for high-contrast, contactless fingerprint images," in *Novel Optical Systems Design and Optimization XII*, R. J. Koshel and G. G. Gregory, Eds., vol. 7429, no. 1. SPIE, 2009. *(Cited on page 117)*

[446] R. Donida Labati, A. Genovese, V. Piuri, and F. Scotti, "Two-view contactless fingerprint acquisition systems: a case study for clay artworks," in *Proceedings of the 2012 IEEE Workshop on Biometric Measurements and Systems for Security and Medical Applications (BioMS)*, Salerno, Italy, September 2012, pp. 1–8. *(Cited on page 117)*

[447] P. D. Kovesi, "MATLAB and Octave functions for computer vision and image processing," Centre for Exploration Targeting, School of Earth and Environment, The University of Western Australia, http://www.csse.uwa.edu.au/~pk/research/matlabfns/. *(Cited on pages 118 and 129)*

[448] J.-Y. Bouguet, "Camera calibration toolbox for Matlab," http://www.vision.caltech.edu/bouguetj/calib_doc/. *(Cited on pages 119, 129, and 134)*

[449] R. Donida Labati, A. Genovese, V. Piuri, and F. Scotti, "Quality measurement of unwrapped three-dimensional fingerprints: A neural networks approach," in *Proceedings of the 2012 International Joint Conference on Neural Networks (IJCNN)*, 2012, pp. 1–8. *(Cited on page 123)*

[450] ——, "Accurate 3D fingerprint virtual environment for biometric technology evaluations and experiment design," in *Proceedings of the 2013 IEEE International Conference on Computational Intelligence and Virtual Environments for Measurement Systems and Applications (CIVEMSA)*, Milan, Italy, July 2013, pp. 43–48. *(Cited on pages 123 and 159)*

[451] ——, "Virtual environment for 3-D synthetic fingerprints," in *Proceedings of the 2012 IEEE International Conference on Virtual Environments Human-Computer Interfaces and Measurement Systems (VECIMS)*, 2012, pp. 48–53. *(Cited on page 123)*

[452] ——, "Low-cost volume estimation by two-view acquisitions: A computational intelligence approach," in *Proceedings of the 2012 International Joint Conference on Neural Networks (IJCNN)*, 2012, pp. 1–8. *(Cited on page 130)*

[453] D. G. Lowe, "Distinctive image features from scale-invariant keypoints," *International Journal of Computer Vision*, vol. 60, no. 2, pp. 91–110, November 2004. *(Cited on pages 140 and 142)*

[454] A. Vedaldi and B. Fulkerson, "VLFeat: An open and portable library of computer vision algorithms," 2008, http://www.vlfeat.org/. *(Cited on pages 140 and 163)*

[455] P. J. Besl and H. D. McKay, "A method for registration of 3-D shapes," *IEEE Transactions on Pattern Analysis and Machine Intelligence*, vol. 14, no. 2, pp. 239–256, February 1992. *(Cited on page 145)*

[456] R. Guerchouche and F. Coldefy, "Camera calibration methods evaluation procedure for images rectification and 3D reconstruction," *Orange Labs, France Telecom R & D*, 2008. *(Cited on pages 170 and 179)*

[457] "Minolta Vivid 910 Noncontact 3D Digitizer," http://www.konicaminolta.it/fileadmin/CONTENT/Measurement_Instruments/Download/Catalogue_Download/vivid910_e9.pdf. *(Cited on pages 195 and 196)*

[458] "OpenCV: Open Source Computer Vision Library," http://http://opencv.org/. *(Cited on page 196)*

[459] S. Matuska, R. Hudec, and M. Benco, "The comparison of CPU time consumption for image processing algorithm in Matlab and OpenCV," in *Proceedings of the ELEKTRO 2012*, 2012, pp. 75–78. *(Cited on page 196)*

[460] "NVIDIA CUDA Compute Unified Device Architecture - Programming Guide," http://developer.download.nvidia.com/compute/cuda/1_0/NVIDIA_CUDA_Programming_Guide_1.0.pdf, 2007. *(Cited on page 196)*

[461] K. Pulli, A. Baksheev, K. Kornyakov, and V. Eruhimov, "Real-time computer vision with OpenCV," *Communications of the ACM*, vol. 55, no. 6, pp. 61–69, 2012. *(Cited on page 196)*

[462] L.-C. Chiu, T.-S. Chang, J.-Y. Chen, and N. Y. C. Chang, "Fast SIFT design for real-time visual feature extraction," *IEEE Transactions on Image Processing*, vol. 22, no. 8, pp. 3158–3167, 2013. *(Cited on page 196)*

[463] International Organization for Standards, "ISO 9241-11 Ergonomic requirements for office work with visual display terminals (VDTs) - Part 11: guidance on usability ," 1998. *(Cited on page 197)*

A

PUBLICATIONS

Some ideas and significant results present in this thesis were published in:

1. "*Touchless Fingerprint Biometrics: a Survey on 2D and 3D Technologies*"

   R. Donida Labati, A. Genovese, V. Piuri, and F. Scotti

   Journal of Internet Technology, 2014 (*To appear*).

   ABSTRACT: Traditional fingerprint recognition systems require that the users touch a sensor to perform biometric acquisitions. In order to increase the usability, acceptability, and accuracy of fingerprint recognition technologies, touchless systems have recently been studied. With respect to touch-based biometric techniques, these systems present important differences in most of the steps of the recognition process. Studies in the literature can be classified into technologies based on two-dimensional and three-dimensional methods. These studies also present important differences in terms of accuracy and required level of user cooperation. This paper presents a brief survey on touchless recognition technologies, proposing a classification of two-dimensional and three-dimensional biometric recognition techniques.

2. "*Accurate 3D Fingerprint Virtual Environment for Biometric Technology Evaluations and Experiment Design*"

   R. Donida Labati, A. Genovese, V. Piuri, and F. Scotti

   Proceedings of the 2013 IEEE International Conference on Computational Intelligence and Virtual Environments for Measurement Systems and Applications (CIVEMSA 2013), Milan, Italy, July 15–17, 2013.

   ABSTRACT: Three-dimensional models of fingerprints obtained from contactless acquisitions have the advantages of reducing the distortion present in traditional contact-based samples and the effects of dirt on the finger and the

sensor surface. Moreover, they permit to use a greater area for the biometric recognition. The design and test of three-dimensional reconstruction algorithms and contactless recognition methods require the collection of large databases. Since this task can be expensive and time-consuming, some methods in the literature deal with the generation of synthetic biometric samples. At the best of our knowledge, however, there is only a preliminary study on the computation of small areas of synthetic three-dimensional fingerprints. In this paper, we extend our previous work and describe a virtual environment for the generation of complete three-dimensional fingertip shapes, which can be useful for the research community working in the field of three-dimensional fingerprint biometrics. The method is based on image processing techniques and algorithms designed for biometric recognition. We validated the realism of the simulated models by comparing them with real contactless acquisitions. Results show that the method is feasible and produces realistic three-dimensional samples which can effectively be processed by biometric recognition algorithms.

3. "*Contactless Fingerprint Recognition: a Neural Approach for Perspective and Rotation Effects Reduction*"

   R. Donida Labati, A. Genovese, V. Piuri, and F. Scotti

   Proceedings of the 2013 IEEE Symposium on Computational Intelligence in Biometrics and Identity Management (CIBIM 2013), Singapore, April 16–19, 2013.

   ABSTRACT: Contactless fingerprint recognition systems are being researched in order to reduce intrinsic limitations of traditional biometric acquisition technologies, encompassing the release of latent fingerprints on the sensor platen, non-linear spatial distortions in the captured samples, and relevant image differences with respect to the moisture level and pressure of the fingertip on the sensor surface. Fingerprint images captured by single cameras, however, can be affected by perspective distortions and deformations due to incorrect alignments of the finger with respect to the camera optical axis. These non-idealities can modify the ridge pattern and reduce the visibility of the fingerprint details, thus decreasing the recognition accuracy. Some systems in the literature overcome this problem by computing three-dimensional models of the finger. Unfortunately, such approaches are usually based on complex and expensive acquisition setups, which limit their portability in consumer devices like mobile phones and tablets. In this paper, we present a novel approach able to recover perspective deformations and improper fingertip alignments in single camera systems. The approach estimates the orientation difference between two contactless fingerprint acquisitions by using neural networks, and permits to register the considered samples by applying the estimated rotation angle to a synthetic three-dimensional model of the finger surface. The generalization capability of neural networks offers a significant advantage by allowing processing a robust estimation of the orientation difference with a very limited need of computational resources with respect to

traditional techniques. Experimental results show that the approach is feasible and can effectively enhance the recognition accuracy of single-camera biometric systems. On the evaluated dataset of 800 contactless images, the proposed method permitted to decrease the equal error rate of the used biometric system from 3.04% to 2.20%.

4. "*Two-view Contactless Fingerprint Acquisition Systems: a Case Study for Clay Artworks*"

   R. Donida Labati, A. Genovese, V. Piuri, and F. Scotti

   Proceedings of the 2012 IEEE Workshop on Biometric Measurements and Systems for Security and Medical Applications (BioMS 2012), Salerno, Italy, pp. 1–8, September 14, 2012.

   ABSTRACT: The detection of latent fingerprints can be a great aid in determining the authenticity of ancient artworks. In fact, a commonly used technique for the authentication of artworks consists in the comparison of fingerprints present on the surface of an artifact with other available latent fingerprints of an artist. This kind of analysis is particularly important for the authentication of clay artifacts. The clay, in fact, is often modeled barehanded, causing a great number of fingerprints left on the surface. In many cases, the artworks are very valuable or fragile and the latent fingerprints cannot be acquired using classical forensic methods. For this reason, contactless acquisition techniques have been proposed. Most of these techniques are based on the use of a single camera. In single-view acquisition systems, however, it can be difficult to properly estimate the size of the captured area, the obtained images can suffer from problems related to perspective distortions, and a calibration task cannot be performed in all the cases. In this paper, we propose a two-view acquisition system able to capture the latent fingerprints left on a clay artwork, and to compute their three-dimensional metric reconstruction. The obtained results show that the proposed approach is feasible and the reconstructed models provide a metric, view-independent, and less-distorted reconstruction of the fingerprint. In particular, we describe the application of the proposed method on a specific clay artwork associated by experts to the famous sculptor Antonio Canova (Italy, 1757–1822).

5. "*Virtual Environment for 3-D Synthetic Fingerprints*"

   R. Donida Labati, A. Genovese, V. Piuri, and F. Scotti

   Proceedings of the IEEE International Conference on Virtual Environments, Human-Computer Interfaces and Measurement Systems (VECIMS 2012), Tianjin, China, pp. 48–53, July 2–4, 2012.

   ABSTRACT: Contactless biometric recognition performed using three-dimensional fingerprint models has the advantages of reducing problems related to the deformations of the skin, dust on the sensor, and spoofing of latent fingerprints. Moreover, the fingerprint area usable for the recognition is wider

than the one captured by traditional contact-based acquisition techniques. The design of fingerprint recognition systems based on three-dimensional models, however, requires the collection of large datasets of samples. This task is expensive and time consuming, and can also require the implementation of new hardware setups. For this reason, the use of virtual environments for the computation of realistic synthetic models can be useful for the evaluation of new biometric algorithms. In the literature, there are methods for the computation of synthetic fingerprint models that resemble fingerprint images acquired using a touch-based sensor. However, at the best of our knowledge, there are no works dealing with the computation of synthetic three-dimensional models of fingerprints. In this paper, we propose a virtual environment able to compute synthetic three-dimensional fingerprints, which can be useful for the entire research community working in the fields of biometrics and three-dimensional reconstruction. The method is based on image processing techniques and algorithms designed for fingerprint recognition applications. The method is validated by comparing the results obtained with contactless fingerprint acquisitions. Results show that the method is feasible and produces three-dimensional models that are realistic and visually comparable with real fingerprints.

6. "*Weight Estimation From Frame Sequences Using Computational Intelligence Techniques*"

   R. Donida Labati, A. Genovese, V. Piuri, and F. Scotti,

   Proceedings of the IEEE International Conference on Computational Intelligence for Measurement Systems and Applications (CIMSA 2012), Tianjin, China, pp. 29–34, July 2–4, 2012.

   ABSTRACT: Soft biometric techniques can perform a fast and unobtrusive identification within a limited number of users, be used as a preliminary screening filter, or combined in order to increase the recognition accuracy of biometric systems. The weight is a soft biometric trait which offers a good compromise between distinctiveness and permanence, and is frequently used in forensic applications. However, traditional weight measurement techniques are time-consuming and have a low user acceptability. In this paper, we propose a method for a contactless, low-cost, unobtrusive, and unconstrained weight estimation from frame sequences representing a walking person. The method uses image processing techniques to extract a set of features from a pair of frame sequences captured by two cameras. Then, the features are processed using a computational intelligence approach, in order to learn the relations between the extracted characteristics and the weight of the person. We tested the proposed method using frame sequences describing eight different walking directions, and captured in uncontrolled light conditions. The obtained results show that the proposed method is feasible and can achieve a view-independent weight estimation, also without the need of computing a complex model of the body parts.

7. "*Quality Measurement of Unwrapped Three-dimensional Fingerprints: a Neural Networks Approach*"

   R. Donida Labati, A. Genovese, V. Piuri, and F. Scotti,

   Proceedings of the 2012 International Joint Conference on Neural Networks (IJCNN 2012), Brisbane, Australia, pp. 1–8, June 10–15, 2012.

   ABSTRACT: Traditional biometric systems based on the fingerprint characteristics acquire the biometric samples using touch-based sensors. Some recent researches are focused on the design of touch-less fingerprint recognition systems based on CCD cameras. Most of these systems compute three-dimensional fingertip models and then apply unwrapping techniques in order to obtain images compatible with biometric methods designed for images captured by touch-based sensors. Unwrapped images can present different problems with respect to the traditional fingerprint images. The most important of them is the presence of deformations of the ridge pattern caused by spikes or badly reconstructed regions in the corresponding three-dimensional models. In this paper, we present a neural-based approach for the quality estimation of images obtained from the unwrapping of three-dimensional fingertip models. The paper also presents different sets of features that can be used to evaluate the quality of fingerprint images. Experimental results show that the proposed quality estimation method has an adequate accuracy for the quality classification. The performances of the proposed method are also evaluated in a complete biometric system and compared with the ones obtained by a well-known algorithm in the literature, obtaining satisfactory results.

8. "*Iris Segmentation: State of the Art and Innovative Methods*"

   R. Donida Labati, A. Genovese, V. Piuri, and F. Scotti

   Cross Disciplinary Biometric Systems, ser. Intelligent Systems Reference Library, C. Liu and V.K. Mago (eds.), Springer Berlin Heidelberg, vol. 37, pp. 151–182, 2012.

   ABSTRACT: Iris recognition is nowadays considered as one of the most accurate biometric recognition techniques. However, the overall performances of such systems can be reduced in non-ideal conditions, such as unconstrained, on-the-move, or non-collaborative setups. In particular, a critical step of the recognition process is the segmentation of the iris pattern in the input face/-eye image. This process has to deal with the fact that the iris region of the eye is a relatively small area, wet and constantly in motion due to involuntary eye movements. Moreover, eyelids, eyelashes and reflections are occlusions of the iris pattern that can cause errors in the segmentation process. As a result, an incorrect segmentation can produce erroneous biometric recognitions and seriously reduce the final accuracy of the system. This chapter reviews current state-of-the-art iris segmentation methods in different applicative scenarios. Boundary estimation methods will be discussed, along

with methods designed to remove reflections and occlusions, such as eyelids and eyelashes. In the last section, the results of the main described methods applied to public image datasets are reviewed and commented.

9. "*Fast 3-D Fingertip Reconstruction Using a Single Two-View Structured Light Acquisition*"

   R. Donida Labati, A. Genovese, V. Piuri, and F. Scotti

   Proceedings of the 2011 IEEE Workshop on Biometric Measurements and Systems for Security and Medical Applications (BioMS 2011), Milan, Italy, pp. 1–8, September 28, 2011.

   ABSTRACT: Current contactless fingertip recognition systems based on three-dimensional finger models mostly use multiple views (N > 2) or structured light illumination with multiple patterns projected over a period of time. In this paper, we present a novel methodology able to obtain a fast and accurate three-dimensional reconstruction of the fingertip by using a single two-view acquisition and a static projected pattern. The acquisition setup is less constrained than the ones proposed in the literature and requires only that the finger is placed according to the depth of focus of the cameras, and in the overlapping field of views. The obtained pairs of images are processed in order to extract the information related to the fingertip and the projected pattern. The projected pattern permits to extract a set of reference points in the two images, which are then matched by using a correlation approach. The information related to a previous calibration of the cameras is then used in order to estimate the finger model, and one input image is wrapped on the resulting three-dimensional model, obtaining a three-dimensional pattern with a limited distortion of the ridges. In order to obtain data that can be treated by traditional algorithms, the obtained three-dimensional models are then unwrapped into bidimensional images. The quality of the unwrapped images is evaluated by using a software designed for contact-based fingerprint images. The obtained results show that the methodology is feasible and a realistic three-dimensional reconstruction can be achieved with few constraints. These results also show that the fingertip models computed by using our approach can be processed by both specific three-dimensional matching algorithms and traditional matching approaches. We also compared the results with the ones obtained without using structured light techniques, showing that the use of a projector achieves a faster and more accurate fingertip reconstruction.

10. "*Measurement of the Principal Singular Point in Contact and Contactless Fingerprint Images by using Computational Intelligence Techniques*"

    R. Donida Labati, A. Genovese, V. Piuri, and F. Scotti

    Proceedings of the IEEE International Conference on Computational Intelligence for Measurement Systems and Applications (CIMSA 2010), Taranto, Italy, pp. 18–23, September 6–8, 2010.

ABSTRACT: Biometric systems identify individuals by comparison of the individual biometric traits, such as the fingerprint patterns. In the literature, many relevant methods are based on the localization of a reference "pivot" point of the fingerprint, called principal singular point (PSP). Most of the time, the PSP is selected from the list of the estimated singular points (SPs) that are identified by specific local patterns of the fingerprint ridges, called cores and deltas. The challenge is to provide an automatic method capable to select the same PSP from different images of the same fingertip. In this paper, we propose a technique that estimates the position of all the singular points by processing the global structure of the ridges and extracting a specific set of features. The selection of the reference point from the candidate list is then obtained by processing the extracted features with computational intelligence classification techniques. Experiments show that the method is accurate and it can be applied on contact and contact-less image types.

COLOPHON

This document was typeset using the typographical look-and-feel `classicthesis` developed by André Miede. The style was inspired by Robert Bringhurst's seminal book on typography *"The Elements of Typographic Style"*. `classicthesis` is available for both LaTeX and LyX at: http://code.google.com/p/classicthesis.